FOREWORD

This final report on the program for Research Investigation of Hydraulic Pulsation Concepts was prepared by Republic Aviation Corporation, Farmingdale, New York, under USAF Contract AF33 (657)-10622.

It summarizes the work performed by Republic from 15 February 1963 to 15 August 1964, and concerns an investigation into the feasibility of hydraulic power transmission by pulsating flow or pressure, the layout design of functional components that would be peculiar to a pulsating system, the analysis of the dynamic characteristics of pulsating systems, components, and power transmission. Work conducted on this program at Republic Aviation Corporation was under the direction of Mr. W. E. Mayhew, with Mr. F. H. Pollard as Principal Investigator, and with the assistance of personnel of the Fluids Systems Staff of the Research Division and the Hydrospace Division. Prof. J.L. Shearer, Pennsylvania State University, was consultant on the analytical portion of the program.

USAF Contract AF33 (657)-10622 was initiated under Project Task 812807 by the Transmission Technology Section of the Air Force Aero Propulsion Laboratory, Research and Technology Division, Wright-Patterson Air Force Base, Ohio. The work was administered under the direction of Mr. B.P. Brooks of the Aero Propulsion Laboratory.

ABSTRACT

This final report covers a program during which Republic made a research investigation of the technical feasibility of the transmission and utilization of hydraulic power through the use of pulsating pressure or pulsating flow concepts. It was concluded that the pulsating flow means were suitable for power transmission, whereas pulsating might be adapted for signal transmission. The type of system currently in greatest use in aerospace vehicles is the constant pressure flow demand system that utilizes a pressure-compensated variable delivery pump. Republic believes that an adaptation of this system to the requirements of a pulsating system will produce the most desirable means of control from the standpoints of efficiency, simplicity, and reliability. Our major efforts have therefore been concerned with the design of such an adaptation.

The research investigation was carried on by two methods: 1) the design effort, and 2) the analytical method. The laboratory effort was limited to relatively simple experiments intended to verify or facilitate analytic results. The system analysis was augmented and verified by data derived from a miniaturized pulsating hydraulic system.

As a result of its research investigation, Republic recommends that the effort be continued and that a representative operating pulsating system be investigated to confirm the analytic data and that further investigations be made into the applicability of pulsating hydraulic concepts for vehicular use.

TABLE OF CONTENTS

TABLE OF CONTENTS (CONT'D)

LIST OF ILLUSTRATIONS

LIST OF ILLUSTRATIONS (CONTINUED)

LIST OF ILLUSTRATIONS (CONTINUED)

LIST OF ILLUSTRATIONS (CONTINUED)

LIST OF ILLUSTRATIONS (CONTINUED)

LIST OF ILLUSTRATIONS (CONTINUED)

LIST OF TABLES

SECTION I - INTRODUCTION

This Final Report covers a program for the research investigation of hydraulic pulsation concepts. To permit a better understanding of a pulsating hydraulic system's characteristics, a discussion of its nature and an analogy to electrical systems is desirable. Heretofore, hydraulic systems have been of the continuous-flow type. In such a system one line is used for downstream or pressure flow and another is used for upstream or return flow, and up to the directional control valves each line is unidirectional in flow. Downstream of the directional control valves the lines are used for bidirectional flow, but for any preset direction of actuation the flow in each line is unidirectional. Thus a continuous-flow hydraulic system can be likened to a direct current electrical system, and the directional control valve to a double pole - double throw switch. In a pulsating system the flow or pressure pulsates in the lines. As will be shown later, a pulsating flow system was selected as being more desirable than a pulsating pressure system for the transmission of hydraulic power. Considering any incremental volume of fluid, the fluid merely moves back and forth in the transmission line and the motion in the transmission line is bidirectional. Thus a pulsating flow hydraulic system can be likened to an alternating current electrical system. Further analogies to direct current and alternating current electrical systems can be drawn. In a direct current electrical system the pressure or voltage can be decreased by a resistor (pressure-reducing valve) and the drop in voltage is dissipated by heat in the resistor and represents lost power.

Increase in voltage in a direct current electrical system is rather complex, as is increase in pressure in a continuous flow hydraulic system. With alternating current electrical systems voltage increase or decrease is readily accomplished in a transformer as a function of the number of turns in the primary and secondary coils. So also with pulsating hydraulics, pressure can be transformed to either increase or decrease as a function of the areas of the input and output ends of the transformer.

Electrical alternating current can be phased, so also can pulsating hydraulic power, as a function of the power generation pickoffs. Electrical alternating current is capable of rectification to direct current, as is pulsating hydraulic power. Thus pulsating hydraulic systems have a very close analogy to alternating current electrical systems, just as continuous flow hydraulic systems have an analogy to direct current electrical systems. The advantages that alternating current electrical systems have over direct current systems are by and large those that pulsating hydraulic systems will have over continuous flow hydraulic systems.

The basic intent of the program was an investigation of the feasibility of the utilization of pulsating flow hydraulics. The investigation was carried on through two methods: 1) the design effort, and 2) the analytical method. The laboratory effort was limited to relatively simple experiments intended to verify or facilitate analytic results.

Manuscript released (September 1964) for publication as an RTD Technical Documentary Report.

The first method of investigation entailed the derivation of layout designs of component parts (pumps, valves, etc.) which would be peculiar to a pulsating hydraulic system rather than the conventional continuous flow hydraulic system. These components were then schematically combined into a simulated aileron control system which would be capable of operation under the operating loads and rates of motion specified in the work statement. This system was then submitted to various analyses to determine the functional characteristics, operating requirements, and failure modes. The design criteria of pulsating power transmission were studied as they affected tubing size and wall thickness, with the resultant effect on line weight. The relative weights of pulsating and continuous flow hydraulic systems were also studied.

The second method of investigation was analytical. For ease of comparison, electrical equivalents were derived not only of the various system components, but also of the over-all system in a simplified form. The transmission line flow effects were not only studied analytically but a simple laboratory setup was also used to verify the analytic data. The system analysis was augmented and verified by data derived from a miniaturized pulsating hydraulic system. The miniaturized system was also used to assist in indication of the optimum pulsation frequency and in derivation of system efficiency data.

In the course of the program it was realized that new terms were necessary to describe operating characteristics and components that were not used in conjunction with continuous flow hydraulics. In order to avoid confusion in this new terminology, a recommended list of nomenclature for pulsating hydraulics was established. This list is presented in Appendix I.

SECTION II - SYSTEM DESIGN

A. GENERAL

As is true in the design of continuous flow hydraulic systems, the design of pulsating hydraulic systems or subsystems must be varied so as to conform to and augment the functional requirements of the services being actuated by the hydraulic system. Two basic approaches to system design utilizing pulsation concepts should be evaluated and the type that better conforms to the desired function chosen. The first basic type is the pure pulsating system in which the mechanical energy is converted to hydraulic energy in a pulsating form. The second type is the combined system in which the energy is converted to hydraulic energy in a continuous flow form and then altered to pulsating flow.

B. PURE PULSATING SYSTEM

When direct conversion from mechanical energy to pulsating hydraulic energy is made, the entire system (aside from rectification at the actuator) should be a pulsating system. For a system other than a small single-actuator or motor system, the weight and design penalties that must be accepted will prove such a system to be impractical. Moreover, it is preferred that the actuator demand a fairly constant flow level. This is due to the design requirements and complexities that are inherent in a pressure-compensated pulsating flow generator.

For a single-line or two-line system (where a fairly constant output flow or velocity is required) a single- or double-ended hydraulic actuating cylinder can be employed as the hydraulic pulsating flow generator, as in the miniaturized system described later in this section.

A typical single-line pure pulsating system is shown in Figure II-1. It will be noted that a relief valve is shown between the pump and the fluid replenishment unit, upstream of the transformer. This valve is necessary in case the actuator is permitted to bottom or its directional control valve is placed in neutral to prevent excessive system pressurization. Locating this valve between the "pressure" and "return" ports of the directional control valve will accomplish the same result.

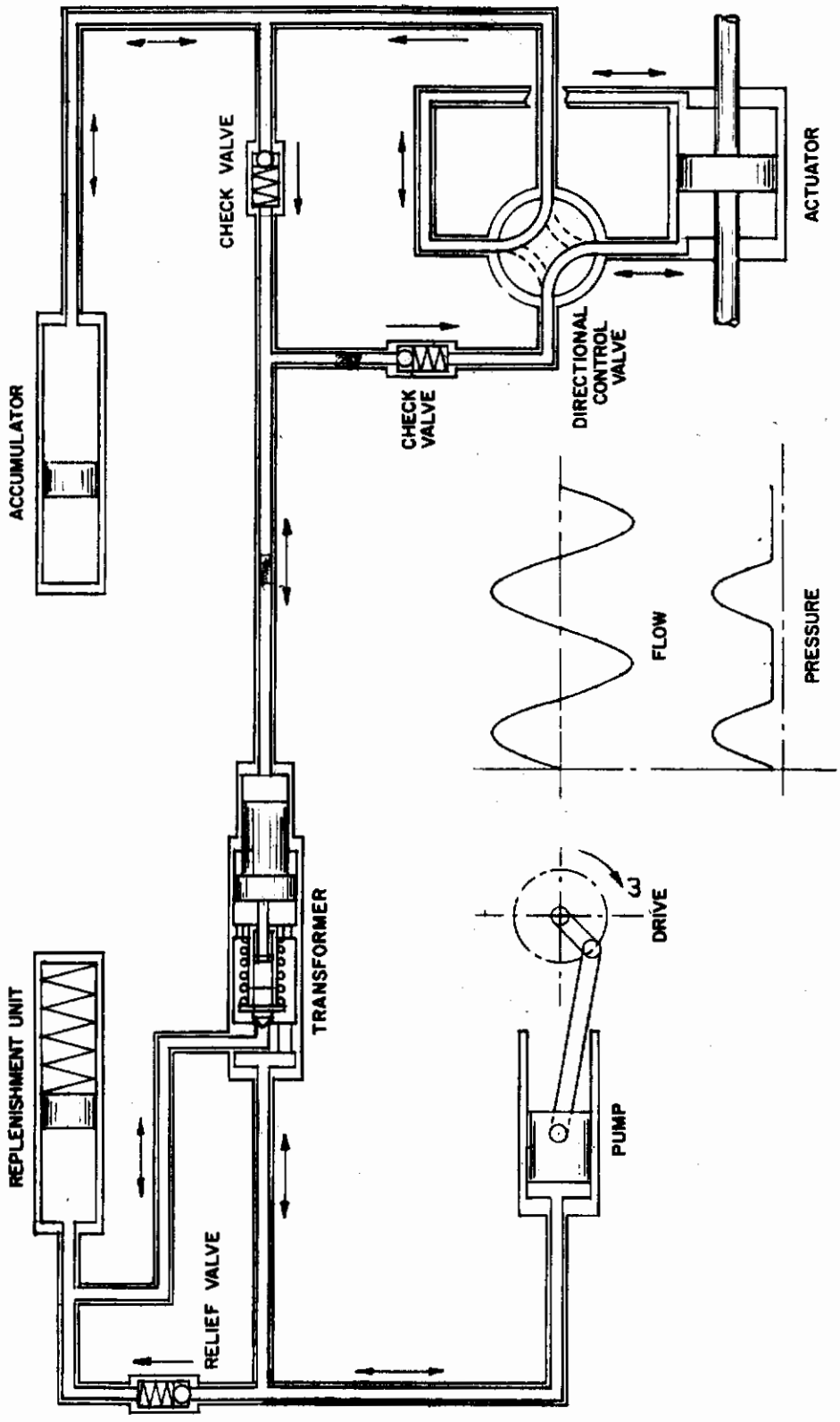

Figure II-1. Single-Line Pulsating System

Conversely, for a single-line type of transmission system, a pure pulsating system is practically mandatory. The reasons for this will be discussed later in this section.

C. COMBINED SYSTEM

For the average application, the combined continuous-pulsating flow type of system will be found to have many advantages over the pure pulsating system. In such a combined system, an evaluation can be made of each subsystem to determine whether the functional requirements and environment indicate the over-all advantage to lie with a pulsating system or a continuous flow system. Where a pulsating system is indicated by the evaluation, a further analysis must be made to determine the optimum number of transmission lines to meet the system's functional requirements.

A typical combined system is shown in Figure II-2. It will be noted that the hydraulic energy is generated in continuous flow form. In general, a pressure-compensated variable delivery pump will be used for this purpose. For the subsystems where pulsating flow is desired, the continuous flow will be converted to pulsating flow by an alternator valve. The balance of the subsystem will then be designed to meet the design conditions.

D. TRANSMISSION LINES

Transmission of the pulsating flow energy through the plumbing lines of a pulsating hydraulic system was considered to be a function of system design. The determination of the optimum number of transmission lines will be one of the first items that must be decided in the design of any pulsating hydraulic system or subsystem.

Since the simulated aileron loads and rate of actuation are identical to those specified under Contract AF33(616)-7454, for a system to meet the work statement requirements, it is desirable to utilize for this program an actuator constructed for that contract and designed to operate at a pressure of 4000 psi. During Republic's work on the above-mentioned contract, where the maximum flow from the pump was 8 gpm, the system was found to be somewhat marginal and flow-limited. For this reason, it is recommended that the pump and components for this system be sized-based on 10 gpm continuous flow at 4000 psi, which is roughly equivalent to 13 1/3 gpm at 3000 psi.

1. Single-Line Pulsating System

For a single-line pulsating system to produce a rectified flow with the power of a continuous flow of 10 gpm at 4,000 psi lines, flows and pressures must be as follows. Rectification of single-line pulsating flow will produce an interrupted half-wave as shown in Figure II-1. Assuming that the pump output is sinusoidal and a rectified flow of 10 gpm is required, then the pump must deliver a peak flow of $10/.318 = 31.4$ gpm.

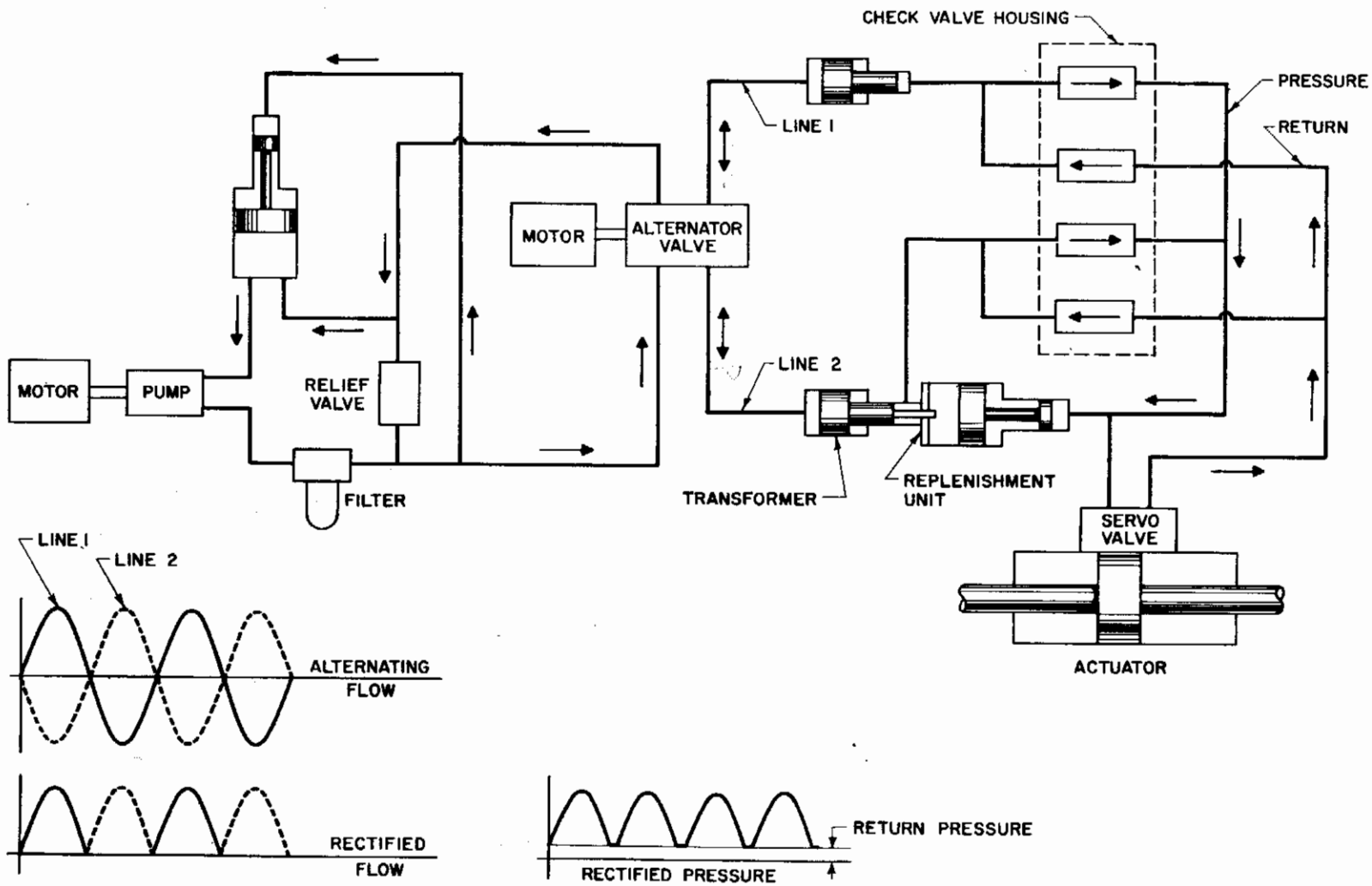

Figure II-2. Two-Line Pulsating System

The average pulsed flow is .637 (the average of a sine wave) times 31.4 = 20 gpm. If the pump piston stroke is limited to 0.5 in. (which will result in a piston velocity that is not excessive) and the pulsation frequency to 8 cps (the desired average frequency), the piston diameter required for an average flow of 20 gpm is 3.06 in. The speed of the eccentric drive would be 8 cps times 60 = 480 rpm. It is readily apparent that for operation at a pulsation frequency of 8 cps the pump would be relatively large and heavy.

The line size required for an average flow rate of 20 gpm will be determined by limiting the fluid velocity to 15 ft/sec. The tube I.D. is calculated as follows:

$$A = \frac{Q}{V} = \frac{20 \times 231}{60 \times 15 \times 12} = .428 \text{ in.}^2$$

$$d = 1.128 \sqrt{.428} = 1.128 \times .654 = .748 \text{ in.}$$

A 1-inch O.D. tubing is the smallest standard tubing size that could be used to obtain a flow passage of .748 diameter or larger.

To obtain an average pressure during each pulse of 4,000 psi, a peak pressure of 4000/.637 = 6,280 psi will be necessary. Assuming an ultimate tensile strength of the tubing of 145,000 psi (the value for Inconel-X) and the conventional factor of 4 between working pressure and burst pressure, the required tubing wall thickness from Barlow's formula would be:

$$w = \frac{DP}{2S} = \frac{1 \times 25,120}{2 \times 145,000} = .087 \text{ in.}$$

The nearest standard wall thickness would be .095 in. and the weight per foot of 1 x .095 tubing .918 lb. Moreover, the motion of a controlled actuator would be quite jerky.

2. Two-Line Pulsating System

A typical two fluid-line pulsating system is shown in Figure II-2. A high-speed continuous flow pump would be used to develop the required flow. The continuous flow would be converted to pulsating flow by the alternator valve. The alternator produces pulses in the two outlet lines, which are 180° out of phase and make full-wave rectification possible.

With full wave rectification, the average flow in the lines is .637 times the peak flow. If a rectified flow of 10 gpm is required, then the alternator valve must supply a peak flow of 10/.637 = 15.7 gpm in each of the two lines. The continuous flow pump will be sized to provide a maximum delivery of 15.7 gpm.

For an average pulsed flow of 10 gpm, the tubing O.D. required to limit the fluid velocity to 15 ft/sec would be 5/8 in.

The advantage of the two-line system over the one-line is that power generation would be more efficient and lighter in weight due to the use of a high-speed multi-piston pump.

Again, for an average pressure of 4,000 psi, a peak pressure of 6,280 psi will be necessary and tubing wall thickness will be as follows:

$$w = \frac{.625 \times 25,120}{2 \times 145,000} = .054 \text{ in.}$$

The nearest standard wall thickness is .058 in. and the weight per foot .351 lb or .702 lb/ft for two tubes.

3. Three-Line Pulsating System

In a three-line system (see Figure II-3), the average rectified flow is .954 times the peak flow. Thus, for the desired average rectified flow of 10 gpm, the peak flow will be 10/.954 or 10.45 gpm. Since the average flow in each line will be .637 times the peak flow, a three-line system will require an average flow of .637 x 10.45, or 6.65 gpm in each tube. Again using an average flow velocity of 15 feet per second, we find that a 1/2 in. O.D. tube will suffice.

Since the summed flow (as indicated in Figure II-3) will be rather constant with only a slight ripple, a peak pressure of 4,000/.954, or 4,200 psi, should be readily attainable. Thus, applying Barlow's formula, wall thickness is

$$w = \frac{.5 \times 16,800}{2 \times 145,000} = .029 \text{ in.}$$

The nearest standard wall thickness is .028 in.; however, due to the high cyclic loading the tubing must endure, the next heavier wall, .035 in., is recommended. This will weigh .174 lb/ft or .522 lb/ft for three tubes.

Summarizing the above from the tubing weight standpoint, we find the following:

No. of Lines	Tube	Wt. Ft.	Total Wt. Ft.
1 Line	1 in. x .095	.918 lb	.918 lb
2 Line	5/8 in. x .058	.351 lb	.702 lb
3 Line	1/2 in. x .035	.174 lb	.522 lb

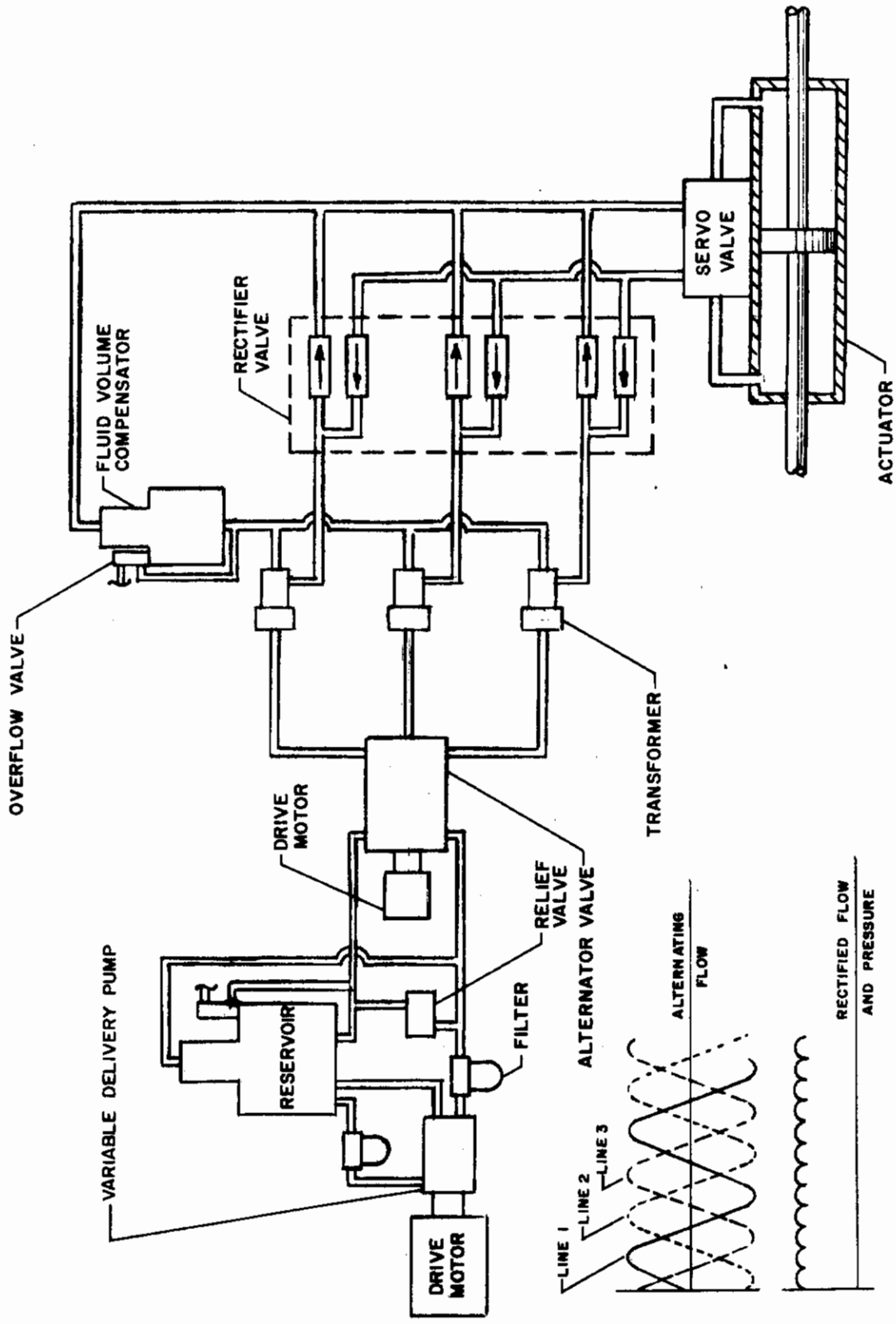

Figure II-3. Three-Line Pulsating System

The tubing line weight relationship will be carried over into other weight considerations. From the functional standpoint, the relatively low ripple of rectified three-line flow will be rapidly attenuated during flow through lines and components and the smooth actuation desirable in a servo system, in particular, will be readily attained. With a two-line system, ripple filtration will be desirable to produce smooth actuation. The addition of the inductance/capacitance required for this purpose will increase the weight disadvantage of a two-line system and reduce its over-all reliability. To produce relatively smooth flow from a single-line system is believed to be wholly impracticable.

E. CONCEPTUAL SYSTEM

In order to centralize system design efforts and place the design and analytic results of the program on a basis which would facilitate comparison with that of a previous Air Force sponsored R&D program, the work statement specified that a conceptual system for an aileron power control be investigated. The actuation deflection rate and loads were specified as follows:

(1) The aerodynamic hinge moment shall be 70,000 in.-lb minimum.

(2) The surface inertia hinge moment shall be 120 in.-lb minimum.

(3) The moment of inertia of the aileron shall be 5 slug/ft^2 minimum.

(4) The aileron surface rate shall be 25°/sec.

(5) The aileron deflection shall be 30°.

The work statement also specified an ambient temperature of 1400°F at the actuator. However, since the program covered by this phase of work was largely a determination of pulsating system feasibility, the temperature requirement merely indicated one area of usability of pulsating hydraulics (see Section VIII).

For a typical pulsating hydraulic system which can readily be sized to meet the specified actuation regime, see Figure II-3. It will be noted that this system generates the hydraulic energy as continuous flow. For the aileron actuation subsystem, the flow is converted to three-line pulsating flow by an alternator valve. The rotary speed of the drive for the alternator valve extablishes the pulsation frequency. The motor for the alternator drive will be a small hydraulic motor and will incorporate a flow control valve to control the pulsation frequency. For the purpose of the test system, however, a needle valve will be substituted for the more sophisticated flow control valve. This will facilitate laboratory investigation of the effects of pulsation frequency variation. This method of pulsation generation from continuous flow by means of an alternator valve is recommended in preference to direct pulsation at the hydraulic energy generating device. It permits the use of a combined continuous flow - pulsating flow system where each basic type is employed to its best advantage.

One of the basic features of pulsating hydraulic systems not normally found in continuous flow systems is pressure transformation. The pulsating hydraulic equivalent of the alternating current electrical transformer can transform hydraulic pressure levels on the basis of area ratios of the input and output ends of the unit in much the same manner that the electrical transformer, on the basis of the number of turns in the primary and secondary windings, transforms the electrical voltage. In addition to its pressure range feature, the hydraulic transformer presents another feature not offered by or pertinent to electrical transformers. It can serve as a fluid separation point so that one fluid may be used on the input side and another on the output side. This feature is further discussed in Section III. The conceptual system will therefore incorporate a transformer. In the general application of pulsating hydraulics, pressure transformation will not be the dominant feature necessitating use of the unit; we believe that the feature of fluid separation will be the main requirement necessitating use of a transformer.

Since the fluid downstream of the transformer will be isolated from the balance of the system, provision must be made for thermal expansion and contraction of the fluid and for a certain amount of fluid loss by leakage. If the volume of fluid downstream is large and the thermal range is wide, the volumetric fluid compensation that must be provided will be large. In general, it will be impractical to provide for this volumetric variation in the transformer; therefore, a separate fluid volume compensator unit must be provided. This unit (and the valving involved in its operation) is described in Section III.

For the average power application, a continuous application of the energy will be desirable; therefore, rectification of the flow from pulsating to continuous will be necessary. Check valves (the hydraulic equivalent of electrical diodes) will perform this function. Once the flow has been rectified from pulsating to continuous, the balance of the conceptual system will employ conventional continuous flow hydraulic elements. To meet the simulated aileron load requirements stated above, an artificial loading device will be used. Calculations of the torque and inertia elements of such a device, together with a typical actuator installation and actuator size calculation, are shown in Appendix II.

F. WEIGHT AND EFFICIENCY

One of the requirements listed in the work statement for the conceptual system is "the ambient temperature at the aileron shall be 1400°F." Although no minimum acceptable duration for this high ambient temperature was specified, Republic believes that this condition rules out a direct comparison between the conceptual system and a continuous flow hydraulic system. Without a major advance in the current state of the art, a continuous flow system of the specified power level cannot be constructed and operated. This statement is based on the following facts.

A hydraulic system of a power level identical to that of the work statement was investigated by Republic under Contract AF33(616)-7454. The maximum operating temperatures of this contract were 1000°F fluid temperature and 1200°F ambient

temperature at the aileron. The fluid used in the system was a mixed polyphenyl ether, one of the best of the organic fluids in resistance to thermal degradation. It was estimated that, even with circulation of the fluid from the lower temperature level portions of the system, the maximum duration of operation at 1000° and 1200°F that could be obtained was about four hours. Since the rate of fluid degradation was logarithmic with temperature, an increase of the ambient temperature at the aileron to 1400°F would so drastically reduce the duration of operation as to make the system impractical.

Because of the oscillatory motion of the fluid in the pulsating system, there is no flow from cooler portions of the system to the extreme temperature areas. Therefore, the system fluid temperature will eventually be equal to or slightly higher than the local ambient temperature and the fluid must be capable of withstanding it.

1. Comparison of Components and Relative Sizes

Comparing the number of components and their relative sizes for a three-line transmission system (as shown in Figure II-3) with those for a two-line system (Figure II-2), it will be noted that the three-line system requires three transformers and a three-bank rectifier as compared with two transformers and a two-bank rectifier for a two-line system. This might lead to the conclusion that the advantage the three-line system has in a smoother rectified flow will be offset by a weight increase. However (as indicated above in Subsection D), the average flow in a three-line system is 6.65 gpm as compared with 10 gpm in a two-line system. Each transformer would therefore be smaller. Moreover, if the system functional requirements make the provision of a relatively ripple-free actuator motion desirable, it will be necessary to add a ripple filter to the rectified continuous flow portion of a two-line system. This ripple filter would be a restrictor and an accumulator. The weight of these would almost certainly equal that of a transformer and a bank in the rectifier valve. With a three-line pulsating system, the ripple would be very small and would attenuate to an unnoticeable level after a short run. In addition, the weight of the transmission lines per foot of length would be 0.180 lb less with a three-line system than with a two-line system. In assessing the over-all relative weight, no fixed value can be set for this weight-saving, as it is a function of the vehicle configuration.

In a continuous flow type of system, the transmission lines will be sized as for a two-line system, hence their relative weight will be the same as that of a two-line pulsating system. It must be noted that in the continuous flow case, one of the transmission lines will be a return line and thus will not be subjected to full system pressure. In some vehicles a lighter weight material has been used for this line; however, it is felt that this is not a good design practice. Assembly errors may easily be made; the lighter weight (and hence weaker return tubing) may inadvertently be used for pressure lines. Therefore, for the purposes of this report, it will be assumed that a pulsating hydraulic system with three transmission lines will indicate a weight-saving in the power transmission lines over a similar continuous flow system.

This weight comparison also points up the desirability, in a combined continuous flow/pulsating flow system, of locating the alternator unit as far upstream as

is practicable. By this means a maximum length of pulsating transmission line will be achieved. An additional advantage will often be obtained by this location of the alternator valve. In most systems where pulsating hydraulics will be used, temperature will also be a problem. It is the tendency of high-temperature systems to have areas of highest temperature in the vicinity of the actuators rather than in the vicinity of power generation. In most cases, an alternator valve located as close as is practicable to the pumping unit will also be in an area of lower ambient temperature. Accordingly, the design requirements of the alternator valve will be diminished.

However, for this specific case with a continuous flow type of system, because of the temperature at the actuator it will be necessary to maintain a fixed minimum rate of flow through the actuator at all times to minimize fluid breakdown due to thermal decomposition. Even with this precaution, there may be a certain amount of fluid that will be more or less stagnant in the actuator that will tend to break down with a resulting deposit of solids. This deposit will, in time, gradually fill all stagnant areas in the actuator and other components and will cause malfunction. Therefore, from this standpoint alone, a continuous flow system cannot logically be used except for very short service life under the conditions of the conceptual system, and any weight or efficiency comparison is fallacious.

2. System Effect

In addition to component weights of pulsating and continuous flow hydraulic systems, the over-all system effect must be considered. For example, with a two-fluid pulsating system such as the conceptual system, the fluid volume control unit does not wholly represent an item of increased system weight. One of the basic functions that it performs is to provide space for the increase in fluid volume due to thermal expansion. Since the volumetric expansion of the fluid is a function of system temperature rather than system design, space for it would have to be provided in the system reservoir in a continuous flow system with a resulting increase in reservoir size and weight.

The isolation of heat that is possible with a two-fluid system suggests another area (not readily apparent) in which a pulsating system will save weight over a continuous flow system. In such a system the transformer acts as a separation point between the high-temperature fluid of the pulsating portion of the system and the fluid of the lower temperature continuous flow portion. It will therefore be located in a relatively low-temperature area and the heat from the high-temperature portion of the system will not be transmitted throughout the entire system. As a result, most of the system components can be fabricated of lighter weight, more readily machined materials, thereby also achieving a cost saving.

In addition to providing a weight-saving, a further feature of pulsating hydraulics that will result in an increase in system reliability and a decrease in maintenance requirements lies in the area of system cleanliness and freedom from contamination. Since in the pulsating portion of the system there will be no flow through the transmission lines, there will be no transfer of contaminants from one

portion of the system to another. The main contaminant-generating component in a hydraulic system is the pump. Since the pump will be isolated from the pulsating system, its contaminants will not reach any contaminant-critical component, such as an electro-hydraulic servo valve. The small and compact continuous flow loop that will exist downstream of the rectifier valve can be brought to the desired cleanliness level during assembly and filling and with reasonable care should remain clean. The installation of filters should be unnecessary.

In a servo-type system, such as is represented by the conceptual system, maximum efficiency is achieved instantaneously with the system operating at its maximum output velocity and at the point of maximum hinge moment. Since this condition is seldom met except in laboratory tests, it is in effect merely an indicated efficiency; it is not normally a basic design consideration, for other design criteria are usually dominant. In Republic's "Investigation of Techniques for 1000°F Hydraulic Systems" (ASD-TDR-62-674), a step input velocity of 40° per second aileron motion was achieved at 900°F fluid temperature. The total hinge moment at maximum deflection was 73,500 inch pounds.

The output horsepower at this instant was:

$$HP = \frac{TN}{63025}$$

T = Torque in inch pounds
N = Velocity in rpm

$$HP = \frac{73,500\ (6.67)}{63025} = 7.78$$

No record was made of the input torque to the pump at this time, but the hydraulic horsepower delivered by the pump was:

$$HP = psi \times gpm \times .000583$$

$$HP = 4000 \times 8 \times .000583 = 18.6$$

Thus the system efficiency was

$$\text{Percent of Efficiency} = \frac{\text{Output Power} \times 100}{\text{Input Power}}$$

$$\text{Percent of Efficiency} = \frac{7.78 \times 100}{18.6} = 41.7\%$$

3. Some Conclusions

Republic believes that an inorganic fluid is necessary for practical 1400°F operation. Molten salts and liquid metals are the outstanding candidate

fluids for the specified operating temperature. In the course of the above-referenced contract, molten eutectic salt mixtures were investigated and utilized for some portions of the program. The melting point of the salt utilized was approximately 280°F; its use at 1400°F would be impractical, due to thermal decomposition.

This leaves liquid metal as a candidate fluid under the terms of the work statement. The outstanding candidate liquid metal eutectic is NaK_{77}. This fluid, in common with all other caustic metal fluids, exhibits very poor lubricity, high corrosivity, and other undesirable characteristics. Although work under Government-sponsored contracts has been in progress for several years, the construction of a system of the specified power level has not been accomplished; however, in a pulsating system such as the conceptual system, we believe that the undesirable characteristics of NaK_{77} will be minimized. The basic hydraulic energy will be generated by using some readily pumped fluid of good lubricity; it will then be transmitted to the liquid metal through a transformer, preferably of the diaphragm type.

Summing up, for certain applications it is apparent that a pulsating system will perform where a continuous flow system will not perform. It is therefore considered that where the thermal conditions are such that an organic fluid cannot be used, a pulsating system is mandatory. At lower temperature ranges, heat isolation by means of fluid separation by a transformer will reduce or eliminate the need for system cooling penalties.

G. MINIATURIZED SYSTEM

Early in the program, a decision was made to construct a miniaturized pulsating hydraulic system utilizing components that were at hand. The system constructed was approximately one-tenth the size of the system that would be required to meet the design loads and rates specified for an analytic basis in the contract. The system was fully instrumented so that it could be used to derive functional data. A schematic diagram of the miniaturized system is shown in Figure II-4. Figures II-5, II-6, and II-7 show the setup and the instrumentation. MIL-H-5606 fluid was used.

The same part number cylinder was used for both the pump and the output actuator -- a tandem cylinder with a working area of 0.405 sq. in. Since the two halves were plumbed in parallel, an effective working area of 0.81 sq. in. resulted. The pumping cylinder drive had an adjustable offset so that the cylinder stroke could be varied as desired. A strain gage was located on the piston rod of the pumping cylinder to indicate input force and phase relationship.

The pumping cylinder was driven through the offset link and roller chain by a vari-drive motor. Two vari-drives were used: 1) the low-speed drive could cycle the pumping cylinder at a frequency of 1 to 8 cps.; 2) the high-speed drive produced a frequency range of 8 to 54 cps. A by-pass valve was connected as close as possible to the pumping cylinder to permit pump unloading for drive check out.

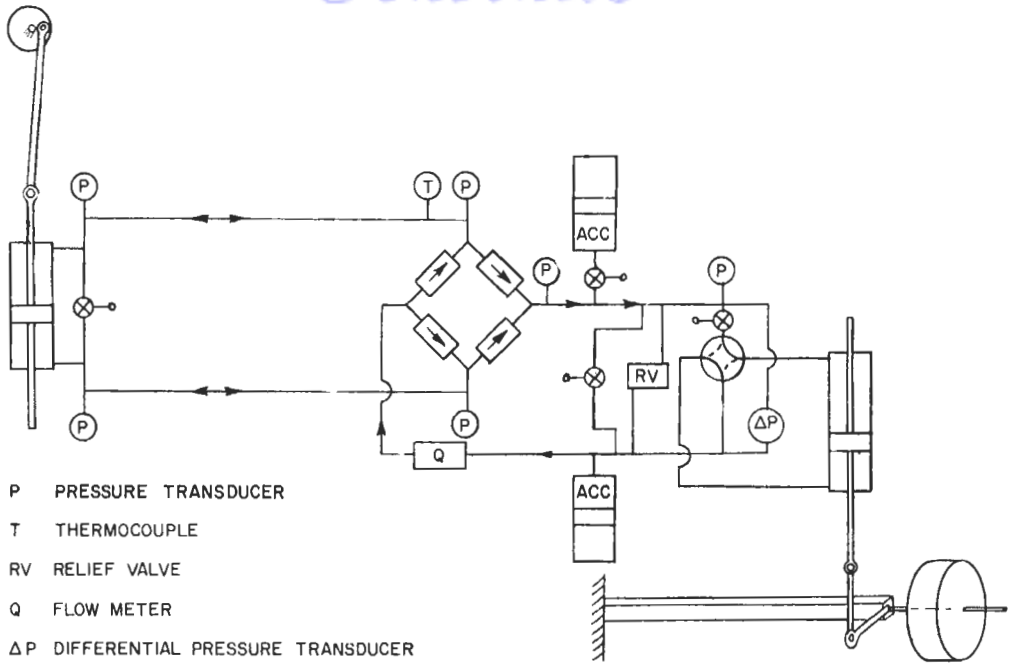

Figure II-4. Miniaturized Pulsating System - Schematic Diagram

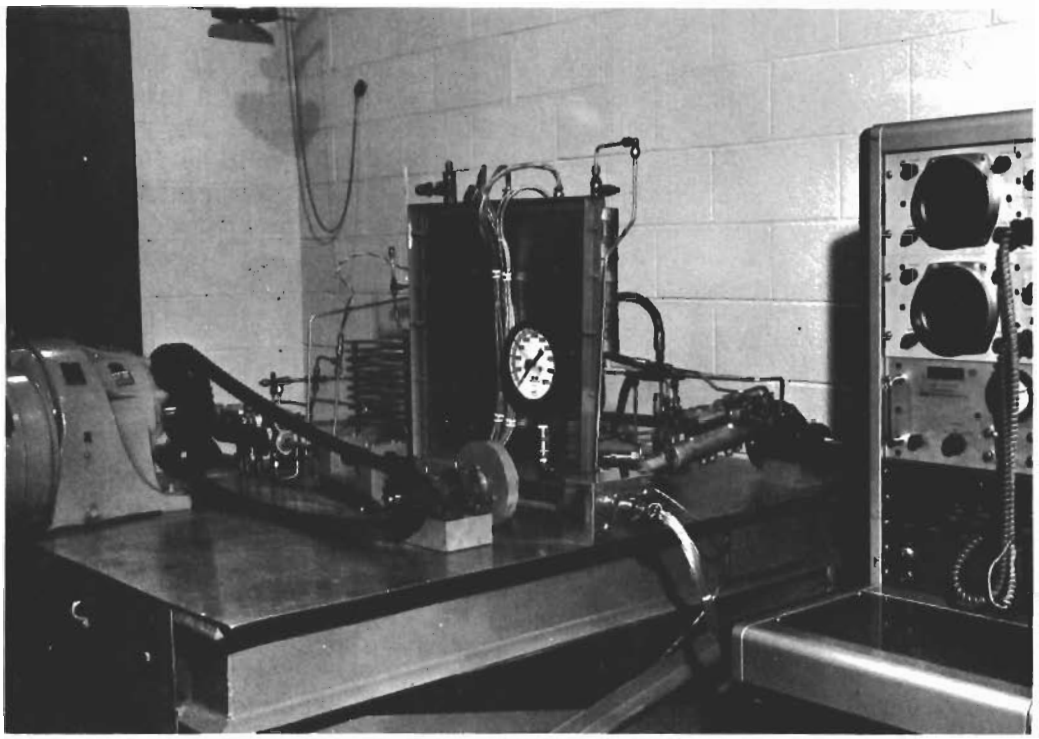

Figure II-5. Miniaturized Pulsating System - Pumping End

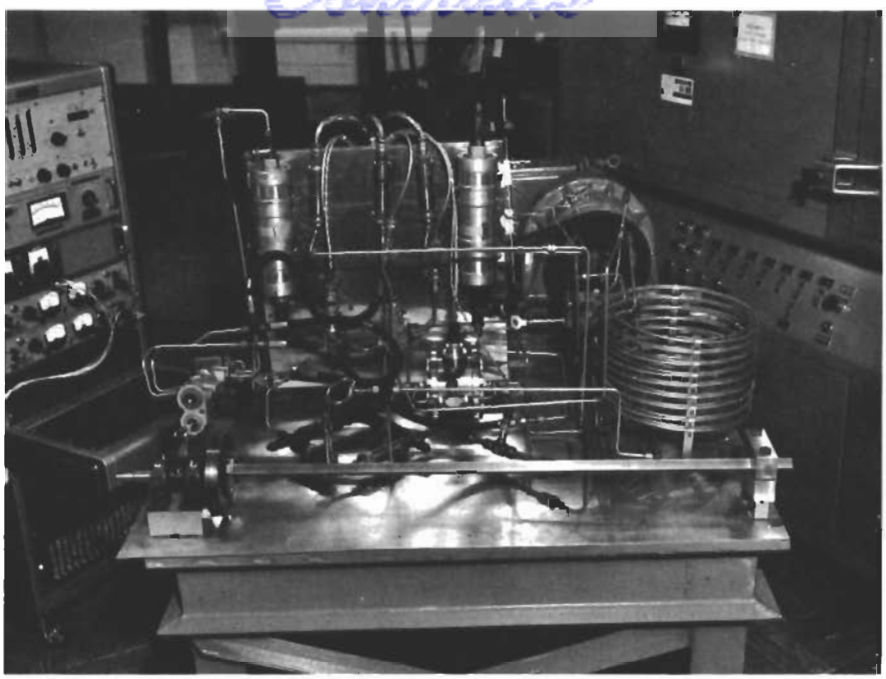

Figure II-6. Miniaturized Pulsating System - Output End

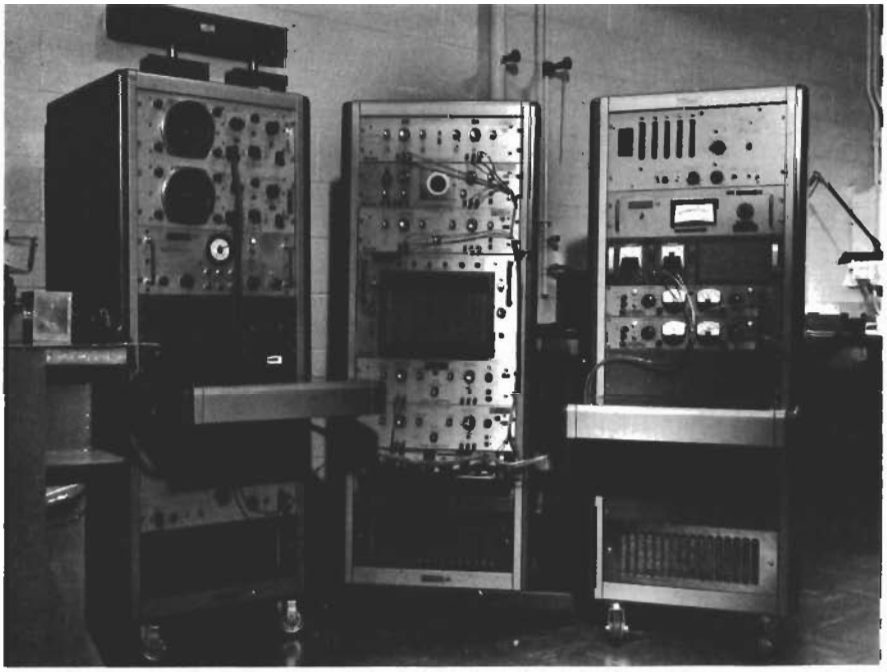

Figure II-7. Miniaturized Pulsating System - Instrumentation

The transmission lines between the pumping cylinder and the check valve rectifier bridge consisted of two lengths of tubing (1/4 in. O.D. x 0.035 in. wall). Each tube was approximately 25 ft. long and was wound in a coil approximately one foot in diameter to save space. As shown in Figure II-4, a pressure pickup was located at both ends of each transmission line. These are high-response transducers and were coupled to electronic recording equipment. From them, transmission line loss data, pulse pressure waveform, and phasing data were derived. These data were used as a basis for the impedance, line characteristics, and efficiency data shown in Section IV. A temperature pickup was located in the line to indicate changes in fluid temperature and thus the fluid viscosity.

A rectifier bridge consisting of four hydraulic check valves terminated the transmission lines and converted the pulsating flow to rectified continuous flow. The functional operation of the check valve rectification is described in Section III under "Rectifier Valve". A pressure pickup was located immediately adjacent to the continuous flow "pressure" connection of the rectifier. From it, data were derived indicating the ripple characteristics of the rectified continuous flow. Functionally associated with the rectifier bridge were two hydraulic accumulators. The one in the pressure line functioned as a ripple filter and had a pre-charge level somewhat lower than the peak pressure indicated by the transducer adjacent to the rectifier. A pressure transducer was located downstream of the high-pressure accumulator to indicate the degree of ripple filtration produced. In the course of the test program, the pre-charge level was varied to determine its efficiency as a ripple filter. A solenoid-operated shut-off valve in the line to the accumulator facilitated its isolation. The second or low pressure accumulator was located in the return line to the rectifier and served a dual function. The pre-charge pressure was very low. The first function of the unit was to maintain a minimum fluid pressure level to overcome transmission line pressure losses during the negative flow portion of a cycle of pulsation and thus ensure filling of the pumping cylinder during the suction portion of its stroke. Various pre-charge pressure levels were tested to indicate their effect on pump performance. The second function of the low-pressure accumulator was to act as a reservoir or fluid volume control. Since the system shown on the schematic is basically a closed loop, provision must be made for volumetric expansion of the fluid as a result of operating heat up. The accumulator also compensated volumetrically for fluid lost from the system due to leakage.

Two system loading devices were provided so that an indication of the working performance of a pulsating hydraulic system could be derived. One was merely a needle valve by-pass from pressure to return. The system used was of the constant flow (for any vari-drive speed and crank offset setting) demand pressure type. Thus, the restriction of the needle valve acted as a constant load on the system and variation of the restriction changed the pressure demand. The other loading device was a cylinder identical to the pumping cylinder. It was connected through a bellcrank to a torque bar sized to require a differential pressure of 1000 psi across the cylinder at each end of the stroke. Since the cylinder that was selected had an integral directional control valve, reversal of porting for stroking was readily accomplished. A shut-off valve was located in the pressure line to the cylinder so that the unit could be isolated when the needle valve was used for system loading. A differential pressure transducer was connected between pressure and return to record the working pressure load. A turbine type flow transducer was located in the return line to record the working flow.

We realized that a pulsating hydraulic system requires a very tight and gas-free system, otherwise it would be spongy and response and efficiency would suffer. Therefore, vacuum filling was used and very little difficulty was experienced in producing a tight system. The data derived from the miniaturized system were used to confirm and amplify analytic data and therefore will be included in that portion of this report.

H. FAILURE ANALYSIS

To further verify the design of the conceptual system, a failure analysis was made. The only unanticipated failure effect indicated by the analysis was that if overfilling or overheating occurred downstream of the transformer, there would be no method of venting excess fluid from the low pressure chamber of the fluid volume compensator. As a result, the negative pulse pressure would increase until a rupture occurred at the weak point of the system. An overflow valve (of the type used by Republic when utilizing boot-strap or differential area reservoirs) will eliminate the possibility of such a failure by venting excess fluid overboard. The failure analysis is tabulated on the following pages.

TABLE II-1

FAILURE ANALYSIS TABULATION

Component	Failure	Direct Effect	Indirect Effect
Variable Delivery Pump	Internal leakage	Reduced delivery and increased by-pass flow added heat rejection	
	External leakage	Deplete system fluid	
	Seized pumping element	No flow or reduced flow	
	Failed spline shaft	No flow	
	Jammed compensator - Open - Closed	Constant flow With excessive pressure No flow	Relief valve open and hot
Reservoir	External leakage	Deplete system fluid	
	Jammed piston	Pump cavitation or high system back pressure	Failure at system weak point
	Underfilled	Pressure fluctuating	Pump cavitation
	Overfilled	Overflow valve opens and compensates	
Filter	External leakage	Deplete system fluid	
	Clogged element	High pressure drop (down-stream pressure low)	
	Collapsed element	Continuous flow portion of system contaminated	
Relief Valve	External leakage	Deplete system fluid	
	Internal leakage	Reduced system flow and/or fluid overheat	
	Jammed mechanism - Open	No flow past unit - fluid overheat	Pump wide open

TABLE II-1

FAILURE ANALYSIS TABULATION (cont'd.)

Component	Failure	Direct Effect	Indirect Effect
Relief Valve (cont'd.)	Jammed Mechanism - Closed	No effect without double failure	Pump compensator failure must be primary
Alternator Valve	External leakage	Deplete system fluid	
	Internal leakage	Reduced system flow and fluid overheat	Pump compensator open
	Seizure Failed drive Failed motor	No flow or continuous flow	Pump feathered
	High friction	Motor overheat	Downstream pressure low
	Off speed motor	Off cycle flow	
Transformer	External leakage	Deplete system fluid	
	Seizure of piston	No flow	Pump compensator fluctuating
	High friction piston	Reduced system pressure Possible fluid overheat	Downstream pressure low
Fluid Volume Compensator	External leakage	Deplete system fluid	
	Jammed piston	Partial to complete loss of flow due to cavitation, or partial to complete loss of pressure differential and possible system rupture.	Pump feathered
	Check valve stuck - Open	Loss of system flow	Pump wide open
	- Closed	Same as jammed piston	Pump feathered

TABLE II-1

FAILURE ANALYSIS TABULATION (cont'd.)

Component	Failure	Direct Effect	Indirect Effect
Rectifier	External leakage	Deplete system fluid	
	Pressure check Stuck - Open	Reduced flow - return pressure high and fluctuating	Pump compensator fluctuating
	Pressure check - Closed	Reduced flow - return pressure normal - pressure fluctuating	Pump compensator fluctuating
	Return check Stuck - Open	Reduced flow - return pressure high and fluctuating	Pump compensator fluctuating
	- Closed	Reduced flow - pressure fluctuating	Pump compensator fluctuating
Servo valve	External leakage	Deplete system fluid	
	Excessive internal leakage	Reduced flow available for actuation	Actuator sluggish, fluid overheat
	Open coil	Hard-over signal in opposite direction	Actuator hard over
	Coil shorted to ground	Loss of control	Actuator to neutral
	Internal coil short	Tendency to excess signal in opposite direction	
	Jammed flapper	Hard-over signal unless jam in neutral	
Actuator	External leakage	Deplete system fluid	
	Excessive internal leakage, 1st stage rod seal	Reduced flow available for actuation	Actuator sluggish, fluid overheat

TABLE II-1

FAILURE ANALYSIS TABULATION (cont'd.)

Component	Failure	Direct Effect	Indirect Effect
Actuator (cont'd.)	Piston head seal excessive leakage or failure	Little or no effect except on hard-over signal - then sluggish to partial deflection	
	Jammed	(Improbable) no actuation	

SECTION III - COMPONENT DESIGN

A. GENERAL

Many of the component parts used in pulsating hydraulic systems will be either identical or similar to those used in continuous flow hydraulic systems. Moreover, in the case of a mixed system, where one portion of the system is continuous flow and another portion is pulsating, both continuous flow and pulsating components will be used. Even in the pulsating components, it will be noted that the various elements which comprise the component are conventional continuous flow elements in an unusual combination. That there are no basically new or unfamiliar functional component elements to be derived and studied goes far to indicate that the use of hydraulic pulsation concepts will be feasible from the standpoint of component design.

In the detail design of pulsating components, attention must be paid to the fatigue effects of cyclic stress loading due to pulsation. As a general case, component housings have very low stress levels and their design will not be affected by the high cyclic stress requirement. The excess strength is due to designing to the very low stress levels required to resist handling damage and to a deflection limitation being generally used rather than an ultimate stress. Helical springs are normally designed for a very high cyclic life; as a result, the cyclic loading from the pulsation will be well within normal life expectancy. Such elements as diaphragms will require special consideration because of pulsation fatigue effects. Elements which slide due to the pulsation will also require special attention, but this will also result from wear rather than fatigue. In such cases, wear and abrasion-resistant surface finishes must be applied.

Because of the fact that there is no functional flow from pulsating components, contamination effects from sources external to the component will be greatly reduced. By careful handling, they can be practically eliminated. Flow due to fluid volume change from thermal effects and fluid volume exchange from leakage will be the main means of contaminant ingestion by components. By the same token, however, wear and degradation products generated within a component will not be carried from the component by flow. Therefore, each pulsating component must be tolerant of its self-generated contaminants.

The thermal environment of pulsating components will basically determine the temperature of the fluid they contain as well as the thermal design requirement of the components. The fluid temperature within the components will be somewhat higher than the ambient temperature because of fluid and moving part friction losses.

B. PULSATION GENERATOR

The type of hydraulic system currently in greatest use in aircraft is the constant pressure, flow demand system which utilizes a pressure-compensated variable delivery pump. An adaptation of this type of system to the requirements of a pulsating system will produce a desirable means of control from the standpoints of efficiency, simplicity, and reliability. Major efforts have therefore been concerned with the design of such an adaptation, which is shown in Figure III-1.

The generator was designed to deliver 10 gpm at 4000 psi with a pulsation frequency of 8 cps. Two single-acting cylinders were chosen to deliver the alternating flow pulses with two discharge strokes or pulses obtained for each cycle. A piston stroke of one inch was arbitrarily selected to minimize piston side forces and to provide reasonable piston thrust forces. The piston diameter was calculated as follows.

$$10 \text{ gpm} = \frac{10 \times 231}{60} = 38.5 \text{ cu. in./sec}$$

$$38.5/8 \text{ cps} = 4.8125 \text{ cu. in./cycle}$$

The eccentric drive shaft speed required is: 8 cps x 60 sec/min = 480 rpm. Each cylinder discharges once for each cycle or revolution of the eccentric drive shaft. Therefore, each cylinder is required to deliver:

$$4.8125/2 = 2.4062 \text{ cu. in./cycle}$$

$$\text{Piston Area} = \text{Displacement/Stroke} = 2.4062/1 = 2.4062 \text{ sq. in.}$$

This area is very close to that of a 1.75-inch diameter circle (2.405). A nominal diameter of 1.75 in. was therefore established for the piston. The piston driving force required is 4,000 psi x 2.405 = 9,620 lb.

A double-acting balanced cylinder was not designed because this would entail the use of two piston rod seals in addition to the piston head seals. Also, to avoid the detrimental effects of piston rod side forces on the rod seals, a crosshead would have been necessary.

In the single-acting cylinder design shown, the extended piston accomplishes the purposes of a crosshead and transmits the piston side forces to the bearing surfaces of the cylinder bore and end cap. The elongated pistons are then subject to the conditions imposed on the plungers of a typical aircraft hydraulic pump.

Some fluid leakage is expected to occur past the piston head seals, especially when piston rings are used. This leakage will serve to lubricate the walls of the cylinder bore and bearing end cap. To avoid leakage past the end cap bearing,

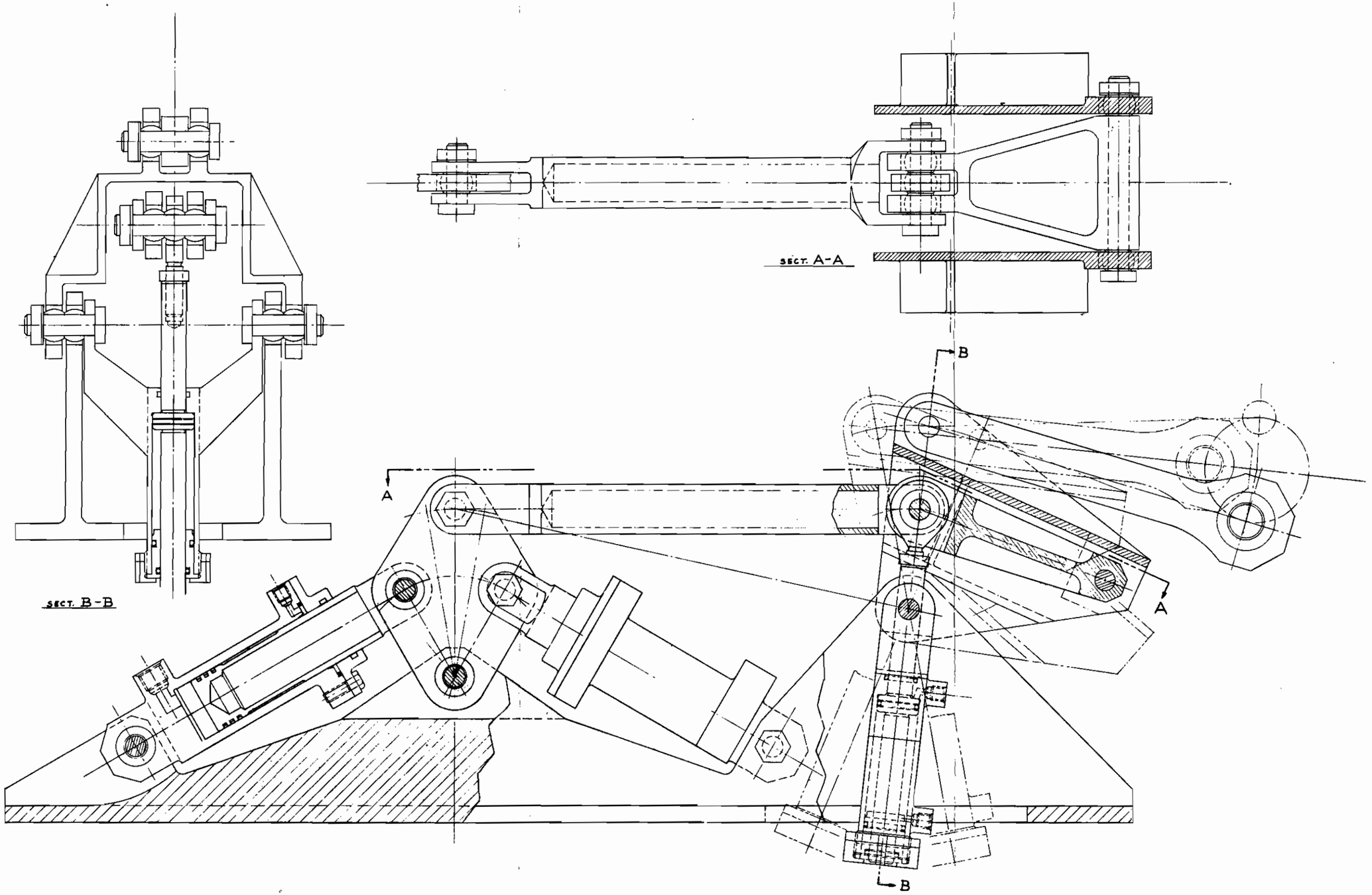

Figure III-1. Variable Delivery Pulsating Flow Generator

however, a seal is installed to accomplish a wiping action on the piston skirt. This leakage will be collected and conducted away by the drain port shown at the end of the cylinder.

A Scotch yoke and cam mechanism that would impart a simple harmonic motion to the pistons and result in a sinusoidal flow output was initially investigated as a driver for the pistons. This mechanism was abandoned because of the relatively large drive forces required and the mechanical complexities introduced in attempting to vary the piston stroke.

The eccentric drive mechanism finally chosen was so proportioned that the the deviation of the piston from a simple harmonic motion due to the "connecting-rod effect" has been minimized.

Variable delivery is obtained in the design shown in Figure III-1 by varying the piston stroke. This is accomplished in the following manner. The eccentric drive shaft continuously oscillates the "saddle" bellcrank through the connecting rod. The "saddle" bellcrank is connected to the cylinder bellcrank through the toggle links. The pistons and linkage are shown in the midstroke position with the toggle set for full piston stroke. The piston stroke is varied by varying the radial distance of the pivoted joint connecting the two toggle links from the "saddle" bellcrank pivot. The radial position of the toggle pivot is held and varied by the toggle cylinder. The position of the toggle cylinder, and therefore the toggle pivot, would be determined by a slide valve sensing system pressure and operating in the same manner as an aircraft pump sensing valve. Thus, piston displacement would be made to vary with system pressure. When no flow is demanded by the system, the pressure would rise and cause the toggle cylinder to pull the toggle pivot towards the "saddle" bellcrank pivot until both pivots coincide. When this occurs, oscillation of the cylinder bellcrank (and therefore piston stroking) ceases. When the system demands flow, the drop in system pressure causes the toggle cylinder to move the toggle pivot to the radial position, giving the required piston displacement.

In this design, the mechanical advantage afforded by the toggle linkage helps keep down the size of the actuator required to hold and/or shift the position of the toggle pivot. The maximum force required from the toggle cylinder occurs at the maximum stroke position shown in the drawing. This force was calculated to be 2,453 lb from the geometry shown in Figure III-2, as explained below.

$$P = \frac{9620 \times 3}{5 \times \cos 12^\circ} = \frac{28,860}{5 \times 0.9781} = 5,900 \text{ lb}$$

$$F = \frac{P \times 5.25}{13.94} = \frac{5900 \times 5.25}{13.94} = 2,230 \text{ lb}$$

Allowance for bearing friction = 10% x 2230 = 223 lb

Toggle cylinder thrust required = 2230 + 223 = 2,453 lb

Effective area of toggle cylinder = $\frac{2,453 \text{ lb}}{4,000 \text{ psi}}$ = 0.613 sq. in.

This area may be approximated by using a piston rod diameter of 0.750 in. and a cylinder bore of 1.187 in.

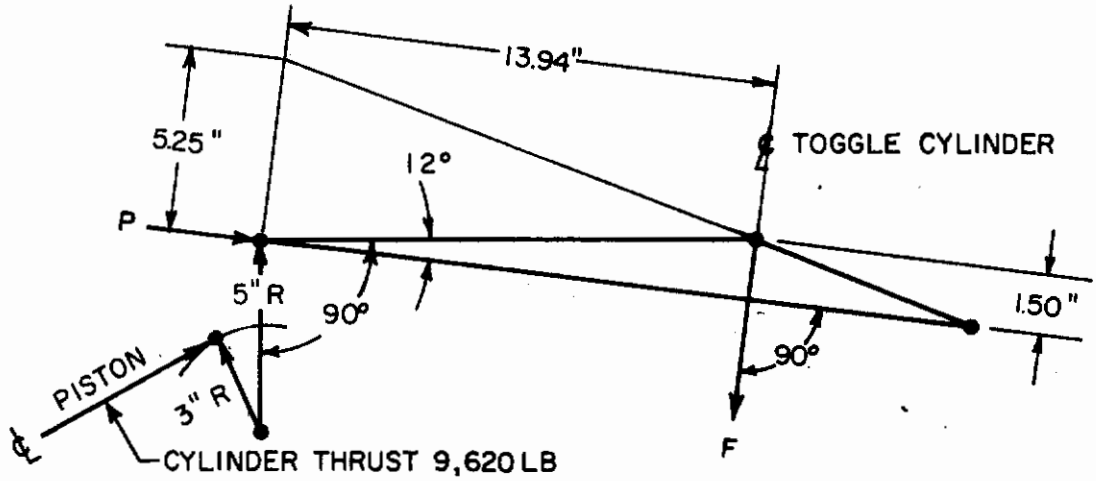

Figure III-2. Toggle Linkage Drive

C. ALTERNATOR VALVE

An alternator valve is a component which converts continuous hydraulic flow to pulsating hydraulic flow. For hydraulics, it performs the same basic function as its electrical counterpart, which converts direct current to alternating current. As described in Section II, the use of an alternator valve makes it possible for a hydraulic system to be partially continuous flow and partially pulsating flow.

The design of a three-phase rotary pulsating generator or "alternator" is shown in Figure III-3. Fluid is ported between the rotor and stator at the lapped interface of these elements where sliding contact occurs.

The rotor incorporates two pairs of radially opposed slots, as shown in Figure III-3, Section B-B. One of these opposed pairs communicates with the port located on the rotor axis and is used to distribute the pressurized flow pulses. The other pair communicates with the valve housing fluid and collects the return flow pulses.

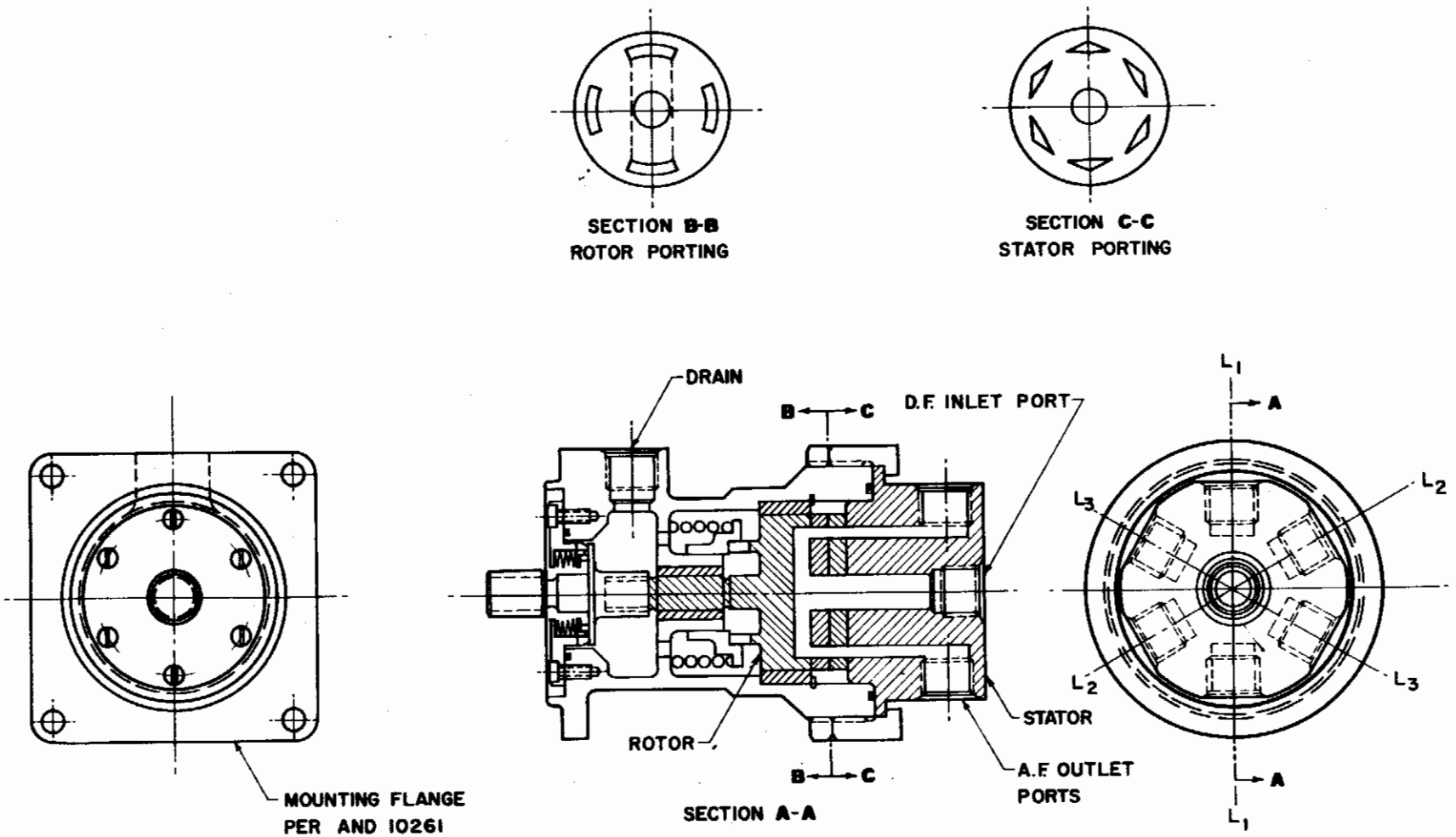

Figure III-3. Three-Phase Alternator

As shown in Figure III-3, Section C-C, the stator of the three-phase alternator incorporates three pairs of radially opposed transmission line ports.

The rotor was designed to incorporate a pair of distribution ports and a pair of return ports with each pair symmetrically located about the axis of rotation to effect a balanced loading condition on the rotor face. This in turn made it necessary to incorporate a pair of symmetrically located ports in the stator face for each transmission line. Each pair of ports would be joined externally to feed one of the three transmission lines.

Another advantage in using a pair of ports for each of the transmission lines is that two cycles (two pressure and two return flow pulses) are generated in each transmission line for each revolution of the rotor. Therefore, for any desired pulsation frequency, the rotor speed need be only half of that required for a two-port rotor (one distribution port and one return port).

The three-phase alternator design shown in Figure III-3 can be readily converted to a single-phase alternator by replacing the stator element only. The single-phase stator would incorporate two pairs of symmetrically located transmission line ports spaced 90° apart. In the three-phase stator, the ports are spaced 60° apart. In both the single-phase and three-phase alternator, a complete cycle (one pressure flow pulse and one return flow pulse) is generated in each transmission for every 180° rotation of the rotor.

The four-port rotor is analogous to a four-pole alternator because a cycle will occur twice in each revolution. Therefore, in an electrical or hydraulic alternator having P pairs of poles or ports respectively, there will be P cycles generated for each revolution of the rotor. If the generator is driven at a speed of s revolutions per second, the frequency in cycles per second will be $f = Ps$. For a frequency of 8 cps, the speed of the 4-port rotor will be 8/2, or 4 revolutions per sec (240 rpm). It is apparent, therefore, that the speed of the motor driving the rotor is the basic control of system pulsation frequency.

The system return port as originally designed was also located in the stator element, but this arrangement was abandoned in favor of the present location for the following reasons:

(1) It further complicated the fabrication of rotor and stator.

(2) The alternator housing would still require a drain port to drain off the leakage of pressurized fluid that would normally occur at the rotor and stator interface.

By porting the system return flow through the rotor and into the alternator housing, the alternator drain port performs the double function of draining off leakage flow and returning system fluid to the reservoir. The return fluid also provides circulation of the fluid within the housing and promotes cooling of the rotor bearing surfaces and shaft seal faces.

A three-line or three-phase pulsating hydraulic system is presented in Figure III-4. If the hydraulic flow is assumed to be sinusoidal, it can be shown mathematically that the average power available in a three-phase system is .954 times the peak power. In the two-line single phase system, the average power available is .637 times the peak power; in the single-line pulsation system, the average power is only .318 times the peak power.

The alternator requires a separate, relatively low-speed drive, but it can be readily utilized with existing high-speed, high-efficiency continuous flow aircraft pumps to create a pulsating hydraulic system. (See Figure III-4.)

An alternate solution is to incorporate the rotor and stator elements of the alternator within the housing of a conventional aircraft pump. Here, the conventional valve plate is replaced by a valve plate containing three ports spaced 120° apart. The valve plate is rotated by means of gearing at the desired rps, which is equivalent to the frequency in cps. The pump then becomes a three-phase pulsation generator.

As an example, a pump driven at 8,000 rpm with its valve plate driven through a 16.67/1 reduction will generate 8 cps of pulsating hydraulic power.

D. TRANSFORMER AND FLUID VOLUME COMPENSATION

The normal function of a transformer is to act as a pressure amplification or reduction device. However, in a pulsating flow system it performs an equally important function in that it also acts as a fluid separator. Because of this function, the transformer is also a logical device in which to incorporate some type of fluid replenishment unit. Hence, for this program the transformers and replenishment units were designed as a single package and also included provisions for relieving thermally expanded fluid.

Initial design work was centered about a piston-type transformer and a piston-pressurized fluid replenishment unit.

1. Piston-Type Transformer

The transformer was sized for a three-phase, three-line, pulsating hydraulic system operating at a frequency of 8 cps and delivering a rectified flow of 10 gpm at 4,000 psi.

Assuming the generator in this system produces sinusoidal flow with a peak value of 10 gpm in each of the three lines, by integrating the sine curve an average flow of 6.37 gpm is obtained in each of the three lines.

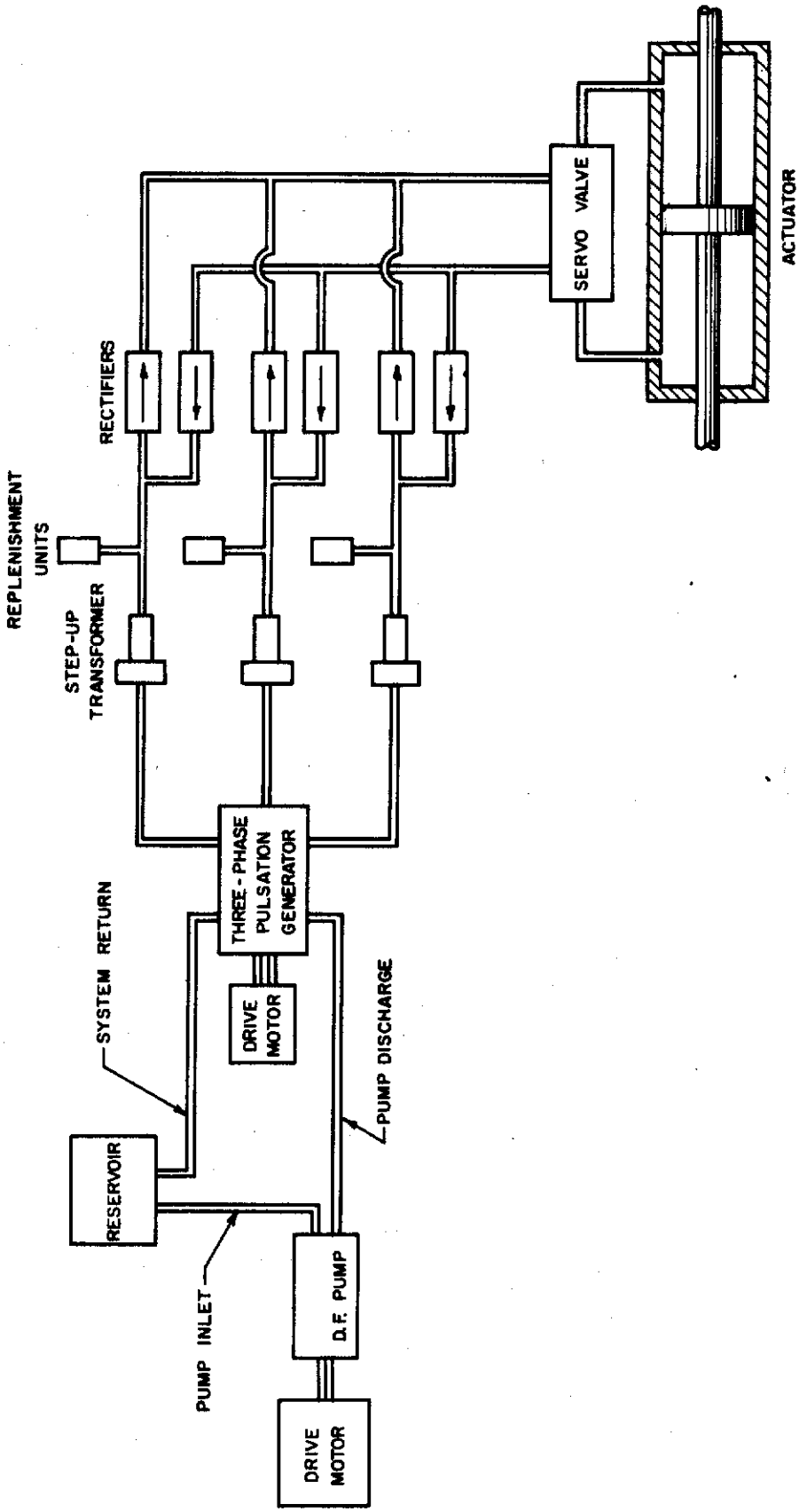

Figure III-4. Three-Phase Pulsating Hydraulic System

The transformer piston displacement was determined as follows:

$$6.37 \text{ gal/min} = 6.37 \text{ gal/min} \times 231 \text{ in.}^3/\text{gal} \times \frac{1}{60} \text{ min/sec} = 24.5 \text{ in.}^3/\text{sec}$$

For a pulsation frequency of 8 cps, the period is $1/f = 1/8$ cps $= .125$ sec/cyc. Since the average flow for each half-cycle is 24.5 in.^{3}/sec, the amount of fluid displaced in each half-cycle is $24.5 \times .125/2 = 1.535$ in.^{3}

Based on tests conducted at Republic on the miniaturized system, a piston stroke of 1/2 in. was selected as being compatible with the assumed pulsation frequency of 8 cps. The piston diameter was then determined from the known displacement and stroke.

$$\text{Piston area} = \frac{\text{displacement}}{\text{stroke}} = \frac{1.535}{.5} = 3.07 \text{ sq. in.}$$

$$\text{Piston diameter} = 1.128 \sqrt{3.07} = 1.975 \text{ in.}$$

The piston diameter was rounded out to a nominal diameter of 2.00 in., for which piston rings and seals are available.

As shown in Figure III-5, the piston is a double-ended design with a 1:1 ratio. A center land is provided to prevent mixing of any leakage flow past the seals at the two end of the piston. A drain is provided on each side of the center land to segregate the leakage.

For a three-phase, three-line, two-fluid system, three transformers and one fluid replenishment unit will be required. For a three-phase, three-line, three-fluid system, six transformers and four fluid replenishment units will be required, as shown in Figure III-6. The four piston transformers shown joined to the fluid replenishment units will incorporate a slightly modified piston. These pistons will be provided with a stud at one end to enable actuation of the thermal expansion check valve, as explained below.

To be of any practical value, fluid replenishment must be accomplished while the system is in operation.

To transfer fluid from a reservoir to a closed system, some pressure must be applied to the fluid in the reservoir. Pressurizing the fluid by means of an inert gas was ruled out because of the following problems:

(1) Additional system complexity

(2) Additional system weight

(3) Reduced reliability

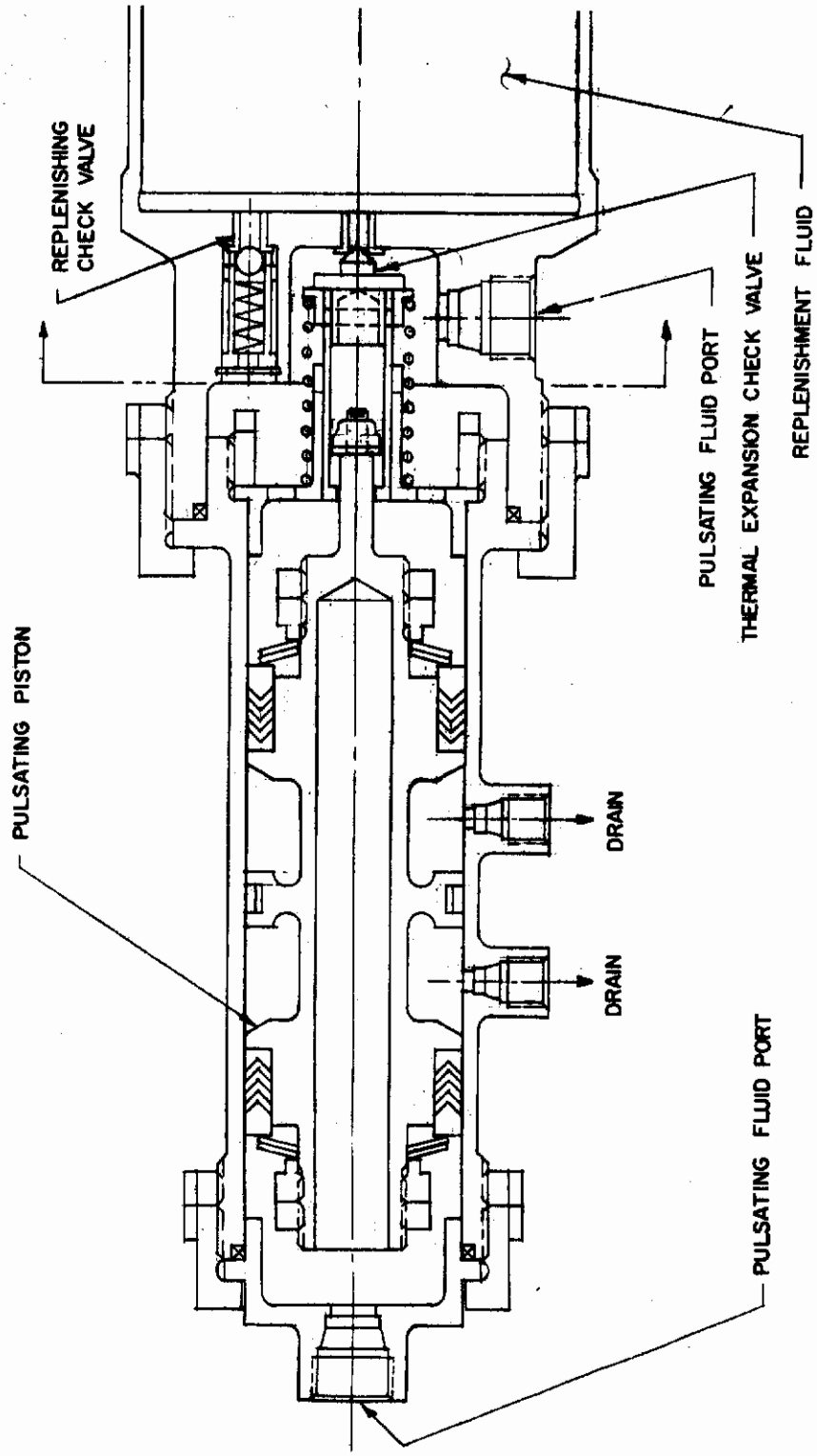

Figure III-5. Transformer and Fluid Level Control Unit

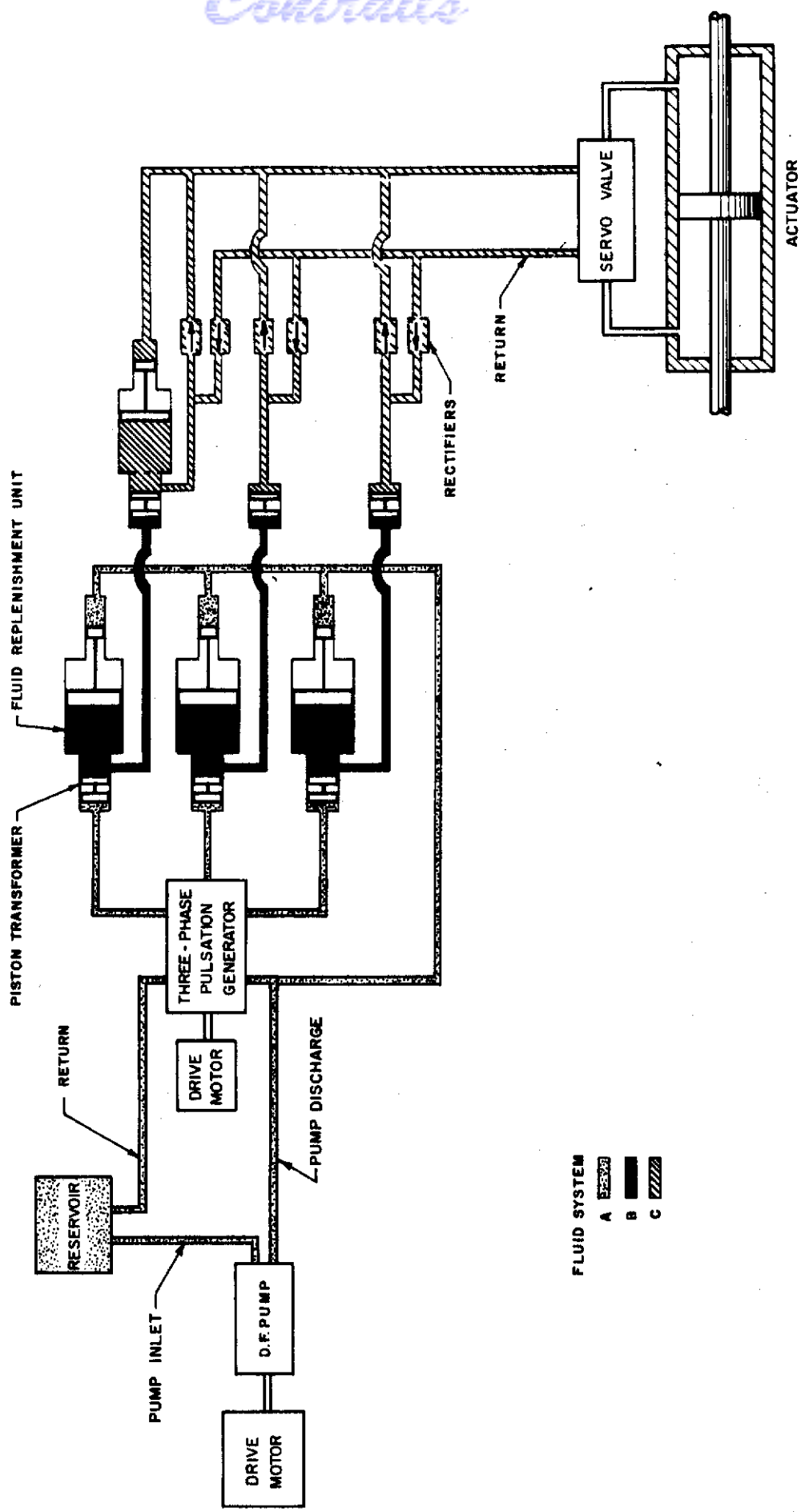

Figure III-6. Three-Phase, Three-Fluid Pulsating Hydraulic System

Such a system would require the use of stored pressurized gas to maintain the fluid at constant pressure. A replenishment unit designed along the lines of a precharged bladder or piston-type accumulator would be impractical because accumulators cannot maintain constant gas pressure with varying ambient temperatures.

In order to overcome the above problems, it was decided to design the replenishment unit similar to a piston-type reservoir.

In the piston-type replenishment unit, two methods were available for applying a force to the piston: 1) the use of mechanical springs, and 2) the use of bootstrap pressure.

A replenishing fluid pressure of 100 psi and 0.25 gallon of fluid were tentatively selected to enable initial sizing of the unit.

Design layouts, on both the spring-loaded and bootstrap pressure loaded piston units, were made to determine the weight difference of the two configurations.

The cylinder dimensions to enclose 0.25 gallon (57.75 $in.^3$) of fluid were determined from the following formulas, which give the minimum surface area (and therefore weight) of a cylinder to enclose a given volume:

$$\text{DIAMETER} = 2\sqrt[3]{\frac{\text{Volume}}{2\pi}} = 2\sqrt[3]{\frac{57.75}{6.28}} = 4.19 \text{ in.}$$

$$\text{LENGTH} \cong 1.1\sqrt[3]{\text{Volume}} = 1.1\sqrt[3]{57.75} = 4.26 \text{ in.}$$

The piston diameter was reduced to a nominal 4.00 in., for which piston rings are readily available. The cylinder length was proportionately increased to 4.60 in. to maintain the same volume.

For the spring-loaded piston configuration, a pair of nested springs were designed to provide the required piston force. Several nested spring combinations as well as single springs were investigated from the standpoints of compactness and weight before the final nested combination was arrived at.

The nested spring design afforded an over-all weight saving of 2.27 lb and a reduction in length of 3.55 in. over the best single spring design.

In the bootstrap pressure-loaded piston design, the over-all length of the cylinder was 3.75 in. less than that for the spring-loaded piston design and 11.2 lb lighter.

As shown in Figure III-6, use of the bootstrap pressurized replenishment unit requires the addition of only two pressurizing lines for a three-phase, three-fluid, pulsating system. The constant pressure of System "A" is utilized to pressurize the replenishment unit for System "B". The rectified pressure of System "C" pressurizes its own replenishment unit, in a real "bootstrap" sense.

The design studies of the two types of replenishment units point out the big weight advantage of the bootstrap version over the spring-loaded version. Another advantage of the bootstrap version is that it will maintain constant pressure on the fluid regardless of the amount of fluid lost through leakage.

In the spring-loaded version, the pressure of the fluid decreases as the volume decreases due to leakage. When nearly all of the fluid is lost through leakage (short of piston bottoming), the fluid pressure decreases to 16 psi. The total load exerted by both springs at this point would be 204 lb. This minimum spring load is also depended upon to overcome the piston seal friction.

The only disadvantage of the bootstrap replenishment unit is the requirement of additional lines, fittings, and piston seals which tend to lessen the over-all reliability of the unit.

The fluid replenishment unit incorporates two check valves to control fluid level. One of the check valves is a ball type that operates automatically to replenish fluid during the return pulse of the cycle. The second check valve utilizes a conical poppet and relieves thermally expanded fluid. It is mechanically lifted off its seat by the transformer piston when the piston oscillates about a center other than its normal center of travel. Off-center travel is induced by unequal thermal expansion of the pulsed fluids.

2. Diaphragm-Type Transformer

In addition to the piston-type transformer, the design of a diaphragm-type transformer was also investigated. Of the two designs, the diaphragm transformer better accomplishes fluid separation because it eliminates the requirement for dynamic seals. However, inherent in the diaphragm transformer is the 1:1 transformation ratio that makes it incapable of transforming pulsating pressure and flow from one amplitude to another. The piston transformer, which must rely on dynamic seals to perform the function of fluid separation, is better suited to accomplish "step-up" or "step-down" of pressure from one level to another, which are the functions of a transformer.

In those systems, where pressure transformation is not a requirement but leak-proof separation of corrosive or otherwise hazardous fluids is an absolute requirement, the diaphragm transformer appears to offer the most promising solution. If pressure transformation is required a piston type transformer can be used, followed immediately by a diaphragm type unit, both within the same housing. The fluid separation point would then be in the diaphragm portion of the unit.

The design of the diaphragm (Figure III-7) is discussed in detail in the following paragraphs.

The diaphragm transformer, like the piston transformer previously discussed, was designed to be used in a hypothetical three-line pulsating system operating at a frequency of 8 cps and delivering a rectified flow of 10 gpm at 4,000 psi. The same design parameters were used for both transformers to permit a size and weight comparison of the two types. It was shown that in a three-line, 8-cps, 10-gpm system, the volume of fluid displaced during each pulse is 1.535 $in.^3$ This is the volume of fluid the diaphragm is required to displace when it is deflected from one extreme position to the other.

To simplify volume calculations, it was assumed that the shape of the deflected diaphragm is that of a sphere. Actually, the shape would vary slightly from that of a sphere or paraboloid.[1] Based on this assumption, some trial calculations were made using the formula for the volume of a spherical segment ($V = \pi h\ (c^2/8 = h^2/6)$ to find the chords (c) corresponding to given heights (h) of several spherical segments having the same volume. The chord and height of the spherical segment correspond to the diameter and deflection at the centerline of the diaphragm, respectively. Since the diaphragm deflects an equal amount on each side of the mean position, the volume solved for in the above formula is doubled to obtain the full diaphragm displacement. A diaphragm diameter of 6.00 in. and a deflection of 0.054 in. each side of neutral gave the required displacement of 1.535 $in.^3$ and resulted in a reasonably low value for the maximum diaphragm stress.

The diaphragm stresses and deflections are determined from formulas given in the following paragraphs. The formulas are applicable to thin, circular membranes, edges fixed, with uniform loads applied at right angles to the plane of the membrane.

The maximum deflection at the centerline is determined as follows:[2]

$$\max y = 0.662\ a\sqrt[3]{\frac{wa}{Et}}$$

where

a = radius to fixed edge of diaphragm, in.

w = unit applied load, psi

E = modulus of elasticity, psi

t = thickness of diaphragm, in.

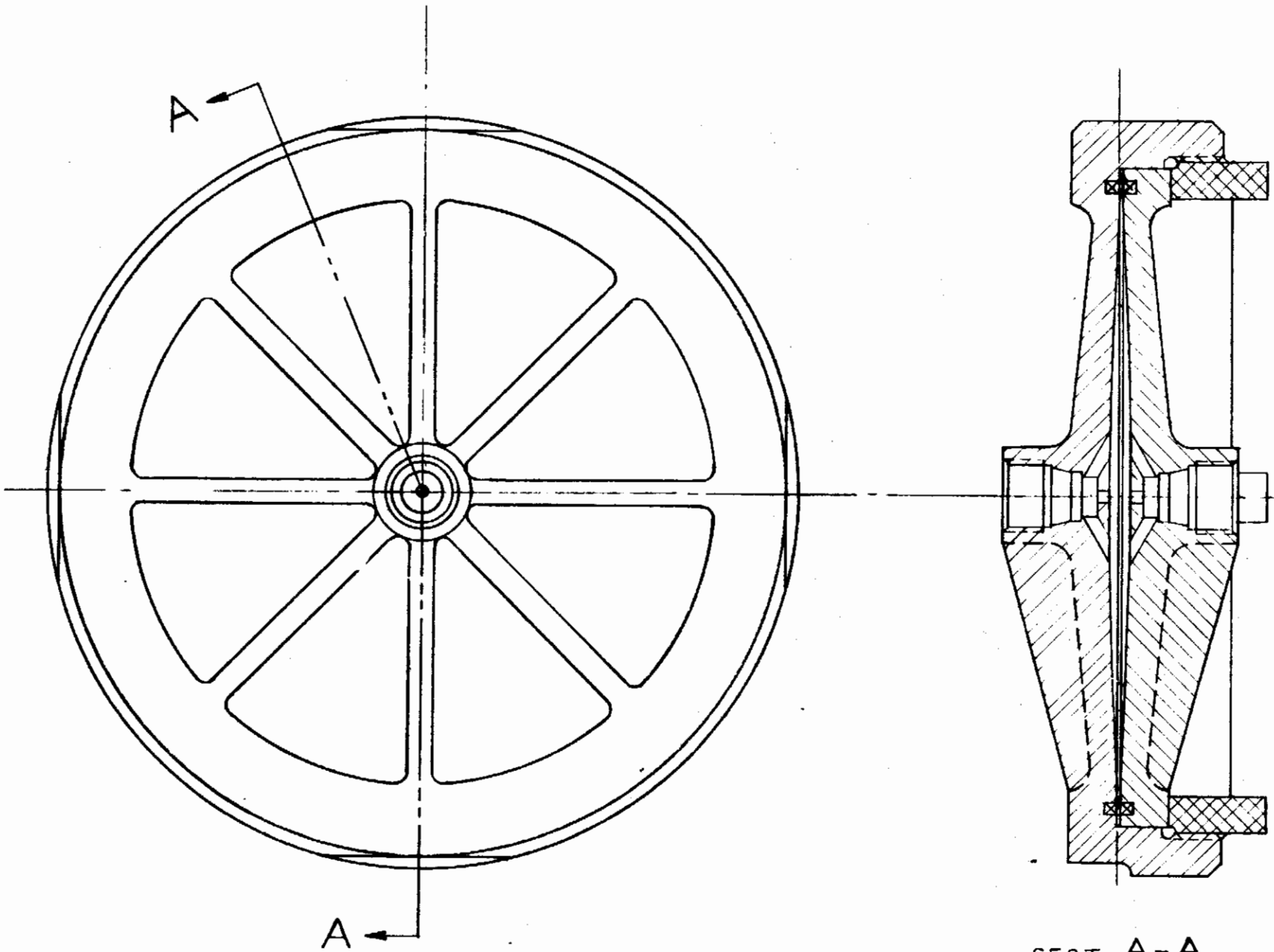

Figure III-7. Diaphragm Design

Since the diameter and maximum deflection of the diaphragm have already been established, the formula was rearranged and solved for w, using different values for t. A thickness of 0.010 in. was found to give the desired results.

$$w = \frac{y^3 Et}{(.662)^3 a^4} = \frac{(.054)^3 (29 \times 10^6) (.010)}{(.662)^3 (3)^4}$$

$$= \frac{(.000157) (29 \times 10^4)}{.290 \times 81} = 1.94 \text{ psi}$$

The diaphragm stresses are determined from the following formulas:[2]

Stresses at center $S_d = 0.423 \sqrt[3]{\frac{Ew^2 a^2}{t^2}}$

$$= 0.423 \sqrt[3]{\frac{29 \times 10^6 (1.9)^2 (3)^2}{(.010)^2}}$$

$$= 0.423 \times 10^3 \sqrt[3]{9450}$$

$$= 0.423 \times 10^3 \times 21.2$$

$$= 8,950 \text{ psi}$$

Stresses at edge $S_d = 0.328 \sqrt[3]{\frac{Ew^2 a^2}{t^2}}$

$$= 0.328 \times 21,200 = 6,950 \text{ psi}$$

The contour of the diaphragm cavity is usually made to correspond to the contour of the deflected diaphragm so that, on bottoming, the diaphragm is supported and kept within its stress limits. The contour of the cavity can be determined from the following formula which gives the deflection of the diaphragm at any distance (r) from center.[2]

$$y = \max y \left(1 - 0.9 \frac{r^2}{a^2} - 0.1 \frac{r^5}{a^5}\right)$$

Another method for developing the contour of the cavity is by the use of two radii.[3] The two radii (one at the centerline and the other at the edge) are selected so that the resulting contour permits the diaphragm to bottom initially at the centerline, where the stresses are highest. The diaphragm edges, which are forced to bottom last, develop higher stresses. The net result is a nearly uniform stress distribution over the entire surface of the diaphragm.

The total working space in the cavity is usually designed to be larger than the normal displacement of the diaphragm. This is to permit the diaphragm to oscillate through its full amplitude without being pressed against the cavity contour at either end of its stroke. Thus, the diaphragm in actual operation never bottoms and operates only within the maximum stress levels permitted. Even so, the "designed-in" overtravel is still calculated to provide a margin of safety. Moreover, it is necessary to permit some variation in system fluid volume prior to compensation.

The design shown in Figure III-7 provided for a maximum diaphragm deflection of 0.100 inch on either side of the unloaded position. The load and stress at full deflection are:

$$w = \frac{y^3 Et}{(.662)^3 a^4} = \frac{(.1)^3 \ 29 \times 10^6 \ \times \ .010}{(.662)^3 \ (3)^4}$$

$$= \frac{290}{.290 \times 81} = 12.35 \text{ psi}$$

$$S_d = 0.423 \sqrt[3]{\frac{Ew^2 a^2}{t^2}}$$

$$S_d = 0.423 \sqrt[3]{\frac{29 \times 10^6 \ (12.35)^2 \ (3)^2}{(.010)^2}}$$

$$= 0.423 \sqrt[3]{29 \times 10^{10} \times 152.5 \times 9}$$

$$= 0.423 \times 10^3 \sqrt[3]{398,000}$$

$$= 31,200 \text{ psi}$$

The diaphragm transformer was designed for operation at 500°F. The materials selected were 446 stainless steel for the diaphragm and titanium for the housing. The two static seals required could be either elastomeric or metallic. The total weight of the unit was calculated to be 8.75 lb.

As in the case of the piston transformer, some method of fluid level control was necessary for the diaphragm transformer. Figure III-8 shows a thermal expansion check valve that would be incorporated in the diaphragm housing.

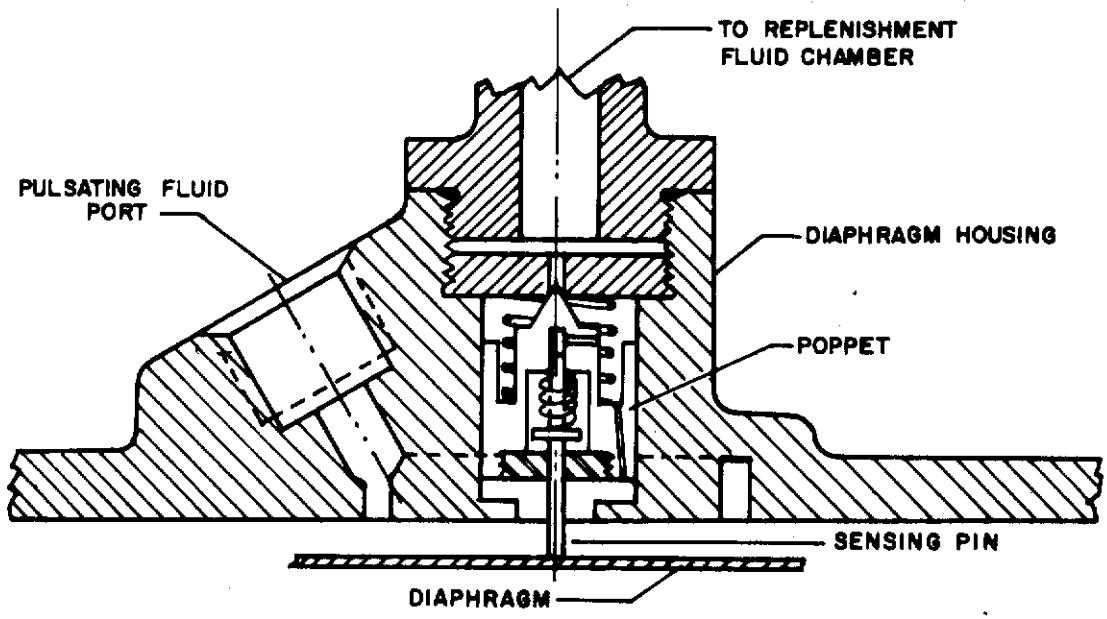

Figure III-8. Thermal Expansion Check Valve

During operation at normal pressure levels, the sensing pin in contact with the diaphragm will move freely within the poppet. Increasing pressure (due to thermal expansion) will deflect the diaphragm beyond its normal operating range and cause the sensing pin to bottom against the poppet. Further motion of the diaphragm will then cause the spring-loaded poppet to unseat, thereby releasing the excess fluid.

A check valve similar to that shown for the piston transformer (Figure III-5) will be used to supply make-up fluid to the system.

One disadvantage of a diaphragm transformer is that failure of the diaphragm could cause two incompatible fluids to mix, with serious results. An approach to this problem would be the use of a doubled diaphragm, as shown in Figure III-9. Here, failure of either diaphragm would be detected by external leakage that would come from the area between the diaphragms.

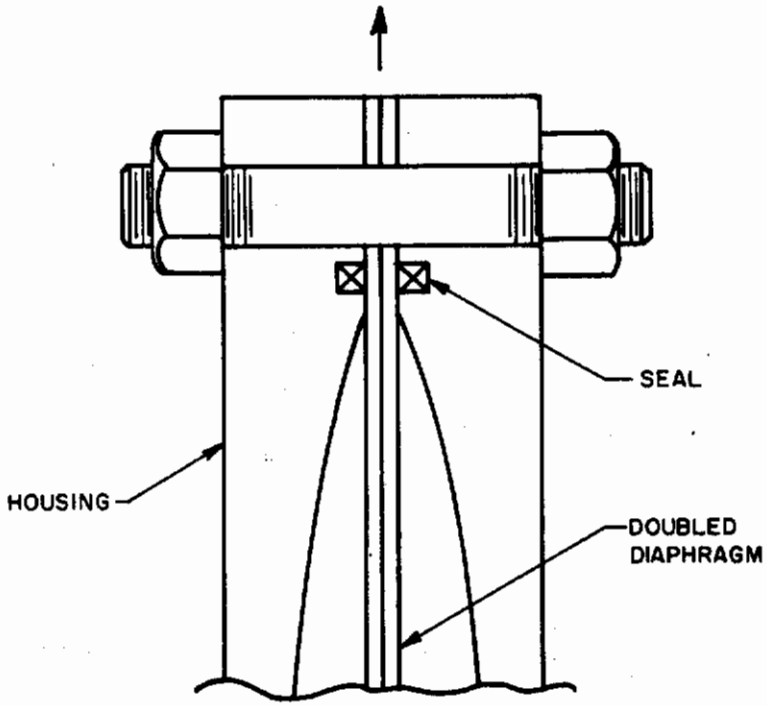

Figure III-9. Doubled Diaphragm

E. RECTIFIER VALVE

To rectify pulsating flow to continuous flow, a hydraulic check valve provides a very convenient tool; it is the mechanical equivalent of an electrical diode. Two check valves are used in each pulsating line: one with free flow leading from the pulsating line to the continuous flow pressure circuit; the other with free flow leading toward the pulsating line from the continuous flow return circuit. For a two-line pulsating transmission system (180° interline phase shift), two pairs of check valves will be required to produce full-wave rectified continuous flow. For a three-line pulsating transmission system (120° interline phase shift) three pairs of check valves will be required for rectification to continuous flow.

A design study made to determine the advisability of combining two or more check valves in a single housing showed that, for the rectification of a single pulsating line, there is little or nothing to be gained by the provision of a combined or dual unit. The number of plumbing connections necessary will be reduced from

four to three (pulsating line, continuous pressure, and continuous return). Even with a single line, there will be an elimination of the possibility of reversed assembly of the individual check valves when a dual unit is provided, however, such a unit must accept some slight penalty of installation convenience. For the rectification of a pulsating system consisting of two or more lines, there appears to be a definite advantage in providing for a combined unit. The space requirement for the rectifier is considerably reduced from that taken by individual check valves. The elimination of a possible reversed connection still applies. The system reliability will be enhanced because of the reduction in the number of plumbing connections (in a three-line system, 5 connections will be required for a combined unit as against 12 connections for individual units), and the system weight will thus be decreased.

The conventional check valve design currently being used in hydraulic components utilizes a conical or a ball type poppet seated against a sharp edge by a spring. Since in a pulsating circuit a rectifying check valve will unseat and seat for each cycle of pulsation, the resultant requirement of cyclic life will be in excess of that which can be expected with an edge-seating poppet. Therefore, a design study was made of a rectifier valve utilizing check valves with face-seating poppets. As shown in Figure III-10, this type of poppet is ground with a flat surface which seats against a similar surface. Such a seat has a much higher leakage than an edge-seating poppet, which can brinell a full seating ring; however, the unit bearing force is so drastically reduced that its endurance will be greatly increased and should result in a unit which will be satisfactory for the high cyclic life necessary for a pulsating system.

F. SYNCHRONOUS MOTOR AND MECHANICAL RECTIFIER

1. Synchronous Motor

Along with the ability to generate a three-phase pulsating hydraulic flow, it appeared desirable to investigate the hydraulic equivalent of an associated component - - the three-phase synchronous motor. Two configurations were studied, each incorporating three pistons driving a crankshaft through the usual connecting rods.

In one arrangement, an "in-line" configuration, the crankshaft will have three throws spaced 120° apart. In another arrangement, the three pistons are located radially 120° apart and the crankshaft will have one throw with all three piston rods attached to it.

Either of the above cylinder arrangements would result in a three-phase synchronous motor. The speed of the motor would be determined by the pulsation frequency employed. For example, a 60 cps pulsation-frequency would drive the motor at 3600 rpm.

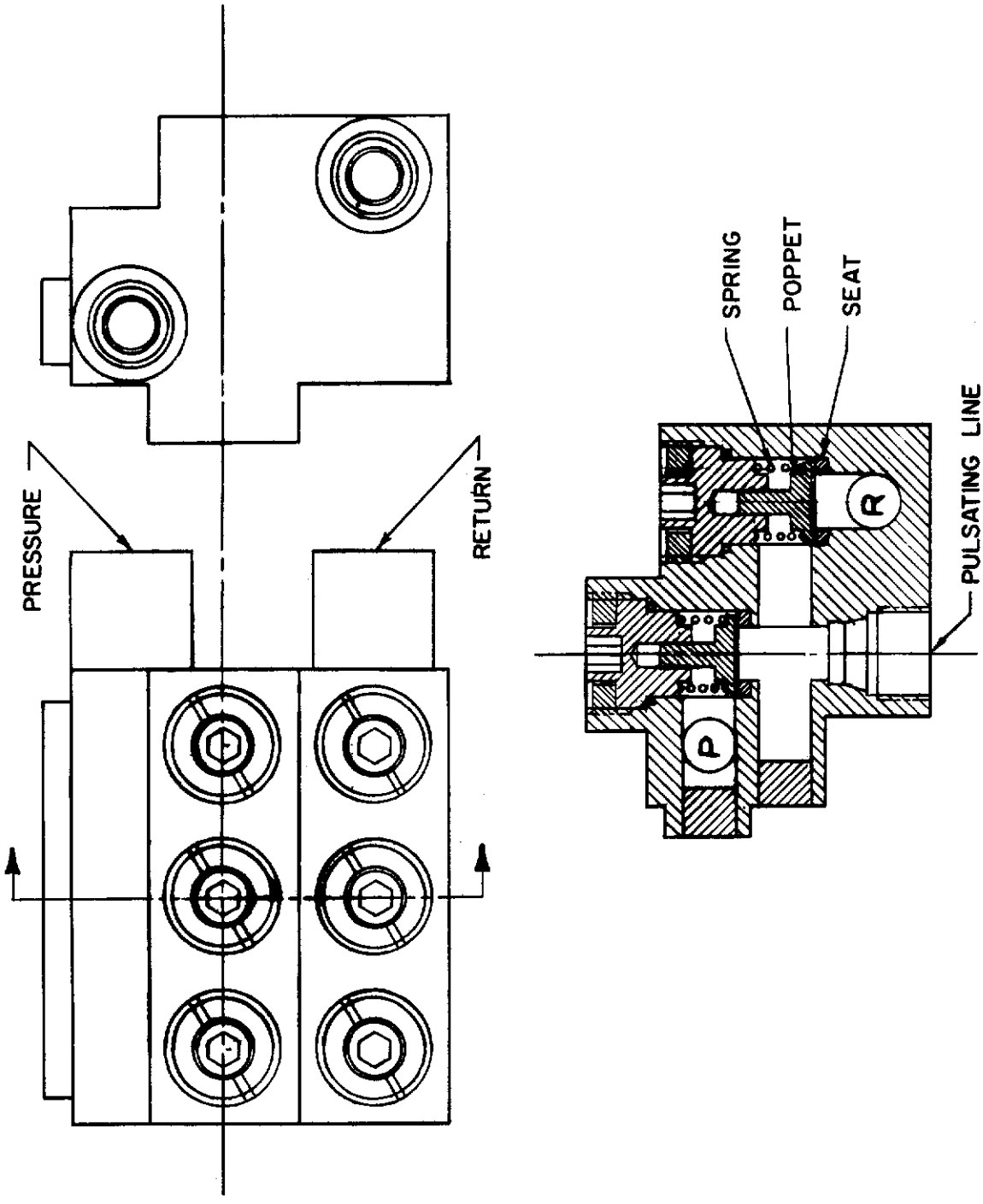

Figure III-10. Rectifier Valve

The direction of rotation of the above three-phase hydraulic motor can be reversed by switching the connections of any two of the three lines, just as is done in reversing the rotation of their electrical counterpart, the three-phase induction motor. The switching of the connections to the hydraulic motor can be accomplished by a four-way selector valve. A schematic drawing of the synchronous motor and reversing valve is shown in Figure III-11.

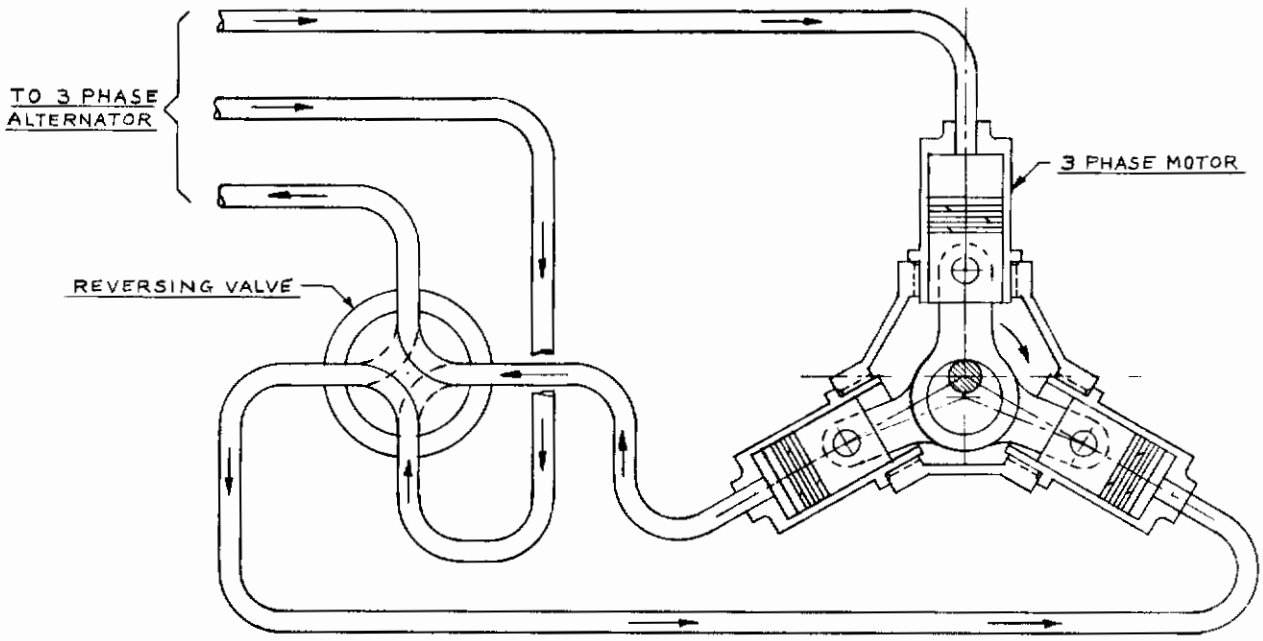

Figure III-11. Three-Phase Hydraulic Motor and Reversing Valve

With the exception of the synchronous pulsating hydraulic motor, all studies of the rectification of pulsating hydraulic energy to continuous energy have been of hydraulic rather than mechanical means. The basic hydraulic rectifier comprises two check valves. One valve, with free flow away from the pulsating line, passes the positive flow portion of the pulse into the continuous flow pressure line; the other, with free flow toward the pulsating line, receives the negative flow portion of the pulse from the continuous flow return line.

In the synchronous pulsating hydraulic motor, the rectification to continuous energy or motion (rotary in this case) is mechanical. The positive flow portion of the pulse in each cylinder provides the basic delivered energy to the eccentric or crank to which each piston is connected. The energy to return the piston during the negative portion of the pulse is provided by the cylinder or cylinders which, due to the line difference, are in the positve portion of the pulse. The flywheel effect produced by the inertia of the rotating mechanism acts as a ripple filter. Since the velocity or rpm is constant (being a function of the pulsating frequency), the motor power will vary with the torque. The motor power is a function of the cylinder thrust. The flow demand of the unit is also a constant since it is a function of pulsation frequency. Therefore, a constant delivery pressure demand type of system is most desirable to provide motor power. A variable delivery type of system which is constant pressure flow demand will be penalized, since the pressure difference between that needed to produce the load torque and the system pressure will represent wasted energy. However, where the motor subsystem is one subsystem of a multisubsystem complex and the motor is operated intermittently, the penalties that must be assumed are of a minor nature.

In starting a synchronous motor, analysis will show that the worst possible starting condition is where the first piston to receive a pulse is fully extended and thus on dead center. Under this condition it is possible for the motor to start in the reverse direction. However, if a "no back" or over-running clutch is used between the motor drive shaft and housing, the start will be delayed until the proper phase relationship is established, at which time the motor will run in the desired direction.

2. Mechanical Rectifier

For linear mechanical rectification, the arrangement shown in Figure III-12 can be used. The figure is semi-schematic and omits bearings, supports, etc. The basic mechanism functions shown can be duplicated for each pulsating line. The pulsating hydraulic input is fed to a cylinder. The positive flow portion of the pulse moves the piston in the extend direction. A spring or accumulator connected to the other end of the cylinder returns the piston to its original position at the end of the positive flow pulse and thus provides the energy for the negative flow portion of the pulsation cycle.

Attached to the piston rod of the cylinder is a double pawl. One half of the pawl is operative for each output direction desired. For output direction reversal, the pawl must be manually rotated so as to engage the opposite ratchet. During the extend motion of the piston rod, the pawl, when set as shown, will engage the ratchet to the left and move it clockwise. During the retract motion of the rod, the pawl will escape from the ratchet. Shafted to the ratchet is a spur gear, which in turn drives a rack. As the ratchet and spur gear move clockwise, the rack will be moved to the left. For the opposite direction of rack motion, the pawl is moved so that its right end will engage the ratchet to the right. Since this ratchet will move counterclockwise, the rack will be moved to the right.

With a single-line system, motion occurs during the positive flow portion of the pulse. Thus, there will be output motion for approximately half the time. During the periods of no motion there will be no force to hold against a load, so it will be necessary for the output mechanism to be irreversible. With a two-line system, the motion will be fairly continuous but may be somewhat rough. To prevent reversal of the output during the period of load shift from one line to the other, an irreversible output is desirable. When a three-line pulsating system is used, the output motion will be fairly smooth and an irreversible output will not be necessary. One or more lines will be in the positive flow pulse phase at all times.

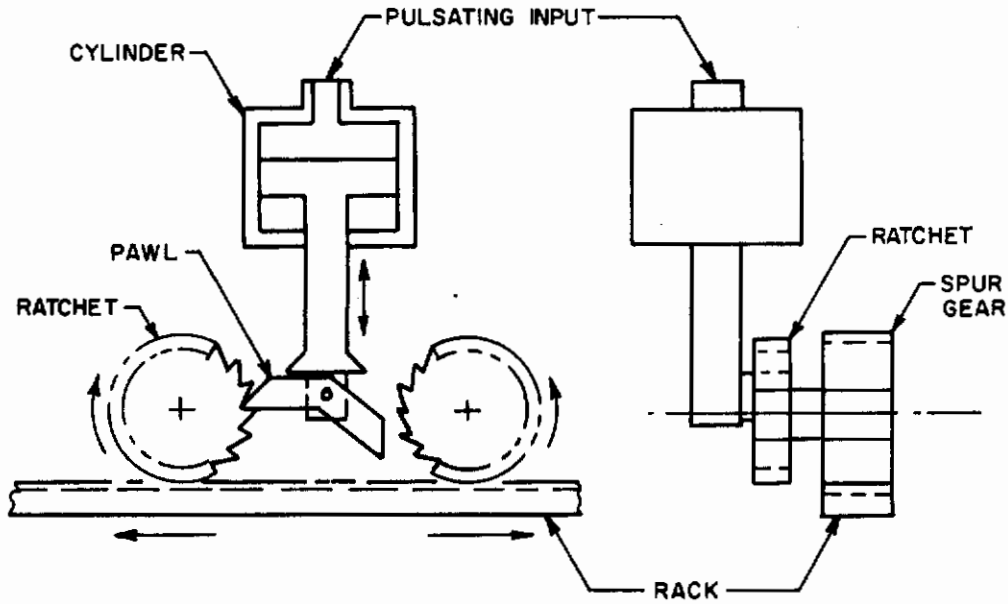

Figure III-12. Possible Arrangement for Linear Mechanical Rectification

In general, where a linear output is required, mechanical rectification will be heavier than hydraulic rectification. Means for directional control will also be heavier and rather awkward; servo control will be difficult in addition to having poor incremental resolution. The efficiency of mechanical rectification is not expected to be any higher than hydraulic. Reliability may be slightly higher than that of hydraulic rectification. It is possible that for some specific application the use of linear mechanical rectification may be preferable to hydraulic, but as a general case the hydraulic means will be found to be more advantageous.

SECTION IV - ANALYTICAL STUDIES

A. GENERAL

1. Method of Approach

In the analysis of systems which are governed by the same equations, the mathematical procedures used in obtaining the solutions are independent of the nature of the systems. In other words, a particular mathematical means of obtaining an electrical system response can also be used to yield a mechanical system response if both systems are governed by the same equations and the excitation functions are the same. An electric equivalent of the mechanical system is, therefore, believed to have the following advantages:

(1) It reduces the mechanical system to a circuit diagram by using the conventional symbols for circuit elements and circuit diagrams which have been developed by electrical engineers.

(2) It allows the use of electric circuit techniques of analysis for obtaining system responses.

(3) It provides an easy means of setting up analog computing diagrams should situations arise which require analog computation.

A four-terminal block diagram is also a powerful means of analyzing engineering problems. It not only clearly describes the governing equations of a component, but also provides a convenient means of interchanging the input and output of both ends of a component in order to match the input and output of upstream and downstream components.

Both the electric equivalent and the four-terminal block diagram method are used in this work study. The electric equivalent is used to study the dynamic response of the over-all system, while the four-terminal block diagram is used to study the viscosity effect of the hydraulic pulsating flow line.

The method of electric equivalent and the comparison between its two different analogies are briefly discussed here.

a. Force-Pressure-Voltage (f-P-V) Analogy

In this analogy, the force, f, or pressure, P, of a mechanical system is set to be analogous to the voltage, V, of an electrical system. The velocity U, and flow rate Q, are set to be analogous to the current, I. These and other relationships between mechanical and electrical parameters are listed in the following chart:

	Mechanical System		Electrical System
	Solid Mechanical System	Hydraulic Mechanical System	
Independent Variables	Force, f	Pressure, P	Voltage, V
	Velocity, U	Flow rate, Q	Current, I
	Linear Displacement, X	Volumetric Displacement, $\int Q dt$	Charge, $q = \int I\, dt$
Passive Elements	Mass, M	Inertance, m	Inductance, L
	Damping Coefficient, b	Resistance, R_h	Resistance, R
	Compliance, K_m	Compliance, K_h	Capacitance, C

b. Force-Pressure-Current (f-P-I)

In this analogy, the force, f, or pressure, P, of a mechanical system is set to be analogous to the current, I, of an electrical system; the velocity, U, and the flow rate, Q, are set to be analogous to the voltage, V. These and other relationships between important mechanical and electrical parameters are listed below.

c. Comparison of Both Types of Analogy

The force-pressure-current analogy seems to be more satisfactory than the force-pressure-voltage analogy from a physical point of view. For instance, a junction in a mechanical system under the force-voltage analogy consideration is equivalent to a loop in an electrical system, while under the force-current analogy consideration it is equivalent to a node. The latter is naturally more realistic in a physical sense. However, the velocity, flow rate, and voltage, analogous to each other in the force-current analogy, can be measured by a vibration pickup, flow meter, and voltmeter, respectively, without disturbing the system or circuit; however, the force and current cannot

be measured without breaking into the system. In addition, difficulty is encountered in establishing the electric equivalent of the hydraulic rectifier by the pressure-current analogy, as can be seen in Figure IV-37.

	Mechanical System		Electrical System
	Solid Mechanical System	Hydraulic Mechanical System	
Independent Variables	Force, f	Pressure, P	Current, I
	Velocity, U	Flow rate, Q	Voltage, V
	Linear Displacement, X	Volumetric Displacement, $\int Q dt$	Flux Linkage, $\int V dt$
Passive Elements	Mass, M	Inertance, m	Capacitance, C
	Damping Coefficient, b	Resistance, R_h	Conductance, G
	Compliance, K_m	Compliance, K_h	Inductance, L

Both types of analogy are used to establish the electric equivalent for the pulsating hydraulic system, so that comparison can be made between both analogies.

2. Types of Pulsating Hydraulic Systems and Their Comparison

Two basic types of pulsating hydraulic systems are possible: 1) standing pressure wave or pulsating pressure systems and 2) pulsating flow systems. From here on, the pulsating flow hydraulic system will be abbreviated as P-F hydraulic system.

In the standing pressure wave systems, the fluid fills a closed hydraulic line and a pressure wave generator is used to generate pressure waves that travel back and forth along the line. When the reflected pressure wave is of the same magnitude and in phase with the incident pressure wave, a standing pressure wave is formed along the line. The following expression and Figure IV-1 show the analytical and graphical expressions of the standing pressure wave.

$$P = 2P_o \sin \omega t \cos \gamma X$$

where: $\gamma = j\omega \frac{\rho}{\beta_e}$ (for nonviscous fluid)

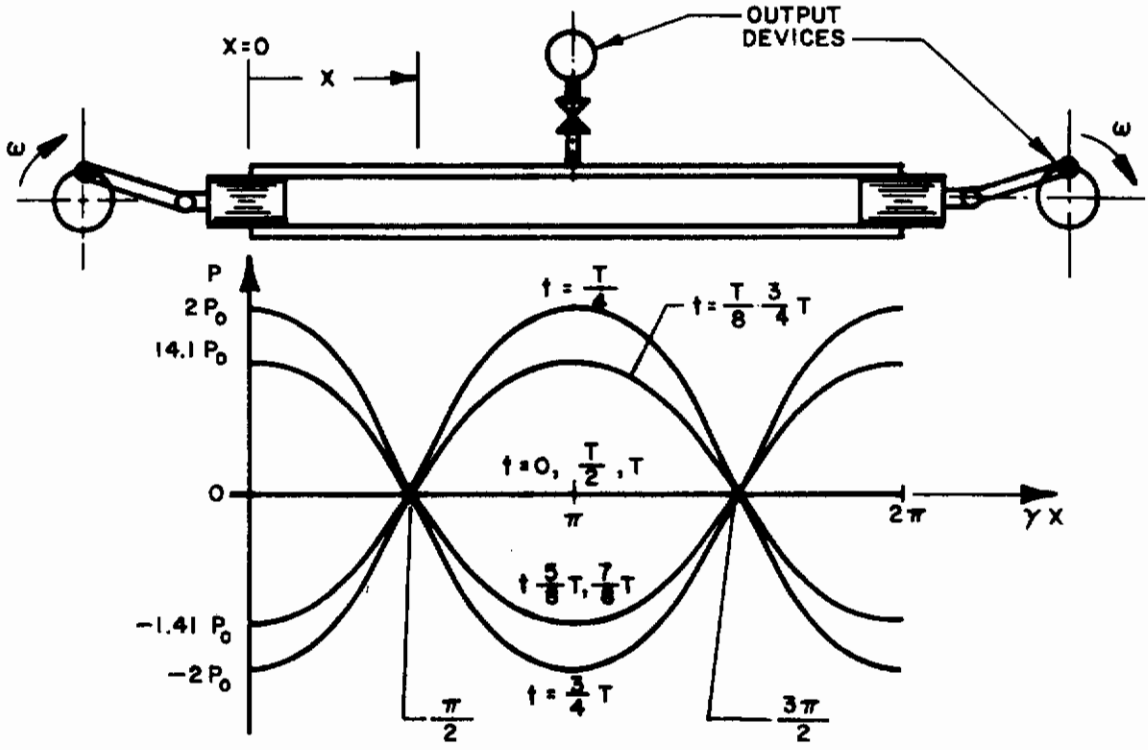

Figure IV-1. Standing Pressure Wave in a P-F Fluid Line of Length, $x = 2\pi/\gamma$

The energy associated with the standing pressure wave can be extracted by devices located at $X = \frac{\pi}{\gamma}$ and $X = \frac{2\pi}{\gamma}$. However, wave systems are believed to be more suitable for control signal transmission than for large power transfer. In power transfer, changes of input impedance of the output devices or of fluid properties resulting from a large amount of power variation will not only change the amplitude and wave length of the standing pressure wave continuously but may destroy it completely. Because the main concern of the study was power transfer, wave systems are not discussed further in this report.

In P-F hydraulic systems, the hydraulic moment and energy are transferred from one end of the transmission line to the other by back-and-forth vibratory motion of the entire mass of the fluid in the line about a mean position. The amount of energy that can be transferred by this type of system seems to be limited by the necessity of moving the entire mass of the fluid, but this limitation is not true. By proper design, P-F hydraulic systems can be used for transmission of large amounts of power. Figure IV-2 is the simplified block diagram of a P-F hydraulic positional control system. Figure IV-3 is the schematic of a three-phase pulsating hydraulic system. The work described in this report was done with this type of system.

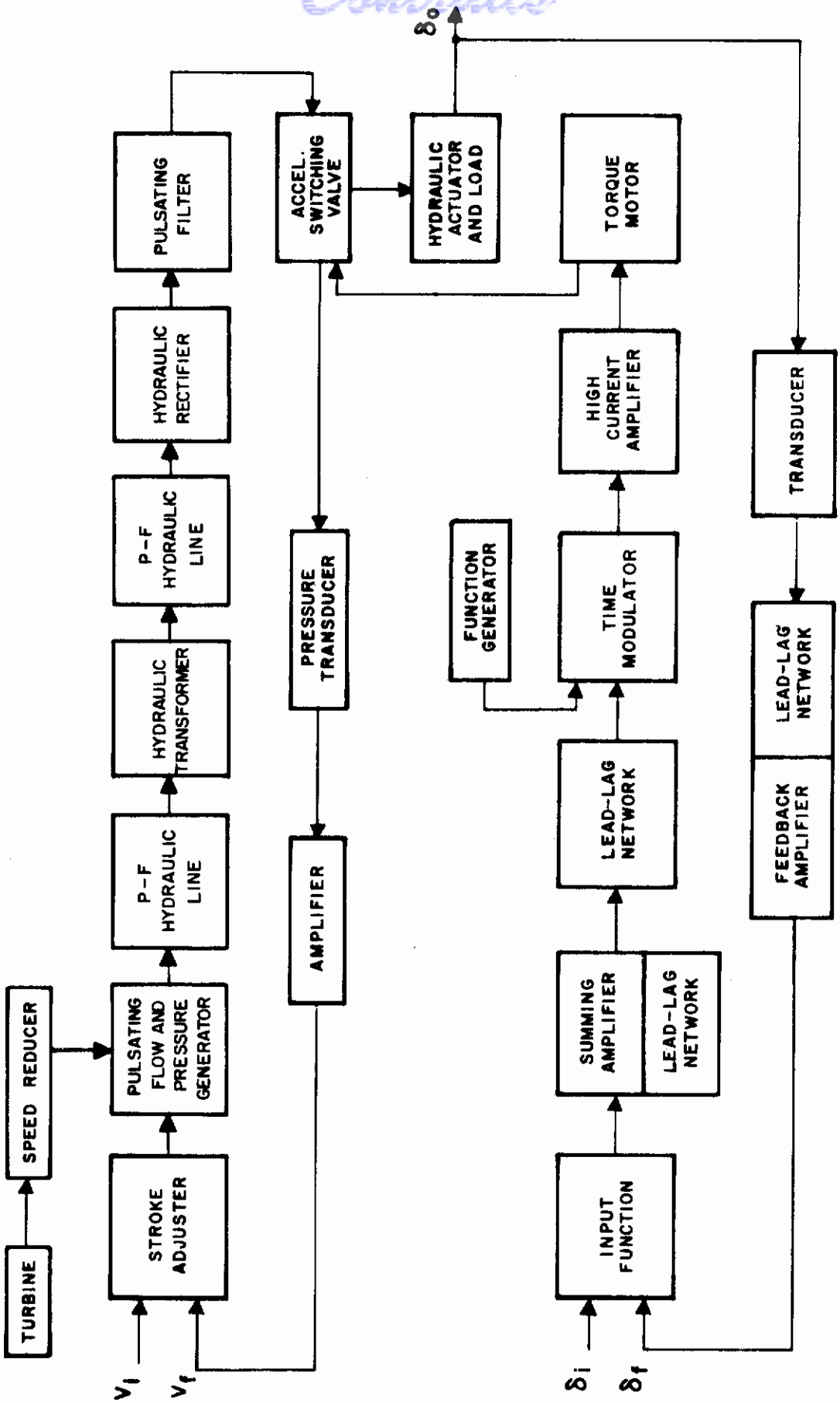

Figure IV-2. Simplified Block Diagram of Pulsating Hydraulic Positional Control System

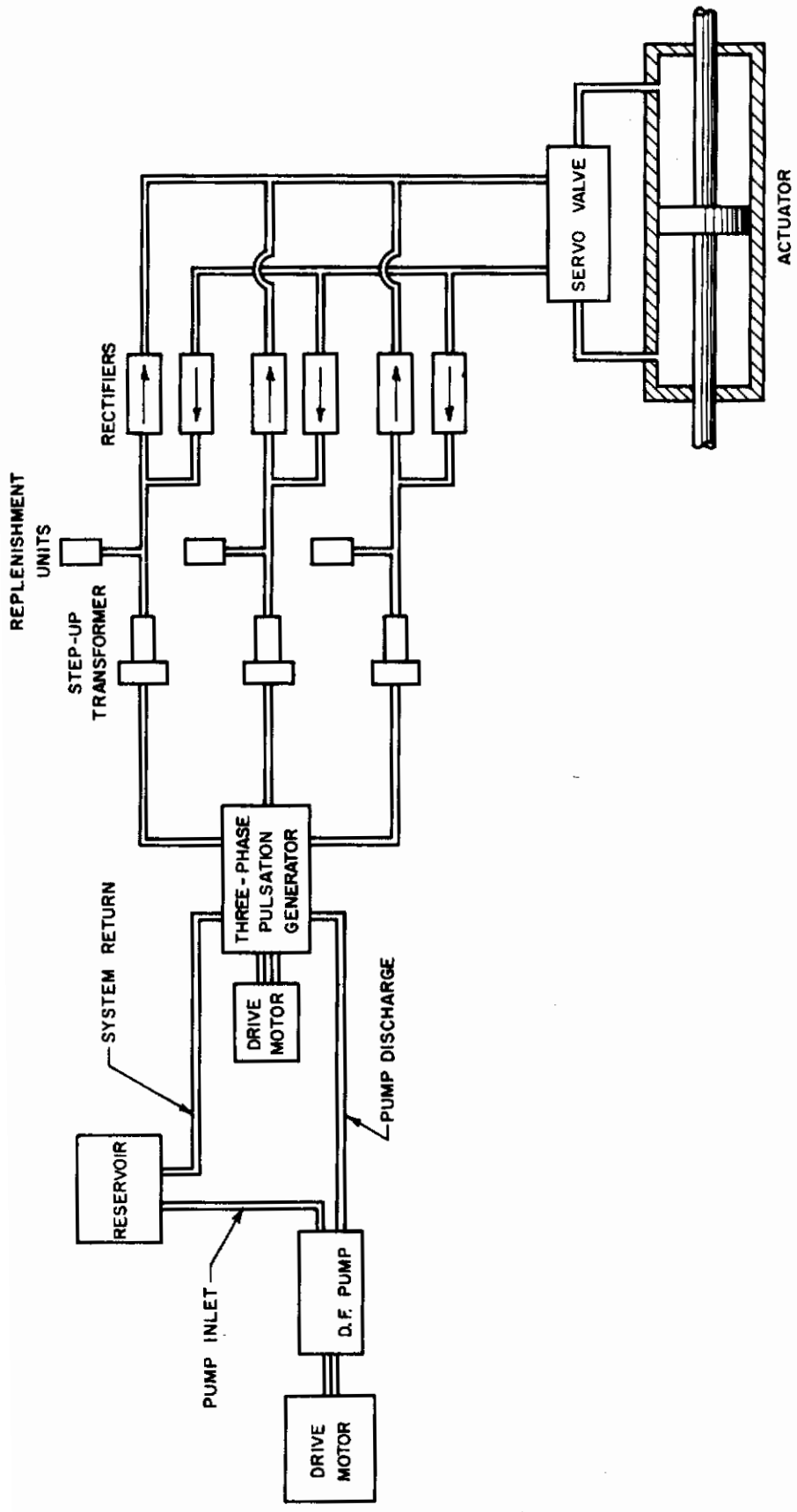

Figure IV-3. Three-Phase, Two-Fluid Pulsating Hydraulic System

B. SYSTEM COMPONENTS AND THEIR ELECTRIC EQUIVALENTS

1. Hydraulic Actuator and its Associated Loads

Figure IV-4 is the schematic diagram of a servo-valve and a hydraulic actuator with its associated loads.

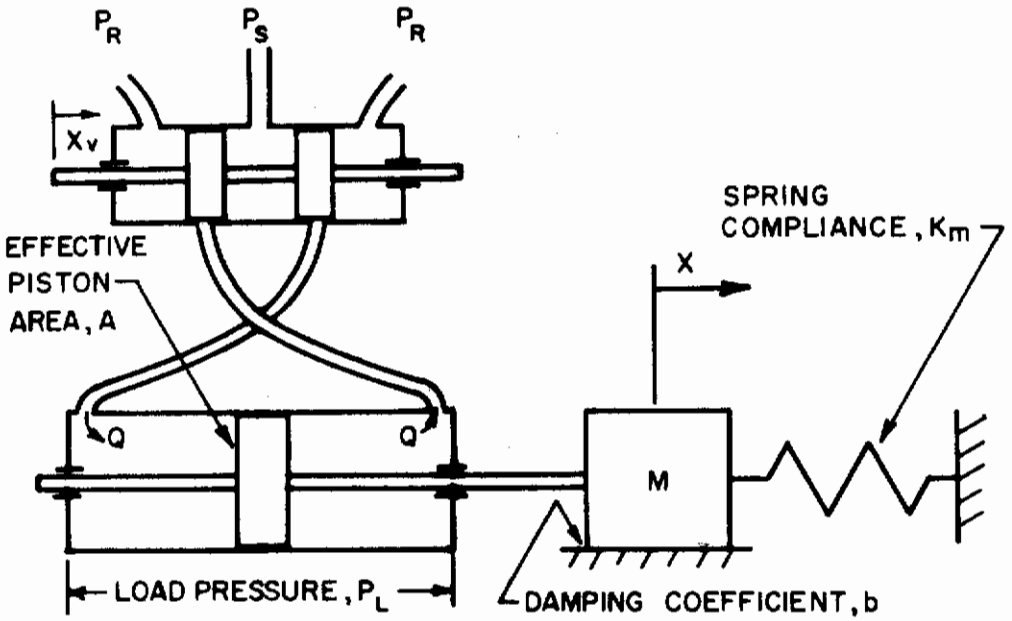

Figure IV-4. Schematic Diagram of Servo-Valve and Hydraulic Actuator with Its Associated Loads

The force equilibrium equation of the hydraulic actuator and its associated loads can be expressed as

$$P_\ell A = \left(MS^2 + bS + \frac{1}{K_m} \right) X. \tag{1}$$

Equation (1) can also be rewritten as

$$P = \left(\frac{MS}{A^2} + \frac{b}{A^2} + \frac{1}{A^2 K_m S} \right) ASX \tag{2}$$

Figure IV-5 is the electric equivalent of the mechanical output of the hydraulic actuator and its associated loads when the pressure-current analogy is used. This is a parallel RCL circuit connected to a current source.

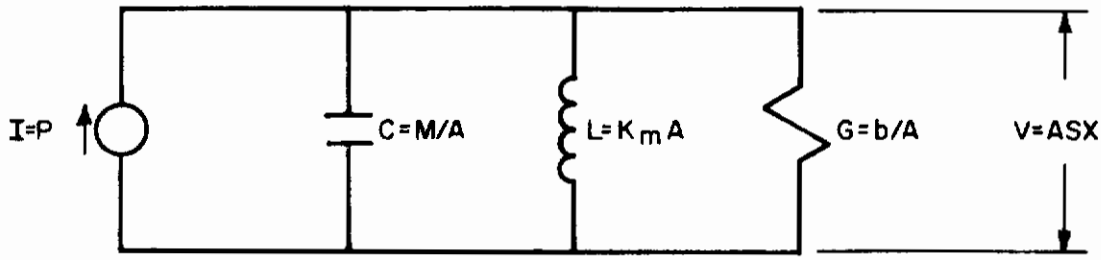

Figure IV-5. Electric Equivalent of the Mechanical Output of the Hydraulic Actuator and Its Associated Loads (Parallel RCL Circuit)

The current equilibrium equation of the circuit is

$$I = \left(CS + G + \frac{1}{LS}\right) V, \tag{3}$$

The similarity between Equations (2) and (3) shows that the mechanical output of the hydraulic actuator and its associated loads can be described by a parallel RCL circuit (with current as its independent variable) if I, C, L, and G are replaced by P, $\frac{M}{A^2}$, A^2K_m, and $\frac{b}{A}$, respectively.

Figure IV-6 is the electric equivalent of the mechanical output of the hydraulic actuator and its associated loads when the pressure-voltage analogy is used. This is a series RCL circuit connected to a voltage source.

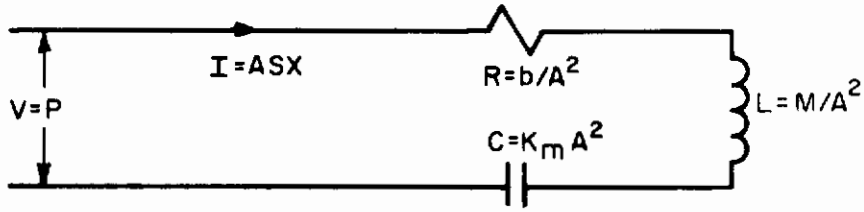

Figure IV-6. Electric Equivalent of the Mechanical Output of the Hydraulic Actuator and Its Associated Loads (Series RCL Circuit)

The voltage equilibrium equation of the circuit is

$$V = \left(LS + R + \frac{1}{CS}\right) I \tag{4}$$

Again, the similarity between Equations (2) and (4) enables representation of the mechanical output of the hydraulic actuator and its associated loads by a simple series RCL circuit if the quantities $\frac{M}{A^2}$, $\frac{b}{A^2}$, and $K_m A^2$ are replaced by L, R, and C, respectively.

2. Hydraulic Servo-Valve

None of the spool displacement vs. flow rate, spool displacement vs. load pressure, and flow rate vs. load pressure characteristics of commercial valves is linear. This is due to the nonlinear characteristics existing between the servo-valve variables. However, linearization of the servo-valve characteristic equations is possible when certain specific restrictions are made. For a closed center four-way valve with constant pressure source, the valve performance can be represented by the following equation:[4, 5]

$$P_L = P_s - \frac{2Q^2}{g^2 X_v^2}, \tag{5}$$

where $g = C_d W \sqrt{\frac{2}{\rho}}$

W = Valve port width

X_v = Spool displacement

When the load is small and the spool is only allowed to oscillate about its neutral position with an amplitude much smaller than its total stroke, the effect of load pressure to the valve flow rate is very small and can be neglected. Equation (5) can, therefore, be approximated by

$$\frac{1}{2} P_s g^2 X_v^2 \simeq Q^2 \tag{6}$$

or

$$Q \simeq K_v X_v, \tag{7}$$

where $K_v = g \sqrt{\frac{P_s}{2}}$.

Equation (7) is the linear expression of a simple displacement-controlled flow source. It should be pointed out here that Equation (7) is not an incremental expression. All variables represent their true values.

Figure IV-7a and IV-7b are the electric equivalents of the hydraulic servo-valve when the pressure-current and pressure-voltage analogies, respectively, are used.

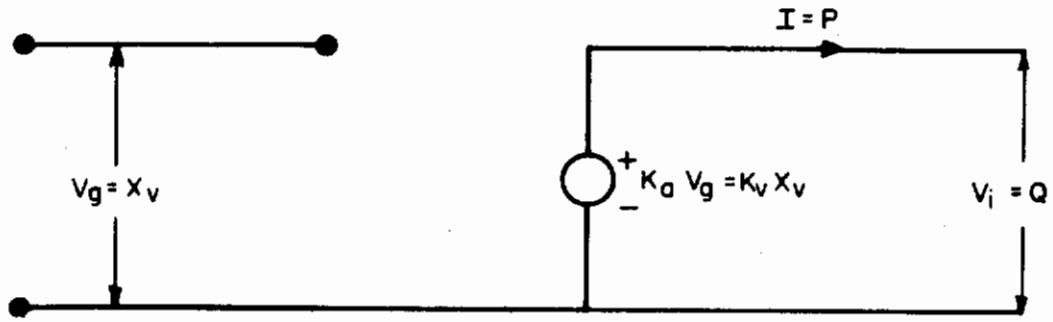

(a) P-C Analogy

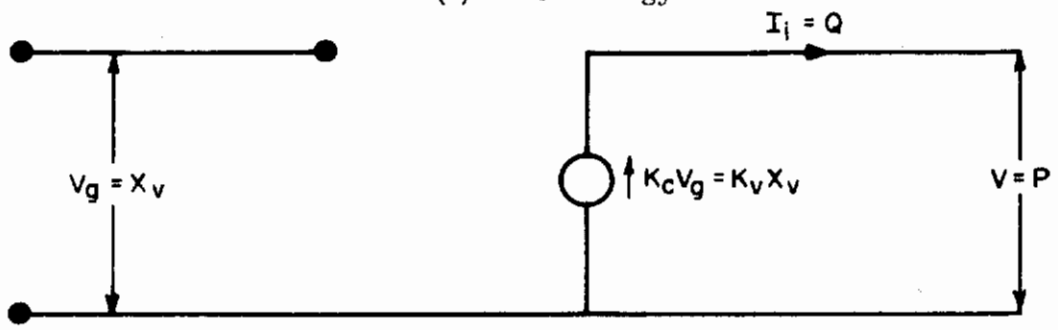

(b) P-V Analogy

Figure IV-7. Electric Equivalent of an Approximate Closed Center Four-Way Valve

Figure IV-7a is an ideal voltage amplifier (generating a voltage-controlled voltage source) which can be described by

$$V_i = K_a V_g, \tag{8}$$

where V_i = Output voltage

V_g = Control voltage

Figure IV-7b is an ideal current amplifier (generating a voltage-controlled current source) which can be represented by the following expression:

$$I_i = K_c V_g, \tag{9}$$

where K_c = Amplifier gain

I_i = Output current

Notice again the similarity among Equations (7), (8), and (9). A point should be mentioned here. The control voltage supplied to both the ideal voltage and current sources is independent of the amplifier output and has importance insofar as the performance of the hydraulic servo-valve is concerned. In a valve of good design, the valve spool displacement, X_v, which is equivalent to the control voltage source of the amplifier, will not be affected by the valve output.

3. Compressibility Effect of the Fluid Between the Servo-Valve and Hydraulic Actuator

Equation (10) can be used to describe the compressibility effect of the fluid between the servo-valve and the hydraulic actuator, if the following conditions exist:

(1) Leakage across the actuator is negligible.
(2) Fluid transmission line is rigid.
(3) Actuator piston is operated near its neutral position.

$$Q - ASX = \frac{\nu_o}{2\beta} SP \tag{10}$$

Parts (a) and (b) of Figure IV-8 are the electric equivalents of the fluid compressibility effect obtained from the pressure-current and pressure-voltage analogies, respectively. The characteristic equation of Part (a) is

$$V_i - V = LSI, \tag{11}$$

while the characteristic equation of Part (b) is

$$I_i - I = CSV. \tag{12}$$

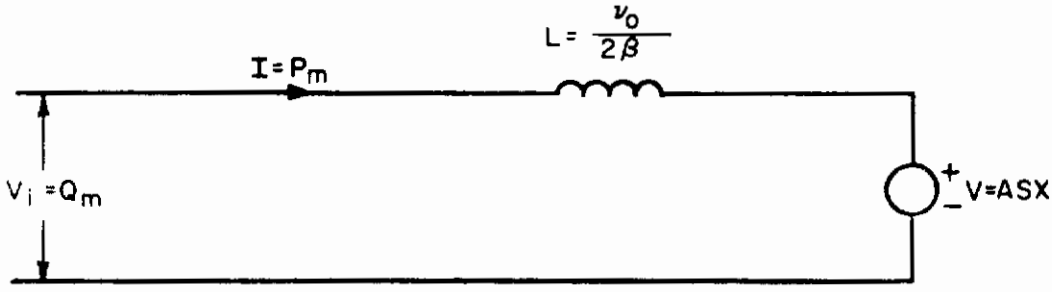

(a) P-C Analogy

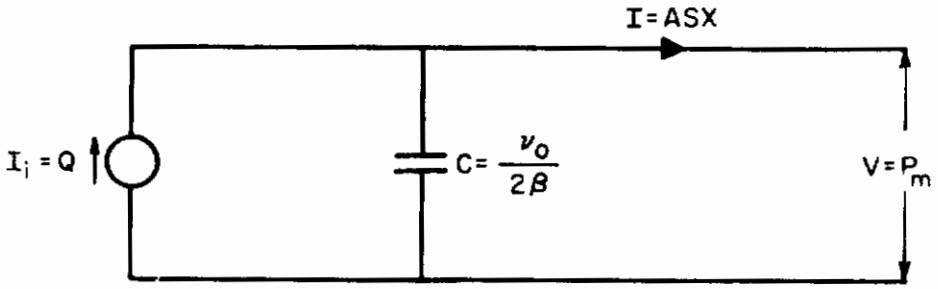

(b) P-V Analogy

Figure IV-8. Electric Equivalent of the Fluid Compressibility Effect

4. The Electric Equivalent of the Servo-Valve and Hydraulic Actuator with its Associated Loads

Figure IV-9 combines the results obtained in the previous discussion, and is the complete electric equivalent of the system shown in Figure IV-4. Part (a) of Figure IV-9 uses the pressure-current analogy, while Part (b) uses the pressure-voltage analogy. Characteristic equations of the components and their electric equivalents are also given.

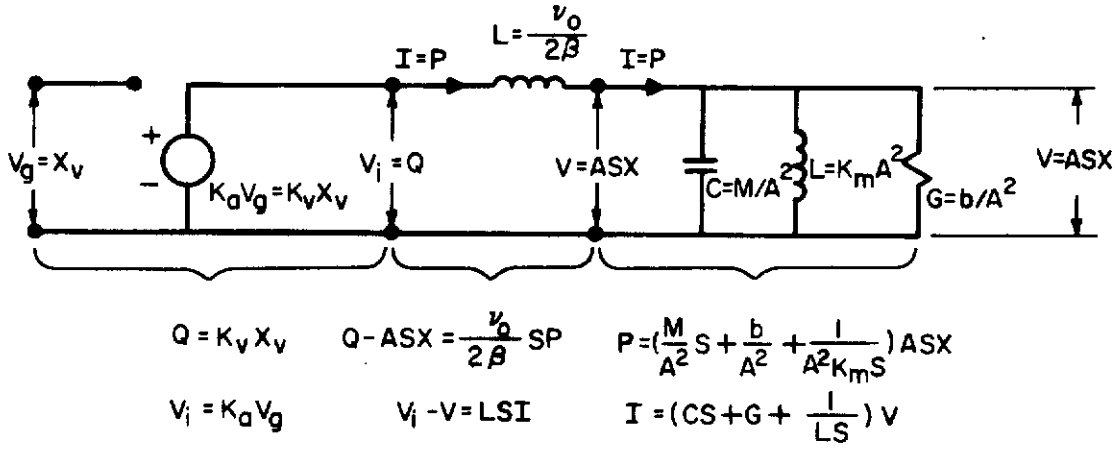

(a) P-C Analogy

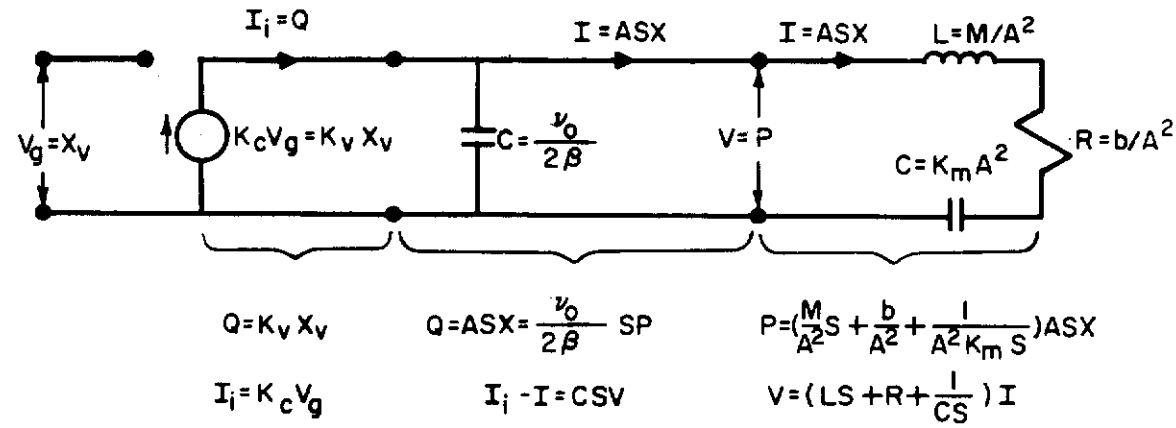

(b) P-V Analogy

Figure IV-9. Electric Equivalent of the Servo-Valve and Hydraulic Actuator with Its Associated Loads and Fluid Compressibility Effect Included

5. Ideal Hydraulic Transformer

Figure IV-10 is the schematic diagram of an ideal hydraulic transformer.

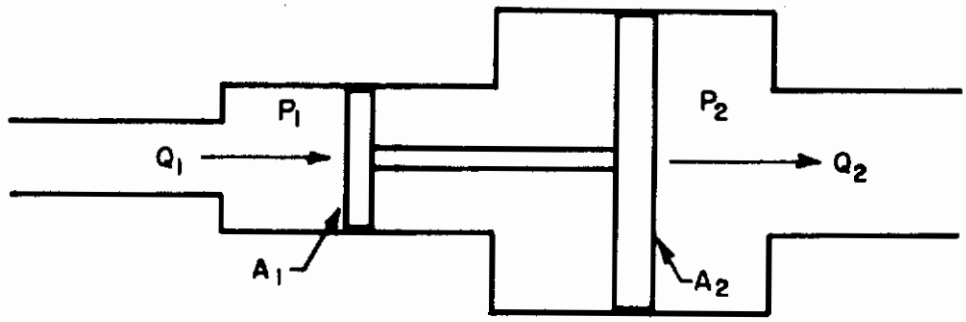

Figure IV-10. Ideal Hydraulic Transformer

The term "ideal" means that the power output equals the power input (i.e., no friction and leakage loss) and that compressibility and inertia effects are negligible. The function of an ideal transformer can best be described by the following equations:

Force Balance Equation

$$\frac{P_2}{P_1} = \frac{A_1}{A_2} \tag{13}$$

Continuity Equation

$$\frac{Q_2}{Q_1} = \frac{A_2}{A_1} \ , \tag{14}$$

where P, A, and Q are pressure, area, and flow rate, respectively.

Figure IV-11 is the schematic diagram of an ideal electric transformer, which is the electric equivalent of the ideal hydraulic transformer. The characteristic equations of the electric transformer are

$$\frac{V_2}{V_1} = \frac{N_2}{N_1} \tag{15}$$

and

$$\frac{I_2}{I_1} = \frac{N_1}{N_2}, \tag{16}$$

where V, I, and N are voltage, current, and coil turns, respectively.

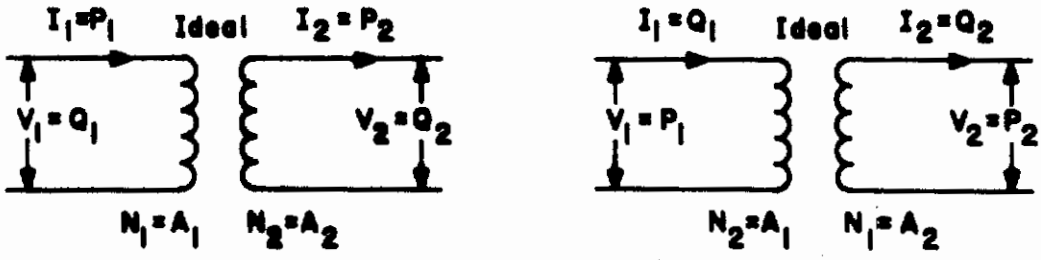

(a) P-C Analogy

(b) P-V Analogy

Figure IV-11. Electric Equivalent of an Ideal Hydraulic Transformer (Ideal Electric Transformer)

Notice again from Figure IV-11 that the pressure-current analogy is a more satisfactory representation than the pressure-voltage analogy from the physical point of view.

6. Non-Ideal Hydraulic Transformer

Figure IV-12 is the schematic diagram of a real hydraulic transformer. The characteristic equations of the transformer are

Momentum Equation

$$P_1 A_1 - P_2 A_2 = (MS^2 + bS + K) X \tag{17}$$

Continuity Equations

$$A_1 SX = Q_1 - \frac{\nu_1}{\beta} SP_1 \tag{18}$$

$$A_2 SX = Q_2 + \frac{\nu_2}{\beta} SP_2, \tag{19}$$

where $\frac{K}{2}$ is the spring constant of the bellows or diaphragm and the other parameters are defined as before.

Combining Equations (17), (18), and (19) and neglecting small order terms, we obtain

$$Q_1 = G_{11} P_1 + G_{12} P_2 \tag{20}$$

and

$$Q_2 = G_{21} P_1 + G_{22} P_2, \tag{21}$$

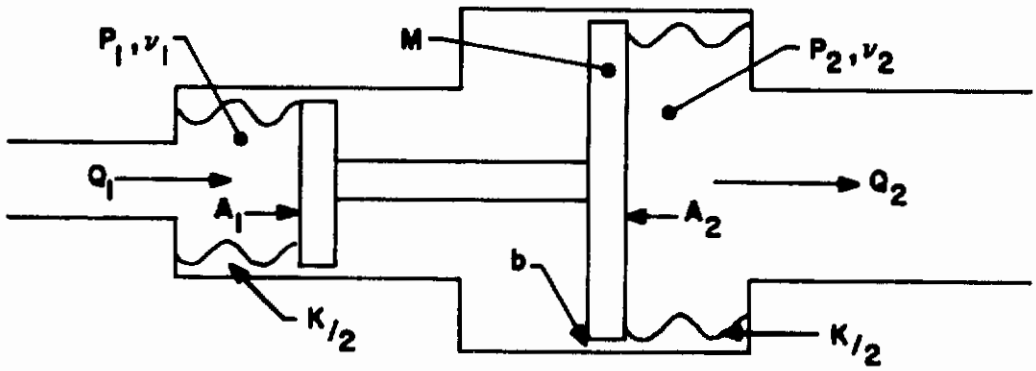

Figure IV-12. Hydraulic Transformer

where

$$G_{11} \simeq \frac{A_1^2 S}{MS^2 + bS + K}$$

$$G_{12} \simeq \frac{-A_1 A_2 S}{MS^2 + bS + K}$$

$$G_{21} \simeq \frac{A_1 A_2 S}{MS^2 + bS + K}$$

$$G_{22} \simeq \frac{-A_2^2 S}{MS^2 + bS + K} .$$

Equations (20) and (21) represent an interacting four-variable system, which can be represented by a four-terminal block diagram, as shown in Figure IV-13.

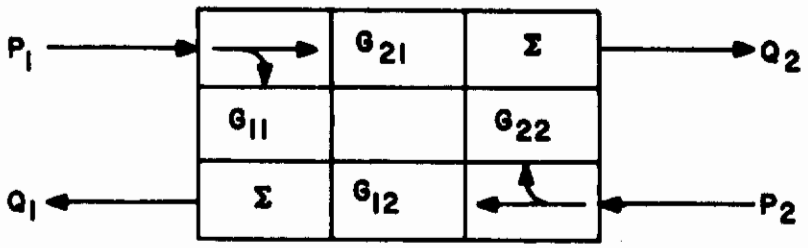

Figure IV-13. Four-Terminal Block Diagram

Equations (20) and (21) can also be transformed into the following useful forms:

$$P_2 = \frac{1}{G_{12}} \left(Q_1 - G_{11} P_1\right) \tag{22}$$

$$Q_2 = \frac{G_{22}}{G_{12}} \left[Q_1 - \left(G_{11} - G_{12}\right) P_1\right]. \tag{23}$$

The equations that govern the performance of a non-ideal electric transformer are 5, 6

$$I_1 - (CS + G + \frac{1}{LS}) V_{01} = I_{01} \tag{24}$$

$$V_{01} = V_1 - \left(L_1 S + R_1\right) I_1 \tag{25}$$

$$\frac{I_2}{I_{01}} = \frac{N_1}{N_2} = \frac{V_{01}}{V_{02}} \tag{26}$$

$$V_2 = V_{02} - \left(L_2 S + R_2\right) I_2 \tag{27}$$

The non-ideal hydraulic transformer characteristic equations (Equations 17, 18, and 19), are rewritten below in a slightly different form:

$$P_1 - \left(\frac{M}{A_1^2} S + \frac{b}{A_1^2} + \frac{K}{A_1^2 S} \right) A_1 SX = P_{01} \tag{28}$$

$$A_1 SX = Q_1 - \frac{\nu_1}{\beta} SP_1 \tag{29}$$

$$\frac{P_2}{P_{01}} = \frac{A_1}{A_2} \tag{30}$$

$$Q_2 = A_2 SX - \frac{\nu_2}{\beta} SP_2 \tag{31}$$

By comparing Equations 24 through 27 with Equations 28 through 30, the equivalent between a non-ideal hydraulic transformer and a non-ideal electric transformer can easily be established, as shown in Figure IV-14.

Several differences exist between the hydraulic and electric transformers. In the pressure-current analogy, the flow leakages through both sides of the hydraulic transformer are equivalent to the voltage drops across the primary and secondary effective resistances of the electric transformer, R_1 and R_2, respectively. The flow leakages through both sides of the transformer are zero when a bellows-type hydraulic transformer is used (see Figure IV-14a), but the voltage drop across the primary and secondary effective resistances of the electric transformer are usually not zero. It is also shown in Figure IV-14a that the hydraulic transformer has an extra pressure drop term, $\frac{M}{A_1^2} S^2 X$ which is equivalent to an additional exciting current term, $C S V_{01}$, that is needed by the primary core of the electric transformer for establishing the mutual flux. This current term, which is non-existent in network analysis, is added to Figure IV-14a by connecting a capacitor, C, in parallel to the reactance, L, and conductance, G.

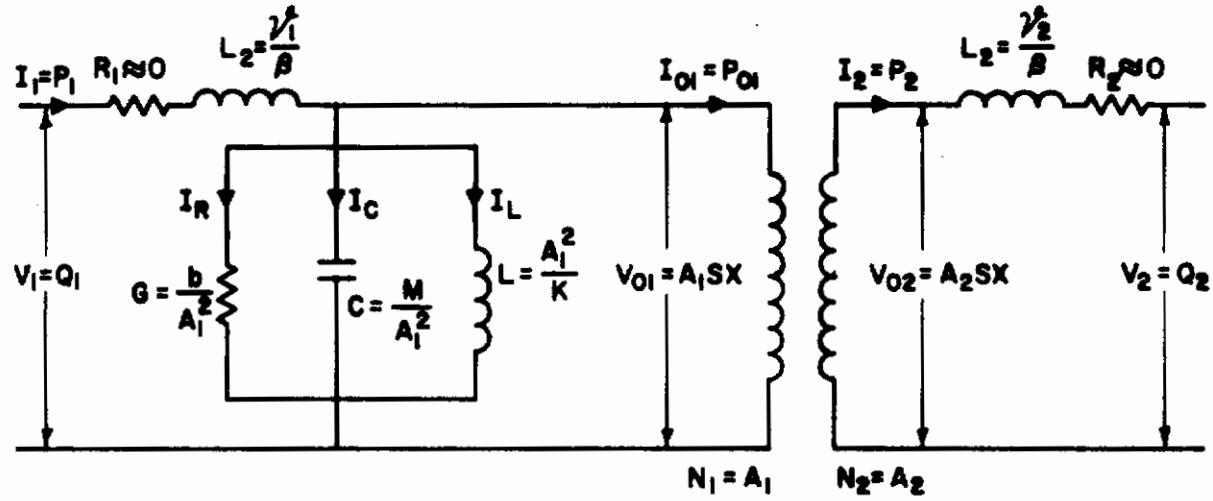

(a) P-C Analogy

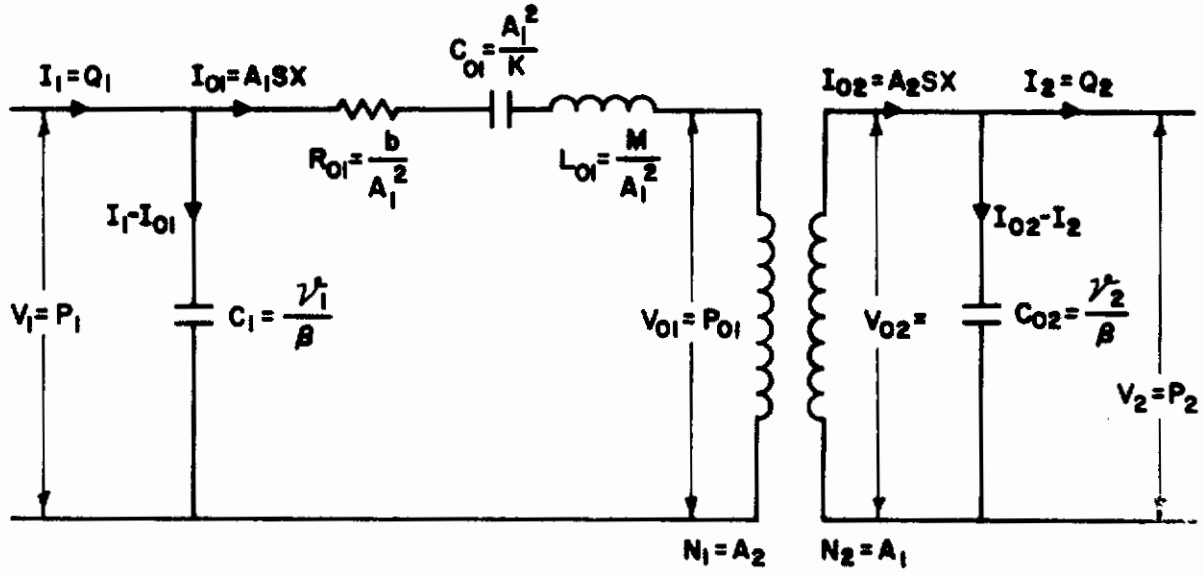

(b) P-V Analogy

Figure IV-14. Electric Equivalent of a Non-Ideal Hydraulic Transformer (Non-Ideal Electric Transformer)

It should be mentioned that for the P-C analogy the area ratio, $\frac{A_1}{A_2}$ is proportional to the turn ratio, $\frac{N_1}{N_2}$, while for the P-V analogy the area ratio, $\frac{A_1}{A_2}$, is inversely proportional to the turn ratio, $\frac{N_1}{N_2}$.

7. Hydraulic Rectifiers

The function of the hydraulic rectifier is to convert an alternative flow (pressure) into a direct flow (pressure). Two types of hydraulic rectifiers are discussed in this subsection. Both types use poppet valves as their rectification means. However, the poppet valve is not the only means that can be used for rectification.

For the purpose of convenience, some basic characteristics of a poppet valve are discussed prior to discussion of the rectifier. Figure IV-15 is a schematic diagram of a conical type poppet valve. Figure IV-16 illustrates the typical flow-pressure relation of a poppet valve.

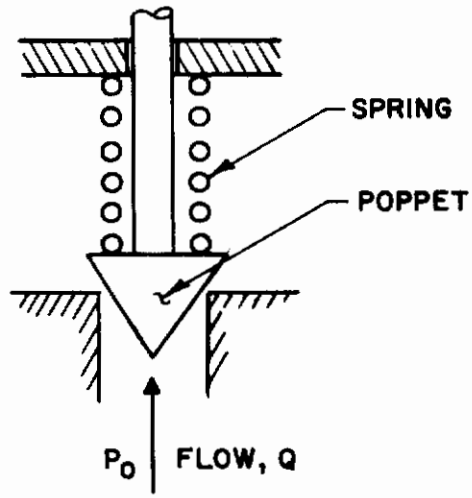

Figure IV-15. Conical Type Poppet Valve

For a poppet valve with adequate force compensation, the flow-pressure relation is a straight vertical line as shown in Figure Figure IV-16. Without force compensation, the pressure drop across the poppet valve (resulting from the change of flow momentum) increases as the flow rate increases. Therefore, the flow-pressure relation of a non-force compensated poppet valve is seen in Figure IV-16 to be a parabolic curve.

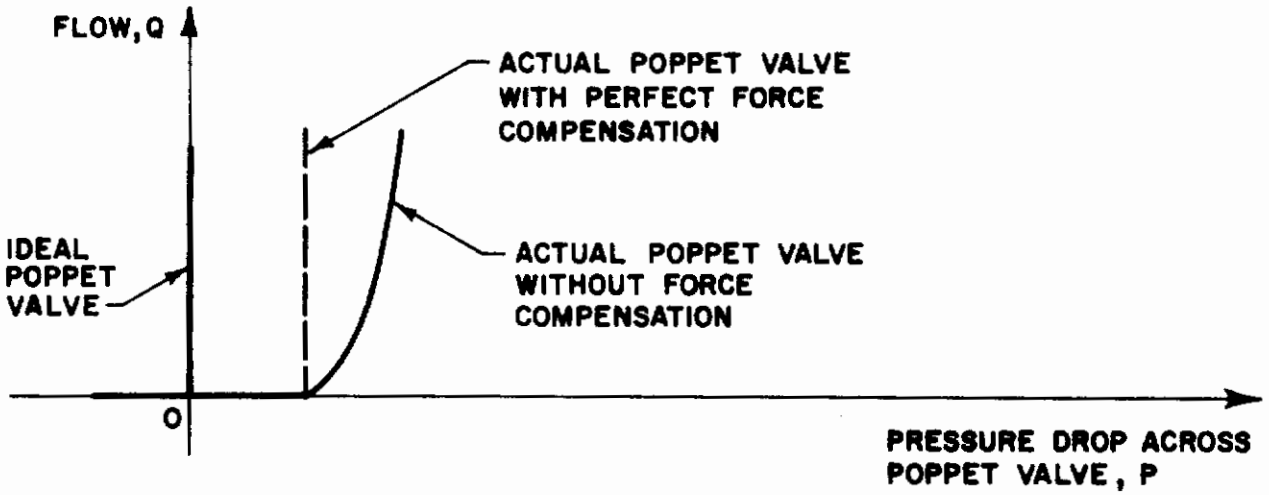

Figure IV-16. Typical Flow-Pressure Characteristics of Poppet Valves

Figure IV-17 is a schematic diagram of the hydraulic full-wave bridge rectifier. In this figure, the rectifier is made of four poppet valves connected to form a hydraulic bridge. During the first half-cycle, the path of the working fluid is line 1, poppet valve 1, load, poppet valve 4, line 2; during the second half-cycle, the path of the working fluid is line 2, poppet valve 3, load, poppet valve 2, line 1. For an ideal hydraulic full-wave bridge rectifier (rectifier made of ideal poppet valves) the flow output is shown in Figure IV-18, which is the graphical representation of the following expression.

$$Q_o = \left| Q_{io} \text{ Sin } \omega t \right|$$

where: Q_{io} is the maximum amplitude of the sinusoid flow input,

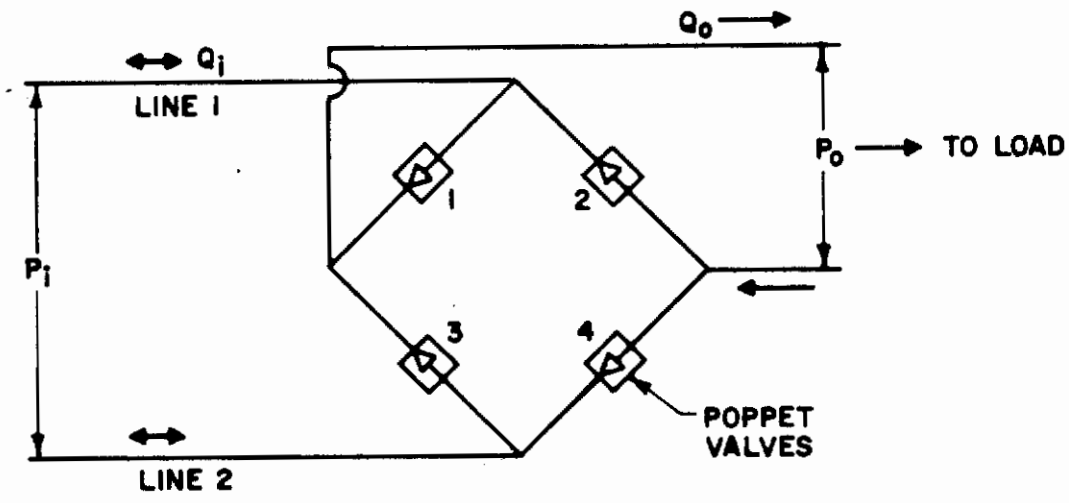

Figure IV-17. Hydraulic Full-Wave Bridge Rectifier

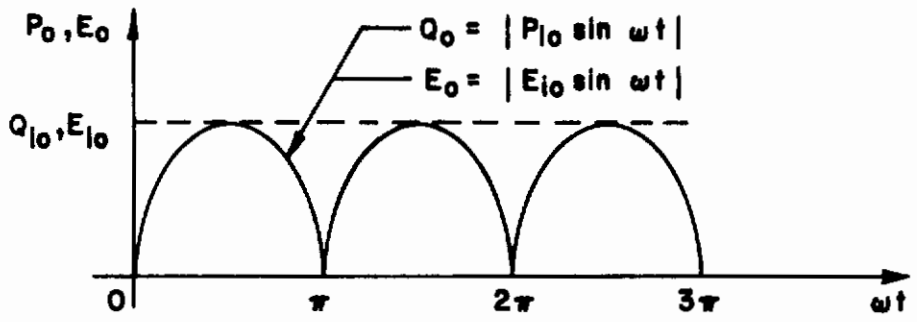

Figure IV-18. Flow and Current Output of an Ideal Hydraulic and Electric Full-Wave Bridge Rectifier

If non-ideal poppet valves are used in the hydraulic rectifier, the flow output shown in Figure IV-18 will be distorted in terms of amplitude and phase. The degree of distortion will depend on the performance of the poppet valves.

The electric equivalent of the hydraulic full-wave bridge rectifier is the electric full-wave bridge rectifier shown in Figure IV-19. The current flow paths of the electric full-wave bridge rectifier are the same as the flow paths of the hydraulic full-wave bridge rectifier.

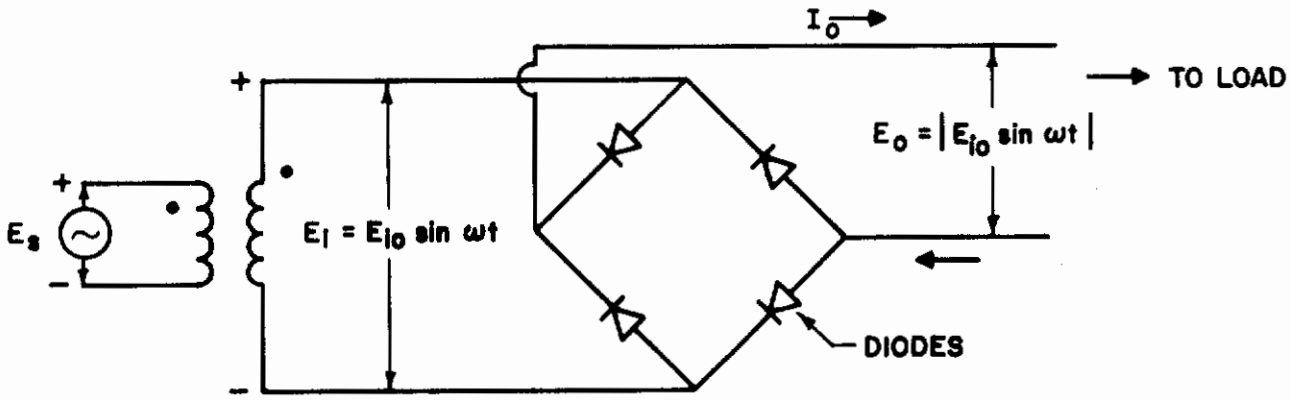

Figure IV-19. Electric Full-Wave Bridge Rectifier

For non-ideal 3-phase rectifiers, amplitude and phase distortion of the output shown in Figure IV-23 will also result. The amount of distortion again depends on the performance of the poppet valves and diodes.

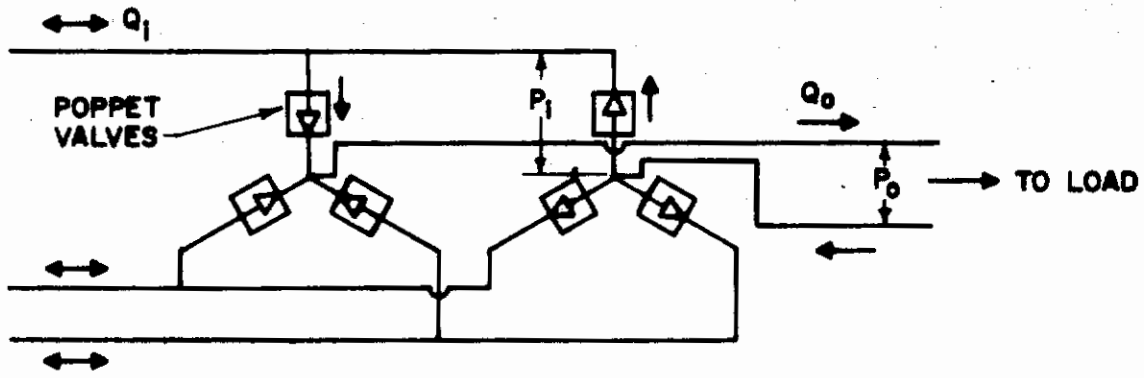

Figure IV-21. 3-Phase Hydraulic Rectifier

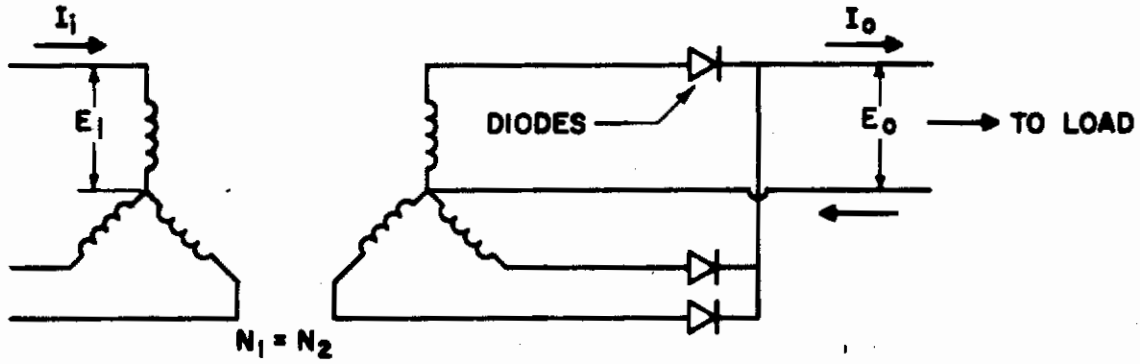

Figure IV-22. Electric Equivalent of the 3-Phase Hydraulic Rectifier, A 3-Phase Electric Rectifier

The voltage output of an ideal electric full-wave bridge rectifier is shown in Figure IV-18, which is the graphical representation of the expression

$$I_o = \left| I_{io} \sin \omega t \right|$$

where: I_{io} = the maximum amplitude of the sinusoid flow input.

Figure IV-20 is the volt-ampere characteristic of a typical silicon P-N junction diode. We notice the similarity between the performance of the poppet valve and diode. The voltage output of a non-ideal electric full-wave bridge rectifier will also be distorted away from that shown in Figure IV-18, again in terms of amplitude and phase. The amount of distortion depends on the characteristics of the diode.

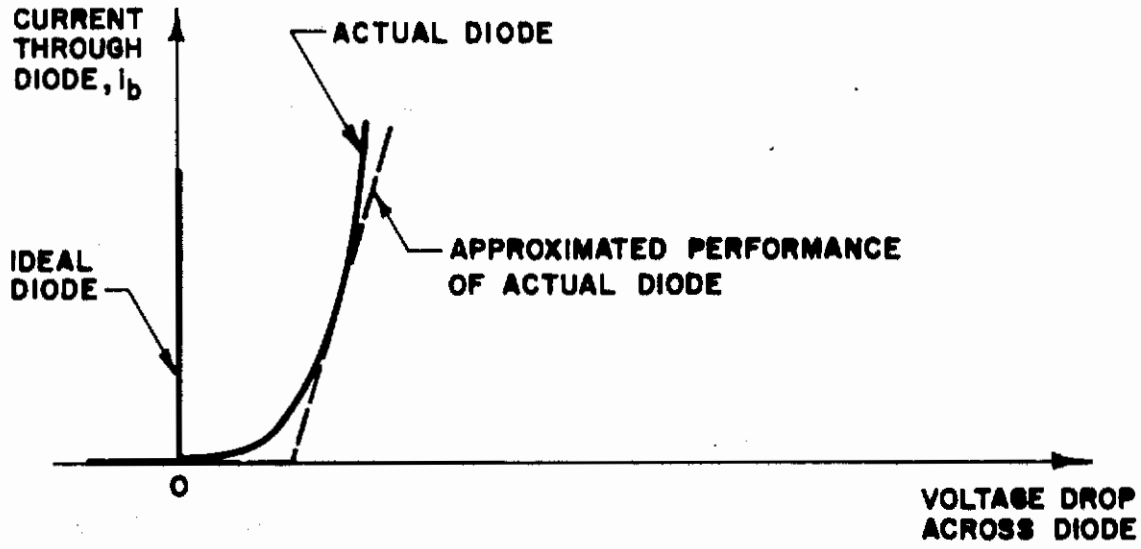

Figure IV-20. Volt-Ampere Characteristic of a Typical Silicon P-N Junction Diode

Figure IV-21 is a schematic diagram of a 3-phase hydraulic rectifier and Figure IV-22 is its electric equivalent, a 3-phase electric rectifier. The flow and current outputs of the ideal 3-phase hydraulic and electric rectifiers are shown in Figure IV-23. The definition of "ideal" is defined as the use of ideal poppet valves and diodes in the hydraulic and electric rectifier, respectively.

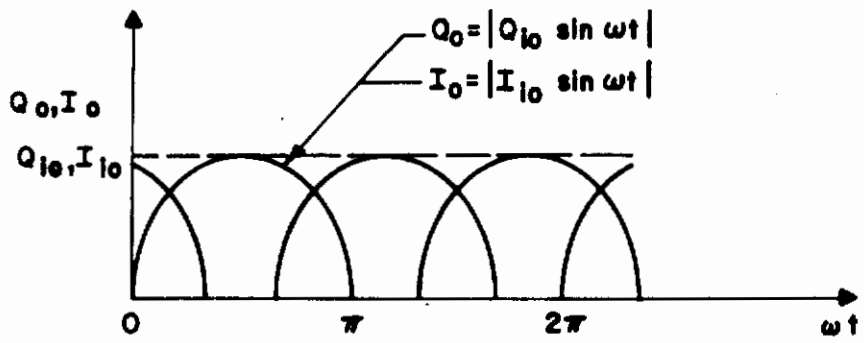

Figure IV-23. Flow and Current Output of Ideal 3-Phase Hydraulic and Electric Rectifiers

For hydraulic rectifiers of the same pressure and flow output, a 3-phase rectifier has certain advantages over a full-wave bridge rectifier. They are:

(1) The line loss is reduced by reducing the flow velocity.

(2) The degree of pulsating filtering requirement is reduced due to the increase of flow pulse per unit time.

(3) The peak pump output pressure, and consequently the peak line pressure, can be reduced due to the increase of pressure pulse per unit time.

The disadvantage of a 3-phase rectifier when compared to a full-wave bridge rectifier is the increase of weight because of the increase of the number of poppet valves.

8. Accumulators

The three types of accumulators commonly used are: 1) spring-loaded, 2) air-loaded, and 3) added-volume. The added-volume accumulator can be used to lower the system natural frequency, but is ineffective for pulsating filtering purposes, therefore, it will not be discussed here.

a. Spring-Loaded Accumulator[4]

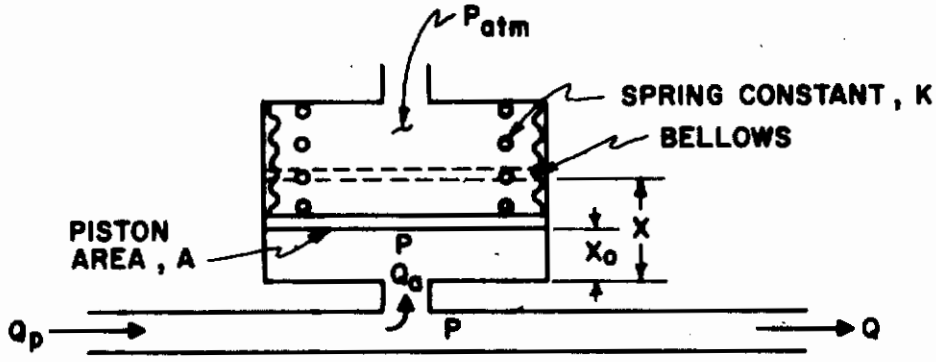

Figure IV-24. Spring-Loaded Accumulator

In Figure IV-24 above, the bellows is used to prevent fluid leakage. Neglecting the damping and mass effect, the force equilibrium equation is:

$$\left(P - P_{atm} \right) A = K \left(X - X_o \right) \tag{32}$$

Differentiating Equation 32 reduces to

$$SP = \frac{K}{A} SX \tag{33}$$

The rate of flow of oil into the accumulator is

$$Q_a = ASX \tag{34}$$

The continuity relation is

$$Q = Q_p - Q_a \tag{35}$$

Then, combining Equations 33, 34, and 35, we obtain the following governing equation:

$$Q = Q_p - \frac{A^2}{K} SP \tag{36}$$

where the symbols are defined in Figure IV-24.

b. Air Loaded Accumulator[4]

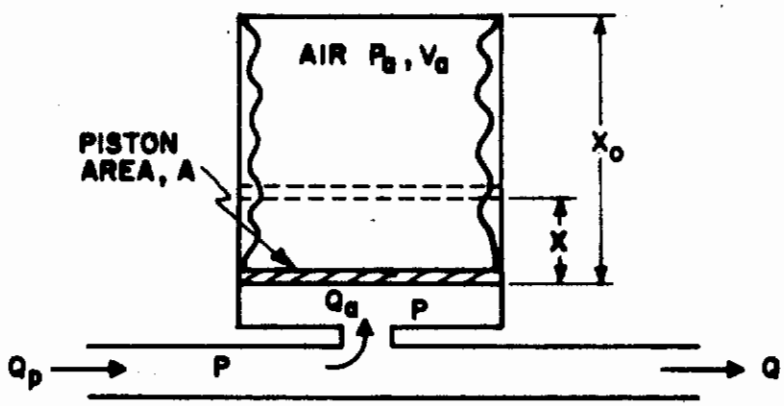

Figure IV-25. Air-Loaded Accumulator

Figure IV-25 is a schematic diagram of an air-loaded accumulator. Neglecting damping and mass effect, the force equilibrium equation is

$$A P_a = AP \tag{37}$$

Assuming the compressed air is a perfect gas and the compression and expansion process is adiabatic and reversible, the equation of state is

$$P_a V_a^{K_r} = P_{ao} V_{ao}^{K_r} \tag{38}$$

and

$$Q_a = ADX \tag{39}$$

where P_{ao} and V_{ao} are initial air pressure and air volume in the accumulator.

Differentiating Equation 38, the following expression is obtained:

$$Q_a = - \frac{1}{K_r} \left(\frac{V_a}{P_a} \right) DP \tag{40}$$

The continuity equation of flow is

$$Q = Q_p - Q_a \tag{41}$$

Neglecting the negative sign of Equation 40, combining it with Equation 41, and then applying the Laplace transformation on the resulting equation, we obtain

$$Q = Q_p - \frac{1}{K_r}\left(\frac{V_a}{P_a}\right) SP \tag{42}$$

It is noticed from Equations 36 and 42 that the flow into and out of the spring-loaded accumulator is proportional to the rate of pressure change. The flow into and out of the air-loaded accumulator is proportional to the rate of change of pressure only when <u>small</u> changes are considered.

The electric equivalent of the accumulator is shown in Figure IV-26.

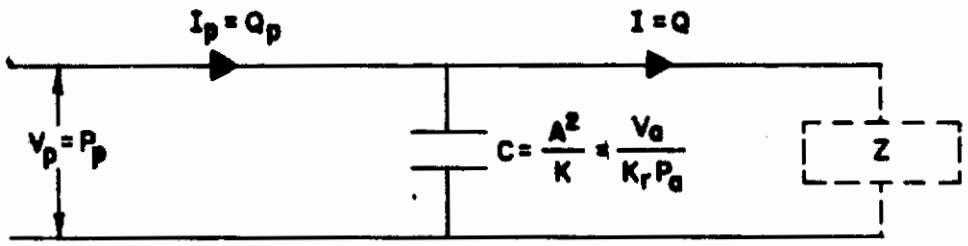

(a) P-V Analogy

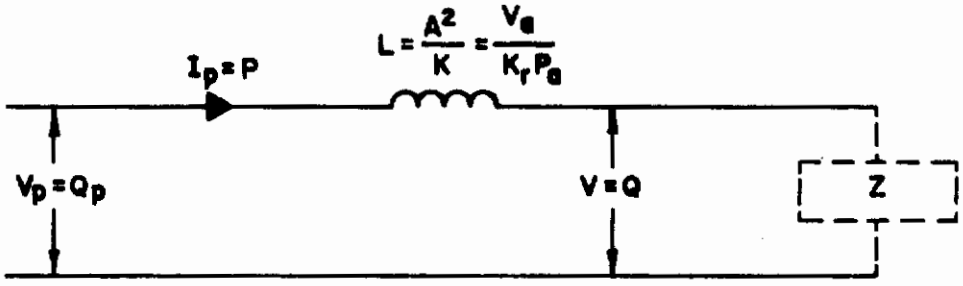

(b) P-C Analogy

Figure IV-26. Electric Equivalent of Accumulator

9. The Linearized Closed-Center, 4-Way Valve in Incremental Form

Equation 6, which describes the performance of an approximated closed center 4-way valve, was linearized from Equation 5 by using the following restrictions.

(1) The spool opening (from neutral position) and load pressure are assumed to be very small.

(2) The effect of the load pressure on the rate of valve output flow can be neglected when Restriction 1 is satisfied.

In this subsection an incremental method is used to transform the valve characteristic equation into its linearized incremental form. Equation 5 is rewritten here for convenience.

$$P_\ell = P_s - \frac{2Q_\ell^2}{g^2X^2} \tag{43}$$

Its linearized incremental form is

$$\Delta Q_\ell = \frac{\Delta X}{Z_1} - \frac{\Delta P_\ell}{Z_2} \tag{44}$$

where:

$$\frac{1}{Z_1} = \left.\frac{\partial Q_\ell}{\partial X}\right]_{P_\ell = \text{const}} = \frac{Q_{\ell r}}{X_r}$$

$$\frac{1}{Z_2} = \left.\frac{\partial Q_\ell}{\partial P_\ell}\right]_{X = \text{const}} = \frac{g^2 X_r^2}{4Q_{\ell r}}$$

$$g = C_d W \sqrt{\frac{2}{\rho}}$$

X_r is the steady spool opening (from neutral position); and $Q_{\ell r}$, the valve flow rate at any particular valve operating point, as shown in Figure IV-27.

ΔQ_ℓ, ΔX, and ΔP_ℓ are the incremental change of valve flow rate, spool opening, and load pressure in reference to their respective steady values, $Q_{\ell r}$, X_r, and $P_{\ell r}$.

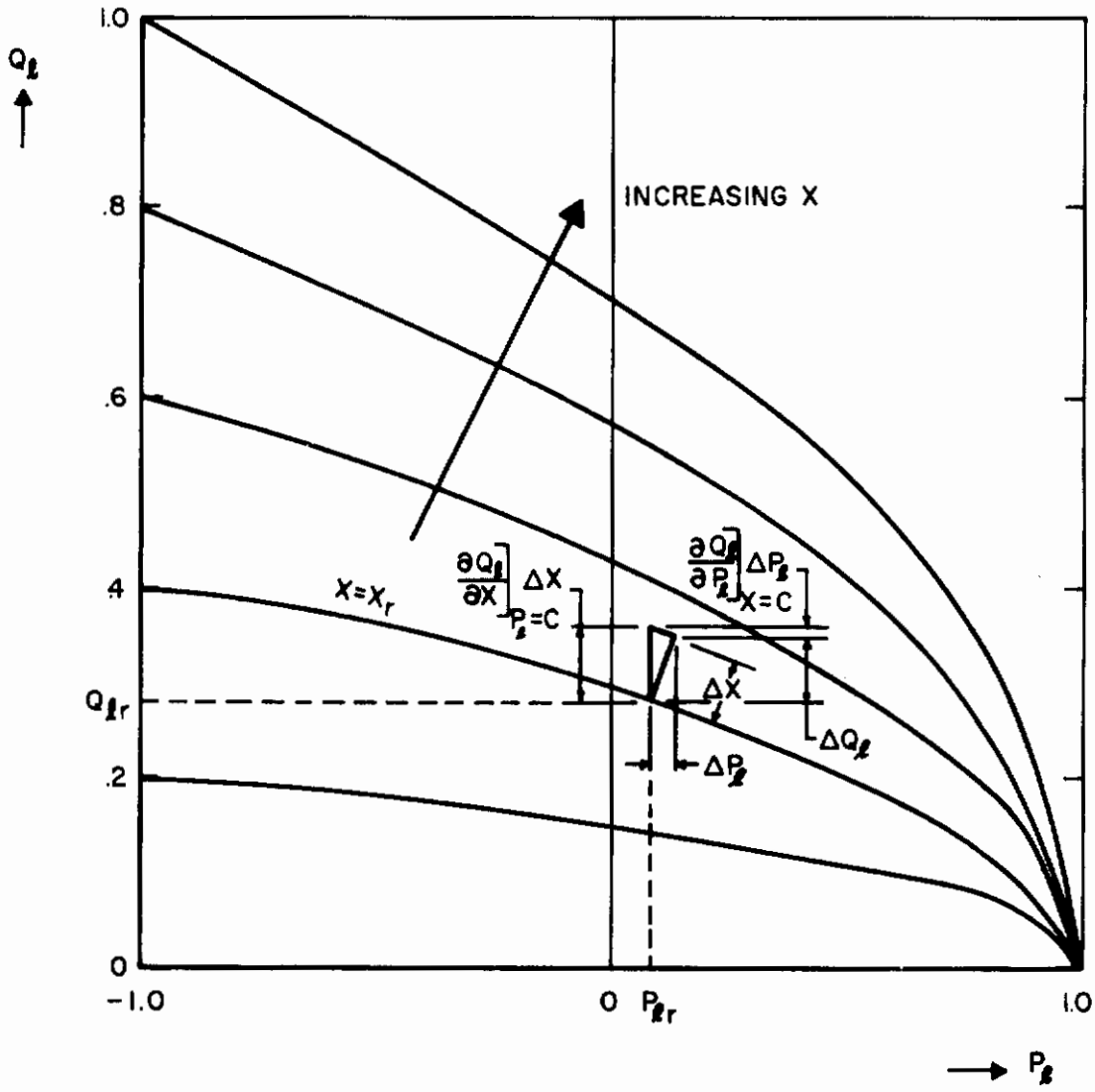

Figure IV-27. Closed Center 4-Way Valve Characteristics

Equation 45 shows that the relation between the incremental change of the valve characteristics, ΔX, ΔP_ℓ, and ΔQ_ℓ, is independent of the supply pressure, P_S. This apparently is due to the fact that for a system of constant pressure and variable flow, the supply pressure, P_S, is independent of the change of the load.

To represent Equation 45 by the electric equivalent network of the P-V analogy, it is rewritten:

$$\left(\frac{Z_2}{Z_1}\right) \quad \Delta X\,(t) = Z_2\ \Delta Q_\ell + \Delta P_\ell$$

or

$$\frac{4\,Q_{\ell r}^{\,2}}{g^2 X_r^{\,3}}\ \Delta X\ (t) = \left(\frac{4\,Q_{\ell r}}{g^2 X_r^{\,2}}\right) \Delta Q_\ell + \Delta P_\ell \qquad (45)$$

The term at the left side of Equation 45 is equivalent to an independent voltage source which is a time function of the incremental spool displacement.

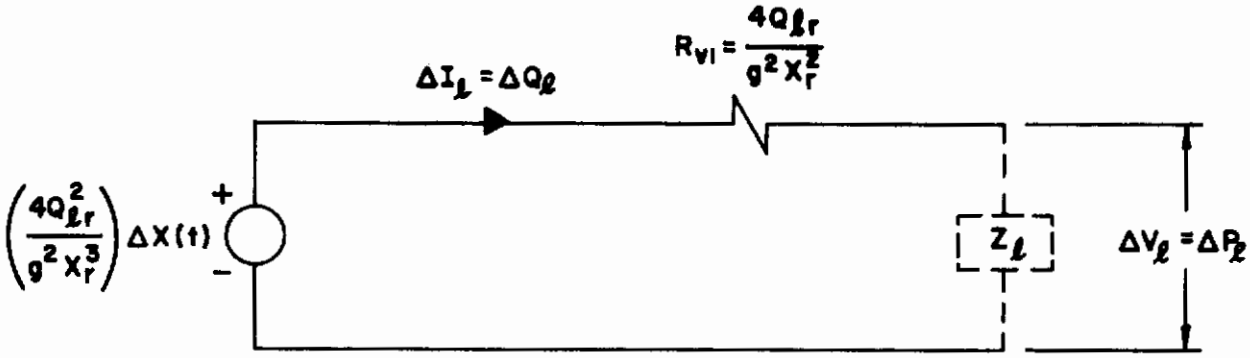

(a) P-V Analogy

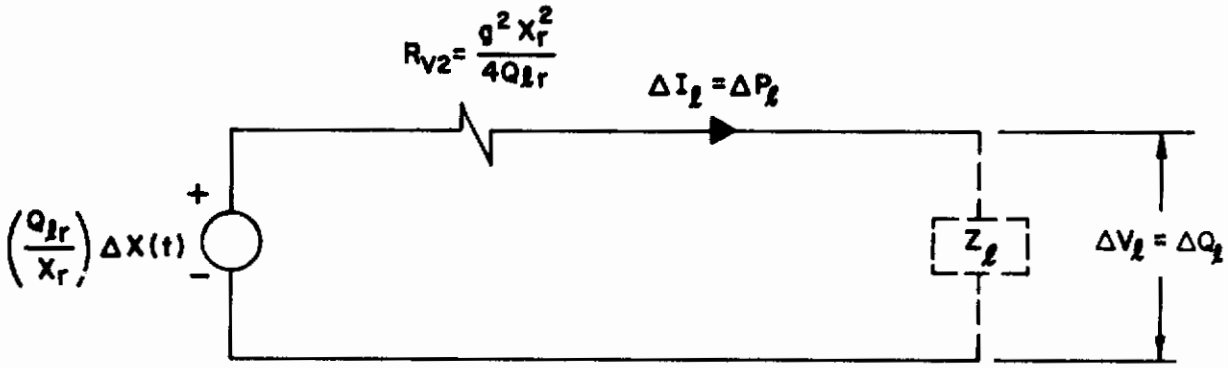

(b) P-C Analogy

Figure IV-28. Electric Equivalent of Incremental Performance of Closed Center 4-Way Valve

Figure IV-28 is a schematic of the electric equivalent of the incremental performance of the closed center 4-way valve.

10. Transmission Line with Lumped Parameters

Whether a transmission line should be treated as lumped or distributed parameters, depends on the relative magnitude between the line length and the wave length of the fluid in the line. A general rule is that when the line length is less than one-eighth of the fluid wave length, the line can be treated as lumped parameters. When the line length equals or exceeds one-eighth of the fluid wave length, the line should be treated as distributed parameters. In this subsection only a line with lumped parameters is discussed.

a. Nonviscous Transmission Line with Lumped Parameters with Flow Input

A nonviscous line of length, L, and cross-section area, A, is represented schematically by Figure IV-29.

(a) Nonviscous Transmission Line (b) Schematic Representation

Figure IV-29. Schematic Representation of Nonviscous Line of Lumped Parameters with Flow Input

The governing equations are [7]

$$Q_a - Q_b = \frac{A\ell}{\beta_e} SP = \frac{T_e}{Z_s} SP \qquad (46)$$

$$P - P_b = \frac{\rho\ell}{A} SQ_b = Z_s T_e SQ_b \qquad (47)$$

The electric equivalent is shown in Figure IV-30.

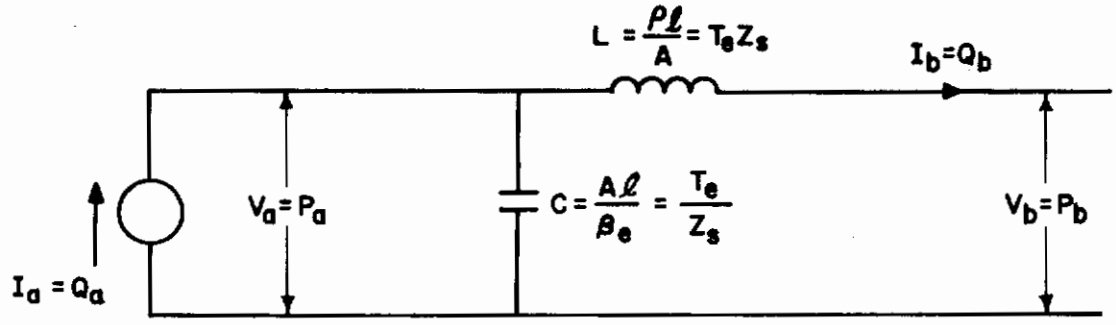

(a) P-V Analogy

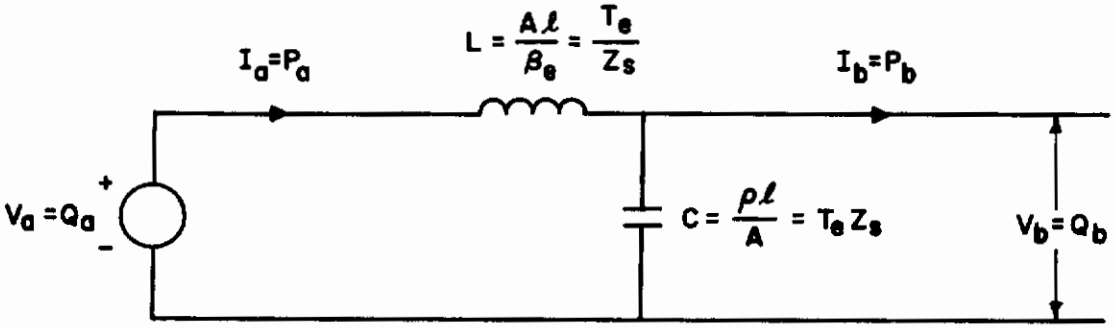

(b) P-C Analogy

Figure IV-30. Electric Equivalent of Nonviscous Line of Lumped Parameters with Flow Input

Equations 46 and 47 can be combined to result in Equations 48 and 49.

$$Q_a = Y_s T_e S P_b + \left(T_e^2 S^2 + 1 \right) Q_b \tag{48}$$

$$P_a \left(T_e^2 S^2 + 1 \right) = P_b + T_e Z_s S Q_a \tag{49}$$

Figure IV-31 is a four-terminal representation of Equations 48 and 49, which shows clearly how the four variables are related to each other.

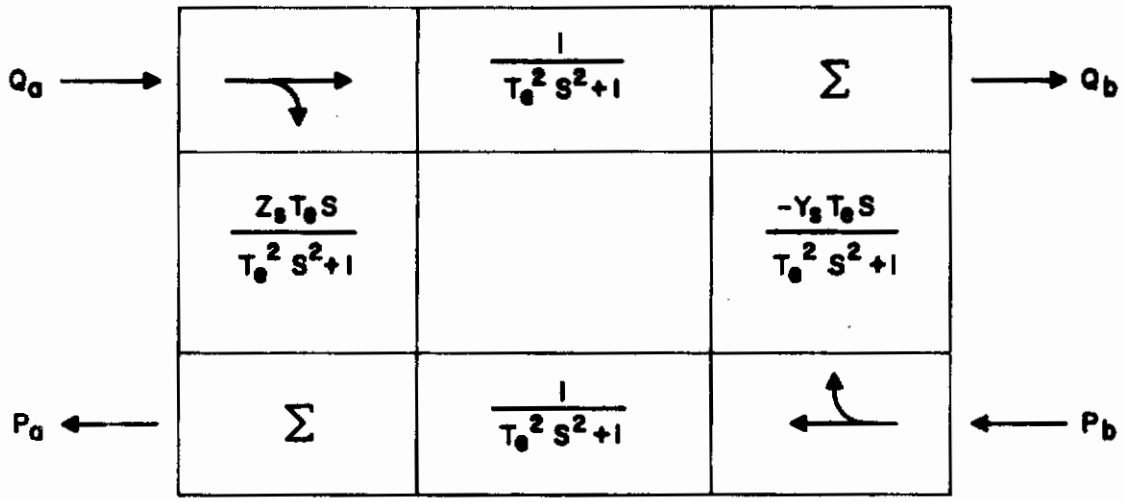

Figure IV-31. Four-Terminal Block Diagram Representation of Nonviscous Line of Lumped Parameters with Flow Input

b. Nonviscous Transmission Line of Lumped Parameters With Pressure Input

When pressure is the input of the transmission line, the inductance of Figure IV-30 should be moved upstream of the capacitance, and the inductance of Figure IV-30 should be moved downstream. This is due to the reason that force always associates with mass. Equations 50 and 51 are the analytical representation. Figure IV-32 is the four-terminal block diagram representation.

$$P_a = P_b \frac{1}{\left(\frac{T_e^2 D^2}{2} + 1\right)} + Q_a \frac{T_e D \left(\frac{T_e^2 D^2}{4} + 1\right)}{Y_s \left(\frac{T_e^2 D^2}{2} + 1\right)} \tag{50}$$

$$P_a \frac{1}{\left(\frac{T_e^2 D^2}{2} + 1\right)} = P_b + Q_b \frac{T_e D \left(\frac{T_e^2 D^2}{4} + 1\right)}{Y_s \left(\frac{T_e^2 D^2}{2} + 1\right)} \tag{51}$$

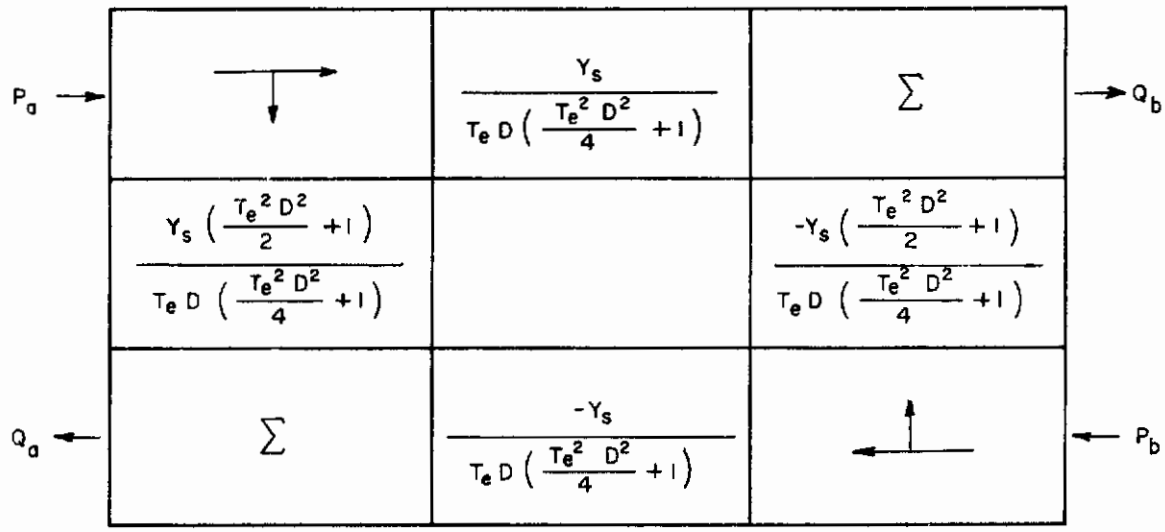

Figure IV-32. Four-Terminal Block Diagram Representation of Nonviscous Line of Lumped Parameters with Pressure Input

c. Viscous Transmission Line of Lumped Parameters with Flow Input

Figure IV-33 is a schematic representation of a viscous line of lumped parameters. Part (a) and (b) of Figure IV-33 represent a line with laminar and turbulent flow, respectively.

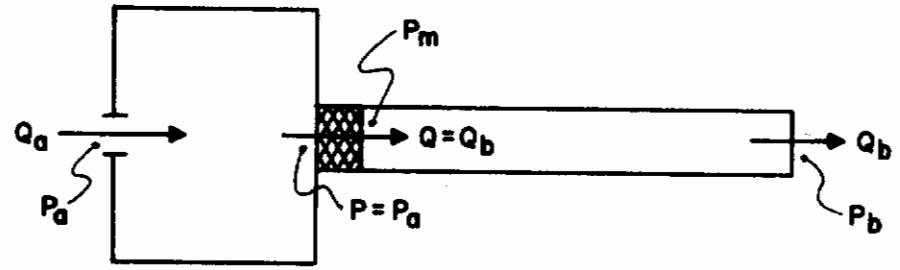

(a) Line with Laminar Flow

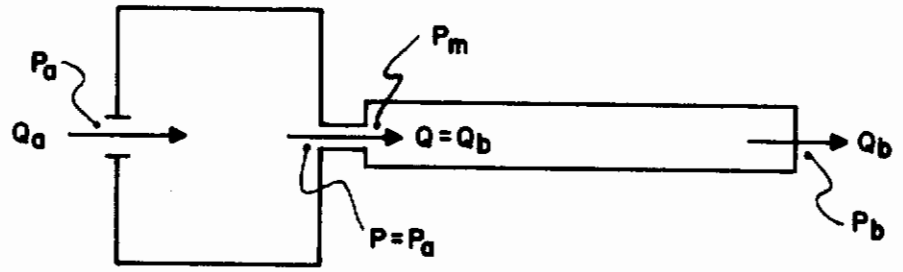

(b) Line with Turbulent Flow

Figure IV-33. Schematic Representation of Viscous Line of Lumped Parameters with Flow Input

The governing equations are [7]

$$Q_a - Q_b = \frac{A\ell}{\beta_e} SP_a = \frac{T_e}{Z_s} SP_a \qquad (52)$$

$$P_a - P_m = R_h Q_b \qquad (53)$$

$$P_m - P_b = \frac{\rho \ell}{A} S Q_b \qquad (54)$$

where: R_h = constant for laminar flow

$R_h = K Q_b$ for turbulent flow

K = constant

The electric equivalent of a viscous line of lumped parameters with flow input can be easily obtained as shown in Figure IV-34. However, for the line with turbulent flow, the resistance, R_h is not a constant but varies proportionally with the flow, Q_b.

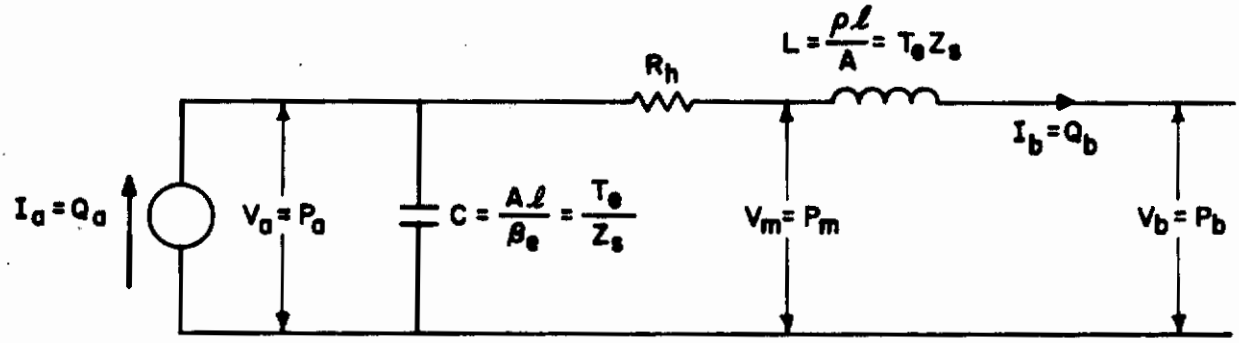

(a) P-V Analogy

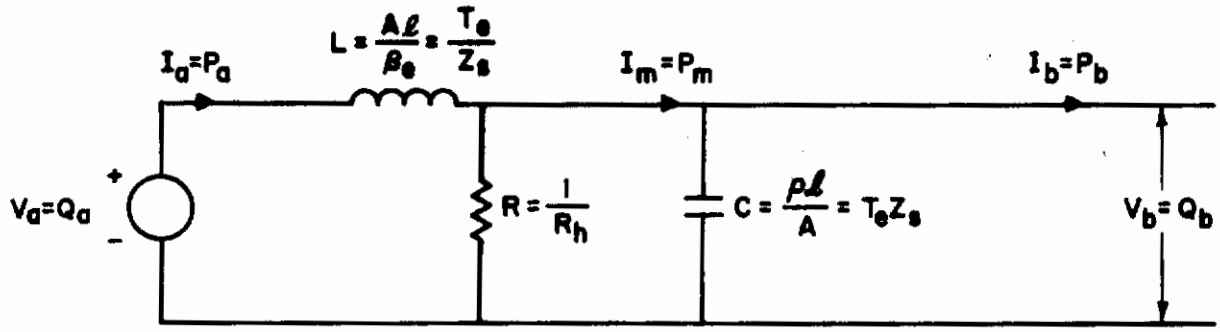

(b) P-C Analogy

Figure IV-34. Electric Equivalent of a Viscous Line of Lumped Parameters with Flow Input

d. Viscous Transmission Line of Lumped Parameters with Pressure Source

The governing equations can be easily derived

$$P_a - P_m = \frac{\rho \ell}{A} SQ_a = Z_s T_e SQ_a \quad (55)$$

$$Q_a - Q_b = \frac{A \ell}{\beta_e} SP_m = \frac{T_e}{Z_s} SP_m \quad (56)$$

$$P_m - P_b = R_h Q_b \quad (57)$$

Where R_h is defined as for Equation 31.

11. Viscous Transmission Line of Distributed Parameters

The transmission line of distributed parameters can be represented by lumped parameters if the line is divided into several sections; the lumped parameters are shown in Figures IV-30 and IV-34. Figure IV-35 is the electric equivalent of a viscous line of distributed parameters.

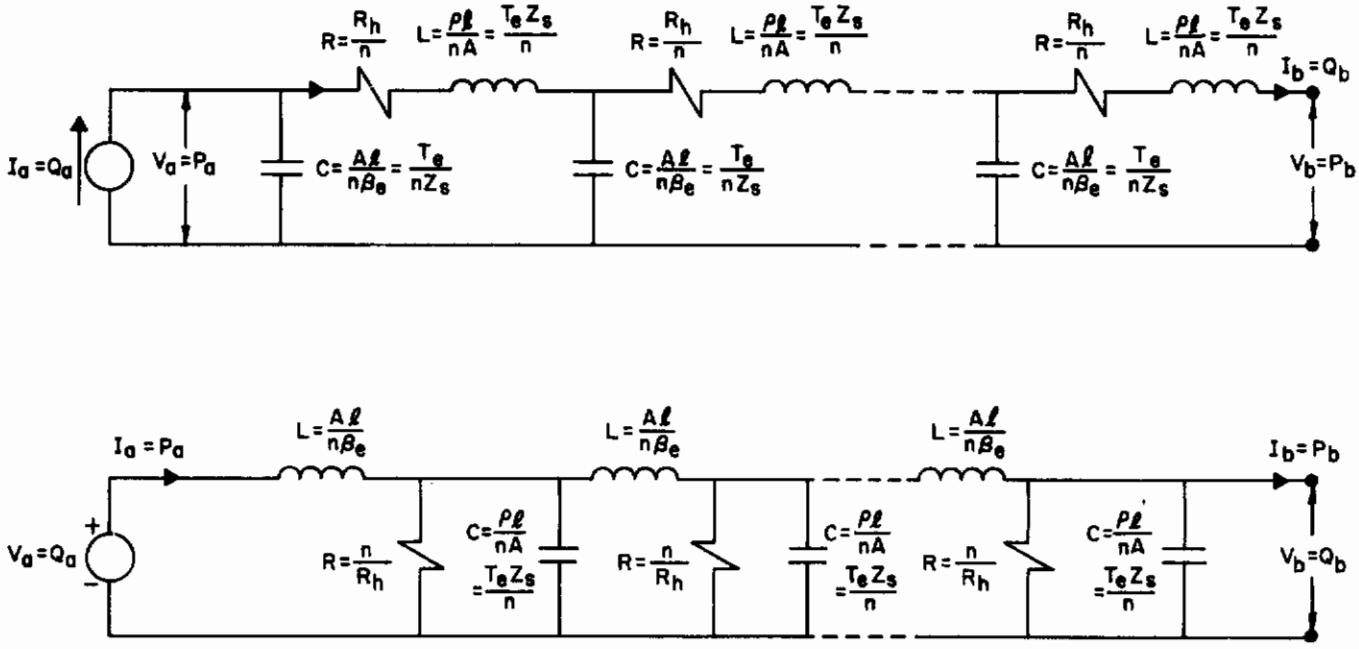

Figure IV-35. Electric Equivalent of Viscous Line of Distributed Parameters by a n-Section of Lumped Parameters

12. Viscous Transmission Line of Distributed Parameters with Low Average Flow Velocity

For an unsteady, compressible, low average velocity, and one-dimensional flow in a uniform tube, the following pair of wave equations can be used to describe its wave propagation. (See Appendix for the derivation of the equations in this subsection.)

$$\frac{\partial^2 P}{\partial X^2} - \gamma^2 P = 0 \tag{58}$$

$$\frac{\partial^2 Q}{\partial X^2} - \gamma^2 Q = 0 \tag{59}$$

where γ, propagation constant $= \sqrt{ZY}$

The solutions of the above wave equations are

$$P = P_1 e^{j\omega t} e^{\gamma X} + P_2 e^{j\omega t} e^{-\gamma X} \tag{60}$$

$$Q = -P_1 \sqrt{\frac{Y}{Z}}\, e^{j\omega t}\, e^{\gamma X} + P_2 \sqrt{\frac{Y}{Z}}\, e^{j\omega t} e^{-\gamma X} \tag{61}$$

The characteristic impedance of the line, which is the ratio of Equation 60 and 61 is

$$Z_s = \sqrt{\frac{Z}{Y}} = \frac{1}{Y_s} \tag{62}$$

The general impedance expression of the line at a distance X looking toward the load is found to be

$$Z_X = Z_s \frac{Z_\ell + Z_s \tanh \gamma X}{Z_s + Z_\ell \tanh \gamma X} \tag{63}$$

where Z_ℓ is load impedance.

Equation 63 shows that the hydraulic line impedance is not only a function of the line characteristic impedance Z_s, but is also a function of load impedance, Z and the propagation constant, γ.

Replacing the hydraulic line characteristic impedance, load impedance, and propagation constant of Equation 63 by that of the electric transmission line produces the electrical transmission line impedance.

Equation 63 and its important parameters are discussed in more detail here for both viscous and nonviscous hydraulic lines.

a. Line Characteristic Impedance:

The line characteristic impedance is defined previously as

$$Z_s = \sqrt{\frac{Z}{Y}} \tag{64}$$

Substituting general form of Z and Y into Equation 64

$$Z_s = \sqrt{\frac{\rho\beta_e}{A}} \left[1 + \frac{R_h}{\rho D}\right]^{\frac{1}{2}} \tag{65}$$

Expanding Equation 65 results in

$$Z_s = \sqrt{\frac{\rho\beta_e}{A}} \left[1 + \frac{R_h}{2\rho D} - \frac{1}{8}\left(\frac{R_h}{\rho D}\right)^2 + \cdots\right] \tag{66}$$

For a viscous line with low average flow velocity, the following relation $\frac{R_h}{\rho\omega} << 1$ usually holds so long as the pulsating frequency is not too small. Therefore, the characteristic impedance of the viscous line reduces to

$$Z_s \simeq \sqrt{\frac{\rho\beta_e}{A}} \left(1 - j\frac{R_h}{2\rho\omega}\right) \tag{67}$$

Substituting R_h by zero in Equation 67, the characteristic impedance of the non-viscous line is obtained.

$$Z_s = \sqrt{\frac{\rho\beta_e}{A}} \tag{68}$$

b. Propagation Constant

The propagation constant is defined previously as

$$\gamma = \sqrt{ZY} \tag{69}$$

Substituting general form of Z and Y into Equation 69 produces

$$\gamma = \sqrt{\frac{\rho}{\beta_e}} \quad D \quad \left[1 + \frac{R_h}{\varphi D}\right]^{1/2} \tag{70}$$

Expanding Equation 70 results

$$\gamma = \sqrt{\frac{\rho}{\beta_e}} \quad D \quad \left[1 + \frac{R_h}{2\rho D} - \frac{1}{8} \left(\frac{R_h}{\rho D}\right)^2 + \ldots\right] \tag{71}$$

For a similar reason as used in obtaining characteristic impedance, the propagation constant of viscous line with low average flow velocity is obtained as

$$\gamma \simeq \omega\sqrt{\frac{\rho}{\beta_e}} \left(\frac{R_h}{2\rho\omega} + j\right) = \frac{\omega T_e}{\ell} \left(\frac{R_h}{2\rho\omega} + j\right) \tag{72}$$

For a nonviscous line, the propagation constant is

$$\gamma \simeq j\omega\sqrt{\frac{\rho}{\beta_e}} \simeq j \frac{T_e \omega}{\ell} \tag{73}$$

c. Hydraulic Line Impedance

For a line with low average flow velocity and friction loss, the line impedance is

$$Z_X = Z_s \frac{Z_\ell + Z_s \tanh \gamma X}{Z_s + Z_\ell \tanh \gamma X} \tag{74}$$

The input impedance is obtained by replacing X by total line length, ℓ

$$Z_o = Z_s \frac{Z_\ell + Z_s \tanh \gamma \ell}{Z_s + Z_\ell \tanh \gamma \ell} \tag{75}$$

For a nonviscous line, the line impedance is:

$$Z_X = Z_s \frac{Z_\ell + j Z_s \tan \gamma X}{Z_s + j Z_\ell \tan \gamma X} \tag{76}$$

The input impedance is obtained by replacing X by total line length, ℓ

$$Z_o = Z_s \frac{Z_\ell + j Z_s \tan \gamma \ell}{Z_s + j Z_\ell \tan \gamma \ell} \tag{77}$$

where:

$$\gamma = \omega \sqrt{\frac{\rho}{\beta_e}} = \omega \frac{T_e}{\ell}$$

X = the distance from the load impedance

Z_ℓ = the load impedance

This expression is very useful in finding the line resonance condition.

In order to establish an equivalence between the hydraulic line (with low average flow velocity) and the electric transmission line, the basic properties of the fluid in a line are represented by their equivalent electric properties.

Inertance (inductance):

$$P_a - P_b = \left(M_{dx}\right) \frac{dQ}{dt} \tag{78}$$

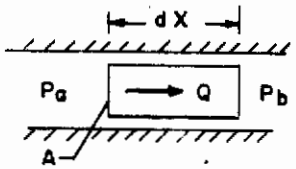

Where m, inertance per unit length of line = $\frac{\rho}{A}$

Capacitance:

$$Q_a - Q_b = \left(C_{dx}\right) \frac{dP}{dt} \tag{79}$$

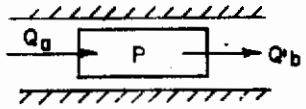

where C_h, capacitance unit length of line = $\frac{A}{\beta_e}$

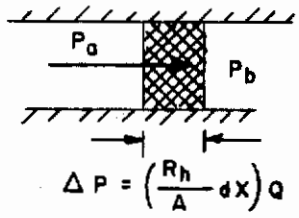

Resistance:

$$\left(P_a - P_b\right) = \left(\frac{R_h}{A} \quad dX\right) \qquad Q \tag{80}$$

Where $\frac{R_h}{A}$, fluid resitance per unit length of line

The equivalents between the characteristic impedance and propagation constant of the hydraulic and electric line are shown in Table IV-1.

TABLE IV-1

THE CHARACTERISTIC IMPEDANCE AND PROPAGATION CONSTANT OF THE HYDRAULIC AND ELECTRIC LINE

		Characteristic Impedance, Z_s	Propagation Constant, γ
Hydraulic Line	With Small Loss	$\sqrt{\frac{m}{C_h}}\left[1 + j\left(\frac{S}{2\omega C_h} - \frac{R_h/A}{2\omega m}\right)\right]^*$ $= \frac{1}{A}\sqrt{\rho\beta_e}\left(1 - j\frac{R_h}{2\rho\omega}\right)$	$\omega\sqrt{m\,C_h}\left[\frac{1}{2\omega}\left(\frac{R_h/A}{m} + \frac{S}{C_h}\right) + j\right]^*$ $= \omega\sqrt{\frac{\rho}{\beta_e}}\left(\frac{R_h}{2\rho\omega} + j\right)$
	Loss-Less	$\sqrt{\frac{m}{C_h}} = \frac{1}{A}\sqrt{\rho\beta_e}$	$j\omega\sqrt{m\,C_h} = j\omega\sqrt{\frac{\rho}{\beta_e}}$
Electric Line	With Small Loss	$\sqrt{\frac{L}{C}}\left[1 + j\left(\frac{G}{2\omega C} - \frac{R}{2\omega L}\right)\right]$	$\omega\sqrt{LC}\left[\frac{1}{2\omega}\left(\frac{R}{L} + \frac{G}{C}\right) + j\right]$
	Loss-Less	$\sqrt{\frac{L}{C}}$	$j\omega\sqrt{LC}$

* The leakage per unit length of hydraulic line, s, is assumed to be zero.

C. THE ELECTRIC EQUIVALENT OF THE PULSATING HYDRAULIC SYSTEM WITH PRESSURE-CONTROLLED FLOW SOURCE

1. Electric Equivalent of the System by P-V Analogy

The completion of the derivation of the characteristic equations and electric equivalents of the basic system components enables us to establish the electric equivalent of the entire pulsating hydraulic system. The system represented by Figure IV-35 is a constant pressure flow-demand system with its source controlled by the system pressure. The following explanations are given to clarify and define certain parts of the figure.

Figure IV-36 is the electric equivalent of the system that is derived from the P-V analogy. It is shown in the figures as well as in the previous subsections that the electric equivalent of the components of the pulsating hydraulic system are generally made of two electric lines of different voltage levels (the live line and the ground line) connected by a condenser and other passive elements. The size of the condenser represents the compressibility effect of the working fluid within the component. The solid and dotted arrows shown in the rectifier represent the flow directions of the rectifier for the first and second half-cycles, respectively. The resistance, R_r, is the total resistance of the two poppet valves of the rectifier that are connected in series. The fluid compressibility of the rectifier is neglected. Therefore, its electric equivalent does not have a condenser connected across the live and ground lines. Hence, the ground lines are not shown in the figure. The system is precharged to pressure P_{pc}. The compressibility effect of the return lines is neglected.

The incremental model is related to the true value model by a dotted arrow, as can be seen from the figure. This is done to indicate that the incremental change of the flow rate and pressure within the components shown in the incremental model will not change the pressure downstream of the high pressure accumulator.

The sinusoid flow inputs to both transmission lines written in Laplace transform are:

$$Q_i = Q_0(P)\left[\frac{2\pi/T}{S^2+\left(\frac{2\pi}{T}\right)^2}\cdot\frac{1}{1-e^{-TS/2}}\right] \tag{81}$$

$$Q_i = Q_0(P)\left[\frac{2\pi/T}{S^2+\left(\frac{2\pi}{T}\right)^2}\cdot\frac{e^{-TS/2}}{1-e^{-TS/2}}\right] \tag{82}$$

The $e^{-TS/2}$ term in Equation 82 shows that the flow in the two transmission lines have a phase difference of 180°.

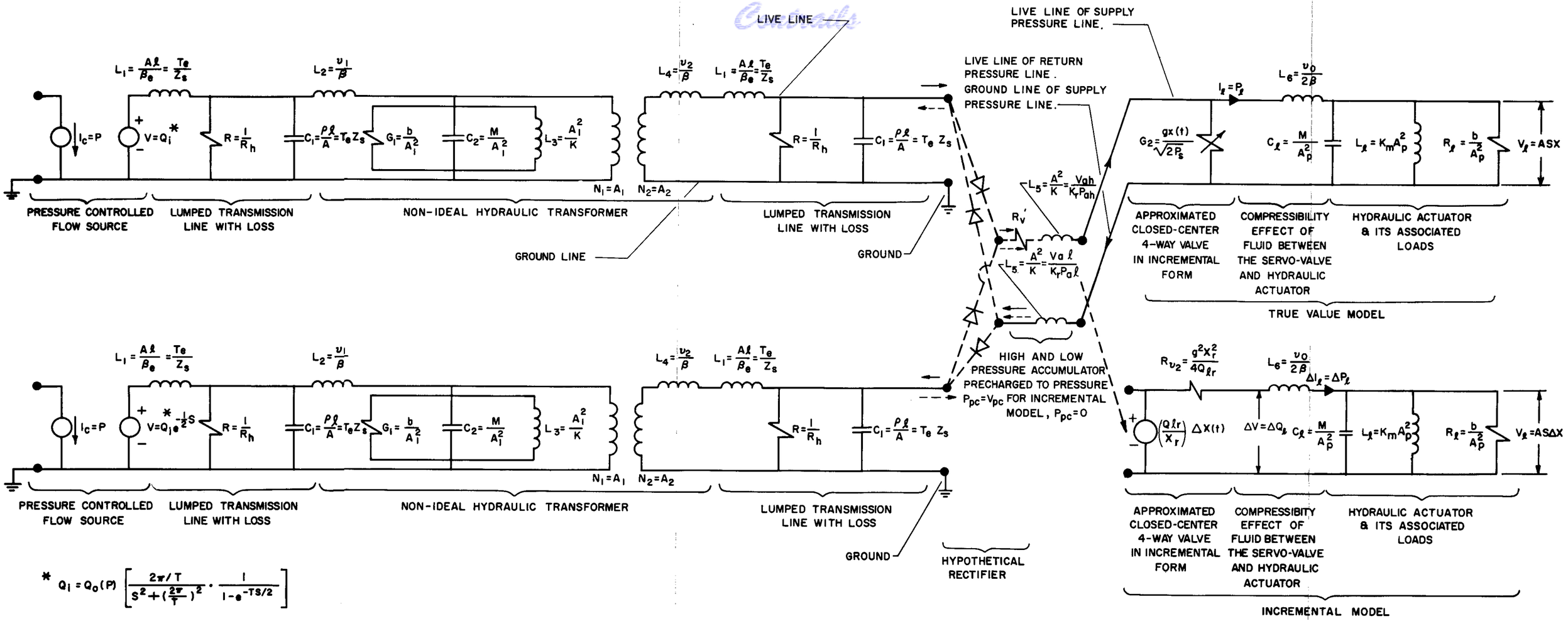

Figure IV-36. True Value Model and Incremental Model of the Electric Equivalent of the Pulsating Hydraulic System with Pressure Controlled Source (P-V Analogy)

2. System Electric Equivalent by the P-C Analogy

Figure IV-37 is the electric equivalent of the system that derived from the P-C analogy. The figure is self-explanatory. Detailed explanations given in the previous subsection will not be given here.

It should be noted that the electric equivalent of the hydraulic rectifier by the P-C analogy is not obtainable without resulting in an impossible physical condition. The electric equivalent obtained by P-C analogy results in the condition that when the voltage equals negative value, the current becomes infinite negative. The rectifier shown in Figure IV-37 is, therefore, drawn in a dotted line and the caption "Hypothetical Rectifier" is used.

D. THE EFFECT OF FLOW PARAMETERS TO THE SYSTEM COMPONENT PERFORMANCES

1. Resonance in a Nonviscous Fluid Line of Distributed Parameters

The resonant frequency of a hydraulic line is defined as that at which the reactive component of the input impedance reduces to zero.

Let the load impedance be

$$Z_\ell = R_\ell + j X_\ell \tag{83}$$

For convenience the load impedance is replaced by

$$Z_\ell = Z_s \ (\alpha + j \beta) \tag{84}$$

where

$$\alpha = \frac{R_\ell}{Z_s}, \quad \beta = \frac{X_\ell}{Z_s}, \quad \text{and } Z_s = \frac{\rho \epsilon}{A}$$

Substituting Equation 84 in the input impedance

$$Z_o = Z_s \frac{Z_\ell + j Z_s \tan \frac{\omega}{\epsilon} \ell}{Z_s + j Z_\ell \tan \frac{\omega}{\epsilon} \ell} \tag{85}$$

and letting the reactive component be zero, produces the resonant condition

$$\beta \tan^2 \frac{\omega}{\epsilon} \ell + (\beta^2 + \alpha^2 - 1) \tan \frac{\omega}{\epsilon} \ell - \beta = 0 \tag{86}$$

If α and β are much smaller than unity, Equation 86 can be simplified to

$$\tan \frac{\omega}{\epsilon} \ell = -\beta \tag{87}$$

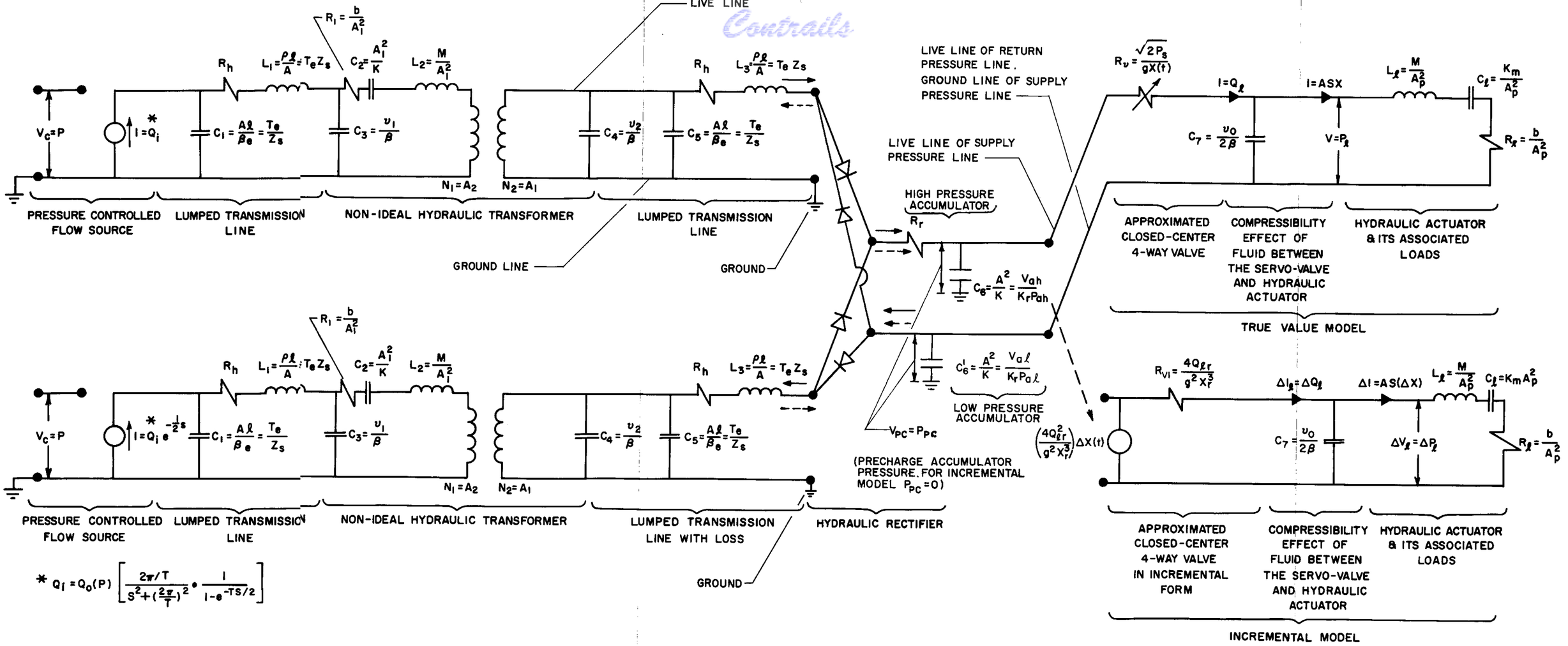

Figure IV-37. True Value Model and Incremental Model of the Electric Equivalent of the Pulsating Hydraulic System with Pressure Controlled Source (P-C Analogy)

The resonant frequency can be predicted by Equation 86 or Equation 87 when the fluid properties, load impedance, and line length are known.

2. Resonance in a Viscous Fluid Line of Distributed Parameters with Low Average Flow Velocity

The input and line characteristic impedance of a distributed line with friction loss and low flow velocity are

$$Z_o = Z_s \frac{Z_\ell + Z_s \tanh \gamma \ell}{Z_s + Z_\ell \tanh \gamma \ell} \tag{88}$$

and

$$Z_s = \frac{\rho \epsilon}{A} \left(1 - j \frac{R_h}{2\rho\omega} \right) , \tag{89}$$

respectively.

Where the propagation constant

$$\gamma = \frac{\omega}{\epsilon} \left(\frac{R_h}{2\rho\omega} + j \right) \tag{90}$$

The load impedance is

$$Z_\ell = R_\ell + j X_\ell = Z_s (\alpha + j \beta) \tag{91}$$

where:

$$\alpha = \frac{R_\ell - \frac{X_\ell R_h}{2\rho\omega}}{\frac{\rho\epsilon}{A} \left[1 + \left(\frac{R_h}{2\rho\omega} \right)^2 \right]} \tag{92}$$

$$\beta = \frac{X_\ell + \frac{R_\ell R_h}{2\rho\omega}}{\frac{\rho\epsilon}{A} \left[1 + \left(\frac{R_h}{2\rho\omega} \right)^2 \right]} \tag{93}$$

The resonant condition can be obtained by substituting Equations 90 and 91 into Equation 88 and letting the reactive component of the final result be equal to zero. The mathematical expression of the resonant condition is rather complicated. However, Equation 87 can be improved to represent the resonant condition by using Equation 93 as its β term. The resonant frequency can, therefore, be predicted once the fluid properties, load impedance, and line length are known.

3. The Effect of Series Condensers on the Pressure Output of the Nonviscous Fluid Line of Distributed Parameters

As the fluid acceleration increases due to the increase of pulsating frequency and stroke, the inertia of the fluid will not only reduce the magnitude but also cause a phase shift of the pressure output. To reduce (or eliminate if possible) the inertia effect, two identical hydraulic condensers can be connected in series with the hydraulic line.

The wave Equations 90 and 95 are solved here in a different manner to show the effect of the series condensers. The wave equations are rewritten here for convenience:

$$\frac{\partial^2 P}{\partial X^2} - \gamma^2 P = 0 \tag{94}$$

$$\frac{\partial^2 Q}{\partial X^2} - \gamma^2 Q = 0 \tag{95}$$

where γ, propagation constant $= \sqrt{Zy}$

For loss-less line, $\gamma = j\omega \frac{\rho}{\beta_e} = j\frac{\omega}{c}$

Equation 86 and 95 reduce to

$$\frac{\partial^2 P}{\partial X^2} + \frac{\omega^2}{c^2} P = 0 \tag{96}$$

$$\frac{\partial^2 Q}{\partial X^2} + \frac{\omega^2}{c^2} Q = 0 \tag{97}$$

The general solutions of Equations 96 and 97 are

$$P = \Psi_1 \cos\frac{\omega}{c} X + \Psi_2 \sin\frac{\omega}{c} X \tag{98}$$

$$Q = \Psi_3 \cos\frac{\omega}{c} X + \Psi_4 \sin\frac{\omega}{c} X \tag{99}$$

Using boundary conditions

$$\left.\begin{aligned} P &= P_o \\ Q &= Q_o \end{aligned}\right\} \text{at } X = 0$$

$$\left.\begin{aligned} \frac{\partial P}{\partial X} &= -j\frac{\omega\rho}{A} Q_o \\ \frac{\partial Q}{\partial X} &= -j\omega\frac{A}{\beta_e} P_o \end{aligned}\right\} \text{at } X = 0$$

the constants reduce to

$$\Psi_1 = P_o, \quad \Psi_3 = Q_o$$

$$-j\frac{\omega\rho}{A} Q_o = \frac{\omega}{C} \left(-C_1 \sin\frac{\omega}{\epsilon} X + C_2 \cos\frac{\omega}{\epsilon} X\right)$$

$$-j\omega \frac{A}{\beta_e} P_o = \frac{\omega}{\epsilon} \left(-C_3 \sin\frac{\omega}{\epsilon} X + C_4 \cos\frac{\omega}{\epsilon} X\right)$$

$$\Psi_2 = -j \frac{\rho\epsilon}{A} Q_o = -j \frac{1}{A}\sqrt{\rho\beta_e}\, Q_o$$

$$\Psi_4 = -j \frac{A\epsilon}{\beta_e} P_o = -j\frac{A}{\sqrt{\rho\beta_e}} P_o$$

Substituting the constants in Equation 98 and 99, produces

$$P = P_o \cos\frac{\omega}{\epsilon} X - j\frac{\rho\epsilon}{A} Q_o \sin\frac{\omega}{\epsilon} X$$

$$Q = Q_o \cos\frac{\omega}{\epsilon} X - j\frac{A\epsilon}{\beta_e} P_o \sin\frac{\omega}{\epsilon} X$$

At $X = \ell$, $P = P_i$ and $Q = Q_i$, therefore the above equations reduce finally to

$$P_i = P_o \cos\frac{\omega}{\epsilon} \ell - j\frac{\rho\epsilon}{A} Q_o \sin\frac{\omega}{\epsilon} \ell \qquad (100)$$

$$Q_i = Q_o \cos\frac{\omega}{\epsilon} \ell - j\frac{A\epsilon}{\beta_e} P_o \sin\frac{\omega}{\epsilon} \ell \qquad (101)$$

The sketch below shows two condensers of equal size connected in series with a hydraulic distributed line.

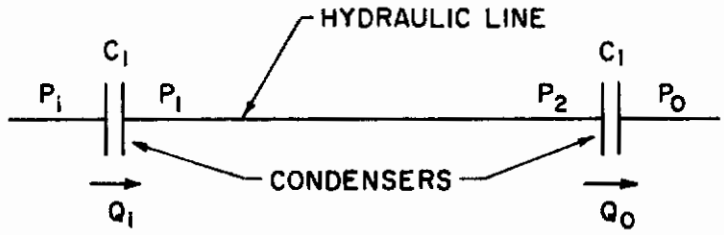

Applying Equation 100 and 101 to the above sketch

$$P_1 = P_2 \cos\frac{\omega}{\epsilon} \ell - j\frac{\sqrt{\rho\beta_e}}{A} Q_o \sin\frac{\omega}{\epsilon} \ell \qquad (102)$$

$$Q_j = Q_o \cos\frac{\omega}{\epsilon} \ell - j\frac{A}{\sqrt{\rho\beta_e}} P_2 \sin\frac{\omega}{\epsilon} \ell \qquad (103)$$

The flow and pressure relation across the condenser is

$$j\omega C_1 (P_i - P_1) = Q_i \quad \text{or} \quad P_j = P_1 - j \frac{Q_i}{\omega C_1} \tag{104}$$

$$j\omega C_1 (P_2 - P_o) = Q_o \quad \text{or} \quad P_2 = P_o - j \frac{Q_o}{\omega C_1} \tag{105}$$

Combining Equations 102, 103, 104, and 105 produce

$$P_i = P_o \left(\cos \frac{\omega}{\epsilon} \ell - \frac{1}{\omega C_1} \frac{A}{\sqrt{\rho \beta_e}} \sin \frac{\omega}{\epsilon} \ell \right) - j Q_o \frac{\sqrt{\rho \beta_e}}{A} \left[\left(1 - \frac{A^2}{\rho \beta_e} \frac{1}{\omega^2 C_1^2} \sin \frac{\omega}{\epsilon} \ell + \frac{2}{\omega C_1} \frac{A}{\sqrt{\rho \beta_e}} \cos \frac{\omega}{\epsilon} \ell \right) \right] \tag{106}$$

$$Q_i = Q_o \left(\cos \frac{\omega}{\epsilon} \ell - \frac{A}{\sqrt{\rho \beta_e}} \frac{1}{\omega C_1} \sin \frac{\omega}{\epsilon} \ell \right) - j P_o \frac{A}{\sqrt{\rho \beta_e}} \sin \frac{\omega}{\epsilon} \ell \tag{107}$$

If the following relation is true

$$\frac{-A}{\sqrt{\rho \beta_e}} \frac{1}{\omega C_1} = \frac{1 - \cos \frac{\omega}{\epsilon} \ell}{\sin \frac{\omega}{\epsilon} \ell} = \tan \frac{\omega \ell}{2\epsilon} \tag{108}$$

then Equations 106 and 107 reduce to

$$P_i = P_o \tag{109}$$

$$Q_i = Q_o - j P_o \frac{A}{\sqrt{\rho \beta_e}} \sin \frac{\omega}{\epsilon} \ell \tag{110}$$

Equations 109 and 110 show that the magnitude and phase of the output pressure are maintained the same as that of the input pressure regardless of the magnitude and phase of the output flow rate.

If the following relation is true

$$\frac{A}{\sqrt{\rho \beta_e}} \frac{1}{\omega C_1} = \frac{1 + \cos \frac{\omega}{\epsilon} \ell}{\sin \frac{\omega}{\epsilon} \ell} = \cot \frac{\omega \ell}{2\epsilon} \tag{111}$$

then Equations 106 and 107 reduce to

$$P_i = -P_o \tag{112}$$

$$Q_i = -Q_o - j P_o \frac{A}{\sqrt{\rho \beta_e}} \tag{113}$$

Equations 112 and 113 show that the magnitude of the output pressure is maintained the same as that of the input pressure, while the phase of the output pressure is maintained 180 degrees different from that of the input pressure, regardless of the magnitude and phase of the output flow rate.

Equations 108 and 111 can further be reduced to

$$C_1 = \frac{A}{\sqrt{\rho \beta_e}} \frac{1}{\omega} \cot \left(\pi - \frac{\omega \ell}{2 \epsilon}\right) \tag{114}$$

$$C_1 = \frac{A}{\sqrt{\rho \beta_e}} \frac{1}{\omega} \tan \frac{\omega \ell}{2 \epsilon} \tag{115}$$

$$= \frac{A}{\sqrt{\rho \beta_e}} \frac{1}{\omega} \cot \left(\frac{\pi}{2} - \frac{\omega \ell}{2 \epsilon}\right)$$

The size of the condensers that should be used in order that Equations 109, 110, 112 and 113 are satisfied is shown in Table IV-2.

TABLE IV-2

AN ANALYSIS OF CONDENSER SIZE WITH RESPECT TO HYDRAULIC LINE LENGTH

Hydraulic Line Length	Relations to be Satisfied	
	$P_i = P_o$ $Q_i \quad Q_i = Q_o - j P_o \frac{A}{\sqrt{\rho \beta_e}} \sin \frac{\omega \ell}{\epsilon}$	$P_i = P_o$ $Q_i = -Q_o - j P_o \frac{A}{\sqrt{\rho \beta_e}} \sin \frac{\omega \ell}{\epsilon}$
$\ell < \frac{\lambda}{2}$		$C_1 = \frac{A}{\sqrt{\rho \beta_e}} \frac{1}{\omega} \tan \frac{\omega \ell}{2 \epsilon}$
$\ell > \frac{\lambda}{2}$	$C_1 = \frac{A}{\sqrt{\rho \beta_e}} \frac{1}{\omega} \cot \pi - \frac{\omega \ell}{2 \epsilon}$	
$\ell = \frac{\lambda}{2}$		$C_1 = 0$
$\ell = \lambda$	$C_1 = 0$	

where λ, wave length $= \frac{2 \pi \epsilon}{\omega}$

4. Representation of Composite Nonviscous Line of Distributed Parameters by a Single Line

The transmission lines in a pulsating hydraulic system may not be continuous but are made up of a series of lines with condenser inertias and leakages in between the lines (such as hydraulic transformer and the leakage through the connecting seals). Therefore, it is important to know that the analytical study performed on a continuous distributed hydraulic line can also be applied to a composite distributed hydraulic line. It is found that by proper distribution of the apparatus along the transmission line, the interruption of the wave (of certain frequency) traveling by the apparatus can be eliminated. The composite distributed hydraulic line can then be treated the same as the continuous distributed hydraulic line. The schematic of the composite distributed hydraulic line is shown below in Figure IV-38.

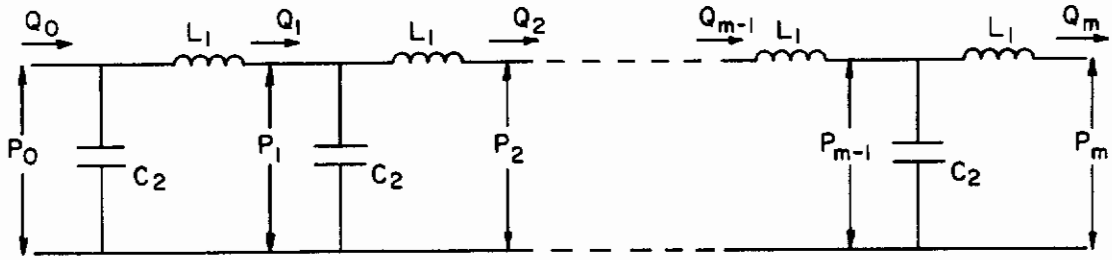

Figure IV-38. Composite Distributed Loss-Less Hydraulic Line

For simplication of analysis, the flow leakage and line loss are assumed to be zero at the present time. The basic pressure drop and flow relation of each individual section of the line can be expressed as

$$P_{n-1} - P_n = L_1 S Q_n \tag{116}$$

and

$$Q_n - Q_{n+1} = C_2 S P_n \tag{117}$$

The condition that the composite distributed line can be treated the same as the continuous distributed line is obtained by the following:

The pressure drop and flow relationship for two adjacent sections of the line are

$$P_{n-1} - P_n = L_1 S Q_n \tag{118}$$

$$P_n - P_{n+1} = L_1 \, S \, Q_{n+1} \tag{119}$$

Equation 109 and Equation 118 produce

$$P_{n-1} - 2 P_n + P_{n+1} = L_1 \, S \, (Q_n - Q_{n+1}) \tag{120}$$

pressure and flow relation across the condenser is

$$Q_n - Q_{n+1} = C_2 \, S \, P_n \tag{121}$$

Substituting Equation 121 into Equation 122 obtains

$$P_{n-1} - 2 P_n + P_{n+1} = L_1 \, C_2 \, S^2 \, P_n \tag{122}$$

Let

$$-L_1 \, C_2 \, S^2 = 2 \sin \frac{\theta}{2}$$

Equation 122 becomes

$$P_{n-1} - 2 P_n \cos \theta + P_{n+1} = 0 \tag{123}$$

Equation 124 is a possible solution of Equation 123

$$P_n = A \cos (m - n) \theta + B \sin (m - n) \theta \tag{124}$$

From Equation 124 we can write

$$\begin{aligned} P_n - P_{n+1} &= A \cos (m - n) \theta + B \sin (m - n) \theta \\ &\quad - A \cos (m - n - 1) \theta - B \sin (m - n - 1) \theta \end{aligned} \tag{125}$$

Substituting Equation 119 in Equation 125 produces

$$\begin{aligned} L_1 \, S Q_{n+1} &= A \cos (m - n) \theta + B \sin (m - n) \theta \\ &\quad - A \cos (m - n - 1) \theta - B \sin (m - n - 1) \theta \end{aligned} \tag{126}$$

If n = m - 1, than Equation 126 becomes

$$L_1 S Q_m = A (\cos \theta - 1) + B \sin \theta \tag{127}$$

Substituting boundary condition

$$P = P_a \text{ at } n = 0$$

and $$P = P_m \text{ at } n = m$$

into Equation 127 and replacing Laplace operator by $j \omega$, obtains

$$P_o = P_m \frac{\cos \left(m - \frac{1}{2}\right)\theta}{\cos \frac{\theta}{2}} + j Q_m \sqrt{\frac{L_1}{C_2}} \frac{\sin m \theta}{\cos \frac{\theta}{2}} \tag{128}$$

By the same method the following flow and pressure relation can also be obtained

$$Q_o = Q_m \frac{\cos \left(m - \frac{1}{2}\right)\theta}{\cos \frac{\theta}{2}} + j P_m \sqrt{\frac{C_2}{L_1}} \frac{\sin m \theta}{\cos \frac{\theta}{2}} \tag{129}$$

The pressure and flow relation of a continuous distributed line had been derived previously and is written here

$$P_o = P_m \cos a \ell + j Q_m \sqrt{\frac{L}{C}} \sin a \ell \tag{130}$$

where:

$$a = \omega \sqrt{LC}$$

$$L = \text{uniform inductance} = \frac{m L_1}{\ell}$$

$$C = \text{capacitance of continuous distributed line} = \frac{m C_2}{\ell}$$

Replacing L and C of Equation 130 by $\frac{m L_1}{\ell}$ and $\frac{m C_2}{\ell}$, produces

$$P_o = P_m \cos a_1 + j Q_m \sqrt{\frac{L_1}{C_1}} \sin a_1 \ell \tag{131}$$

and

$$a_1 = \frac{m \omega}{\ell} \sqrt{L_1 C_1} = 2 \frac{m}{\ell} \sin \frac{\theta}{2}$$

Comparing Equations 128 and 129 with Equations 130 and 131 respectively, obtains

$$\cos a_1 \ell = \frac{\cos \left(m - \frac{1}{2}\right)\theta}{\cos \frac{\theta}{2}} = \cos \left(2 m \sin \frac{\theta}{2}\right) \tag{132}$$

$$\sin a_1 \ell = \frac{\sin m\theta}{\cos \frac{\theta}{2}} = \sin \left(2 m \sin \frac{\theta}{2} \right) \tag{133}$$

If θ is a very small number, then Equation 132 reduces to

$$\theta \sin m\theta = 0$$

or

$$\sin m\theta = 0 \tag{134}$$

Equation 133 results in a trivial solution

$$\sin m\theta = m\theta$$

In order for Equation 134 to be satisfied, the following relation must hold

$$\theta = \pm \frac{K\pi}{m} \tag{135}$$

where $K = 0, 1, 2, \ldots$

From Equation 133

$$a_1 \ell = 2 m \sin \frac{\theta}{2} \approx m\theta \qquad (\text{for } \theta \rightarrow \text{small})$$

Because

$$a_1 = \frac{2\pi}{\lambda} \qquad (\lambda = \text{wave length})$$

We have

$$\frac{2\pi\ell}{\lambda} = m\theta = \pm K\pi$$

or

$$\ell = \frac{K\lambda}{2} \tag{136}$$

Therefore, in order that the composite distributed line can be treated the same as the continuous distributed line, the following two relations must hold

$$\sin \frac{\theta}{2} \approx \frac{\theta}{2}$$

and the length of the composite distributed line should be a multiple of half wave length of the continuous distributed line.

E. THE EFFECT OF SYSTEM COMPONENTS AND FLOW PARAMETERS ON THE SYSTEM PERFORMANCE

The load response of the system can be predicted as long as the input and return pressure of the servo-valve are known and kept constant throughout the system operation. In other words, the load response of a pulsating hydraulic system depends not only on the system control loop, but also on the capability of the system to maintain constant input and return pressure in the continuous-flow section at various flow demand conditions. The capability of maintaining input and return pressures constant is, in turn, dependent on the accumulator size, transmission line dynamics, and the pump response of the system. The discussion of this subsection is, therefore, devoted to the effect of system components on the pressure of the continuous flow section.

1. Effect of High Pressure Accumulator Size on the Pressure and Flow Filtering

For a pulsating hydraulic system with constant flow as its input, the flow downstream of the rectifier can be assumed to be fully rectified sinusoidal pulses, as shown in Equation 137.

$$Q = \frac{2}{\pi} Q_o - \frac{4}{\pi} Q_o \left[\frac{1}{3} \cos 2\omega t + \frac{1}{15} \cos 4\omega t + \ldots \right] \qquad (137)$$

The first term of Equation 137 is a direct component of the flow; the other terms are high-order harmonic components of the flow. Assuming the low pressure accumulator pressure, P_ℓ, remains fairly constant, the high pressure accumulator and system load can be represented schematically by Figure IV-39.

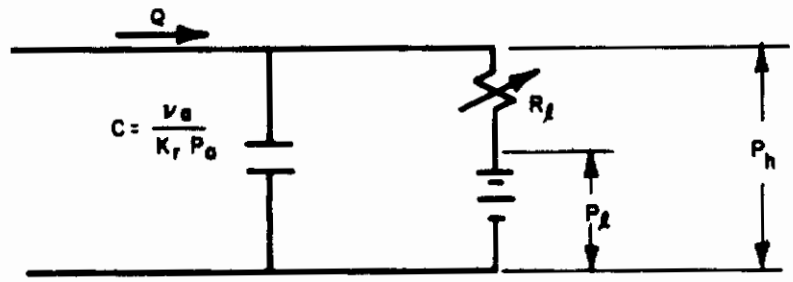

Figure IV-39. **Schematic Representation of High Pressure Accumulator and the Equivalent System Load**

The ratio of pressure variation to the pressure at the accumulator can be obtained from Figure IV-39 as

$$\left| \frac{\Delta P_h}{P_h} \right| \simeq \frac{2}{3} \frac{K_r P_a}{R_\ell \nu_a \omega} \qquad (138)$$

Equation 138 can be used to determine the relationship among the accumulator volume, pulsating frequency, and equivalent load resistance for maintaining pressure ratio, $\left| \frac{\Delta P_h}{P_h} \right|$, to be equal or less than pre-designed value. Figure IV-40 is the graphical representation of Equation 138 for $\left| \frac{\Delta P_h}{P_h} \right| = 0.02$.

For a system that has pressure as its input, the flow downstream of the rectifier is close to fully rectified square wave pulses. Hence, the pulsation filtering is relatively more easily achieved.

2. Effect of Low Pressure Accumulator Size on the System Performance

The purpose of the low pressure accumulator is to provide uniform and constant return pressure at the continuous flow section during the return stroke of the flow. A uniform and constant return pressure in the continuous flow section can force the return flow to satisfy its continuity equation with the lowest pressure amplitude and reduce the harmonic pressure component in the direct flow section.

3. Effect of Pump Response to the System Performance

For a system that has a pulsating flow source as its input (such as the miniaturized system setup), a pressure sensor can be used at various locations to adjust the pulsating flow amplitude, as shown in Figure IV-41. The change of pulsating flow amplitude is necessary to maintain constant input and return pressure between the rectifier and servo-valve during the variation of flow demand. The maximum transient deviation of the input and return continuous pressure from their steady-state value depends on:

- The variation of the rate of flow demand.
- The response of the pressure sensor, pump stroke adjusting mechanism, and the pulsating flow pump.
- The size of the accumulators in the continuous flow section.

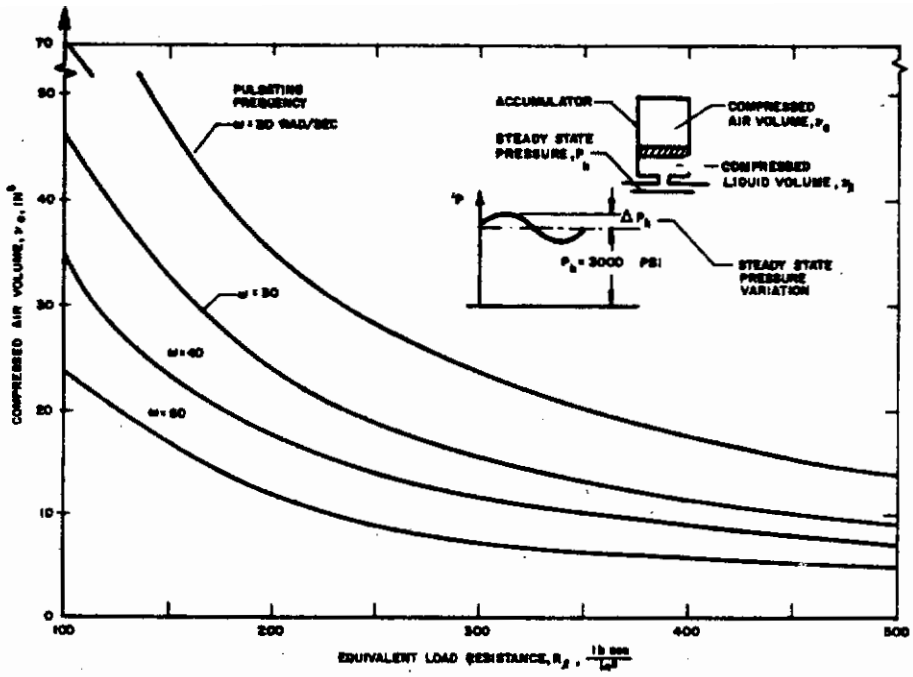

Figure IV-40. Accumulator Volume, Pulsating Frequency, and Equivalent Load Resistance Relationship for Maintaining $\left|\frac{\Delta P_h}{P_h}\right| \leq 0$ for Steady-State System Operation.

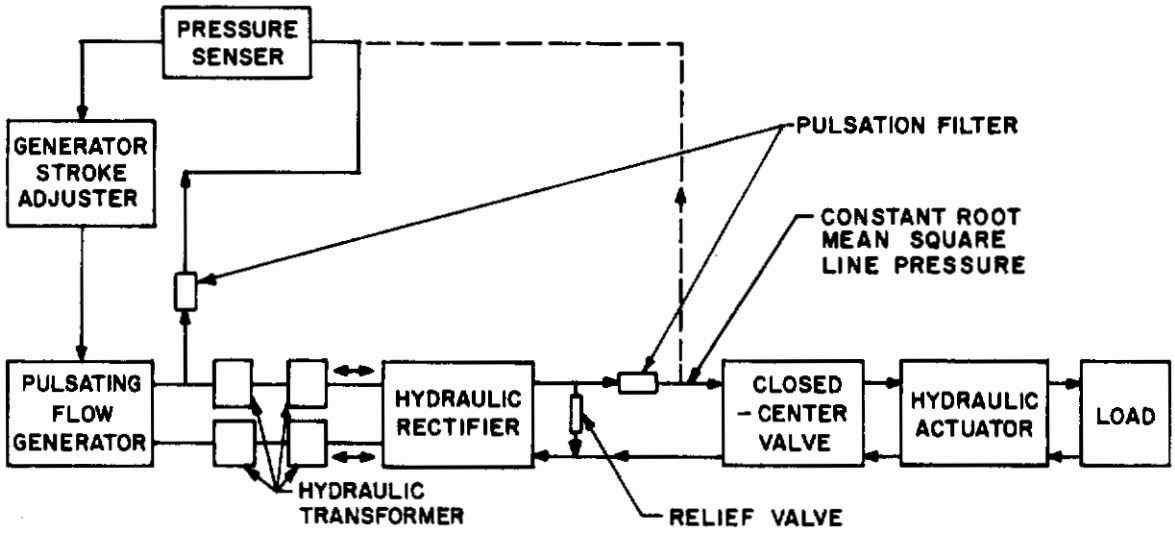

Figure IV-41. Schematic of Flow Amplitude Adjustment

For a known change of the rate of flow demand, increase of the accumulator size and the response of the pressure sensor, pump stroke adjusting mechanism, and pulsating flow pump will reduce the deviation of the input and return continuous pressure from their steady-state value. Optimization is necessary between the size of the accumulator and the response of the pressure sensor, the pump stroke adjusting mechanism, and the pulsating flow pump for actual system design.

For a system that has a pulsating pressure source as its input, the adjustment of flow is achieved by the continuous flow pump. Therefore, both the accumulator size and the pump response are responsible for minimizing the input and return pressure deviation at the servo-valve.

4. The Effect of Fluid Cavitation on System Efficiency and Power Capacity

As anticipated, fluid cavitation was observed during the system efficiency test. The cavitation of fluid was apparently caused by the formation of a vacuous space between the pump piston and its surrounding fluid, due to insufficient fluid pressure in the low pressure accumulator. The low pressure accumulator is located at the low pressure side of the direct flow section. The pressure within it is necessary to overcome the friction, inertia, and capacitance effects of the fluid and the line during operation. Experiments were, therefore, conducted, using both the miniaturized system and the pulsating flow line loss test setup, to obtain the relations among the pulsating frequency, pulsating stroke, and fluid cavitation. Different system precharge pressures (precharge pressure of the low pressure accumulator) were used during the test in order to find their effect on the fluid cavitation. Figure IV-42 shows both the test results and the approximate theoretical predictions. The test results are quite close to the theoretical predictions except at the vicinity of low frequencies. The test results also agree with the theoretical prediction that, for the same precharge system pressure, the value of the critical pulsating frequency that causes fluid cavitation decreases as the pulsating stroke increases. For the same pulsating stroke, the critical pulsating frequency increases as the precharge system pressure increases.

For a pulsating system that has either a pressure source or a flow source, fluid cavitation will reduce the width of the pressure and flow pulses. The amplitude of the pressure and flow pulses will not be reduced unless the vacuous space extends to more than half of the total fluid displacement during each half cycle. Two apparent results are:

- The reduction of average pressure amplitude and lowering of the power capacity of a system of known design.
- The reduction of system efficiency. However, the reduction in this system resulting from the fluid cavitation is not as serious as that in machinery such as the steam turbine, etc.

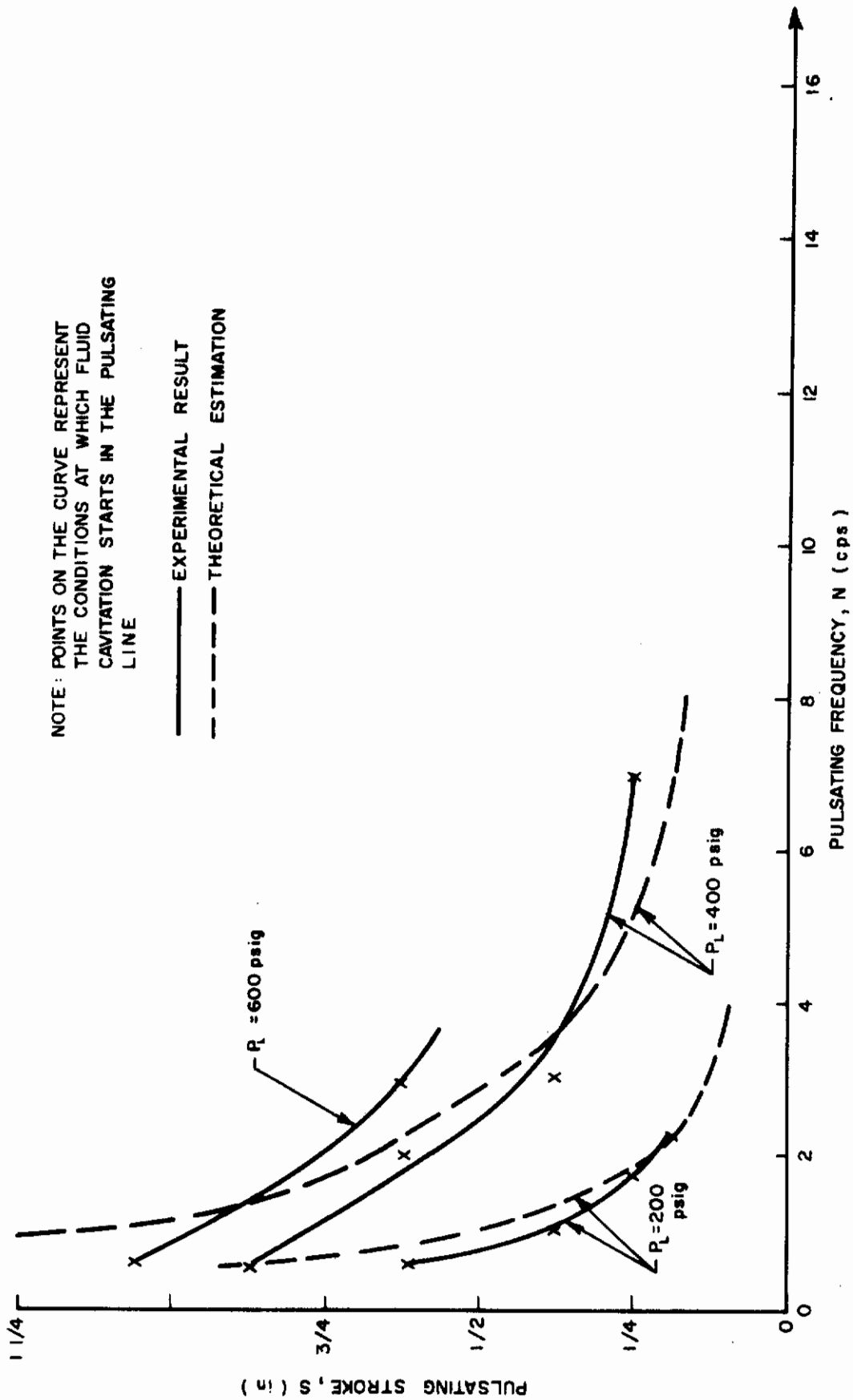

Figure IV-42. Pulsating Frequency, Pulsating Stroke, and Fluid Cavitation Relationships of the Miniaturized Pulsating Hydraulic System for Various System Precharge Pressures

F. COMPARISON OF PULSATING HYDRAULIC SYSTEMS WITH CONSTANT PRESSURE SOURCES AND CONSTANT FLOW SOURCES

For analytical representation, a system with a constant pressure source is defined as one in which the pressure at the input tends to remain constant and the flow varies on demand. Such a system is exemplified by one in which a pressure-compensated variable delivery pump is used and the pulsations are caused by the introduction of an alternator valve.

A constant flow source system is one in which the pulsating energy is generated by a reciprocating cylinder or similar means, as in the miniaturized system. In such a system, the flow is a function of the driving frequency and stroke of the pumping cylinder.

Analytical investigation shows that a pulsating hydraulic system with a constant pressure source has more advantages than a pulsating hydraulic system with a constant flow source. The following is a comparison of the two systems; the advantages of one system are the disadvantages of the other.

1. Advantages of systems with a constant pressure source:

   - Small power is required to drive the pulsating valve; hence the pulsating frequency is more easily controlled and maintained.
   - A commercial pressure-compensated variable delivery pump can be used in combination with a pulsating valve as the hydraulic power unit of the system. No new pump development is necessary.
   - Pressure pulses traveling back and forth in the fluid line are near square-wave shape. For the same power transmitted through the line, the maximum pressure level in the line is thus less than that of the fluid line of a system with a flow source.
   - Depending on the characteristics of the pulsating valve and pump, the flow pulses traveling back and forth in the fluid line can also be made close to square-wave shape, thus reducing the peak flow Reynolds' number. This fact is very important when the Reynolds' number of the flow is near or larger than the critical Reynolds' number.

2. Advantage of systems with a constant flow source:

   - No pulsating valve and its associated driving mechanisms areneeded. The system therefore has fewer components.

It should be indicated here that all the assumptions and boundary conditions used in reaching the above comparisons have been carefully justified. However, verification of the comparisons will not be made experimentally until a full-size pulsating hydraulic system is built and tested.

G. ANALYTICAL STUDY OF VISCOSITY EFFECT ON A PULSATING TRANSMISSION LINE

Little information is currently available on the friction characteristics of a fluid in a pulsating system. Several technical papers dealing with similar problems have been published; however, they dealt mainly with direct flow with sinusoidal flow of small amplitudes superimposed on it. Even though the constantly transient flow of the pulsating system has the same Reynolds' number as the steady, direct flow, it is believed that the friction characteristics of the two are quite different. Therefore, it was decided to emphasize analytical and experimental studies of the pulsating transmission line loss.

An impedance method was used to study the dynamic responses of pulsating flow.

For establishing correct and simplified analytical representations of the P-F fluid line behavior, for rapid analytical study, several simplified four-terminal block diagrams using different fluid-line models were derived in this subsection. Those analytical models that best matched the experimental results were used in the analytical and analog computer study of the P-F hydraulic system efficiency and dynamic response. Experimental results are shown in Subsection H.

1. Viscous Line With Distributed and Lumped Parameters

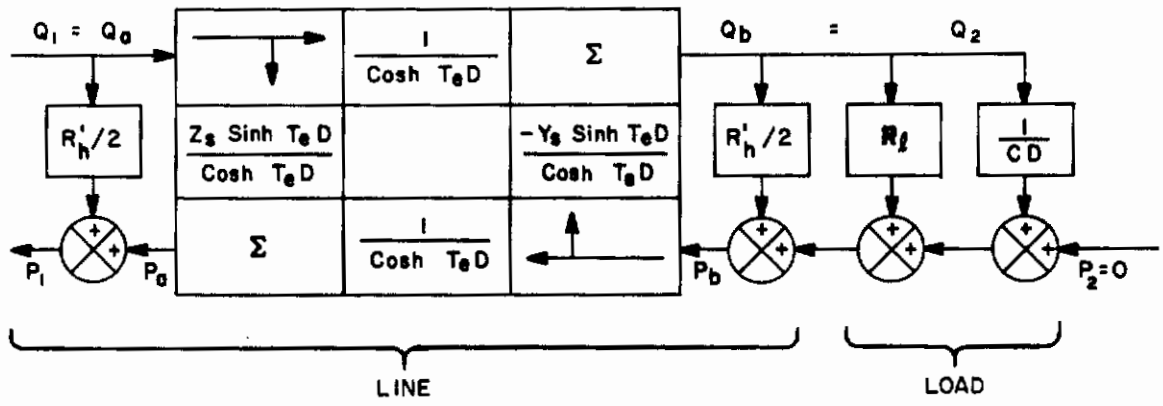

Figure IV-43. 4-Terminal Block Diagram Representation of Fluid Line With Distributed and Lumped Parameters

In this model, the inertia and compliance of the fluid line are assumed to be the distributed parameters, while the resistance is assumed to be a lumped parameter. The lumped resistance is divided into two halves and concentrated at each end of the line. Figure IV-43 is the four-terminal block diagram representation of this model; all variables in Figure IV-43 have incremental values. The accumulator in the test setup is large enough that its impedance, 1/CD, and pressure, P_2, can be assumed to be zero, and the downstream pressure, P_2, is negligible. The imput impedance of the fluid line loss test setup was derived and shown in Equations 139 and 140.

$$\left| Z_i \right| = \left| \frac{P_1}{Q_1} \right| = \frac{1}{C_1} \left(\left[\frac{R'_h C_1}{2} + \alpha Z_s \right]^2 + \left[\frac{Z_s}{2} \quad 1 - \alpha^2 \quad \text{Sin } 2 T_e \omega \right]^2 \right)^{\frac{1}{2}} \tag{139}$$

$$\phi_i = \tan^{-1} \left[\frac{Z_s \left(1 - \alpha^2 \right) \text{Sin } 2 T_e \omega}{\left(R'_h C_1 + 2 \alpha Z_s \right)} \right] \tag{140}$$

where

$$C_1 = \text{Cos}^2 T_e \omega + \alpha^2 \text{ Sin } T_e \omega$$

$$\alpha = \left(\frac{R'_h}{2} + R_\ell \right) \Big/ Z_s$$

Graphical representation of Equations 139 and 140 is shown in Figures IV-54a and IV-54b.

If the total value of the load resistance (R_ℓ) and half of the total line loss $\frac{R'_h}{2}$ is equal to that of the line characteristic impedance, the input impedance of the line can be obtained by

$$Z_1 = \frac{P_1}{Q_1} = \left| Z_1 \right| e^{j\phi} \tag{141a}$$

where $$\left| Z_1 \right| = \left[\left(\frac{R'_h}{2} + \frac{\sqrt{\rho \beta_e}}{A} \right)^2 + \left(\frac{-R_h}{2A\omega} \sqrt{\frac{\beta_e}{\rho}} \right)^2 \right]^{\frac{1}{2}}$$

$$\phi = \tan^{-1} \left[\frac{\frac{R_h}{-2A\omega} \sqrt{\frac{\beta_e}{\rho}}}{\frac{R'_h}{2} + \frac{\rho \beta_e}{A}} \right] \tag{141b}$$

$$R'_h = \frac{128 \mu \ell}{\pi D^4}$$

The load impedance (R_ℓ) was used to match the line characteristic impedance so that no pressure wave would be reflected back.

Since the input flow to the system is

$$Q_1 = R_y \left[Q_o \, e^{j\omega t} \right] , \tag{142a}$$

the input pressure can be expressed as

$$P_1 = R_y \left[\left| Z_1 \right| \, e^{j(\omega t + \phi)} \right] \tag{142b}$$

where Z_1 and ϕ are the same as in Equation 141.

Input impedance and phase angle vs pulsating frequency characteristics of Equation 142 are plotted in Figure IV-44.

2. Non-Viscous Line With Distributed Parameters

Figure IV-45 is the analytical representation of the line loss test setup, with the line considered to be of distributed parameters and frictionless. Again, the impedance (1/CS) and the pressure variation (P_2) due to the input disturbances are assumed to be small. The input impedance of the line can be obtained as the following form;

$$\left| Z_i \right| = \frac{Z_s}{C_1} \sqrt{\alpha^2 + \tfrac{1}{4} \left(1 - \alpha^2 \right)^2 \left(\text{Sin } 2 \, T_e \, \omega \right)^2} \tag{143a}$$

$$\phi_i = \tan^{-1} \left[\frac{\left(1 - \alpha^2 \right) \text{ Sin } 2 \, T_e \, \omega}{2 \alpha} \right] \tag{143b}$$

if the load impedance (Z_ℓ) is equal to the line characteristic impedance (Z_s)

$$Z_1 = \left| Z_1 \right| \, e^{j\varphi} = Z_s = \frac{1}{A} \sqrt{\rho \beta_e} \tag{144}$$

where $\phi = 0$

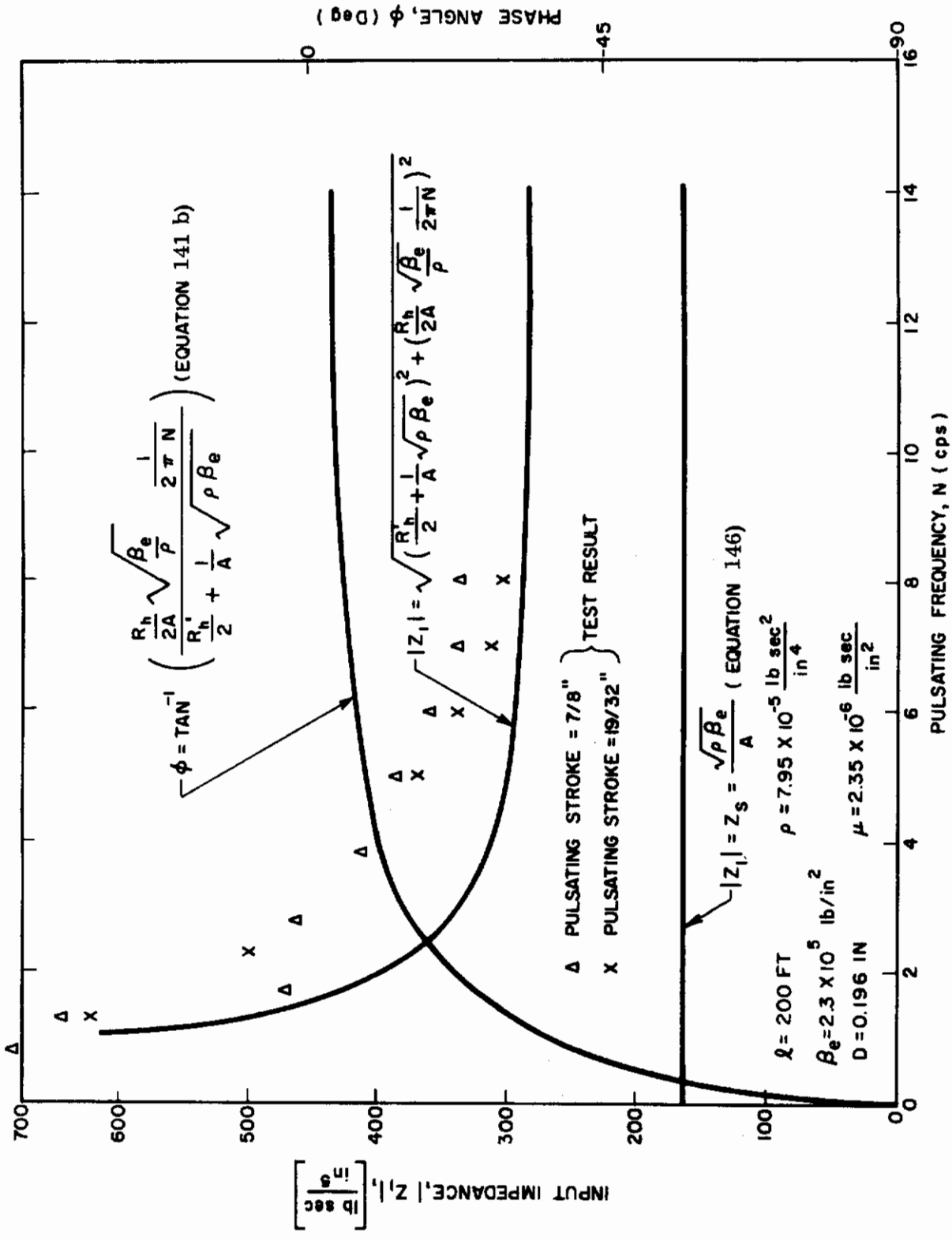

Figure IV-44. Input Impedance vs Pulsating Frequency Characteristics

The input impedance vs pulsating frequency characteristics of Equation 144 are also plotted in Figure IV-44.

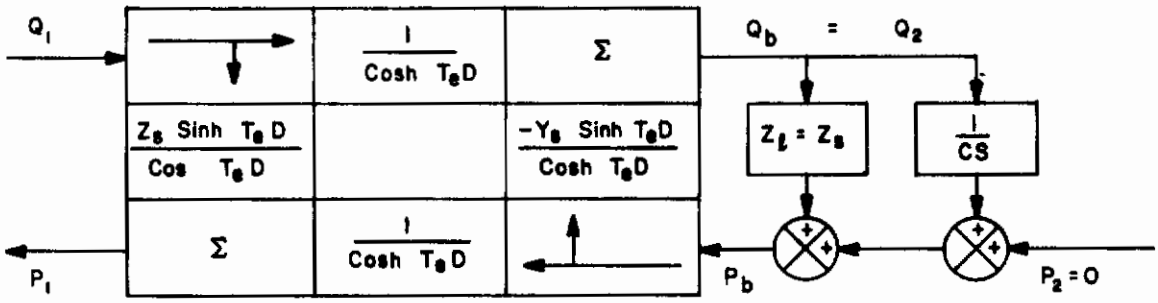

Figure IV-45. 4-Terminal Block Diagram Representation of Nonviscous Fluid Line With Distributed Parameters

3. Viscous Line With Distributed Parameters

The input impedance equation of a distributed line was derived in Appendix A and is rewritten

$$Z_1 = Z_s \frac{Z_\ell - Z_s \tanh \gamma \ell}{Z_s - Z_\ell \tanh \gamma \ell} \tag{145}$$

If the load impedance (Z_ℓ) is equal to the line characteristic impedance (Z_s), or when the line length, ℓ, is very long, the input impedance of the line reduces to

$$Z_1 = Z_s = \frac{\sqrt{\rho \beta_e}}{A} \left(1 - j \frac{R_h}{2 \rho \omega} \right) \tag{146}$$

which is the characteristic impedance of the line.

The input impedance vs pulsating frequency characteristics of Equation 146 are plotted in Figure IV-46. It should be pointed out that Equation 146 will not give accurate results at very low frequency. This is because the assumption $\alpha_1 < r_1$, that was used during the derivation of Equation 146, is not valid when the pulsating frequency is very low.

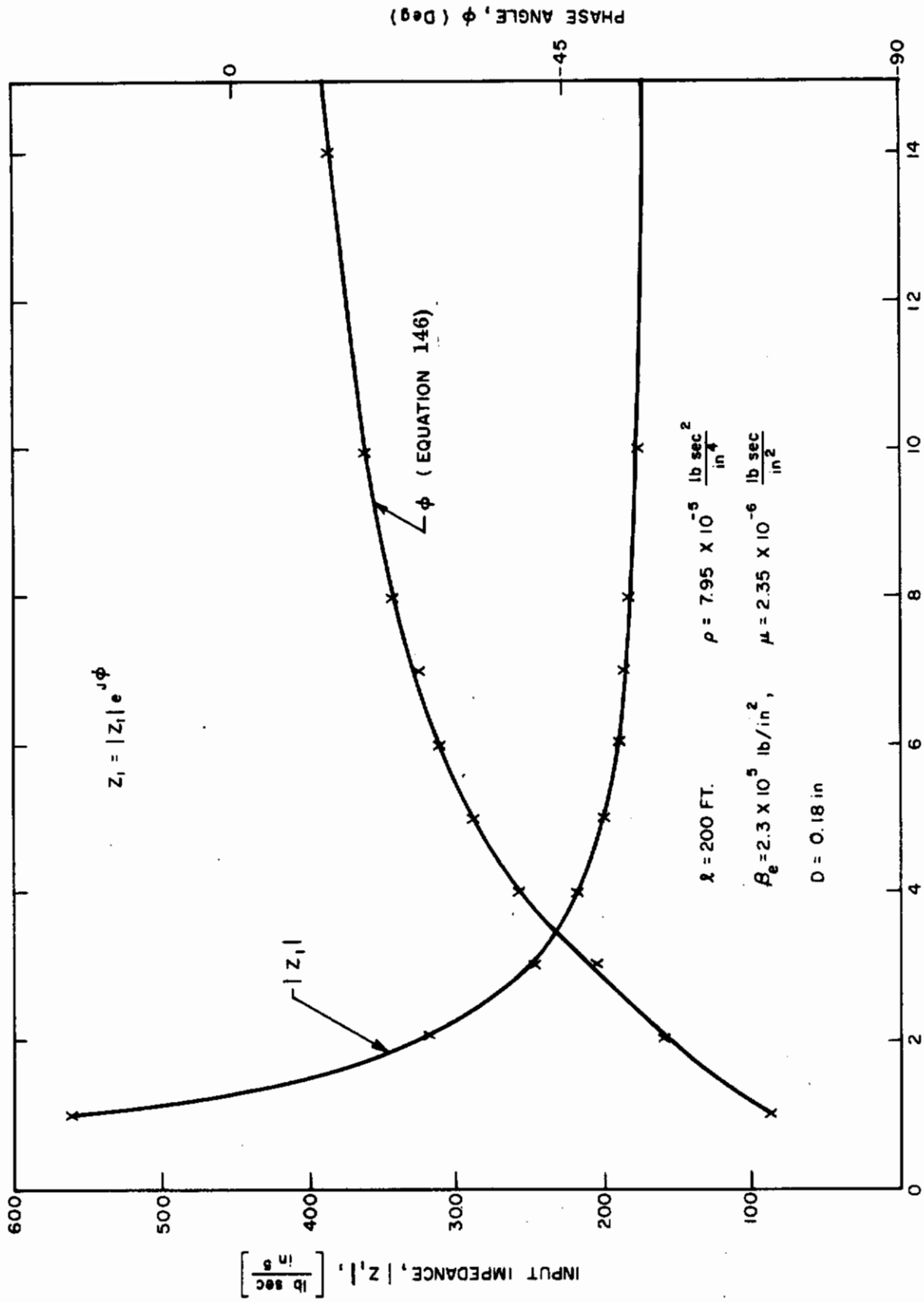

Figure IV-46. Input Impedance vs Pulsating Frequency for Viscous Line of Distributed Parameters When Load Impedance is Equal to Line Characteristic Impedance

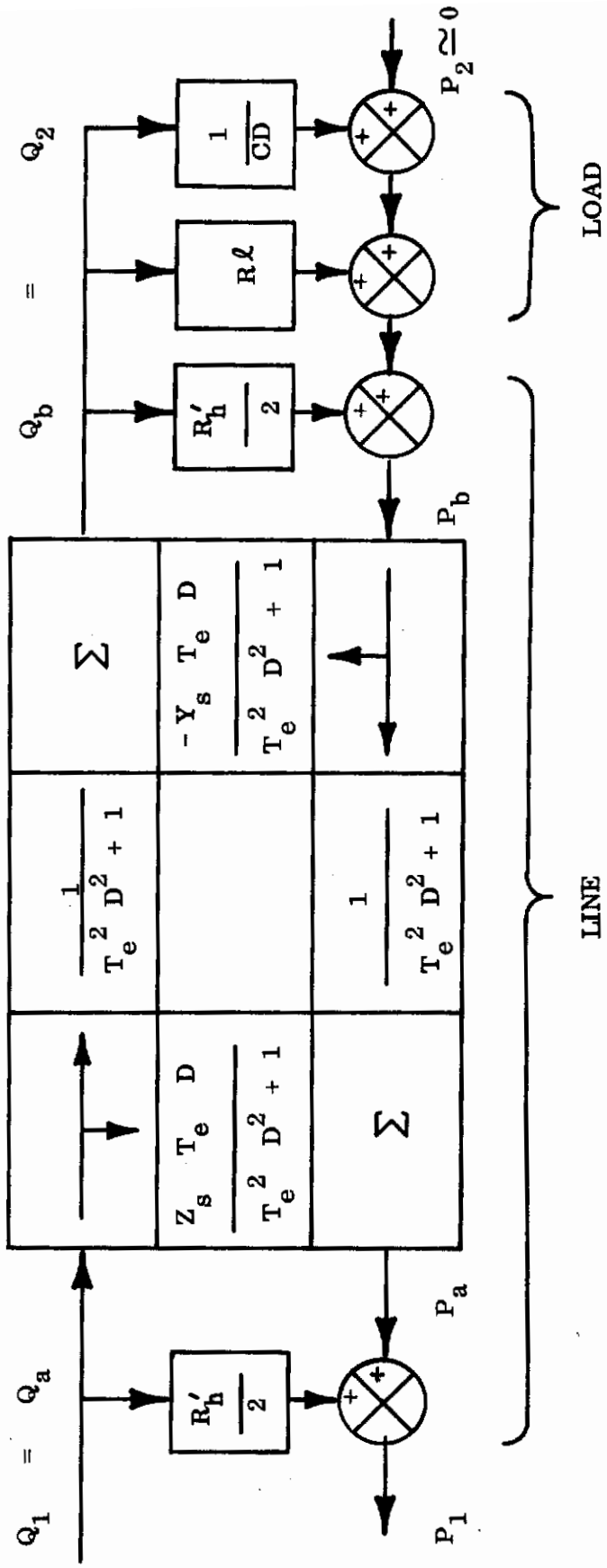

Figure IV-47. 4-Terminal Block Diagram Presentation of Fluid Line With Lumped Parameters

4. Viscous Fluid Line With Lumped Parameters

In this model, all parameters of the fluid line are assumed to be lumped. The lumped resistance is again assumed to be divided into halves, one half concentrated at each end of the line. Figure IV-47 is the four-terminal block diagram representation of the lumped parameter line; its input impedance was similarly derived.

$$\left|Z_i\right| = \left(\left[\frac{R'_h}{2}\left(1+\frac{1}{C_2}\right)\right]^2 + \left(\frac{Z_s\, T_e\, \omega}{1 - T_e^{\,2}\,\omega^2} - \frac{R'_h\, Y_s\, T_e\, \omega}{2\, C_2}\right)^2\right)^{\frac{1}{2}} \tag{147}$$

$$\phi = \tan^{-1}\left[\frac{\dfrac{Z_s\, T_e\, \omega}{1 - T_e^{\,2}\,\omega^2} - \dfrac{R'_h\, Y_s\, T_e\, \omega}{2\, C_2}}{\dfrac{R'_h}{2}\left(1+\dfrac{1}{C_2}\right)}\right] \tag{148}$$

where: $C_2 = \left(1 - T_e^{\,2}\omega^2\right)^2 + \left(\frac{R'_h}{2}\, Y_s\, T_e\, \omega\right)^2$

R_ℓ is assumed to be zero.

H. PULSATING FLOW LINE LOSS TEST SETUP AND EXPERIMENTAL RESULTS

1. Direct Flow Loss of Short Transmission Line

To obtain more accurate comparison between direct flow and pulsating flow losses, tests were carried out to measure direct flow loss using the same transmission line that was used to measure pulsating flow loss. The test setup is shown in Figure IV-48. The line is 117 inches long and is bent to a circular loop that has the same diameter as that of the loops used in the pulsating flow loss test.

Figure IV-49 is the theoretical and experimental direct flow resistance vs flow rate characteristics. Figure IV-50 shows the same result, but is plotted in a different manner. The plots are the friction coefficient vs Reynolds number characteristics. It can be seen from the figures that there is close agreement between the theoretical and experimental results.

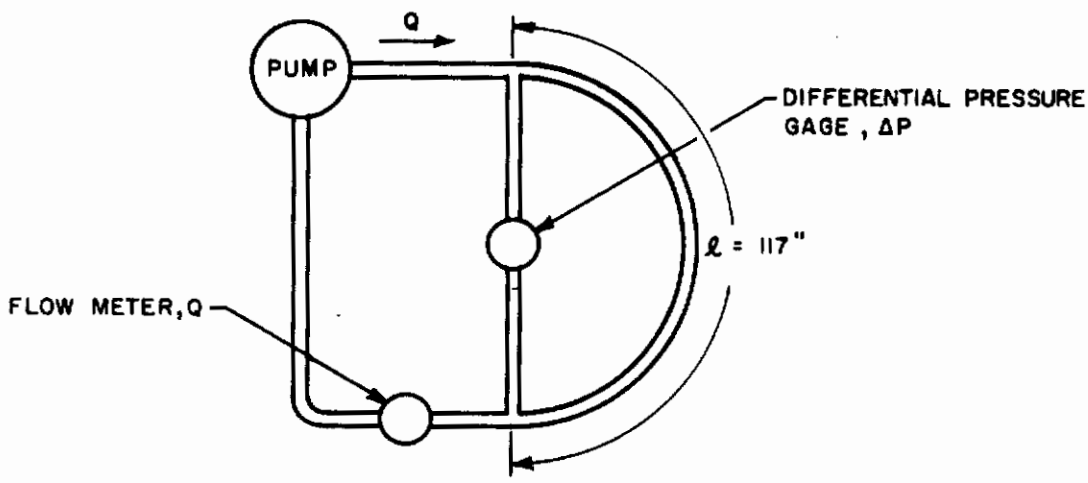

Figure IV-48. Test Setup of Direct Flow Loss Through a Short Line

2. Pulsating Flow Loss of Fluid Line With Distributed and Lumped Parameters

Figures IV-51 and IV-52 are the schematic and photograph of the line loss test setup for studying pulsating flow. During the positive stroke, the pump forces the fluid through the line into the accumulator; then, during the negative stroke, the accumulator pressure forces the fluid back through the line into the pump.

The accumulator precharge pressure was varied during different tests to avoid fluid cavitation. The effect of this variation on the test results is insignificant because of the pressure insensitivity of the fluid bulk modulus, the viscosity, and the mass density. The linear hydraulic resistor shown in the test setup was specially designed and has a linear range from 0.1 to 10 GPM. The purpose of having a linear hydraulic resistor in the test setup was to reduce the amplitude of the reflected pressure wave, during the test, so that a comparison could be made with the experimental input impedance of the same fluid line with no linear hydraulic resistor installed in the test setup. Hydraulic fluid MIL-H-5606 was used during the test.

The Mark V flow transducer of Rampo Instrument Company was used to measure the P-F, which has a flat frequency response of about 100 cps. The flow rate can also be calculated from the pressure drop across the linear resistor. Because the physical length of the linear resistance unit is much shorter than the expected shortest pressure wave length, the flow through the linear resistance can be considered as a slug flow and is essentially in phase with the pressure drop. Several pressure pickups were installed along the hydraulic line to measure the flow pressure. All instruments used during the test have dynamic responses much faster than required for obtaining accurate test results. Tests that were performed include:

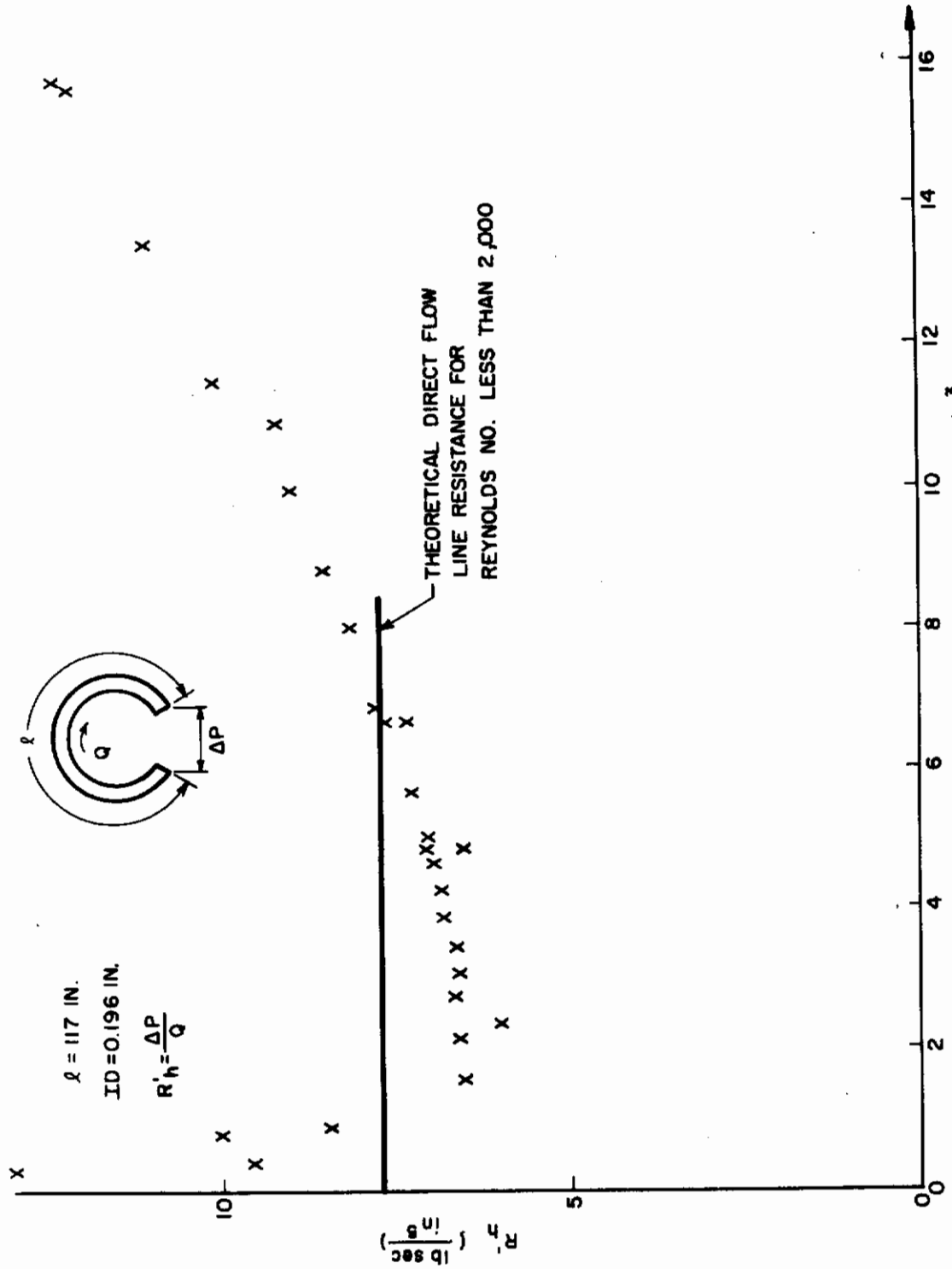

Figure IV-49. Theoretical and Experimental Direct Flow Resistance of Short Line

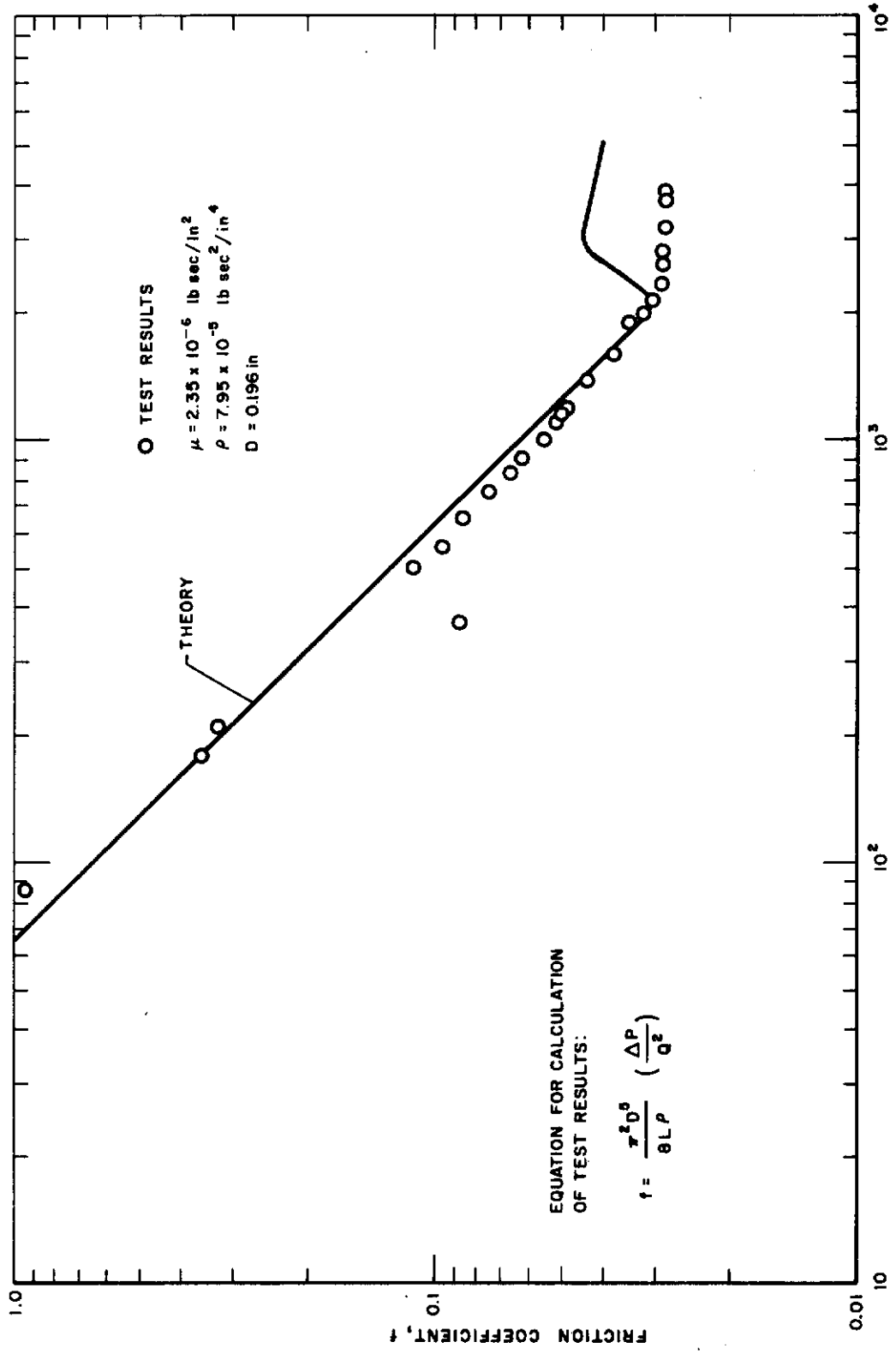

Figure IV-50. Theoretical and Experimental Direct Flow Friction Coefficient of Short Line

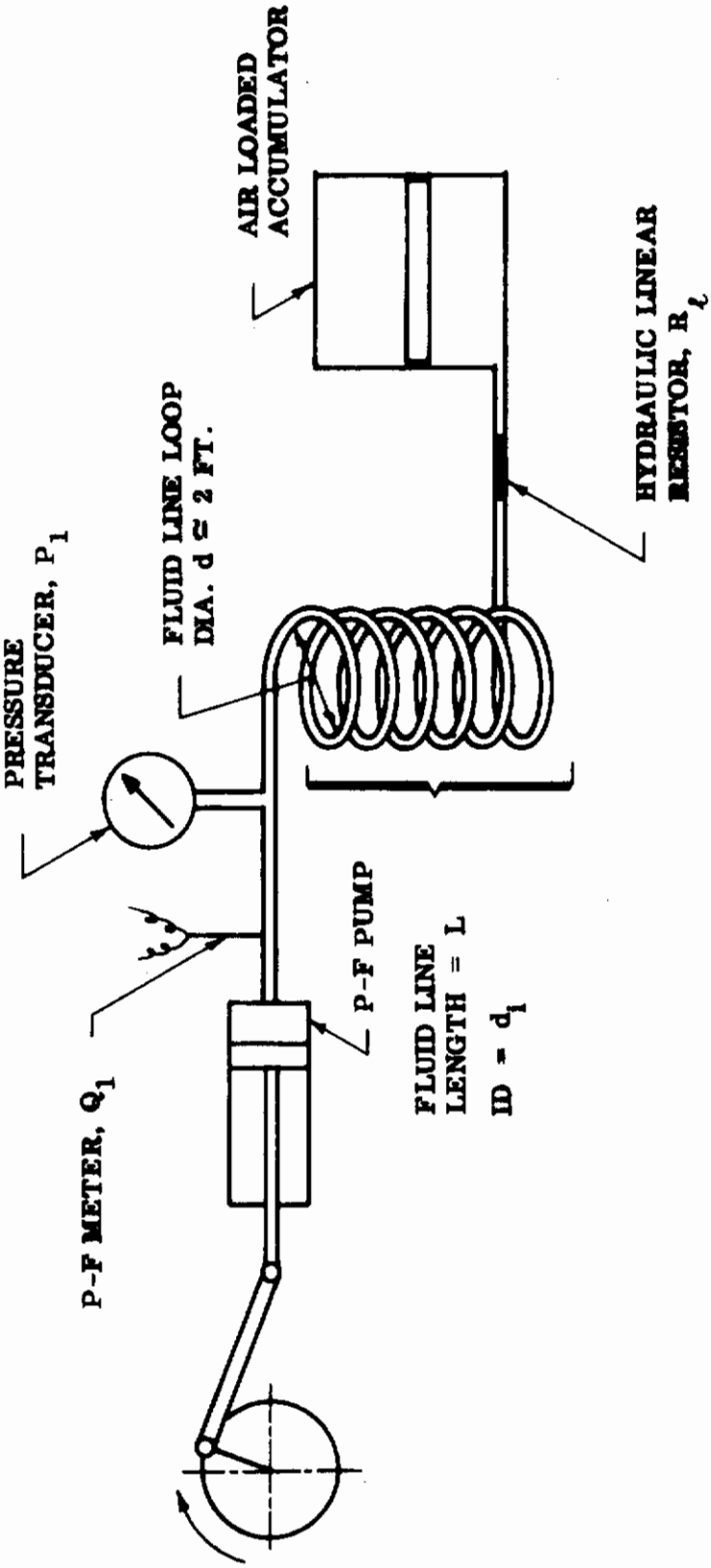

Figure IV-51. Line Loss Test Setup for Pulsating Flow

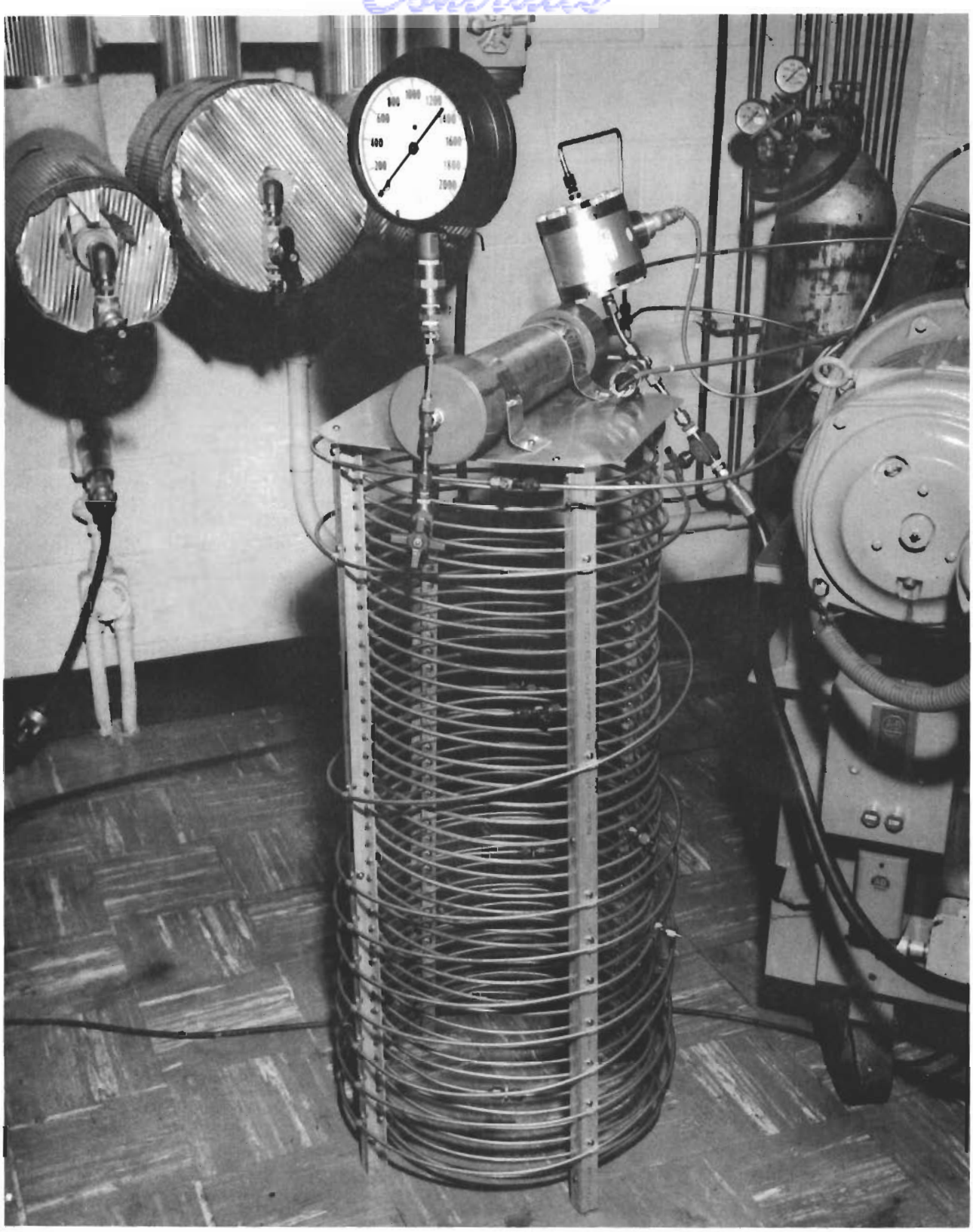

Figure IV-52. Pulsating Flow Loss Test Setup For Line of Distributed Parameters

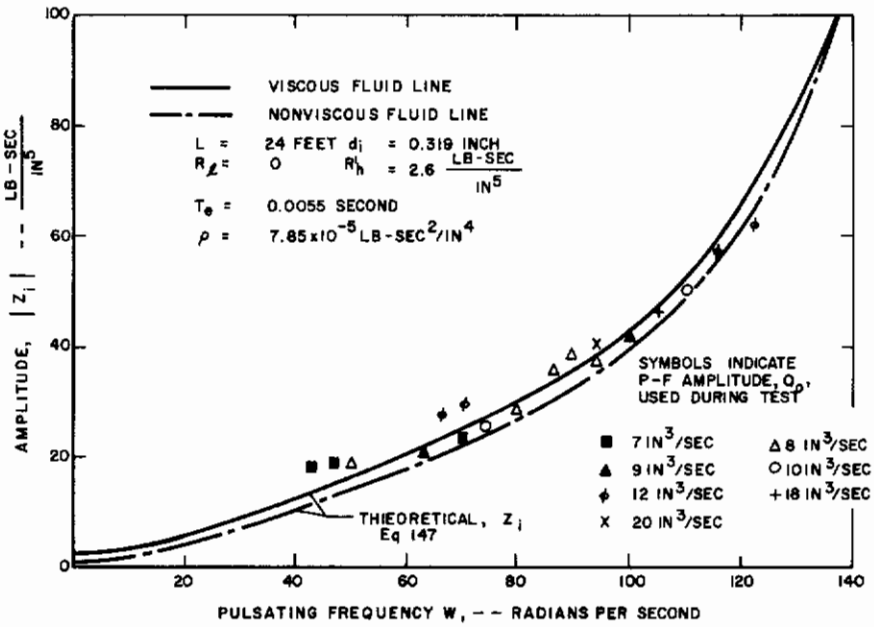

a. Amplitude vs Pulsating Frequency

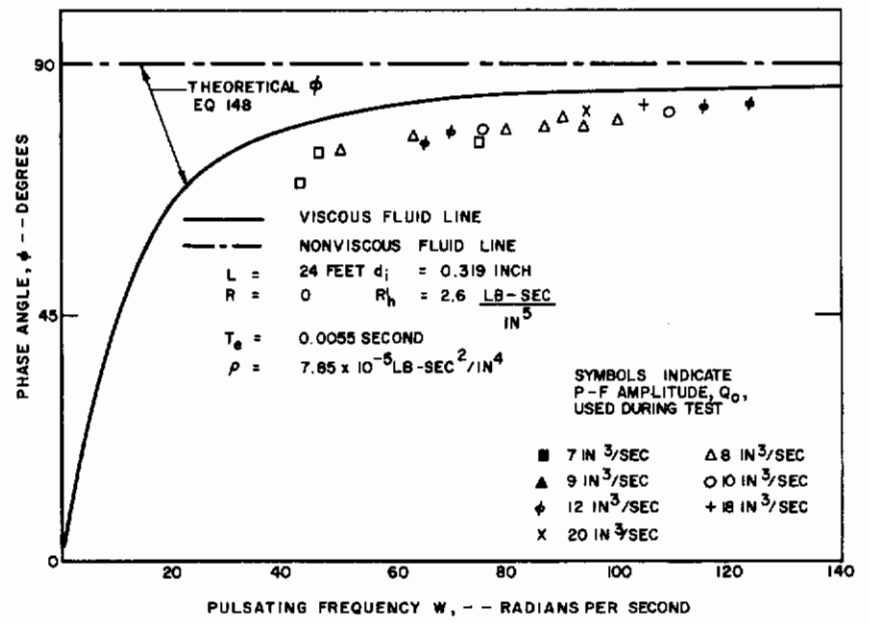

b. Phase Angle vs Pulsating Frequency

Figure IV-53. Theoretical and Experimental Input Impedance of Short P-F Fluid Line

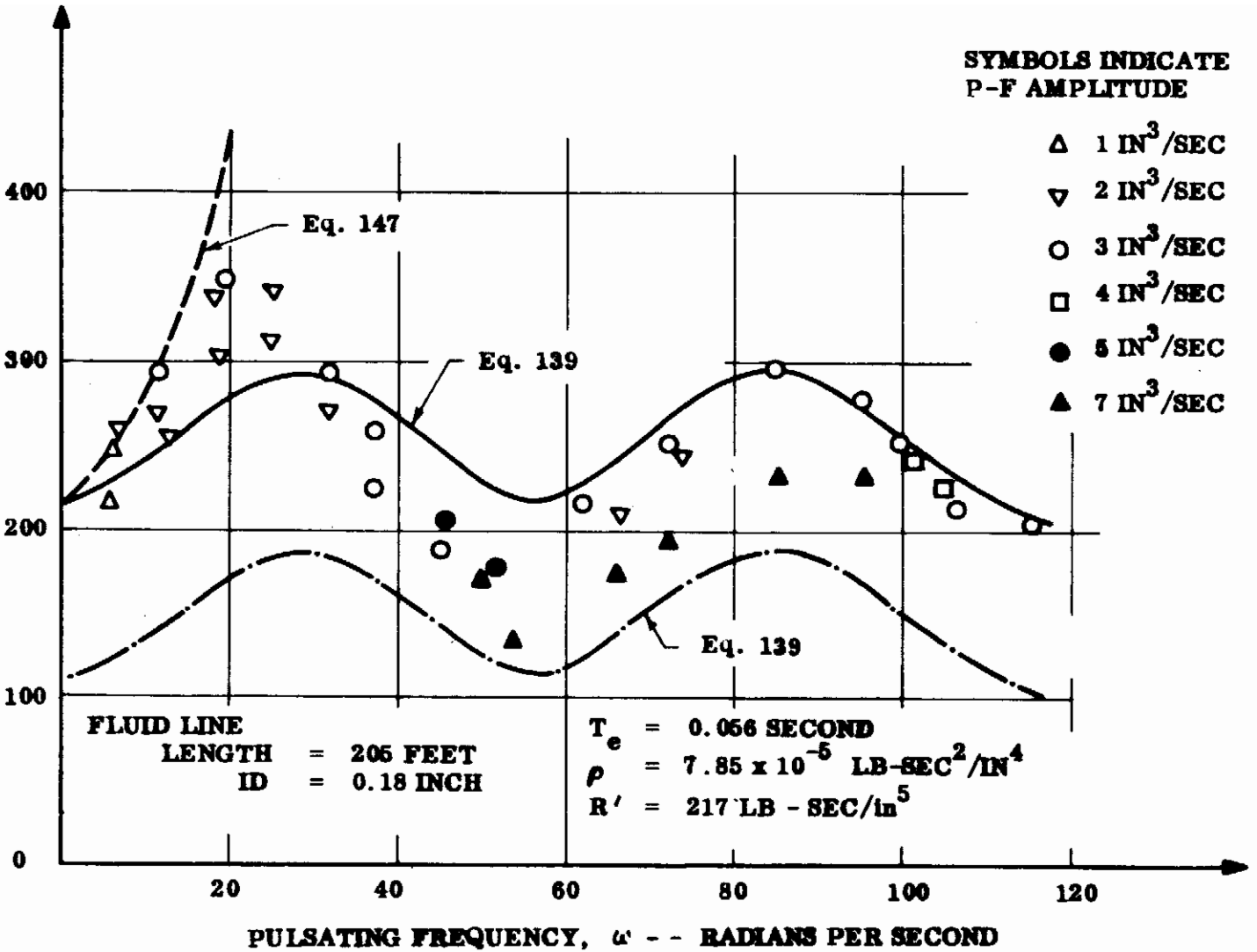

Figure IV-54a.. Theoretical and Experimental Input Impedance of Long P-F Fluid Line With Zero Load Impedance

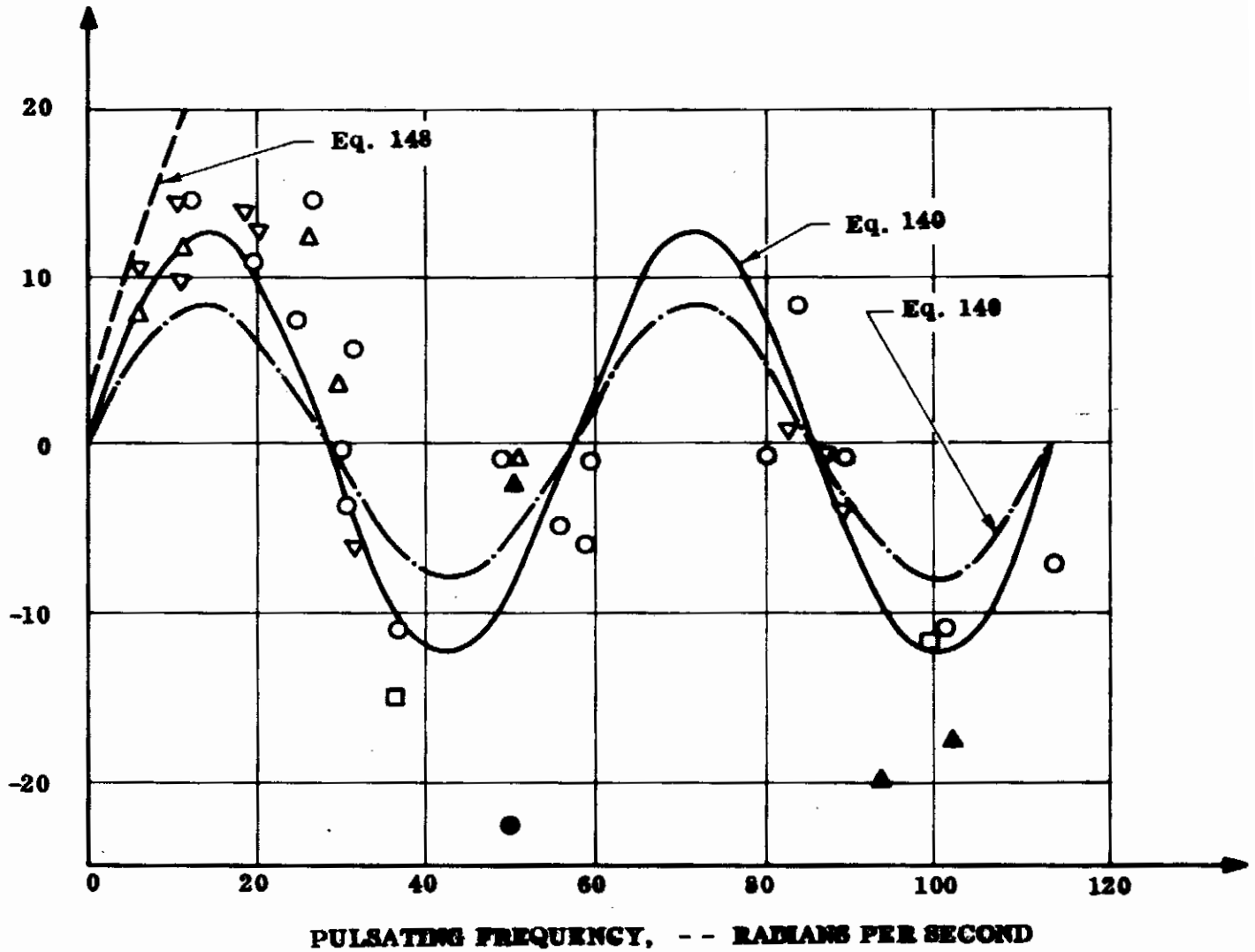

Figure IV-54b. Theoretical and Experimental Input Impedance of Long P-F Fluid Line With Zero Load Impedance

(1) Line loss vs pulsating frequency and stroke (or Reynolds number). (Figure IV-50)

(2) Gain and phase change of pulsating pressure and flow vs pulsating frequency and stroke. (Figure IV-53)

(3) Input impedance of the line. (Figure IV-54a and Figure IV-54b)

(4) Minimum precharge accumulator pressure to avoid flow cavitation. (Figure IV-42)

Test results of the fluid line with lumped and distributed parameters were reduced and plotted in Figures IV-53 and IV-54 respectively.

I. EFFICIENCY ESTIMATE OF THE SIMPLIFIED PULSATING HYDRAULIC SYSTEM MODEL

Figure IV-55 is a simplification of Figure 25a of the Second Quarterly Progress Report, RAC 933-2. The simplifications include:

- No hydraulic transformer is used in the transmission line.
- The losses in the hydraulic rectifier are neglected.
- The system is operated at low load and low flow conditions, so that the impedance downstream of the high pressure accumulator can be approximately represented by the valve impedance, R_v, alone.
- The system is not precharged.

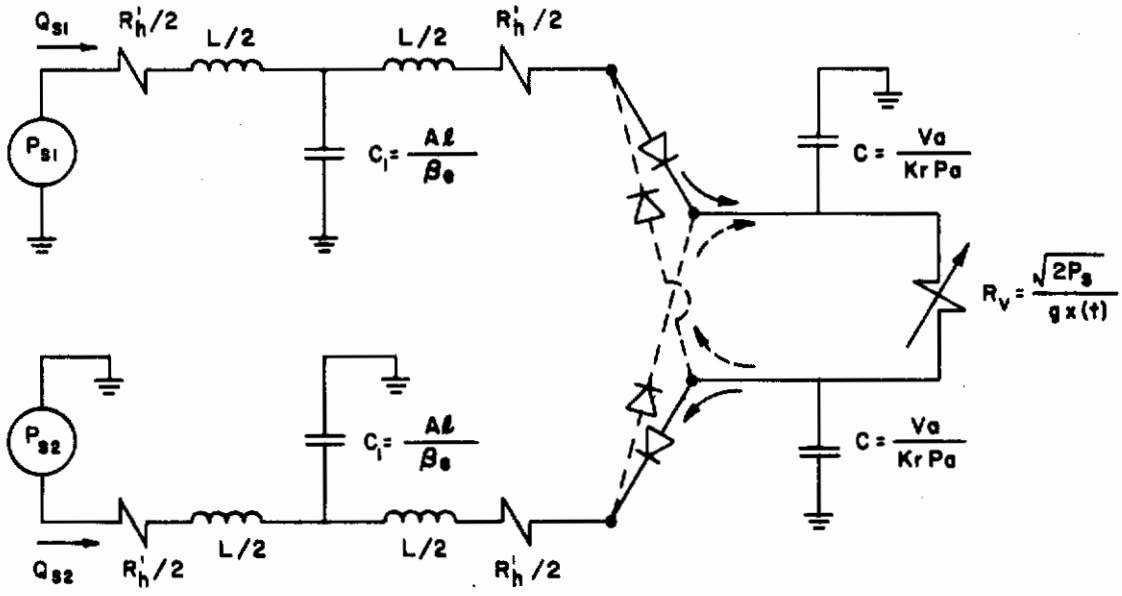

Figure IV-55. Simplified Model of the Pulsating Hydraulic System With Transmission Line of Linear Flow Resistance

The over-all system efficiency estimations are carried out for systems that have either pressure or flow as their source.

1. The Two-Line Pulsating Systems With a Constant Pressure Source

If a pressure-compensated variable delivery pump and a pulsating-flow valve are used, the pressure source, P_{s1}, is a train of pressure pulses forming an offset as shown in Figure IV-56 because of the rectifier's switching action, the pressure level of $P_{\ell 1}$ varies between the high-pressure-accumulator pressure, P_{ah}, and the low-pressure-accumulator pressure, $P_{a\ell}$.

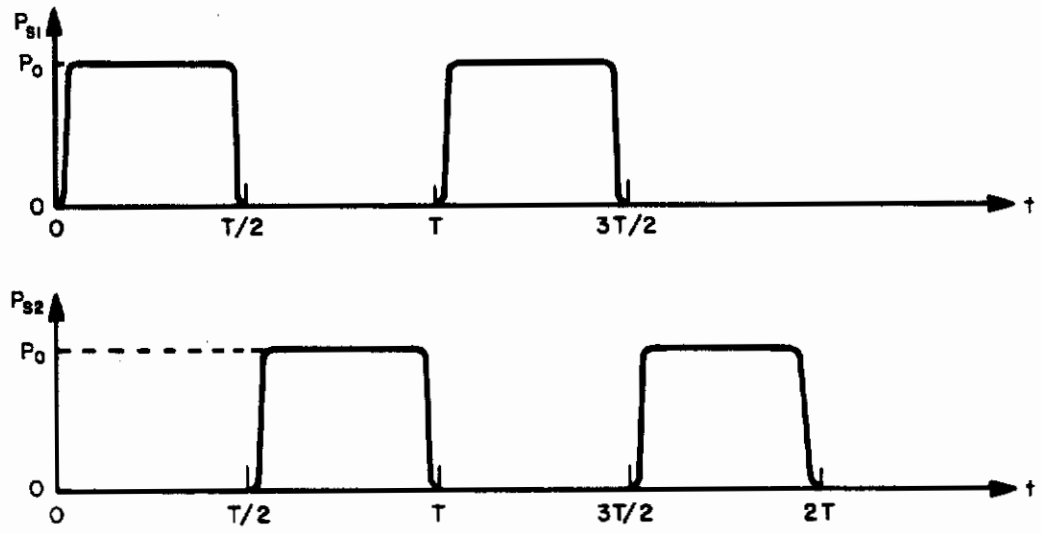

Figure IV-56. Pressure Pulse of Pressure Source

For the convenience of calculation, the pressure pulses are represented mathematically by their complex form:

$$P_{s1}(t) = \sum_{n} \overline{P}_{1n} e^{jn\omega t} \tag{149}$$

$$P_{\ell 1}(t) = \sum_{n} \overline{P}_{2n} e^{jn\omega t} \tag{150}$$

where

$$\overline{P}_{10} = \frac{P_o + P_r}{2}$$

$$\overline{P}_{20} = \frac{P_h + P_\ell}{2}$$

$$P_{1n} = -j\left(\frac{2}{n\pi}\right)\left(P_o - P_r\right)$$

$$P_{2n} = \frac{-2}{n\pi}\left(P_h - P_\ell\right)\left(\sin n\omega t_1 + j\cos n\omega t_1\right)$$

$$n = \pm 1, \pm 3, \ldots$$

As shown in Figure IV-55, two accumulators are used in the direct flow section of the P-F hydraulic system. The accumulator on the high-pressure side provides pressure-pulse filtering; the accumulator on the low-pressure side provides a constant return pressure during the return stroke of the pulsating flow, so that the required peak return pressure is greatly reduced.

During steady-state system operation, both the high-and low-pressure accumulators are maintained at a constant pressure level. Therefore, for steady-state system efficiency calculations, a correct fluid line model with its initial and boundary conditions is all that is needed. Figure IV-55 is further reduced to Figure IV-57. Furthermore, the pressure and flow at any corresponding point of both fluid lines are equal in magnitude and 180 degrees out of phase. Hence, in obtaining system efficiency, only one fluid line needs to be considered, as shown in Figure IV-58.

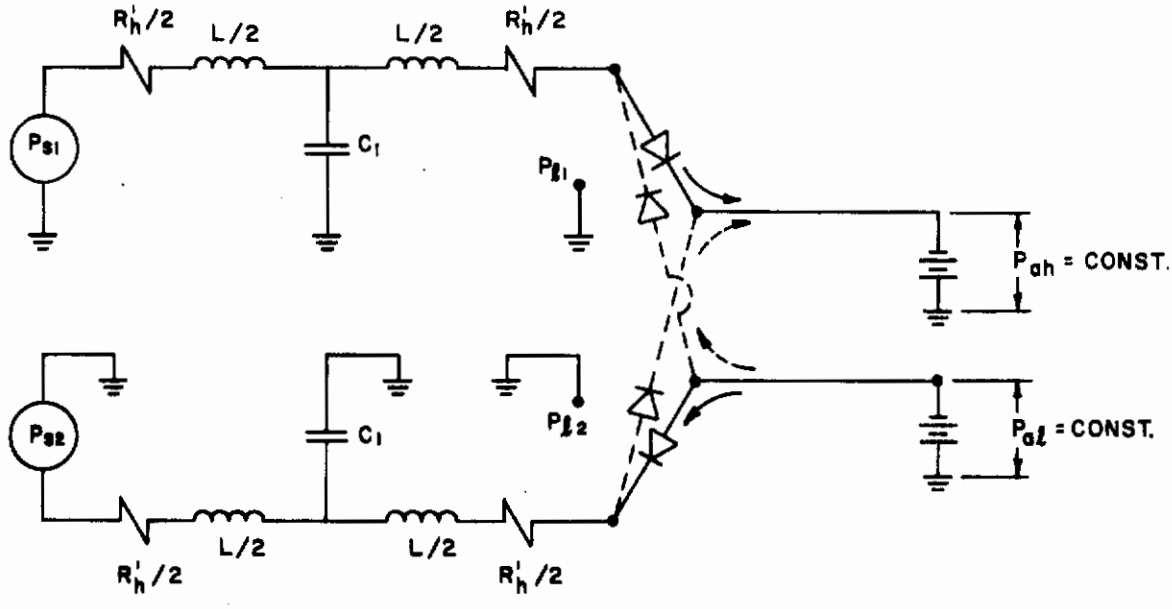

Figure IV-57. Simplified Steady-State Model of the Pulsating Hydraulic System (with Linear Flow Resistance)

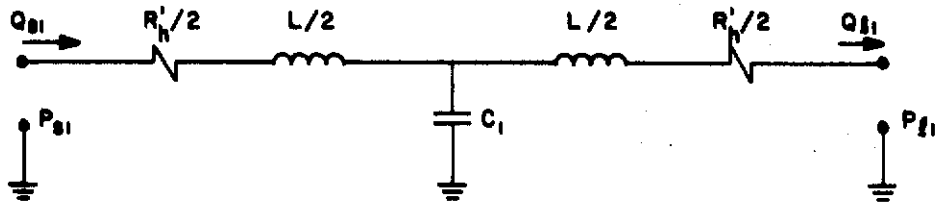

Figure IV-58. Further Simplified Model for Over-all System Efficiency Calculations

Because of the rectifier's switching action, the pressure level of $P_{\ell 1}$ varies between the constant high pressure accumulator pressure (P_{ah}) and the constant low pressure accumulator pressure ($P_{a\ell}$) as shown in Figure IV-59. The phase difference between P_{s1} and $P_{\ell 1}$ is caused by the dynamics of the fluid in the transmission line.

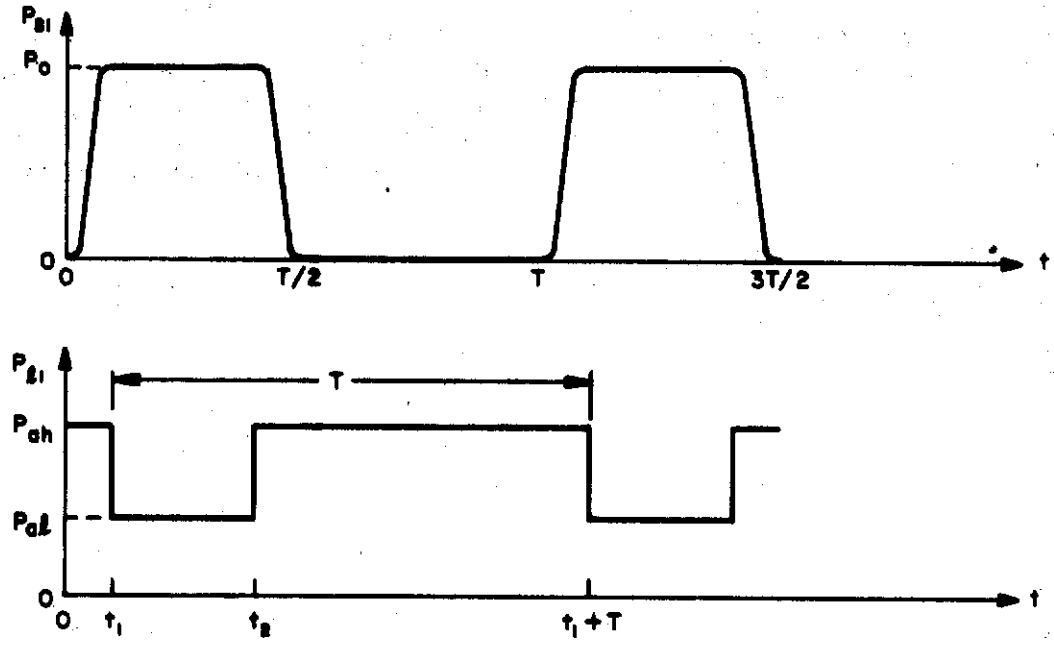

Figure IV-59. Input and Output Pressure Pulses of the Transmission Line

The value of P_{s1} is a given quantity. P_{ah} and $P_{a\ell}$ are the pressure levels that can be maintained by the system by using the correct value of load resistance, R_v, and system precharge pressure. Therefore, both P_{s1} and $P_{\ell 1}$ are known values, except for the time t_1 and t_2, resulting from the fluid line dynamics.

The input and output flow of the line, Q_{s1}, and $Q_{\ell 1}$ can be represented by the following expressions:

$$Q_{s1}(t) = \sum_n G_a(jn\omega)\ \overline{P}_{1n}\ e^{jn\omega t} + \sum_n G_b(jn\omega)\ \overline{P}_{2n}\ e^{jn\omega t} \quad (151)$$

$$Q_{\ell 1}(t) = \sum_n G'_a(jn\omega)\ \overline{P}_{1n}\ e^{jn\omega t} + \sum_n G'_b(jn\omega)\ \overline{P}_{2n}\ e^{jn\omega t} \quad (152)$$

where: $G_a = \left.\dfrac{Q_{s1}}{P_{s1}}\right]_{P_{\ell 1}=0}$; $G_b = \left.\dfrac{Q_{s1}}{P_{\ell 1}}\right]_{P_{s1}=0}$; $G'_a = \left.\dfrac{Q_{\ell 1}}{P_{s1}}\right]_{P_{\ell 1}=0}$;

$$G'_b = \frac{Q_{\ell 1}}{P_{\ell 1}}\quad P_{s1}=0$$

Assuming that the change of fluid density due to pressure variation is negligible, the time t_1, and t_2 can be evaluated from the following two continuity equations:

$$\int_{t_1}^{t_2} Q_{\ell 1}(t)\,dt + \int_{t_2}^{t_2+T} Q_{\ell 1}(t)\,dt = 0 \quad (153)$$

$$\int_{t_1}^{t_2} Q_{s1}(t)\,dt + \int_{t_2}^{t_2+T} Q_{s1}(t) = 0 \quad (154)$$

With the pressures P_{s1} and $P_{\ell 1}$ known and the flow Q_{s1} and $Q_{\ell 1}$ obtained from Equations 151 and 152, the system efficiency can be easily computed from Equation 155.

$$\eta = \frac{\int_0^T P_{\ell 1}(t)\ Q_{\ell 1}(t)\ dt}{\int_0^T P_{s1}(t)\ Q_{s1}(t)\ dt} \qquad (155)$$

2. The Two-Phase Pulsating System With a Flow Source

When a positive displacement pulsating pump (such as the one in the miniaturized pulsating hydraulic system) is used, the flow source has sine wave shape flow pulses as shown in Figure IV-60.

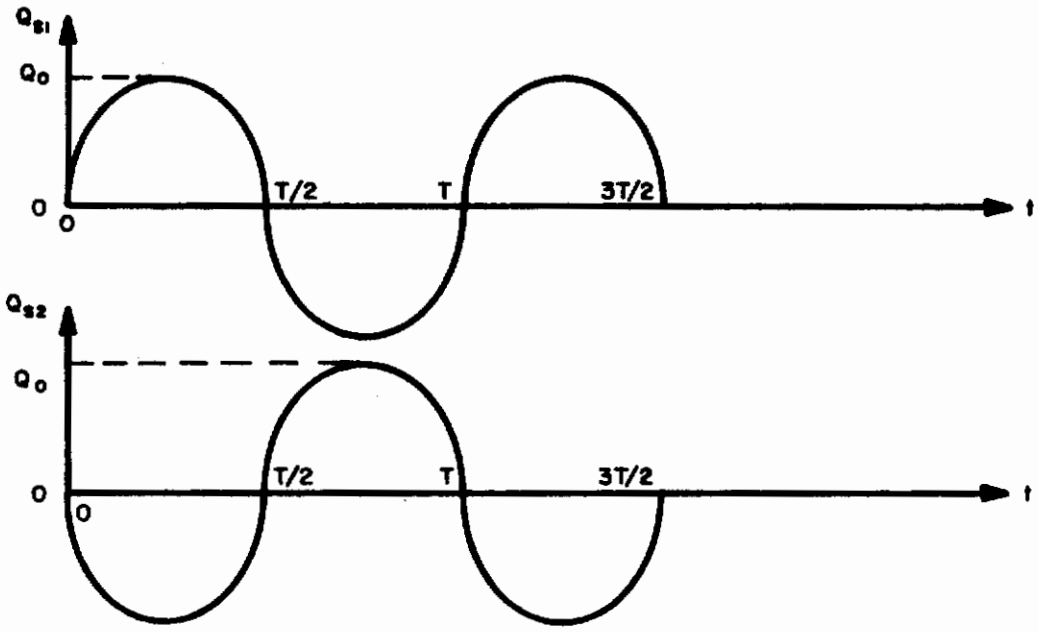

Figure IV-60. Flow Pulses of Flow Source

The switching action of $P_{\ell 1}$ from P_{ah} to $P_{a\ell}$ (or from $P_{a\ell}$ to P_{ah}) is in phase with the change of $Q_{\ell 1}$ from positive to negative (or from negative to positive). The time, t_1, resulting from the phase difference between Q_{s1} and $P_{\ell 1}$ is, therefore, the same as that between Q_{s1} and $Q_{\ell 1}$. The analytical expression of $P_{\ell 1}$ can be obtained by replacing t_1 and t_2 of Equations 153 and 154 with t_1 and $(t_1 + T/2)$, respectively.

By the same method the pressure, P_{s1}, and flow, $Q_{\ell 1}$, can be expressed in functions of the independent variables and other parameters of the fluid line.

$$P_{s1}(t) = \sum_{n=1} G_s(jn\omega)\, Q_{10}\, e^{jn\omega t} + \sum_{n} G_{\ell}(jn\omega)\, \overline{P}_{2n}\, e^{jn\omega t} \quad (156)$$

$$Q_{\ell 1}(t) = \sum_{n=1} G'_s(jn\omega)\, Q_{10}\, e^{jn\omega t} + \sum_{n} G'_{\ell}(jn\omega)\, \overline{P}_{2n}\, e^{jn\omega t} \quad (157)$$

where: $n = \pm 1, \pm 3, \ldots$

$$G_s = \left.\frac{P_{s1}}{Q_{\ell 1}}\right]_{P_{\ell 1}=0}; \quad G_{\ell} = \left.\frac{P_{s1}}{P_{\ell 1}}\right]_{Q_{s1}=0}; \quad G'_s = \left.\frac{Q_{\ell 1}}{Q_{s1}}\right]_{P_{\ell 1}=0};$$

$$G'_{\ell} = \left.\frac{Q_{\ell 1}}{P_{\ell 1}}\right]_{Q_{s1}=0}$$

The Q_{s1} and $P_{\ell 1}$ phase relationship is shown in Figure IV-61. The following continuity equation is used to determine the value of t'_1 and t'_2.

$$\int_{t'_1}^{t'_1 + T/2} Q_{\ell 1}(t)\, dt + \int_{t'_1}^{t'_1} Q_{\ell 1}(t)\, dt = 0 \quad (158)$$

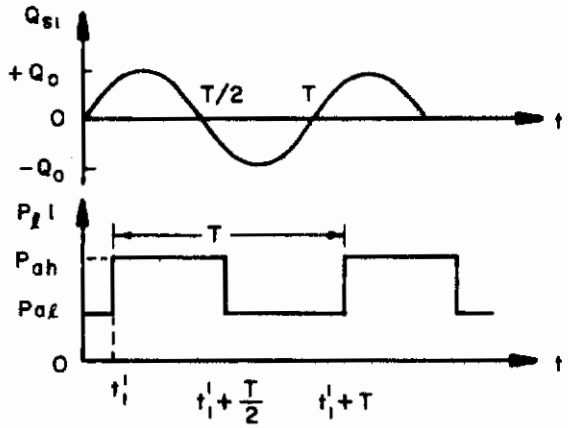

Figure IV-61. Phase Relationship Between Q_{s1} and $P_{\ell 1}$

Again, the over-all system efficiency can be computed from the power ratio as shown in Equation 155.

J. MINIATURIZED TWO-PHASE P-F HYDRAULIC SYSTEM SETUP

Figure II-4 is the schematic of a two-phase miniaturized P-F pulsating hydraulic system setup. The hydraulic rectifier is made of four check valves, each with an undamped natural frequency of 25 cps. No hydraulic transformers were used in the fluid lines. The purpose of this test setup is to verify analytical assumptions, and obtain quantative information about the effect of various fluid and system parameters on the system performance.

Tests were conducted with the following purposes in mind:

(1) To determine the effectiveness of a rectifier constructed with four check valves. Tests included measurement of flow loss, pressure loss, the dynamic response, and the stability of the check valves.

(2) To evaluate the filter characteristics of the high pressure accumulator. Tests included the measurement of cut-off frequency (for particular load impedance conditions) and verification of analytical assumptions.

(3) To determine line losses. The test objectives were to establish line loss characteristics as a function of pulsating frequency, flow velocity profile, and fluid viscosity.

Figures II-5, -6 and -7 are photographs of the miniaturized system and the associated instrumentations. The pump used in the system, which has been converted from an aircraft tandem actuator, is driven by a 3 HP Varidrive unit having a speed range between 59 and 590 rpm. The pump stroke can be varied from zero to one inch by means of an adjustable eccentric drive.

The four ball-seat check valves used to form the rectifier are those used in the 1000°F hydraulic system investigation conducted under Contract AF33(616)-7454. The mass of the balls and guides, as well as the spring rates, have been determined for the purpose of studying the dynamic response of the valves.

The transmission lines from the pump to the rectifier are about 20 feet long. The fluid used during the test was MIL-H-5606 fluid. During the system efficiency tests the servovalve and actuator were disconnected from the system. A needle valve was used as the system load. For each variation of the system parameters (load orifice area and P-F amplitude and frequency), the pressure and flow data were taken after the system had reached the new steady-state conditions.

Although shown separately on the hydraulic schematic, the control valve is an integral part of the actuator. This actuator, which is identical to that used for the pulse generator, is connected to a mechanism for simulating aerodynamic and inertia loads. Connected in parallel to the actuator is a throttling valve, which is essentially a variable restrictor, for use at times when it is desirable to impose a constant load on the system.

Two piston-type air-oil accumulators are used in the system, one on the high pressure side and the other on the low pressure side. The low pressure accumulator is used for fluid make-up as well as fluid expansion, whereas the high pressure one serves as a pulsation filter device.

Instrumentation includes six pressure transducers connected to a Brush recorder as well as a differential pressure transducer connected to a Boonshaft and Fuchs readout. A magnetic pickup with a Hewlett-Packard digital counter is used to monitor pump cycling speed. A flowmeter in the return line and a temperature pickup complete the instrumentation.

K. ANALYTICAL AND EXPERIMENTAL SYSTEM EFFICIENCY OF THE MINIATURIZED PULSATING HYDRAULIC SYSTEM

Figure IV-62 is the theoretical and experimental result of over-all system efficiency of the miniaturized pulsating hydraulic system. Both fluid lines in the setup are 20 feet long and 0.187 inch in diameter. The fluid line model shown in Figure IV-55 and the system efficiency equation (Equation 155) were used in the theoretical efficiency computation. However, the actual calculation was done by analog computer. The hydraulic rectifier was assumed to have negligible friction loss and negligible flow leakage. The experimental efficiency is defined as the ratio of power output through the needle valve to the power input to both P-F fluid lines. The difference between the theoretical and experimental efficiency is believed to be due to the following two reasons:

(1) The friction loss in several "T" or elbow fittings that were neglected in the theoretical computation.

(2) The flow leakage through the check valves of the rectifier due to their low damped natural frequencies (undamped natural frequency of check valves is approximately 25 cps). The damped natural frequencies of the check valves are believed to be much lower than their undamped natural frequencies due to the uncompensated flow reaction force and the fluid viscosity.

For the frequency and flow amplitude range tested, no noticeable difference in system efficiency had been observed for systems under the same load conditions. The maximum power output obtained from the miniaturized hydraulic system during test was 0.5 HP.

L. ANALOG COMPUTER PROGRAM FOR SYSTEM DYNAMICS AND EFFICIENCY STUDY

Because of the limited amount of experimental information that could be obtained from the analytical computation and the miniaturized pulsating hydraulic system, an analog computer program was set up to obtain quantitative information. This information is necessary to optimize system geometry for various power capacity and load conditions.

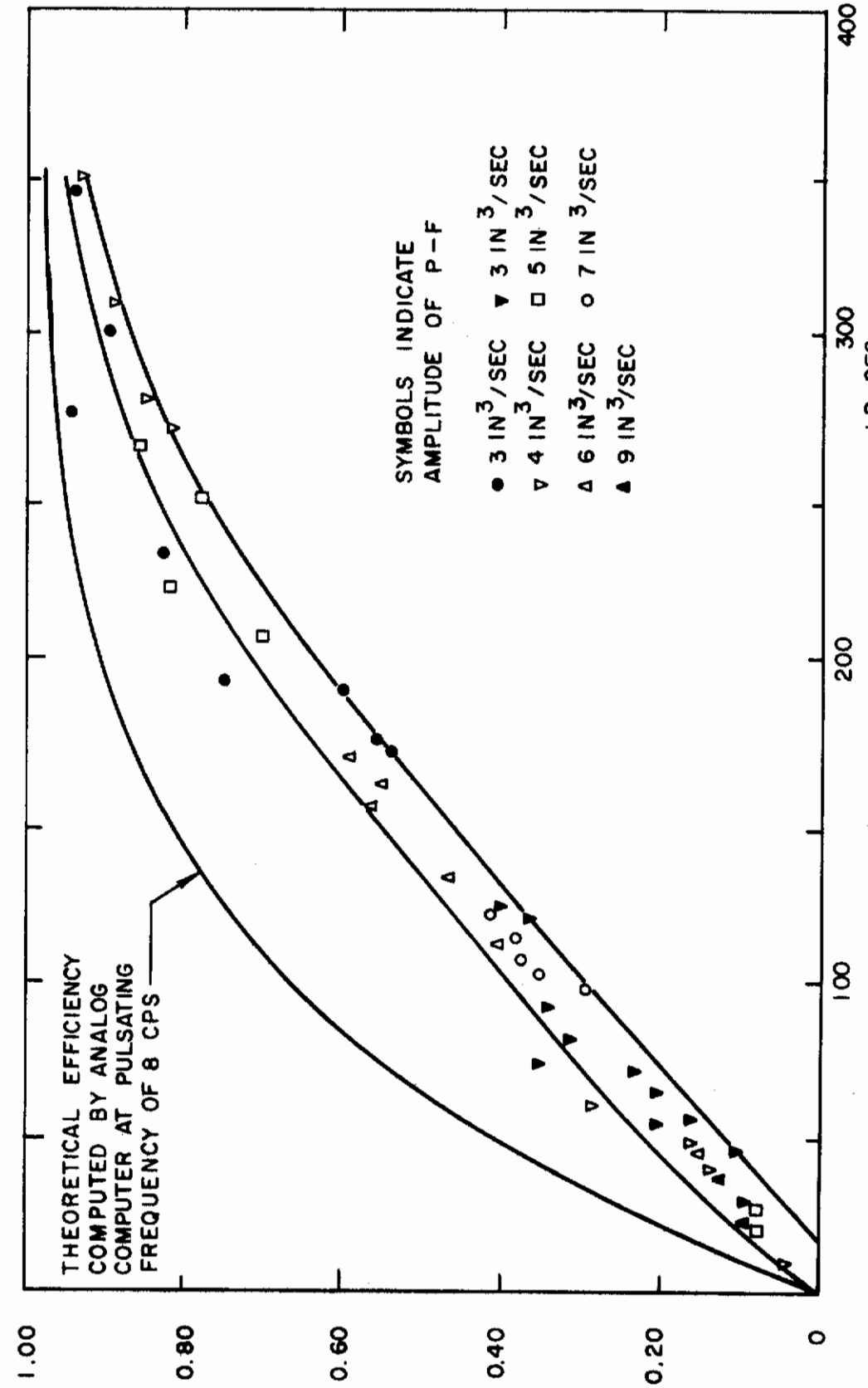

Figure IV-62. Theoretical and Experimental System Efficiency of the Miniaturized P-F Hydraulic System

Figure IV-63 is the four-terminal block diagram of the miniaturized pulsating hydraulic system. Figures IV-64 to -69 are the analog computer programs for the system components. Viscosity results were used in the transmission line analog computer programing.

It should be pointed out here that the analog computer program represents a pulsating hydraulic system that has a controlled flow source (as in the miniaturized system) as its independent input. Comparison of data from the analog computation and the miniaturized pulsating hydraulic system setup,as shown in Table IVL-1 indicates that the analog computer program is adequate and that the machine is functioning correctly.

1. Computer Programing and Operation

The basic system configuration and important variables are shown in Figure IV-63. The 180° phase shift block indicates that the lower transmission line was not included in the computer simulation (due to a limitation in the amount of equipment required) and its outputs (pressure and flow) taken as the outputs of the upper line with a 180° phase shift.

Approximately 40 operational amplifiers, 4 servos, 1 square root function generator, 35 pots, assorted diodes, capacitors, etc., and a six channel recorder were required for the problem.

The following outputs were recorded on the six channel recorder: pump flow and pressure, load flow and high and low pressure accumulator pressures. The last channel was used for various system checkouts.

2. Computer Map Description

The flow generator (Figure IV-64) is the solution of a second-order equation that has the proper initial conditions. Some feedback (adjustable to positive and negative values) was added to take care of any random damping introduced unintentionally into the circuit.

The load (Figure IV-65) is simply an orifice whose equation

$Q = K_c \sqrt{P_H - P_L}$ is solved by a square root function generator.

The hydraulic rectifier (Figure IV-65) is a diode logic device very similar to an actual A.C. rectifier, satisfying the proper pressure-flow relationships.

The accumulator circuit model (Figure IV-66) is somewhat interesting in that the requirement for a function generator is removed by the use of a circuit which utilizes a high gain amplifier. The model is basically an equation of the form

$$\Delta Q = K_1 P^{-k_r} \frac{dp}{dt}$$

It could have been solved in a conventional manner by raising P to the minus K_r power in a function generator, taking the derivative of P and multiplying the two quantities in a servo. The disadvantage of this technique besides the differentiation (which can be removed by integrating both sides with respect to time) is that P has a large range so that if P^{-K_r} is obtained by a function generator it suffers a loss of accuracy for the larger values of P. The basic computing circuit works in this manner (refer to Figure IV-66). ΔQ, which is available, is divided by $K_1 P^{-K_r}$ (where P^{-K_r} is assumed). The resulting quantity which is $\frac{dP}{dt}$ is then integrated to get P. The output of a high gain amplifier is called $\frac{\dot{P}P^{-K_r}}{P}$. This signal is fed into a servo being multiplied by P to give PP^{-K_r}. The same signal is also available from the previous mentioned sources and both are summed in the high gain amplifier to produce $\frac{\dot{P}P^{-K_r}}{P}$. This value when integrated gives P^{-K_r}.

Figure IV-67a shows the circuit and equations corresponding to a lumped parameter transmission line. The block diagram solution of the equations representing the lumped parameter transmission line (Reference 8) is shown in Figure IV-67b. The solution is straightforward except for the use, again, of a high gain amplifier. Q_1 is available as an input and it is also available (Q_1*) from the solution of the equations. These two values must be the same so that both quantities are fed into the high gain amplifier and the only quantity missing that is needed is P_{1b} so the amplifier output is called P_{1b} and fed back to where it was assumed. This circuit forces P_{1b} to the value that makes Q_1 equal to Q_1* and this must then be the proper value of P_{1b}. Figure IV-64 is the complete computer diagram.

As a general rule, a distributed parameter model of the transmission line should be used when the line length exceeds one-eighth of the fluid wavelength.

The distributed parameter transmission line block diagram (Figure IV-68) and computer map (Figure IV-69) is the solution to the partial differentiation equations which describe the pressure and flow relationships in the transmission line, by means of time delay operations (References 9 and 10). The equations are:

$$\frac{\partial P}{\partial t} = - \beta \frac{\partial V}{\partial x}$$

$$\frac{\partial P}{\partial x} = - \rho \frac{\partial V}{\partial t}$$

where

P = fluid pressure

V = fluid velocity

β = fluid bulk modulus

ρ = fluid mass density

The general form of the solution of either equation is:

$$P = F_1\left(t + \sqrt{\frac{\beta}{\rho}}\,x\right) + F_2\left(t - \sqrt{\frac{\beta}{\rho}}\,x\right)$$

where F_1 and F_2 are arbitrary functions. By proper manipulation and utilizing boundary and initial conditions, F_1 and F_2 may be determined, and the time difference equations shown in Figure IV-68 result.

The time delay T_d was approximated by the following second order transfer function:

$$T(s) = \frac{10 - 4.7\,T_d S + T_d{}^2 S^2}{10 + 4.7\,T_d S + T_d{}^2 S^2}$$

This expression gives a time delay which is valid for an $\omega\ T_d$ product (where ω is the frequency of the highest harmonic of the input) of about 4. Therefore, since a line length of 150 feet (the maximum length being considered) produces a 34 millisecond delay, the transfer function would be good to a frequency of about 19 cycles/second (sinusoidal input). For shorter transmission line lengths higher frequencies could be used.

3. Computation Results

The table below is a comparison of computer and experimental values that were obtained from the miniaturized system setup for two separate runs.

Figure IV-70 is a representative steady-state run with typical numerical values for the system variables. Figure IV-71 is the analog computation result of the system efficiency vs various system parameters. It should be pointed out here that more extensive computation results could have been obtained if it was not limited by the amount of budget and time available.

The equation of the air loaded accumulator and the numerical calculation of system efficiency that were used in the analog computer program are shown in Appendix B.

TABLE IV-3. COMPUTER vs. EXPERIMENTAL DATA

Conditions: Transmission line-length 30 feet, diameter 3/16 inch, frequency 7 cycles/sec

	Pump Flow Q_o, in^3/sec	Pump Press. P_{ia}, psig	Load Flow Q_L, in^3/sec	High Press. Accum. Press. P_H, psig	Low Press. Accum. Press. P_L, psig	
Computer	4.5	1080	2.8	720	405	Run 1
Experimental	4.4	1050	2.77	725	355	Run 1
Computer	5.6	1075	3.7	672	484	Run 2
Experimental	5.6	1000	3.54	635	455	Run 2

The data shown in this table are sample figures and are intended to indicate the close conformity that was achieved between experimental and computer data.

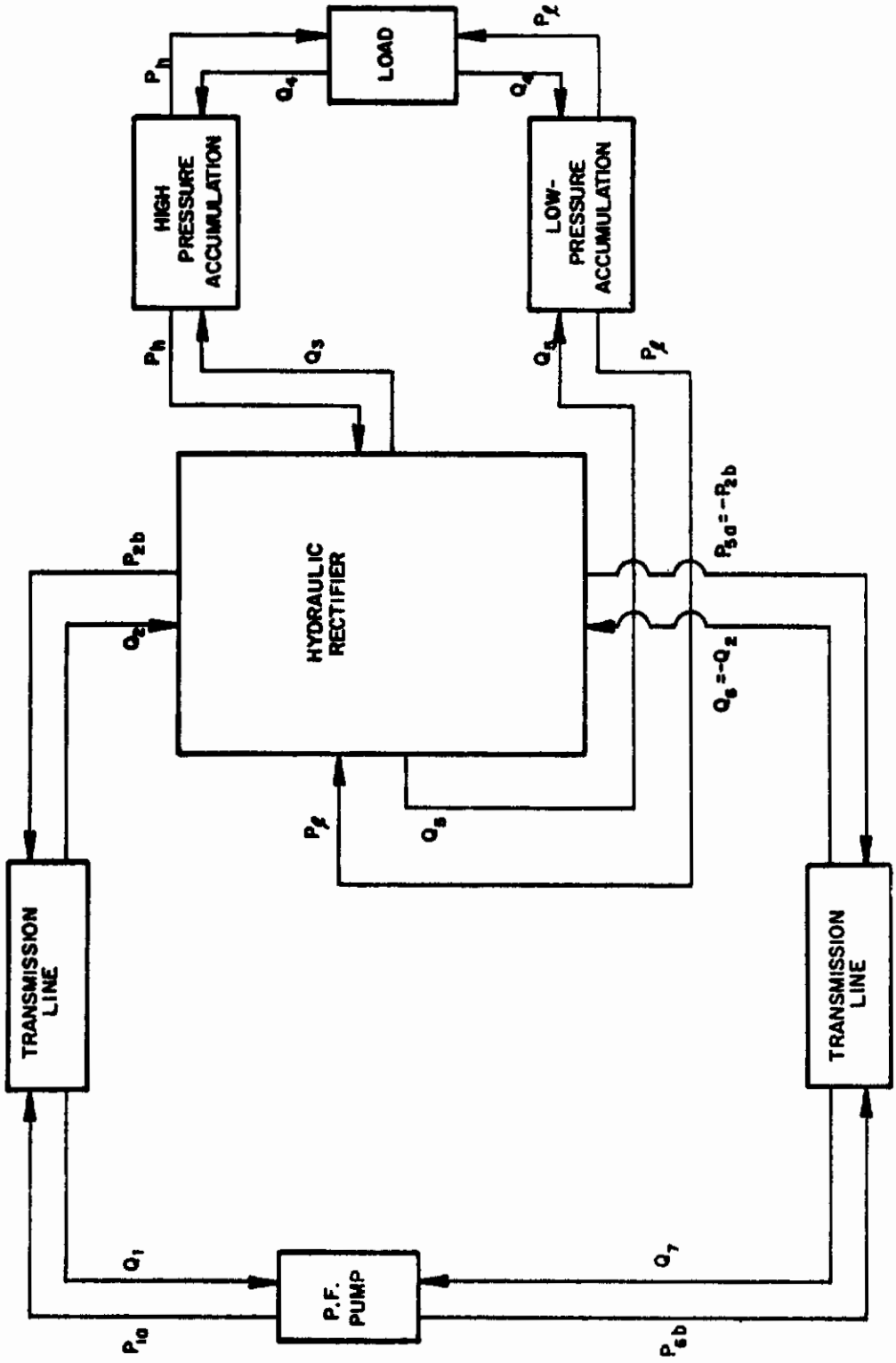

Figure IV-63. Four-Terminal Block Diagram of Pulsating Hydraulic System With Flow Source as Its Input

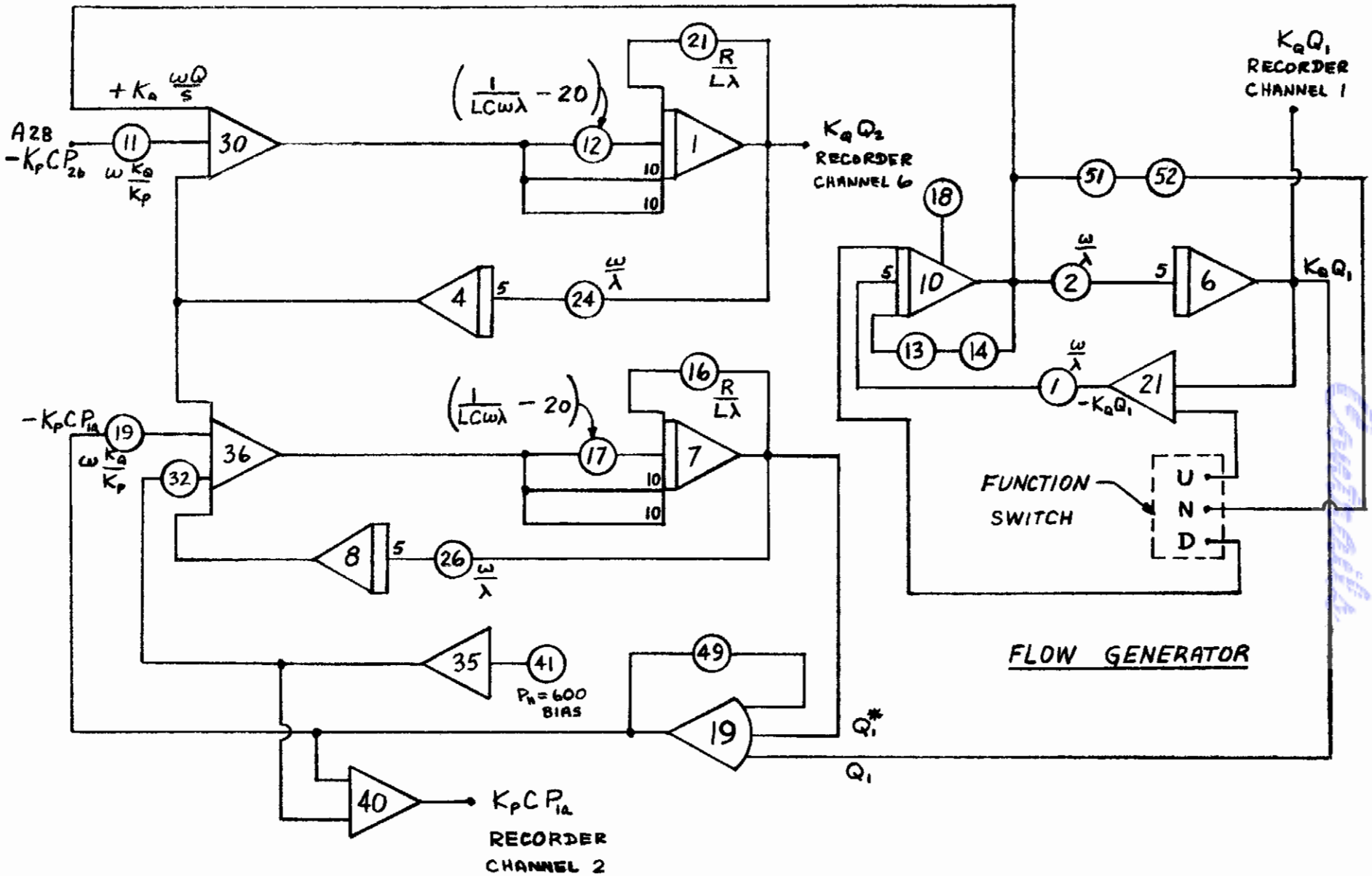

Figure IV-64. Transmission Line - Lumped Parameters

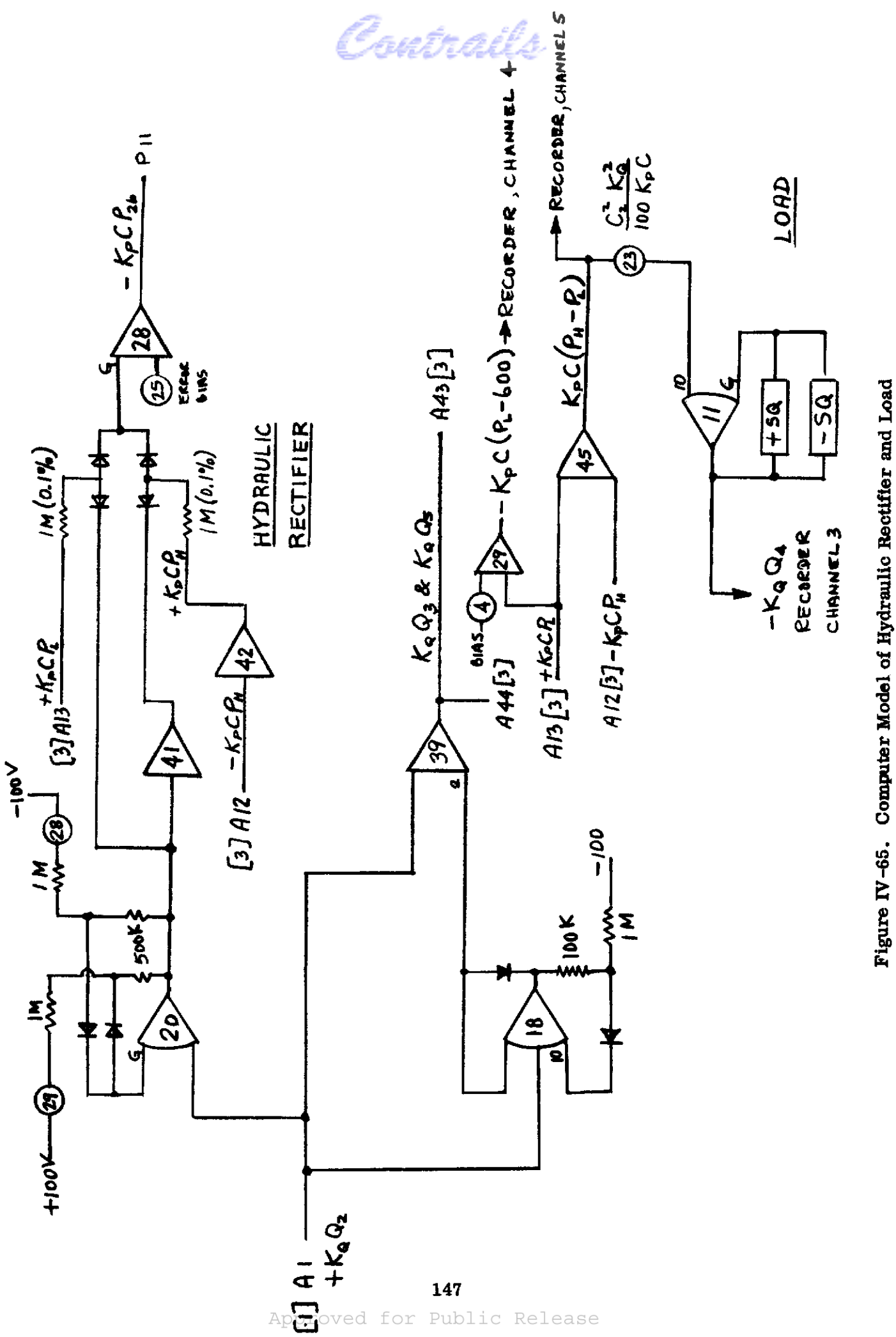

Figure IV-65. Computer Model of Hydraulic Rectifier and Load

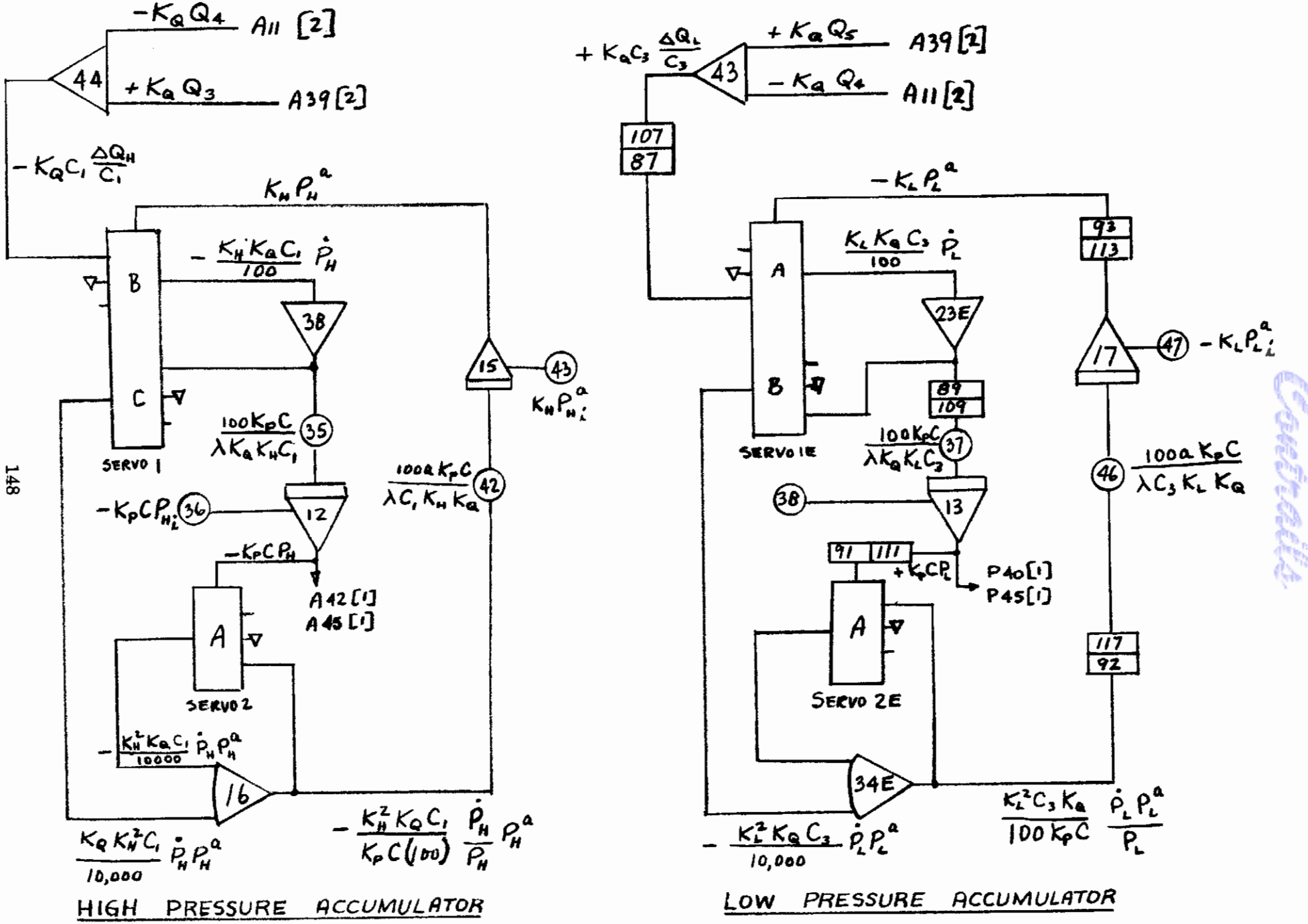

Figure IV-66. Basic Computing Circuit Operation

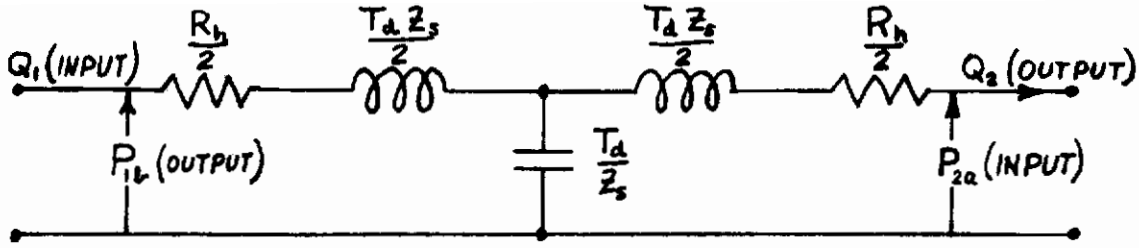

$$DQ_1 = sCP_{1b} + Q_2$$

$$DQ_2 = Q_1 - sCP_{2a}$$

WHERE $D = LCs^2 + RCs + 1$

R_h = RESISTANCE

Z_s = CHARACTERISTIC IMPEDANCE

T_d = PULSE TIME DELAY

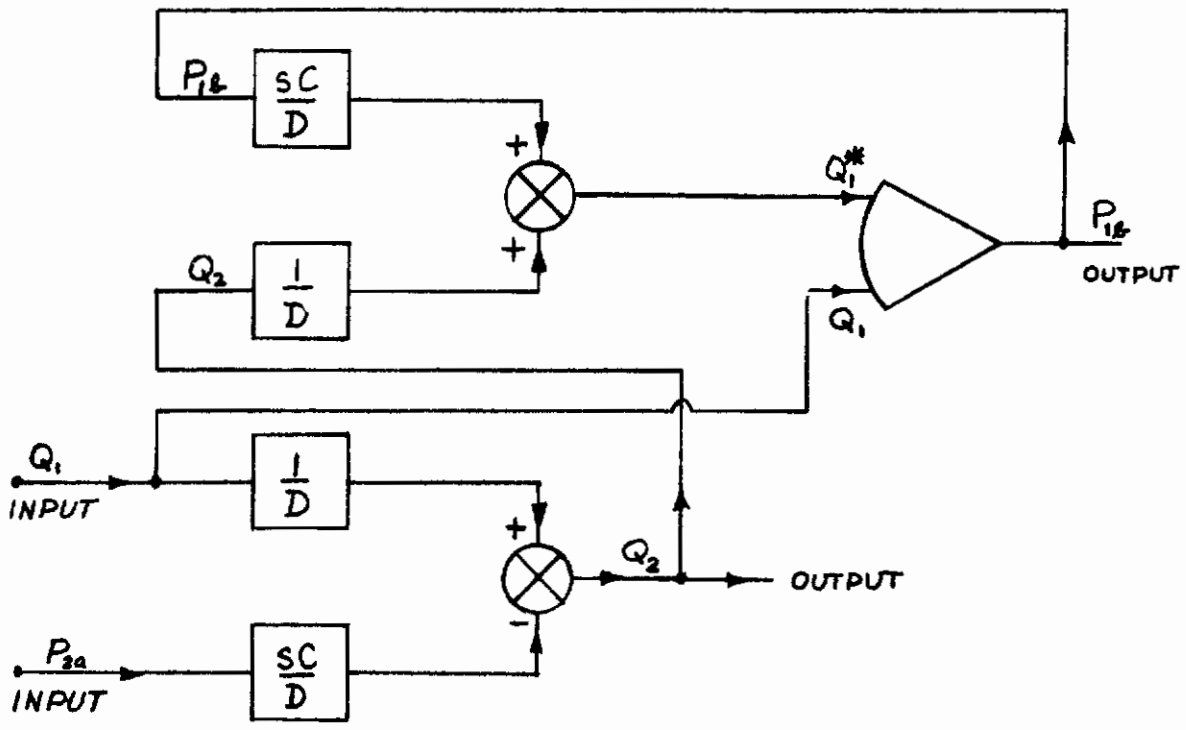

Figure IV-67. Lumped Parameter Transmission Line Block Diagram

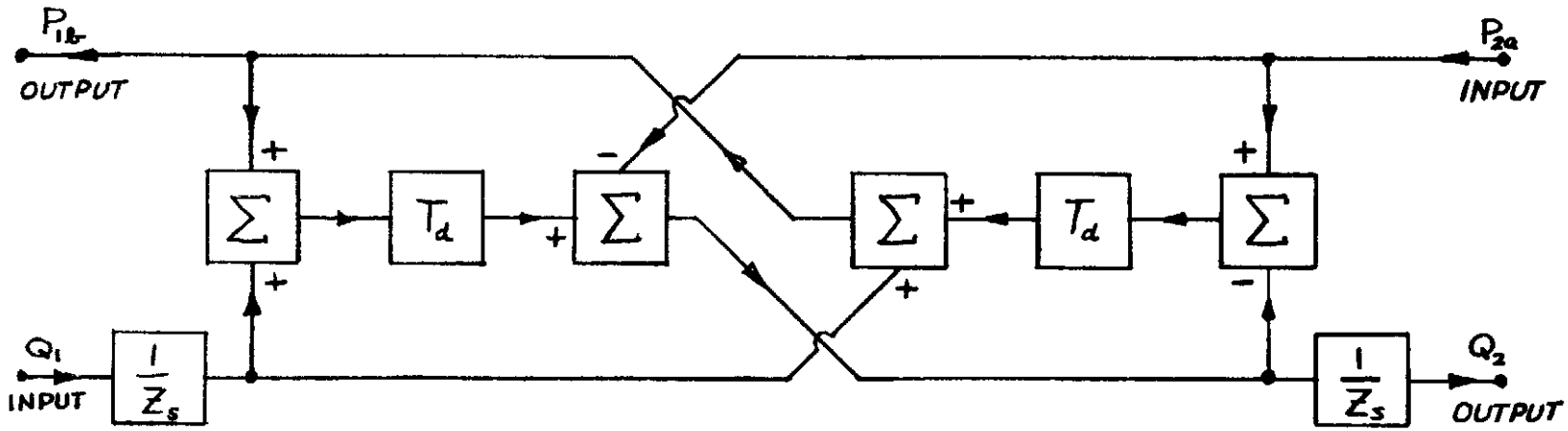

$$P_{2a} + Z_s Q_2 = P_{1b}(t - T_d) + Z_s Q_1(t - T_d)$$

$$P_{1b} - Z_s Q_1 = P_{2a}(t - T_d) - Z_s Q_2(t - T_d)$$

Figure IV-68. Distributed Parameter Transmission Line Block Diagram

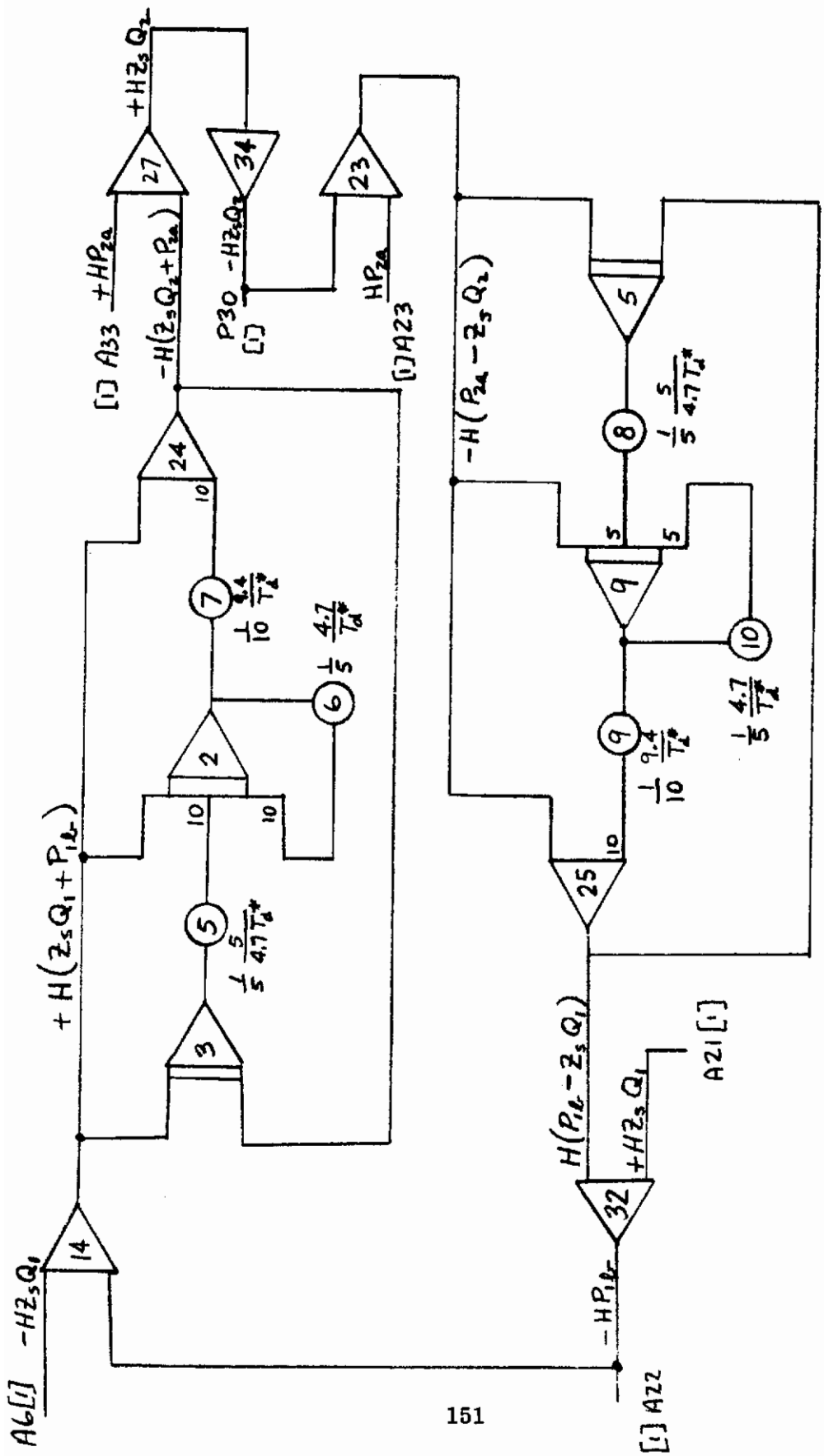

T_d^* = MACHINE TIME DELAY

Figure IV-69. Transmission Line-Distributed Parameters

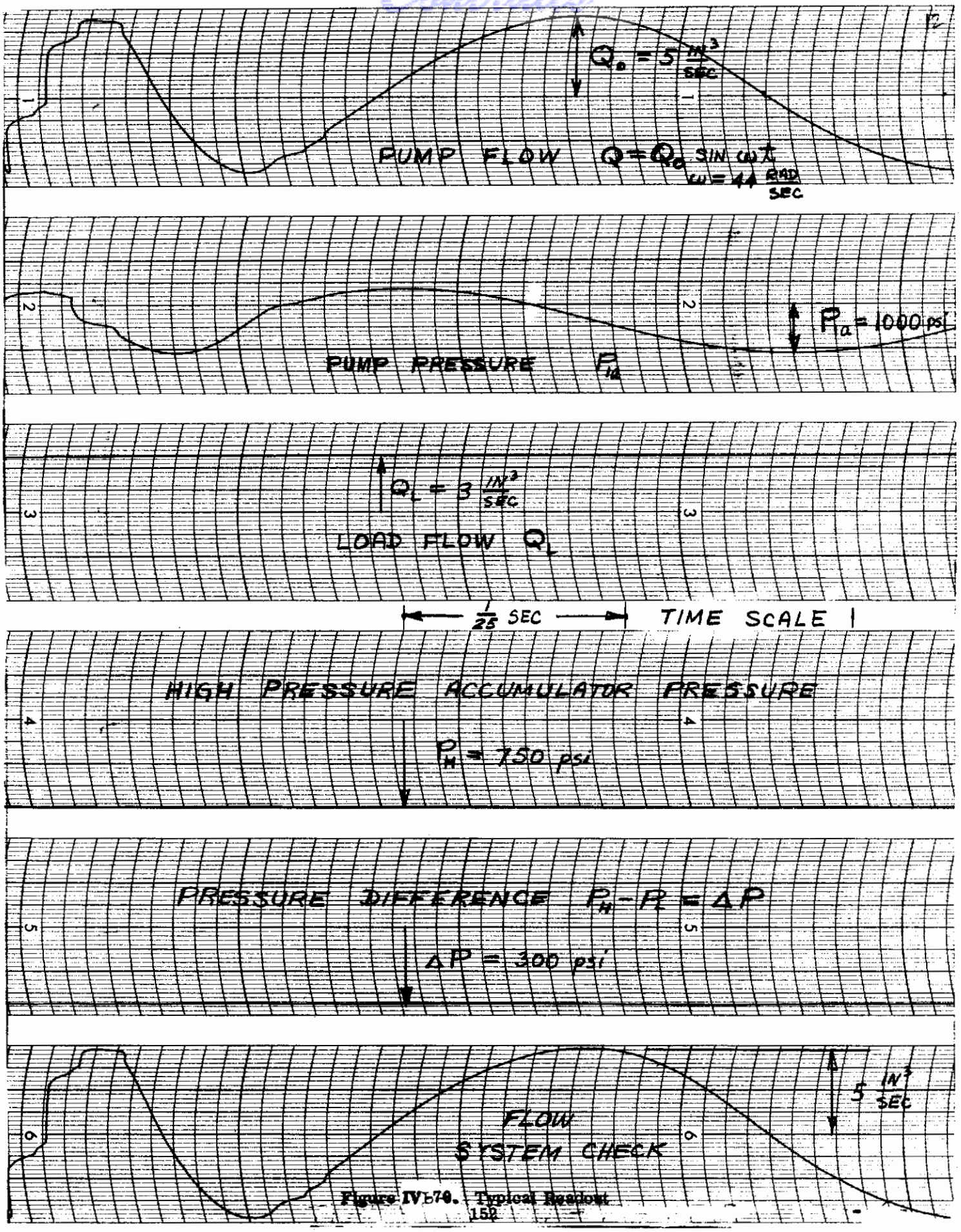

Figure IV-70. Typical Readout

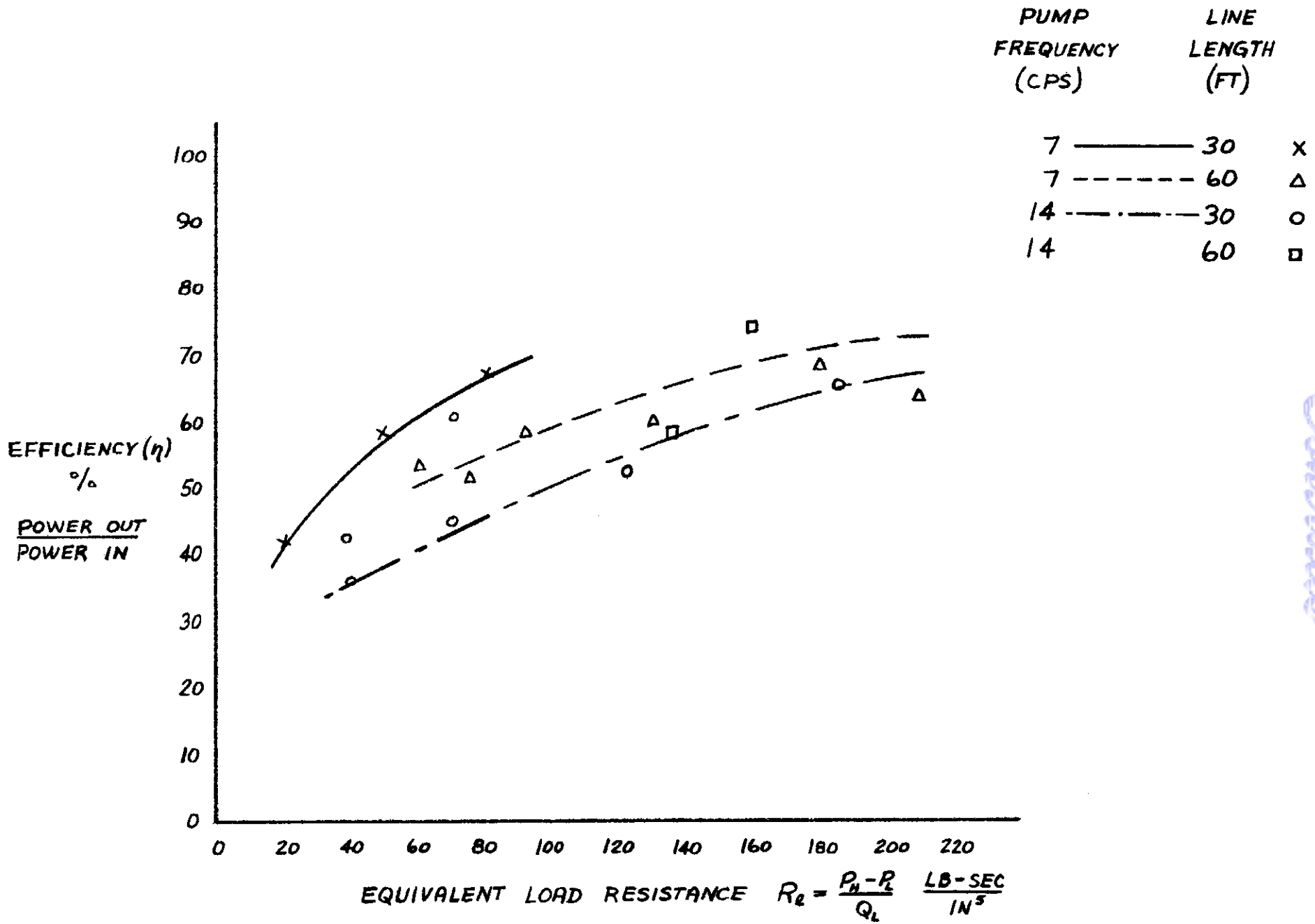

Figure IV-71. Efficiency vs Load

M. OPTIMUM FREQUENCY SELECTION

The optimum operating frequency for a given system configuration will be defined as the frequency which results in maximum power efficiency within reasonable parameter limitations, i.e., the performance of a given amount of work in a certain time should require a minimum power input.

It must be realized that varying the system frequency affects many parameters. In general, as the load input and system (pump or alternator, lines, rectifier, and accumulator) output are more closely matched, the higher is the efficiency. Since impedances are a function of frequency, it can be seen that conversely the efficiency is a function of frequency. From the tests on the miniature hydraulic system, a frequency of 5 cps or more results in a higher efficiency.

Analytically, the efficiency may be computed from

$$\eta = \frac{\frac{1}{T}\int_0^T P_{\ell 1}\, Q_{\ell 1}\, dt}{\frac{1}{T}\int_0^T P_{s1}\, Q_{s1}\, dt}$$

Because of the complex inter-relationships among system parameters, the determination of optimum frequency is not amenable to a closed form solution. To determine the optimum frequency it is desirable to program the particular problem on the computer and then vary the frequency, evaluate the efficiency, and choose the operating frequency which corresponds to the maximum efficiency (within practical equipment limitations). This operating frequency would then be the so-called "optimum frequency."

In general, it can be said that for a range of frequency from 5 to 12 cps (average 8 cps) the effect of frequency variation on the parameters that affect its selection will be quite small. Where the transmission lines are longer than two or three feet, the inertia of the fluid which must be accelerated for each pulsation will be found to be a governing parameter. Since the work of accelerating the fluid is a function of the square of the velocity and the number of accelerations of the fluid per second is a function of the frequency, it can be seen that for the length of transmission line that is found in most applications a low frequency is dictated. Since (as stated earlier) the undamped natural frequency of the check valves of the rectifier is in the order of 25 cps and the damped frequency is somewhat lower, a frequency below this range is desirable. Experience has also indicated that, except where a system is very closely coupled, the natural range of hydraulic system response is 15 cps or less. Therefore, it is considered that the desirable average frequency for a pulsating flow hydraulic system will be approximately 8 cps. Detailed computer analysis may indicate a slightly different frequency for a specific system, but such an analysis will be extremely complex unless the pulsating system is very simple. In cases where a system is very closely coupled and the transmission lines are quite short, higher frequencies in the order of 100 to 200 cps are desirable.

SECTION V - MATERIALS

No materials or process work was accomplished during the course of the contract. A literature survey of materials usable with liquid metals (such as NaK_{77}) at temperatures to 1400°F is presented in Appendix V.

SECTION VI - CONCLUSIONS AND RECOMMENDATIONS

A. GENERAL

As a result of the research investigation performed under this contract, Republic concludes that the construction and operation of a pulsating hydraulic system is feasible. In some cases, a continuous flow hydraulic system may be superior to a pulsating hydraulic system in efficiency and weight. However, as will be indicated below, broad conclusions are valueless when it comes to designing a hydraulic system for a specific vehicle. For certain applications, pulsating hydraulic systems will be found to have a definite advantage over continuous flow hydraulic systems. It is in these areas of application that further studies are recommended to define the efficient use of pulsating hydraulics. Moreover, it will be noted that in some of these areas further studies will be necessary to produce the technology which will make the application of pulsating hydraulics practicable.

B. APPLICATIONS OF PULSATING HYDRAULICS

To permit a more precise conclusion as to the applicability of pulsating hydraulics, it is first desirable to examine those applications where it appears that pulsating hydraulics will have an advantage over continuous flow hydraulics. In general, these lie in the areas of fluid separation or isolation, pressure variation efficiency, and motion or speed synchronization.

1. Fluid Separation or Isolation

The most general application indicating an advantage for pulsating hydraulics over continuous flow hydraulic lies in the ease of fluid separation by use of a barrier or transformer unit. This separation of fluids can be utilized for several purposes, some of which are indicated below.

In a pulsating system, the transformer is a very simple barrier unit with a diaphragm or piston separator that will transmit the energy of the system into a downstream fluid with only minor attenuation due to the diaphragm spring rate or the hysteresis of piston friction. Transmission of continuous flow energy into a different fluid in a barrier unit requires, in addition to the basic barrier unit piston, position sensors and a means of flow switching that will reverse the flow from one portion of the unit to another. Because of the additional elements, this results in a component with great functional complexity and hence reduced reliability.

The type of system in which fluid separation is often not only desirable, but in some cases mandatory, varies considerably. One such case is isolation of nuclear radiation. When a subsystem is required to operate in an area subject to radiation, fluid separation can be utilized to isolate the radiation to a portion of the vehicle that is readily shielded. This will carry with it an additional design advantage in that materials which are susceptible to nuclear degradation can be used in the uncontaminated areas.

In cases where vehicle environments are such that a wide range of ambient temperatures will exist at any given time during the course of a mission, a greater over-all efficiency of system design and reliability of components can be achieved by the use of fluids in the various areas that are more compatible with the thermal range to be encountered. In some cases of continuous flow systems design penalties have been taken in order to utilize a fluid at temperatures in excess of its level of inception of thermal breakdown. In some of these cases, system conditioning has been applied by various means in an effort to keep the fluid from reaching its breakdown temperature.

By-passes and built-in leakage paths (conditioning flow) are supplied in actuators and valves to prevent fluid breakdown. In such cases, there is always danger of fluid stagnation in some portion of the over-temperature components; this may result in local fluid breakdown with attendant coking and other undesirable side effects. The application of the system conditioning also has a very definite reduction in over-all efficiency, since the conditioning flow represents wasted power. This wasted power also increases the basic over-all thermal problem of the system, since it represents energy dissipated in the form of heat. Jacketing and other means have also been applied to components to maintain the fluid temperature within certain limits. This represents not only wasted power for the flow through the jackets in the conditioning system, but also wasted weight and lost performance.

Attempts have been made to use liquid alkali metals as hydraulic fluid where the ambient temperatures are extremely high. However, because of the extremely poor lubricity and corrosion characteristics of these fluids, pumping or energy generation is a very serious problem and has necessitated use of very low efficiency and low power components. With a pulsating system, the energy can be generated in a readily pumped fluid and then transmitted through a barrier unit or transformer to the alkali metal fluid. This permits the use of high efficiency aircraft type pumps and the generation of high power levels.

From time to time, various types of system designs have been employed in an effort to isolate the effects of battle damage or component failure and maintain the balance of a system in a functional condition. Among these means have been the use of 1) open-center systems; 2) a requirement for the automatic return of directional control valves to a blocked neutral; and 3) the introduction of quantity and flow-measuring fuses. The first two of these methods

gave no warning that the system was damaged and that subsequent efforts at operation would result in the loss of the entire system. The fuses were erratic in operation; their response to a slow rate of fluid loss was either absent or highly variable. With a pulsating system, a barrier installation would completely isolate each subsystem. Damage to the subsystem would merely bottom the barrier, from which a signal could be relayed to the central control to advise of subsystem failure.

2. Pressure Variation Efficiency

Another application of pulsating hydraulic systems that will prove an advantage over continuous flows systems stems from the ability to change pressure in the system by the use of a transformer, in much the same manner that an electrical transformer changes the voltage in an alternating current circuit. By the use of different areas on the input and output sides of the transformer, the system pressure can be readily increased or decreased. When a reduced pressure level is required in a continuous flow hydraulic system, a pressure-reducing valve is normally employed. The energy represented by the difference between the reduced pressure and the system pressure at the subsystem flow rate is dissipated in the form of heat. The result is a drastic decrease in system efficiency. In extreme cases, a heat exchanger may also be necessary to dissipate the heat and prevent system overheating. Pressure increase in a continuous flow hydraulic system requires the use of a rather complex component and has seldom been utilized in aerospace system design. With a pulsating system, a transformer is capable of creating any desired pressure reduction or increase, with coincident inverse flow-rate variation and without energy loss other than the hysteresis of the transformer.

In several current aircraft, the fuel system pumps (engine feed and intertank transfer) are being driven by hydraulic motors rather than the electric motors that have heretofore been the conventional drive means. Because of the variation in the flow rates that are required (particularly in the engine feed pumps), it has been necessary to take certain penalties in hydraulic system design to accomplish this. Republic believes that a more efficient fuel pump drive system can be accomplished by the use of pulsating hydraulics in lieu of continuous flow hydraulics.

A typical schematic diagram for a fuel pump drive system which utilizes pulsating hydraulics is shown in Figure VI-1. In this system an alternator valve converts the continuous flow to pulsating flow. The number of lines or phases of the pulsating system will be a function of the number of pumps in the system. Moreover, if it is desired to operate some of the transfer pumps sequentially, they can receive their power from the same line as is shown with the upper pair of pumps.

During the maximum flow condition, the motor pumps that feed the engine (the two lower pumps in the figure) will have the shut-off valve that bypasses the transformer open so as to apply full system pressure to the motor

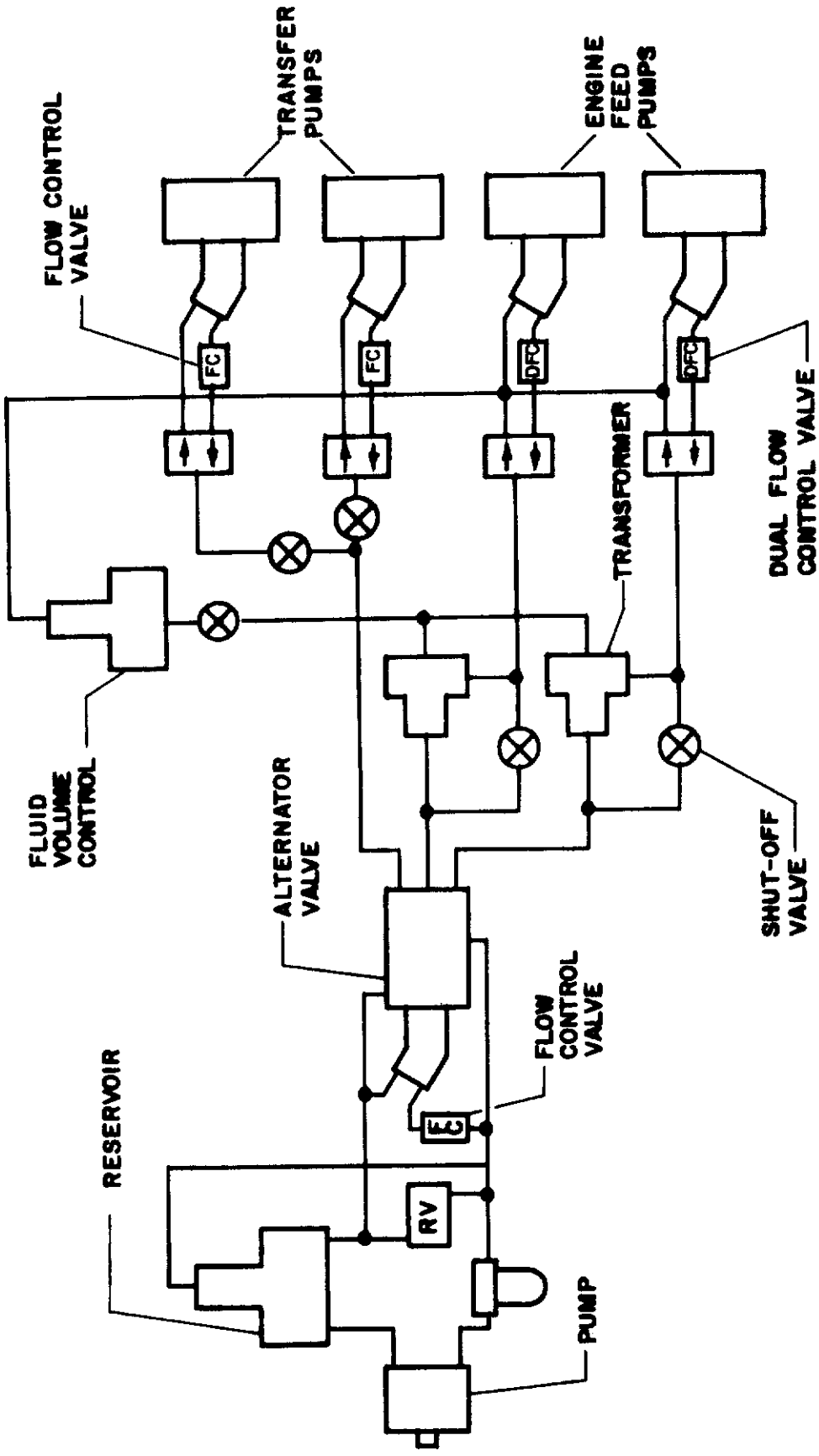

Figure VI-1. Fuel Pump Drive System

for maximum torque output. Since this would also apply full system pressure to the large piston of the volume control unit causing it to overflow, the shut-off valve in this circuit will be closed. Since the motor-pump units will require two operating speeds, a dual flow control valve will be used. The high flow portion will be shut off during cruise operations.

The motor-pumps used for transferring fuel from one tank to another will have only one operating condition and will therefore be fed full system pressure. Since these will be smaller units and, as mentioned above, will in some cases operate sequentially, it is probable that they can all be connected to a single line or phase so as to balance the interline power demand.

3. Motion or Speed Synchronization

In aerospace applications it is often desirable to synchronize the motion of two or more actuating cylinders. Various types of flow dividers have been tried for this purpose, but none has been effective. Specification MIL-H-5440 recognizes this by placing a close restriction on the use of flow dividers.

The alternator valve designed in the course of this project provides an excellent means of accurate flow division. The number of lines coming from the valve will be equal to the number of cylinders to be synchronized. Since the valve will rotate at a fairly constant rate and the variation in rate for a single rotation will necessarily be negligible, the basic flow volume of each pulse will be the same. Figure VI-2 shows a schematic diagram of a possible application of pulsating hydraulics to flow division and actuator synchronization. It will be noted that each pulsating line requires individual rectification and that the motion of the actuator (since it is in effect a single-line system) will be rather jerky; however, for most applications where synchronization is necessary (such as wing flaps), the jerky motion will not be objectionable since it will be in very short steps. By the application of pulsating synchronization, cables, push rods, and other mechanical synchronization devices will be unnecessary, with a considerable weight saving resulting.

A further application for pulsating hydraulics stems from the application of the synchronous hydraulic motor described in Section III. Since the speed of this motor will be a function of the pulsation frequency, a constant rate rotation can readily be achieved by close frequency control. The pulsation frequency is established by the rate of rotation of the alternator valve, or rather by the motor element of this component, which controls the frequency by its speed. Because a combined continuous flow/pulsating flow system is powered by a pressure-compensated variable delivery pump, basically it will be a constant pressure system with the pressure loading of the alternator valve relatively constant. The driving force required from the motor will be largely due to valve friction, which because of constant pressure loadings will also be constant. Therefore, changes in the load of the synchronous motor will not appreciably affect the load on the driving device. As a result, a combination of an alternator valve and a synchronous motor into a single unit will provide a constant speed drive which is not susceptible to frequency or speed variation as a result of major load changes.

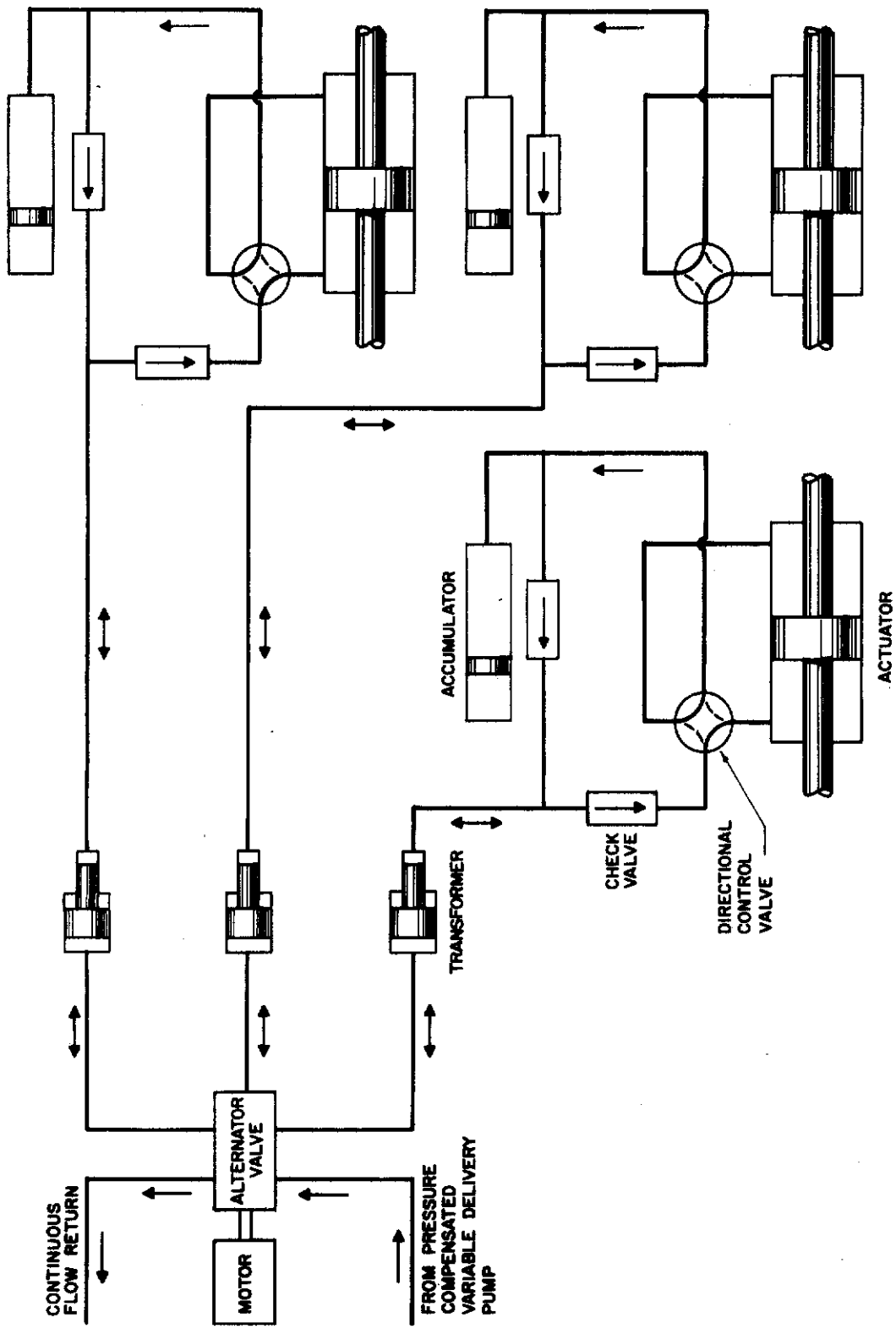

Figure VI-2. Synchronization with Single-Line Systems

C. SUMMARY

The applications that the feasibility study has indicated to be desirable and efficient stem from two of the basic features or elements of pulsating hydraulics which are either not found or inconvenient to produce with continuous flow hydraulics.

The first group deals with the pressure transformer or fluid barrier and energy transmission applications. Some are coupled with extreme temperature applications and utilization of hydraulics and two or more fluids in a system. Others are basically concerned with energy transformation and conservation, which is a feature of the pressure transformation capability. The second general area deals with the action of creating pulsation and resultant pulse control either from flow division, pulse rate, or frequency control. In each group it will be noted that the desirable applications of pulsating hydraulics lie in areas where continuous flow hydraulics suffer penalties in operation.

Because of the additional components that will be necessary in most pulsating systems, such a system would appear to be heavier and less efficient than a continuous flow system. For the specific applications involved, however, pulsating hydraulics will not only be more reliable and lighter in weight, but also more efficient than continuous flow systems.

D. ANALYTIC STUDY CONCLUSIONS

1. Comparison of Theoretical and Experimental Results

Figures IV-53 and IV-54a are the theoretical and experimental input impedances of short and long fluid lines of zero load resistance, respectively. The theoretical impedance is computed from various simplified fluid line models. The short and long lines are defined as lines that have lengths less or more than one-eighth of the pressure wave length. The lumped resistance, R_h, and the time for the pressure wave to travel from one end to the other end of the line, T_e, that were used in the theoretical input impedance calculations were obtained from experiments for the purpose of minimizing the deviation of the theoretical predictions from the test results. Because of the limitation of the test setup, the average flow Reynolds number (over the positive pump stroke) of all the tests did not reach or exceed the critical number of 2000. The maximum average flow Reynolds number during the test was 1700. The maximum pulsating frequency tested was 20 cps. The test results in Figure IV-53 show that within the pulsating frequency range tested, Equations 147 and 148 are a better representation of the short P-F fluid line than a non-viscous fluid line model. Experimental input impedances obtained from another fluid line, 20 feet long and 0.18 inch inside diameter, for the same frequency range, confirm the above result.

The test results plotted in Figure IV-54a and IV-54b show that for pulsating frequencies up to 20 rad/sec., the experimental input impedance of the fluid line that was tested lies between the theoretical input impedances computed from Equations 139 & 140 and 147 & 148. At low pulsating frequencies, the length of line is a relatively small fraction of the pressure wave length; and consequently, the fluid moving back and forth in the line behaves more like a lumped

parameter system, rather than a distributed parameter system. The results in Figures IV-54a and IV-54b also reveal that for frequencies from 20 to 122 rad/sec., the experimental input impedance of the long line that was tested falls between the analytical values obtained from Equations 139, 140 and 143a, 143b. The similar agreement between the computed and experimental input impedances of the same line with load resistance, R_ℓ = 15 lb-sec/in^5, shows that the amplitude of the reflected pressure wave is extremely small. This indicates that the reflected pressure wave component existing in the experimental results is negligible. Figure IV-71 is the analog computated efficiency and Figure IV-62 is theoretical and analog computed efficiency of the miniaturized P-F hydraulic system. Both fluid lines in the setup are 20 feet long and 0.187 inch inside diameter. The fluid line model shown in Figure IV-47 and the system efficiency equation derived in this report were used in the theoretical efficiency computation. However, the actual calculation was done by analog computer. The hydraulic rectifier was assumed to have negligible friction loss and negligible flow leakage. The experimental efficiency is defined as the ratio of the power output through the needle valve to the power input to both P-F fluid lines. The difference between the theoretical and experimental efficiency is believed to be due to the following:

(1) The friction loss in several tee or elbow fittings that were neglected in the theoretical computation.

(2) The flow leakage through the check valves of the hydraulic rectifier due to their low damped natural frequencies. The damped natural frequencies of the check valves are believed to be much lower than their undamped natural frequencies due to the uncompensated flow reaction force and their fluid viscosity.

For the frequency and flow amplitude range tested, no noticeable difference in system efficiency had been oberseved for systems under the same load conditions. The maximum power output obtained from the miniaturized hydraulic system during test was 0.5 HP.

2. Conclusions

With the frequency range and average flow Reynolds number range that were tested, the following conclusions can be reached in regard to the P-F fluid line:

(1) A short P-F fluid line can be represented by a fluid line of lumped parameters that has its total resistance divided into halves and concentrated at each end of the line.

(2) A long P-F fluid line can be represented by a fluid line of distributed inertia and compliance with its total equivalent resistance divided into halves and concentrated at each end of the line. The total equivalent resistance is approximately equal to half of the total lumped resistance of the line.

Within the pulsating frequency and flow amplitude range investigated, both the computed and experimental system efficiency show that:

(1) the system efficiency is very sensitive to the system load impedance;

(2) for the same load impedance, the system efficiency is rather insensitive to the change of pulsating frequency and flow amplitude, so long as the average flow Reynolds number remains less than 2000.

The above results show that, to determine the optimum system pulsating frequency and flow amplitude, other parameters, such as the pulsating flow line input impedance, resonance conditions, number and size of pulsating flow line, etc., rather than the system efficiency will have to play a decisive role. Analytical and experimental results indicate that 5 to 12 cps is a practical pulsating frequency range from practical system design point of view. Low pulsating frequency tends to increase the ripple filtering problem.

E. RECOMMENDATIONS

Based on the research investigations that Republic has performed in the course of the contract, it appears to be thoroughly feasible to construct and operate a pulsating flow hydraulic system. When a pulsating hydraulic system is used under the conditions which are stated in the conclusions, it will be superior and preferable to a continuous flow hydraulic system.

Although the miniaturized pulsating system that was constructed produced very satisfactory results, it should be noted that two of the components that are basic elements of the desired applications of pulsating principles were not constructed but were developed only to the point of layout designs. In order to determine fully the functional characteristics of the alternator valve and the transformer-fluid volume control combination it is desirable that representative components be constructed and tested not only as individual components but in a simulated system.

The miniaturized system which was operated under the contract had a very low power level; although it produced very useful data, it was not representative of the type of pulsating system that would be used for the more representative type of pulsating flow hydraulic system application. Therefore, it is recommended that a higher power level system be constructed and operated at a more representative power level which will be indicative of the capabilities of pulsating system operation. Such a system should contain the alternator and transformer elements referred to above, so applied as to indicate their system compatibility. It is felt that the recommended system operating investigation can be accomplished in a system as envisioned by the load and rate operating requirements that were listed in the work statement. Moreover, since these loads and rates of motion are identical to those employed in the "Investigation of Techniques for 1000°F Hydraulic Systems," the results obtained in the recommended investigation will be directly comparable with data already available.

At the present time the technology of system design and operation at temperatures in excess of 1000°F has not advanced to a point where it is feasible to operate at high power beyond this limit. Therefore, it is recommended that for the present a temperature goal of 500°F to 700°F maximum be authorized.

From this operation and investigation of a representative pulsating system a much more complete evaluation of the feasibility of operation at temperature limits in excess of 1000°F will be achieved. Moreover, the specific operating characteristics and functional problems that may arise in the operation of a full-scale system will be delineated and solutions to the problems will be provided. The work will thus form a solid basis for future expansion to more critical areas of design, since it will be based on an area of investigation where there is a considerable store of experience.

It is also recommended that a further study intended to better delineate the areas of pulsating system usability be undertaken. For this purpose, comparative studies should be made of typical subsystems that appear to offer some advantage under pulsation concepts as contrasted with operation under continuous flow concepts. Further, since investigations to date have indicated the definite superiority of pulsating hydraulics in the area of extreme high temperature applications, it is recommended that preliminary investigations be undertaken along the lines required to advance the technology necessary for pulsating system operation under extreme thermal conditions.

SECTION VII - REFERENCES AND BIBLIOGRAPHY

1. Stevens, H.H., "Behavior of Circular Membranes Stretched Above the Elastic Limit by Air Pressure," Experimental Stress Analysis, Vol. 2, No. 1 (1944).

2. Roark, R.J., Formulas for Stress and Strain, Third Edition, McGraw-Hill Book Co., Inc. (1954).

3. Westerheide, D.E., Clifford, J.C., and Burnet, G., "Design and Test of a Diaphragm Pump for Liquid Metals," Nuclear Science and Engineering, Vol. 17, No. 4 (1963).

4. Blackburn, J.F., Reethof, G., and Shearer, J.L., Fluid Power Control, Cambridge, Technology Press of Massachusetts Institute of Technology (1960).

5. Lynch, W.A., and Truxal, J.G., Principles of Electronic Instrumentations, New York, McGraw-Hill (1957).

6. Fitzgerald, A.E., and Higgenbotham, D.E., Basic Electrical Engineering, New York, McGraw-Hill (1957).

7. Shearer, J.L., Notes prepared for the course "Advanced Automatic Control," M.I.T. Mechanical Engineering Department (1960).

8. "Research Investigation of Hydraulic Pulsation Concepts," Republic Aviation Corporation Quarterly Progress Reports 933-1 to 5.

9. Ezekiel, F.D., and Paynter, H.M., "Computer Representations of Engineering Systems Involving Fluid Transients," Trans. ASME (Nov. 1957).

10. Ezekiel, F.D., "Dynamic Representation of Lossless Distributed Systems," Control Engineering, May 1958.

BIBLIOGRAPHY

1. Constantinesco, G., "Theory of Wave Transmission - A Treatise on Transmission of Power by Vibration" - Walter Haddon, London (1922).

2. Kraus, J.D., "Electromagnetics," McGraw Hill Book Company, Inc., New York (1953).

3. Regetz, J.D., Jr., "An Experimental Determination of the Dynamic Response of a Long Hydraulic Line," National Aeronautics and Space Administration, Washington (1960).

4. Oldenburger, R., and Donelson, J. Jr., "Dynamic Response of a Hydraulic Plant," AIEE Transactions, paper No. 62-167.

5. D'Souza, A.F., Oldenburger, R., "Dynamic Response of Fluid Lines" Journal of Basic Engineering, Transaction, ASME, Paper No. 63-WA-73.

6. Oldenburger, R., and Goodson, R.E., "Simplification of Hydraulic Line Dynamics by Use of Infinite Products," Journal of Basic Engineering, Transaction of ASME, paper No. 62-WA-55.

7. Shearer, J.L., "Notes Used in Course ME 506, Special Topics in Automatic Control," Pennsylvania State University.

8. Ezekiel, F.D., and Paynter, H.M., "Fluid Power Transmission, From Fluid Power Control" by J.F. Blackburn, G. Roethof, and J.L. Shearer, editors, The Technology Press of M.I.T., and John Wiley & Sons, Inc., New York, N.Y. (1960).

9. Paynter, H.M., "Section 20, Fluid Transients in Engineering Systems," from Handbook of Fluid Dynamics, by V.L. Streeter, ed., McGraw Hill Book Company, Inc., New York, N.Y. (1961).

10. Shearer, J.L., "Section 21, Conversion, Transmission, and Control of Fluid Power," from Handbook of Fluid Dynamics by V.L. Streeter, ed., McGraw Hill, Inc., New York, N.Y. (1961).

APPENDIX I - NOMENCLATURE FOR HYDRAULIC PULSATION SYSTEM

Term	Definition
Pulsation	A reversing flow wave. The flow rate is considered as being basically sinusoidal in form.
Alternator	A component which converts continuous flow to pulsating flow.
Pulsation Generator	A component which converts mechanical energy to pulsating hydraulic energy.
Transformer	A component which transforms pulsating pressure and flow from one amplitude to another. It can also act as a barrier or separator between two fluids. The pulsating hydraulic energy is transmitted from one fluid to the other.
Transformer Ratio	The ratio of input to output area.
Rectifier Valve	A component which converts pulsating flow to continuous flow.
Number of Lines	The number of parallel lines in a pulsating transmission circuit. This term is used rather than "number of phases" because the analogy to an AC electrical system is not complete. For example, in a three-phase electrical system a potential is measured between two wires of different phases or between one wire and ground, whereas in pulsating hydraulics pressure is measured in each line or tube.
Line Difference	The angular cyclic difference between the lines of a pulsating circuit. This difference is equal to 360° divided by the number of lines.
Cyclic Shift	The angular deviation from proper cyclic relationship between one line and one or more other lines.
Positive Flow	Flow in a pulsating line in the normal pressure direction away from the power source.
Negative Flow	Flow in a pulsating line in the normal return direction toward the power source.
Fluid Volume Compensator	A component that compensates (either automatically or through a controlled means) for changes in the volume of fluid in a closed hydraulic circuit.
Frequency	The number of complete pulsation cycles in a given time period. Usually stated as "cycles per second" (cps).

This nomenclature is cumulative; it includes symbols from the First, Second, and Third Quarterly Progress Report.

A	=	Area
b	=	Damping coefficient
C	=	Capacitance
C_d	=	Discharge coefficient
~~C~~	=	Sonic velocity
D	=	$\frac{d}{dt}$
E	=	Voltage
f	=	Force
G	=	Conductance
g	=	$C_d \, W\sqrt{\frac{2}{\rho}}$
I	=	Current
K_h	=	Compliance (hydraulics)
K	=	Spring constant
K_r	=	Ratio of specific heat of air
K_a	=	Amplifier gain
K_c	=	Valve orifice constant
K_m	=	Compliance (mechanics)
ℓ	=	Length of line
L	=	Inductance
M	=	Mass
m	=	Inertance per unit length of line
N	=	Number of coil turns
P	=	Pressure
P_ℓ	=	Load pressure
P_s	=	Supply pressure
Q	=	Flow
R	=	Resistance
R_e	=	Real component of a complex number
R_h	=	Distributed hydraulic resistance
R′	=	Lumped hydraulic resistance
R_y	=	Reynolds number
S	=	Laplace operator
s	=	Hydraulic line leakage per unit line length
T_e	=	Wave traveling time through a line of length ℓ
U	=	Velocity
V	=	Voltage
W	=	Valve part width
X	=	Displacement
X_v	=	Spool displacement
X_p	=	Pulsating pump stroke
Y	=	Admittance
Y_s	=	Line surge admittance
Z	=	Impedance
Z_s	=	Line surge impedance (or characteristic impedance)
β	=	Bulk modulus
β_e	=	Equivalent bulk modulus
γ	=	Propagation constant
Δ	=	Increment
ρ	=	Fluid mass density
ω	=	Frequency
ϕ	=	Impedance phase angle
ν	=	Volume
$\frac{\partial}{\partial X}$	=	Partial differentiation with respect to displacement X

APPENDIX II - DESIGN CALCULATIONS

A. TORQUE BAR CALCULATION

The twisting of a 7075 ST aluminum alloy torque bar is used to simulate the aerodynamic hinge moment.

To find the length of bar required, assume a 2.4-in. square bar of 7075 ST aluminum alloy. The stress sustained by the bar for the torque induced is given by

$$S_s = \frac{T}{0.208h^3}$$

where

T = torque, in.-lb
h = depth of square bar = 2.4 in.

$$S_s = \frac{70,000}{0.208(2.4)^3} = 24,400 \text{ psi}$$

This stress is well below the yield point; therefore, permanent deformation will not be a critical parameter.

The length of bar required is calculated by the formula

$$L = \frac{\beta h^4 E_s \theta}{T}$$

where

L = length of bar, in.
β = numerical factor based on bar cross-section (0.141)
h = depth of bar, in.
E_s = modulus of rigidity of bar, psi
θ = angle of twist in radians

substituting:

$$L = \frac{(0.141)\ (2.4)^4\ (3.9 \times 10^6)\ (0.523)}{670,000}$$

$$= 136.00 \text{ in.}$$

B. INERTIA MASS

To find the weight required to simulate a 5 slug ft^2 moment of inertia, assume a lead weight, cylindrical shape, and 1-ft diameter (or 6-in. radius). Using the formula

$$I = \frac{Mr^2}{2}$$

where $M = \frac{W}{g}$

$$I = \frac{Wr^2}{2g}$$

solving for W

$$W = \frac{2Ig}{r^2} = \frac{(2)\ (5)\ (32.2)}{(0.5)^2}$$

$$W = \frac{322.00}{0.25} = 1288 \text{ lb}$$

For ease of handling, the thickness, L, of each lead disk was made 2 in. (0.166 ft).

Net volume of each disk = $\pi R^2 L - h^2 L = (\pi R^2 - h^2)$

substituting:

$$2[\ (3.14)(6)^2 - (2.4)^2\ ] \text{ cu ft} = 214.56 \text{ cu in.} = \frac{214.56}{1728} = 0.124 \text{ cu ft}$$

Density of lead = 710 lb per cu ft
Weight per disk = 710 x 0.124 - 88.04 lb
For fifteen disks in series
W = 88.04 x 15 = 1320.60 lb

Fifteen 1-ft diameter x 2-in. thick lead disks are sufficient to simulate the 5 slug ft^2 moment of inertia.

C. ACTUATOR

A typical actuator for controlling a typical aileron surface with a hinge moment and characteristics in accordance with data specified in the Work Statement is shown in Figure AII-1. Basic data and dimensions of the actuator are given in Table AII-1.

TABLE AII-1 - ACTUATOR DATA

Drawing number	FS3316024
Type	Balanced piston
Total stroke, in.	4.625
Working stroke, in.	4.625
Bore diameter, in.	3.321
Rod diameter, in.	1.475
Net area, instroke, $in.^2$	6.95
Net area, outstroke, $in.^2$	6.95
Volume, actuator instroke, $in.^3$	32.14
Volume, actuator outstroke, $in.^3$	32.14
Exchange volume	0
Time, full stroke (in-out), sec	1.835 sec
Rated flow rate, gpm	4.6
Maximum thrust, lb (4,000 psi)	27,800
Surface movement	± 30°
Surface rate, deg/sec	32.7
Maximum hinge moment, in.-lb	73,500
Moment arm, average, in.	4.39
Thrust required, lb	16,800
Load pressure, net psi	2,367
Actuator hp, load	6.35

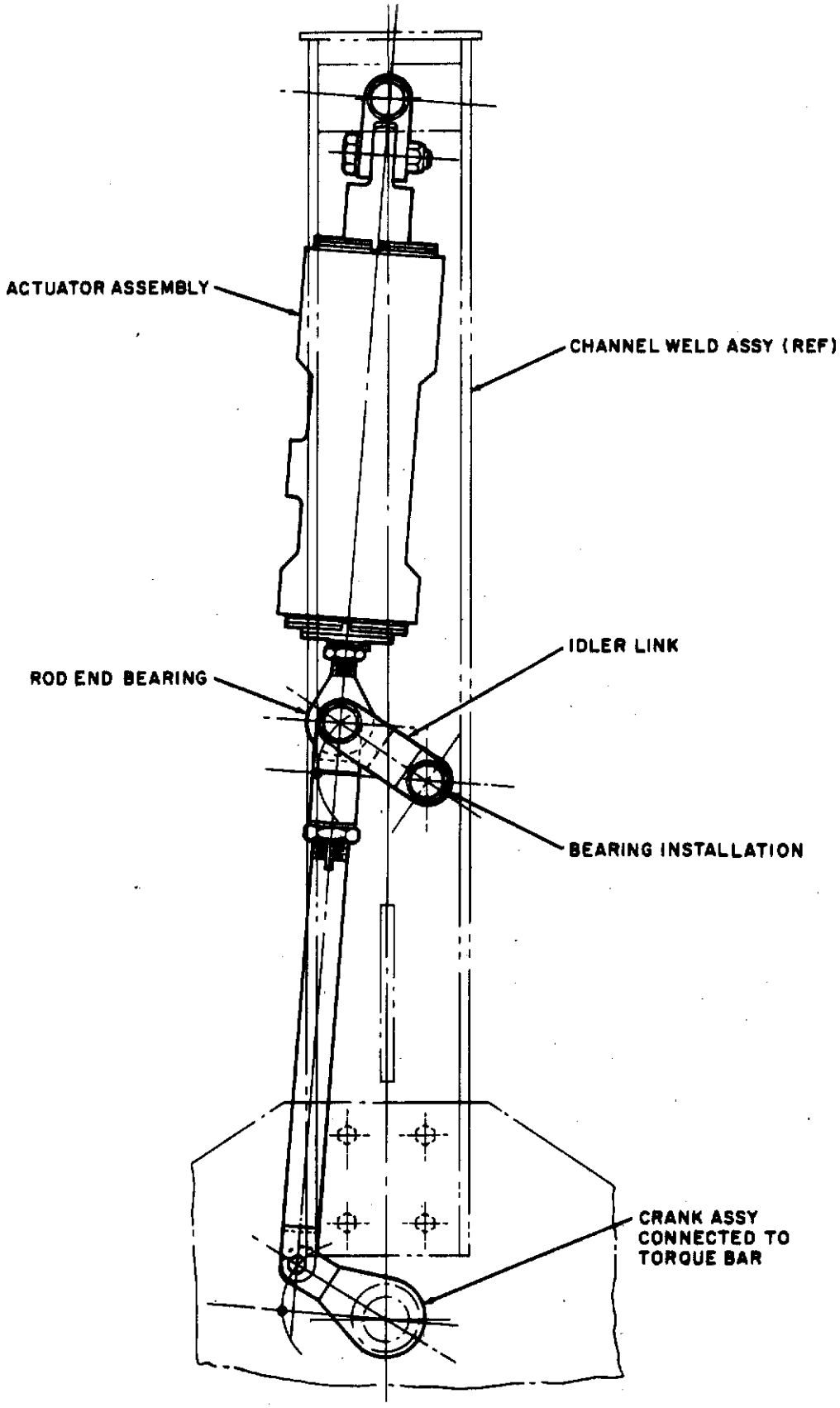

Figure AII-1. Actuator Test, Bearing Installation

APPENDIX III

DERIVATION OF CHARACTERISTIC EQUATIONS FOR TRANSMISSION LINE OF DISTRIBUTED PARAMETERS

UNSTEADY, COMPRESSIBLE AND LOW AVERAGE VELOCITY FLOW IN A UNIFORM PASSAGE

One Dimensional Flow

Figure AIII-1 shows the control volume of an unsteady, compressible and viscous flow in a uniform passage. The average velocity is assumed to be small, and the flow is one dimensional.

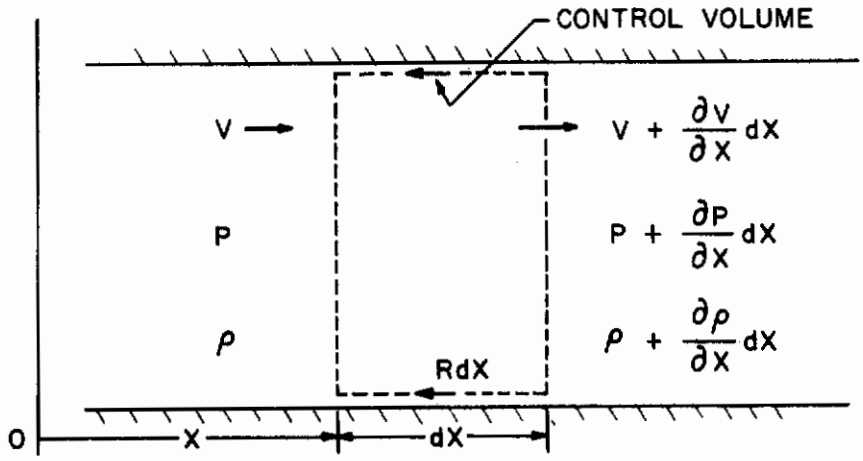

Figure AIII-1 Control Volume of Unsteady, Compressible and One-Dimensional Flow in a Uniform Hydraulic Line

Continuity equation:

$$\rho VA - \left[\rho VA + \frac{\partial(\rho VA)}{\partial x} dX \right] = AdX \frac{\partial \rho}{dt} \qquad \text{(AIII-1)}$$

Equation of state of liquid:

$$d\rho = \frac{\rho}{\beta_e} dP \qquad \text{(AIII-2)}$$

where

$$\frac{1}{\beta_e} = \frac{1}{\beta} + \frac{1}{E\left(\frac{D_o}{D_i} - 1\right)}$$

Combining Equation AIII-1 and AIII-2, results in

$$\rho \frac{\partial V}{\partial X} + \frac{V}{\beta_e} \rho \frac{\partial P}{\partial X} = - \frac{\rho}{\beta_e} \frac{\partial P}{\partial t} \qquad \text{(AIII-3)}$$

When the velocity is low enough we may neglect the second term on the left side of Equation AIII-3. The simplified continuity equation is, therefore, obtained.

$$\frac{\partial V}{\partial X} = - \frac{1}{\beta_e} \frac{\partial P}{\partial t}$$

or

$$\frac{\partial Q}{\partial X} = - \frac{A}{\beta_e} DP \qquad \text{(AIII-4)}$$

where $D \equiv \frac{\partial}{\partial t} \equiv j\omega$

The momentum equation is:

$$PA - \left[PA + \frac{\partial PA}{\partial X} dX \right] - QR_h dX = \left[\rho V^2 A + \frac{\partial (\rho V^2 A)}{\partial X} dX \right] - \rho V^2 A + \frac{\partial}{\partial t} \int_{cv} \rho V dA \, dX \qquad \text{(AIII-5)}$$

Carrying Equation AIII-5 out, and again neglecting the terms that have V as a coefficient, the momentum equation is reduced to

$$-\frac{\partial P}{\partial X} = \rho \frac{\partial V}{\partial t} + \frac{R_h Q}{A}$$

or

$$-\frac{\partial P}{\partial X} = \frac{1}{A}\left(R_h + \rho D \right) Q \qquad \text{(AIII-6)}$$

Let $\frac{A}{\beta_e} D$ and $\frac{1}{A}\left(R_h + \rho D \right)$ be represented by Y and Z, respectively, Equation AIII-4 and AIII-6 can be rewritten as

$$-\frac{\partial Q}{\partial X} = YP \qquad \text{(AIII-7)}$$

$$-\frac{\partial P}{\partial X} = ZQ \qquad \text{(AIII-8)}$$

Equations AIII-7 and AIII-8 are the pair of wave equations that describe the wave propagation in the distributed hydraulic line.

Differentiating Equations AIII-7 and AIII-8 with respect to X and substituting Equation AIII-7 and AIII-8 into the proper terms of the differentiated equations, the following pair of equations can be obtained.

$$\frac{d^2 P}{dX^2} - \gamma^2 P = 0 \qquad \text{(AIII-9)}$$

$$\frac{d^2 Q}{dX^2} - \gamma^2 Q = 0 \qquad \text{(AIII-10)}$$

where γ, propagation constant $= \sqrt{Z\,Y}$

The proper solution form of Equation AIII-9 is

$$P = C_1 e^{\gamma X} + C_2 e^{-\gamma X} \qquad \text{(AIII-11)}$$

Differentiating AIII-11 with respect to X

$$\frac{dP}{dX} = C_1 \gamma e^{\gamma X} - C_2 \gamma e^{-\gamma X} = -ZQ \qquad \text{(AIII-12)}$$

Therefore, the solution of Equation AIII-10 must be in the following form

$$Q = C_1 \frac{\gamma}{Z} e^{\gamma X} + C_2 \frac{\gamma}{Z} e^{-\gamma X}$$

or

$$Q = \frac{-C_1}{Z_s} e^{\gamma X} + \frac{C_2}{Z_s} e^{-\gamma X} \qquad \text{(AIII-13)}$$

where: Z_s, hydraulic line surge impedance $= \sqrt{\frac{Z}{Y}}$

Letting X = 0, Equation AIII-13 reduces to the following expression which is the instantaneous pressure at the section X = 0 on the hydraulic line

$$P = C_1 + C_2 \qquad \text{(AIII-14)}$$

It should be noticed from the above expressions that the quantities C_1 and C_2 are constant with respect to X but vary harmonically with respect to time. Therefore the terms C_1 and C_2 may be of the following form

$$C_1 = P_1 e^{j\omega t}$$

and

$$C_2 = P_2 e^{j\omega t} \qquad \text{(AIII-15)}$$

Substituting AIII-15 into Equation AIII-14, Equation AIII-14 becomes

$$P = P_1 e^{j\omega t} + P_2 e^{j\omega t} \qquad \text{at } X = 0 \qquad \text{(AIII-16)}$$

Substituting Equation AIII-16 into AIII-11 and AIII-13 results

$$P = P_1 e^{j\omega t} e^{\gamma X} + P_2 e^{j\omega t} e^{-\gamma X} \qquad \text{(AIII-17)}$$

and

$$Q = \frac{-P_1}{Z_s} e^{j\omega t} e^{\gamma X} + \frac{P_2}{Z_s} e^{j\omega t} e^{-\gamma X} \qquad \text{(AIII-18)}$$

Let us consider the wave traveling in the positive X direction only. The surge (or characteristic) impedance of the line is obtained by taking the ratio of the pressure and flow rate.

$$Z_s = \frac{P}{Q} = \sqrt{\frac{Z}{Y}} = \frac{1}{Y_s} \qquad \text{(AIII-19)}$$

The phase velocity of the traveling wave is

$$v = \frac{\omega}{\text{Im } \gamma}$$

which is the sonic velocity of the fluid in the line. This velocity may be affected both by the line wall rigidity and the amount of air dissolved in the fluid.

Let us consider a line of surge impedance, Z_s, which is terminated at a load impedance, Z_ℓ as shown in Figure AIII-2.

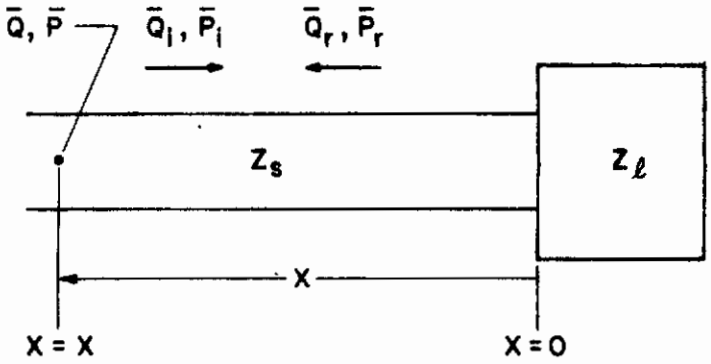

Figure AIII-2. Terminated Transmission Line

$\bar{Q}_i$ and $\bar{P}_i$ are the incident flow and pressure wave. $\bar{Q}_r$ and $\bar{P}_r$ are the reflected flow and pressure wave. They are complex functions of position. The resultant flow and pressure wave are the sum of the incident and reflected components

$$\bar{P} = \bar{P}_i + \bar{P}_r \qquad \text{(AIII-20)}$$

$$\bar{Q} = \bar{Q}_i + \bar{Q}_r \qquad \text{(AIII-21)}$$

where $\bar{P}_i = P_i e^{\gamma X}$

$\bar{P}_r = P_r e^{-\gamma X + j\zeta}$

$\bar{Q}_i = Q_i e^{\gamma X - j\delta}$

$\bar{Q}_r = Q_r e^{-\gamma X + j(\zeta - \delta)}$

ζ is phase shift at load

δ is phase difference between the pressure and flow

At the load (X = 0)

$$\frac{\bar{P}_r}{\bar{P}_i} = \frac{P_r}{P_i} e^{j\zeta} = \bar{\rho}_p$$

$$\frac{\overline{Q_r}}{\overline{Q_i}} = \frac{Q_r}{Q_i} e^{j\zeta} = \overline{\rho_q}$$

where $\overline{\rho}_p$ = reflection coefficient of pressure wave

$\overline{\rho}_q$ = reflection coefficient of flow wave

It follows that

$$\overline{P} = P_i \left(e^{\gamma X} + \overline{\rho}_p e^{-\gamma X} \right)$$

and

$$\overline{Q} = Q_i e^{-j\sigma} \left(e^{\gamma X} + \overline{\rho}_q e^{-\gamma X} \right)$$

By the definition of characteristic impedance we have the following relationship

$$Z_s = \frac{\overline{P}_i}{Q_i} = \frac{P_i}{Q_i} e^{j\sigma} = - \frac{\overline{P}_r}{\overline{Q}_r} = - \frac{P_r}{Q_r} e^{j\sigma} \qquad \text{(AIII-24)}$$

At the load

$$Z_\ell = \frac{\overline{P}}{\overline{Q}} \qquad \text{(AIII-25)}$$

Substituting Equation AIII-24 and AIII-25 into Equation AIII-21 we have

$$\frac{\overline{P}}{Z_\ell} = \frac{\overline{P}_i}{Z_s} - \frac{\overline{P}_r}{Z_s} = \frac{\overline{P}_i - \overline{P}_r}{Z_s} \qquad \text{(AIII-26)}$$

Substituting $\bar{P}$ by Equation AIII-20 we have

$$\frac{\bar{P}_i + \bar{P}_r}{Z_\ell} = \frac{\bar{P}_i - \bar{P}_r}{Z_o}$$

Solving for $\frac{\bar{P}_r}{\bar{P}_i}$ yields

$$\frac{\bar{P}_r}{\bar{P}} = \frac{Z_\ell - Z_s}{Z_\ell - Z_s} = \bar{\rho}_p \qquad \text{(AIII-27)}$$

By a similar method we can obtain

$$\bar{\rho}_q = - \frac{Z_\ell - Z_s}{Z_\ell + Z_s} = - \bar{\rho}_p \qquad \text{(AIII-28)}$$

The impedance Z_x at any point X of the line looking toward the load is defined as

$$Z_x = \frac{\bar{P}}{\bar{Q}} \qquad \text{(AIII-29)}$$

Substituting the appropriate equations into Equation AIII-29, the impedance of a line with linear friction loss is obtained as

$$Z_X = Z_s \left(\frac{Z_\ell + Z_s \tanh \gamma X}{Z_s + Z_\ell \tanh \gamma X} \right) \qquad \text{(AIII-30)}$$

For a frictionless line (γ has imaginary part only) Equation AIII-30 reduces to

$$Z_X = Z_s \left(\frac{Z_\ell + j Z_s \tan \frac{\omega}{c} X}{Z_s + j Z_\ell \tan \frac{\omega}{c} X} \right) \qquad \text{(AIII-31)}$$

APPENDIX IV - EQUATION DEVELOPMENT

1. Air Loaded Accumulator - Equation Development

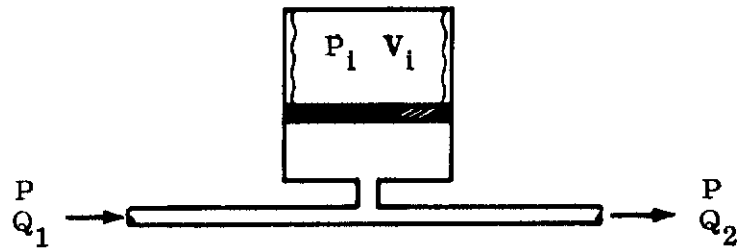

Basic $$PV^{Kr} = P_i V_i^{Kr} \qquad \text{(AIV-1)}$$

Equations: $$Q_2 = Q_1 - \frac{1}{K_r}\left(\frac{V}{P}\right)\frac{dp}{dt} \qquad \text{(AIV-2)}$$

where P_i = initial accumulator pressure

V_i = initial accumulator air volume

K_r = $\frac{C_p}{C_v}$ (ratio of specific heats, isentropic process)

from Equation B-1 $$V = \left(\frac{P_i V_i^{K_r}}{P}\right)^{\frac{1}{K_r}} = P_i^{\frac{1}{K_r}} V_i \frac{1}{P^{\frac{1}{K_r}}}$$

Substituting for V in Equation AIV-2

$$Q_2 = Q_1 - \frac{1}{K_r}\frac{1}{P}\frac{dP}{dt} P_i^{\frac{1}{K_r}} V_i \frac{1}{P^{\frac{1}{K_r}}} =$$

$$Q_1 - \frac{P_i^{\frac{1}{K_r}} V_i}{K_r} P^{-\left(\frac{K_r + 1}{K_r}\right)} \frac{dP}{dt}$$

$$Q_1 - Q_2 = \frac{P_i^{\frac{1}{K_r}} V_i}{K_r} P^{-\left(\frac{K_r + 1}{K_r}\right)} \frac{dP}{dt}$$

2. Power Input

The system efficiency η was computed by use of the equation

$$\frac{(P_H - P_L) Q_L}{\overline{PQ}} = \frac{\text{power output}}{\text{power input}} = \eta$$

where $\overline{PQ} = \frac{1}{T} \int_0^T PQ \, dt$

Due to the irregular waveform of P a numerical technique was used to evaluate the integral. See below:

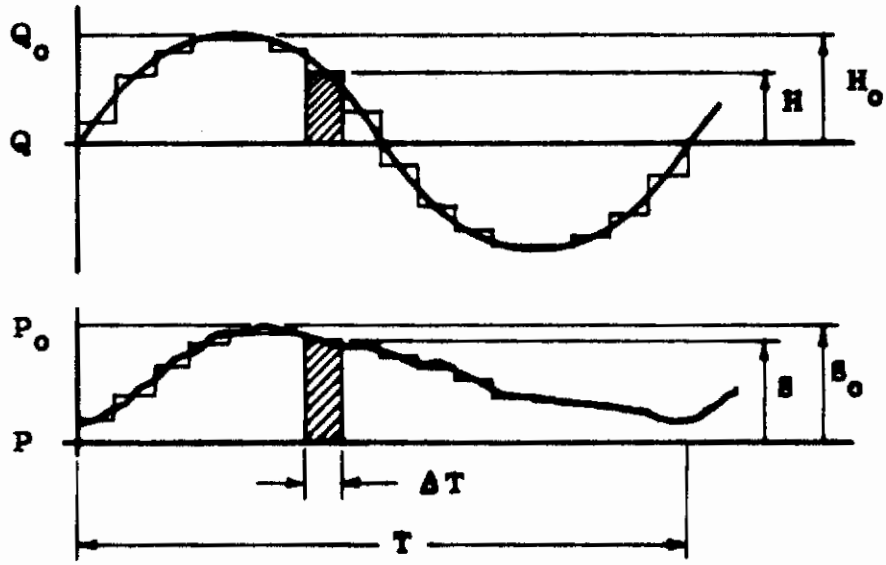

$$Q = \frac{H}{H_o} \quad Q_o \qquad\qquad P = \frac{S}{S_o} \quad P_o$$

$$\overline{PQ} = \frac{1}{T} \int_o^T PQdt = \frac{P_o \; Q_o}{TH_o \; S_o} \int_o^T HS \; dt =$$

$$\frac{P_o \; Q_o}{TH_o \; S_o} \quad \sum_i^N \quad H_i \; S_i \; \Delta \; T$$

APPENDIX V - MATERIALS FOR USE AT 1400°F

As presently designed, the hydraulic system will probably use a fluid such as a mixed polyphenyl ether for operation to 700°F. Since Republic had previous experience with this fluid during developmental work on its 1000°F hydraulic system (Contract AF33(616)-7454), this knowledge will be applied in the selection of materials for use in the 700°F zone.

For operation to 1400°F, the most suitable fluids appear to be the liquid metals, with NaK_{77} (sodium-potassium eutectic) receiving primary consideration. The use of liquid metals will have an effect on the containment materials with respect to corrosion, erosion, deterioration of mechanical properties, and sliding and bearing properties.

A number of materials that are compatible with NaK_{77} for operation at 1400°F are shown in Table AV-1. The austenitic stainless steels as well as the cobalt-base and nickel-base alloys are among those materials with good corrosion resistance. The refractory metals, including columbium, molybdenum, tantalum, tungsten, and chromium are recommended for use in NaK_{77} to 1690°F.

There are many factors which affect liquid metal corrosion, among which are the following:

(1) Temperature

(2) Temperature gradient

(3) Cyclic temperature fluctuation

(4) Surface area-to-volume ratio

(5) Purity of liquid metal

(6) Flow velocity or Reynolds number

(7) Surface condition of containment material

(8) The number of materials in contact with the same liquid metal

(9) Condition of the material (the presence of a grain boundary precipitate, the presence of a second phase, the state of stress of the material, and the grain size)

Liquid metal attack may take place by several fairly common mechanisms. One is a relatively uniform solution attack on the solid surface by the liquid corrodent. Another common method of attack is direct alloying, the interaction between liquid and solid to form surface films or typical layers of intermetallic compounds and solid solutions. These films may form a loosely adherent scale or, if held tightly, may serve as a barrier to slow down additional diffusion.

TABLE AV-1. MATERIALS COMPATIBILITY WITH LIQUID NaK_{77}

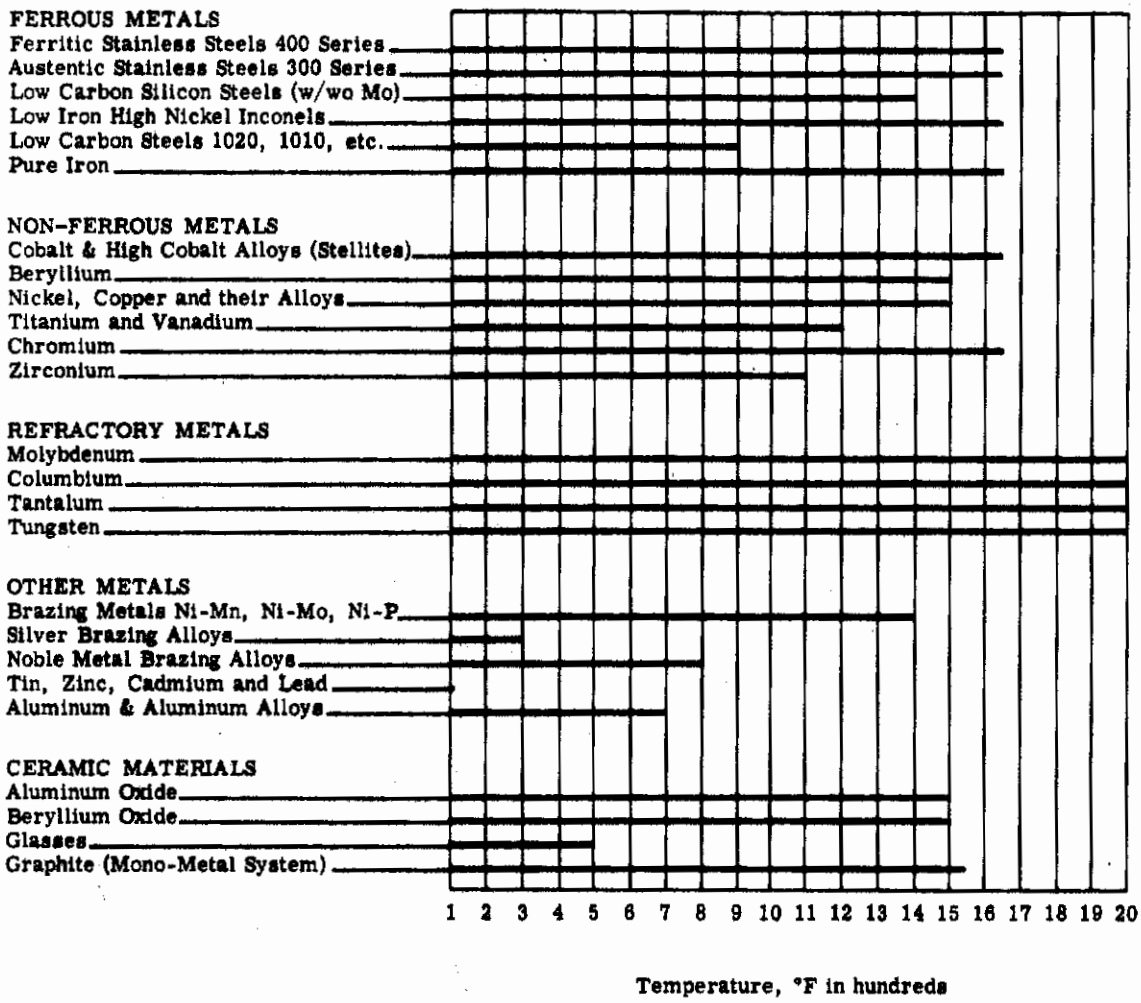

Selective reaction of the liquid metal with minor constituents of the solid may result in intergranular penetration or in the depletion of a dissolved component of a solid. Selective grain-boundary attack can drastically alter the physical properties of a material without appreciably changing its weight or appearance. This type of attack is often accelerated by the application of stress to the solid during exposure to the liquid metal. Particular care will be exercised in designing any part which will be subjected to stresses; a minimum of stress parts will be used.

Attack also results from corrosion by contaminants rather than by the liquid itself. Such contaminants may include oxygen, nitrogen, or carbon, dissolved in the liquid or present as part of a compound in suspension. For example, in oxygen-contaminated systems, the container metal may become coated with a layer of its own oxide if its oxide is more stable than the oxide formed by the liquid metal. The oxide layer, as with alloy layers, is sometimes tenacious and adherent. Hence, the layer acts as a diffusion barrier, thereby inhibiting further attack. On the other hand, the oxide layer may be non-adherent, in which case drastic weight loss ensues, especially under dynamic conditions. There remains the possibility that a film, once formed, can be removed by the fluxing action of other oxides.

One of the major problems inherent in the use of NaK_{77} is the formation of potassium and sodium oxides. The most harmful effects of this oxide contamination are increased corrositivity and cold zone precipitation. The precipitation on close-fitting parts is of primary concern; of almost equal concern is the fact that in a flowing system the oxides may accumulate in a cold zone and plug the system. This will be avoided by keeping NaK_{77} flow out of cooler areas ($<700°F$).

One of the most serious manifestations of liquid metal behavior (in which actual corrosion plays only a small part) is diffusion bonding or welding of solid metal surfaces to each other. Such self-welding takes place when contact with an alkali metal occurs and is intensified if the metals are held together under pressure. This effect becomes increasingly serious with increasing temperature.

Of particular interest in most liquid metal systems is a type of mass-transport, thermal-gradient transfer. This transfer is a result of the coexistence of a temperature differential and an appreciable thermal coefficient of solubility. Even though the actual solubility may be low, large amounts of a solid component may be dissolved from the zone of higher solubility and precipitated in the zone of lower solubility. This continued removal of the dissolved component from the system accelerates corrosion attack in some areas, eventually causing plugging of flow channels. Certain impurities, especially oxygen, may accelerate solution and the thermal-gradient transfer effect.

The selection of materials for the seal surfaces and bearings will be of major importance. Bearings which use hydrodynamic films for lubrication will be carefully designed in view of the exceptionally low viscosities of the liquid metals. Normally, oil lubricants form strong adherent surface films which reduce metal-to-metal contact or remove it entirely. However, with few exceptions, liquid metals tend to promote metal-to-metal contact by reacting with and dissolving protective surface films.

Data on the bearing properties of metals in NaK_{77} is very limited. Compatibility tests have been performed on a variety of materials at 350°F, using a fixed specimen bearing against a rotating sleeve. Material pairs showing the best wear properties include a tungsten carbide-cobalt cermet, a 6-6-2 high strength tool steel, white cast iron, and 17-4PH stainless steel against the tungsten carbide-cobalt cermet (carboloy 779). Austenitic and ferritic stainless steels, low-carbon steel, cobalt-base alloys, and a copper alloy showed poor compatibility in NaK_{77}. Bearing-material compatibility tests in NaK_{77} at temperatures to 950°F have been performed with the following results:

(1) Chromium carbide cermets are unsatisfactory bearing materials.

(2) Porous tungsten carbide cermets gave excellent results and are considered the best for oscillating bearing materials.

(3) A combination of titanium carbide cermet against tungsten carbide cermet has excellent compatibility characteristics and low coefficients of friction.

(4) The lower the percentage of cobalt in the tungsten carbide cermet, the less is the tendency for superficial damage. This is attributed to the increase in hardness and finer grain structure, the latter being considered more important.

(5) There is less tendency for surface damage to titanium carbide cermets if they do not contain a solid-solution type of carbide.

(6) Titanium carbide cermets tested with similar cermets tend to have less superficial surface damage when tested at temperatures below 850°F.

(7) Cermets with equivalent compositions tend to have similar compatibility characteristics.

(8) The compatibility of nickel-bonded cermets compares favorably with the compatibility characteristics of cobalt-bonded cermets.

(9) Metal-cermet and cermet-cermet combinations have fractional compatibility characteristics which are directly proportional to temperature.

(10) Copper and some copper alloys are most compatible with chromium or cermets at temperatures up to 600°F.

(11) Nickel and nickel alloys, with the possible exception of Colmonoy 6, do not have good compatibility characteristics at high temperatures.

(12) The chromium-tungsten-cobalt alloys showed fair compatibility characteristics at 600°F; however, above this temperature performance was poor.

(13) Iron-base alloys are also unsatisfactory at temperatures above 600°F.

(14) Surface-treated materials behaved according to their substrate materials.

(15) Surface finish is suspected to be an important factor in the compatibility of low-shear-strength materials which do not weld readily to the complementary material.

APPENDIX VI - MAJOR EQUATIONS FOR ANALYTIC STUDIES

Of the equations shown in Section IV, the following are those that are of greater importance for analytic studies of pulsating hydraulic systems:

Equation	
46, 47	Non-viscous line of lumped parameters with flow input.
50, 51	Non-viscous line of lumped parameters with pressure input.
52, 53, 54	Viscous line of lumped parameters with flow source.
55, 56, 57	Viscous line of lumped parameters with pressure source.
	Distributed Parameters
62	Characteristic impedance of viscous line, general.
63	Input impedance at distance X.
67	Characteristic impedance of viscous line, low flow velocity.
68	Characteristic impedance of non-viscous line, flow velocity.
72	Propagation constant of viscous line.
73	Propagation constant of non-viscous line.
75	Input impedance of viscous line.
77	Input impedance of non-viscous line.
88, 90, 91	Line resonance conditions.
138	Flow filtering effect, pressure variation ratio to accumulator pressure.

Equation	
141a, 141b	Line input impedance, lumped resistance at ends.
143a, 143b, 144, 146	Non-viscous line input impedance (distributed parameters).
147, 148	Viscous line input impedance (lumped parameters).
151, 152	Input and output pressure-flow of line (pressure source).
153, 154	Continuity Equation (pressure source).
155	System Efficiency.
156, 157	Input and output pressure-flow of line (flow source).
158	Continuity Equation, flow source.